nano bio & med 2017

nov. 22-24, barcelona (spain)

www.nanobiomedconf.com

abstracts book

Organisers

PHANTOMS foundation

IBEC
Institute for Bioengineering of Catalonia
EXCELENCIA SEVERO OCHOA

BOKU
Universität für Bodenkultur Wien
University of Natural Resources
and Applied Life Sciences, Vienna

NANOMED
S P A I N

Index

On behalf of the Organizing Committee, we take great pleasure in welcoming you to Barcelona (Spain) for the NanoBio&Med2017 International Conference.

This event, after successful editions organized within ImagineNano in Bilbao 2011 & 2013, and in Barcelona in 2014, 2015 & 2016, is going to present the most recent international developments in the field of Nanobiotechnology and Nanomedicine and will provide a platform for multidisciplinary communication, new cooperations and projects to participants from both science and industry. Emerging and future trends of the converging fields of Nanotechnology, Biotechnology and Medicine will be discussed among industry, academia, governmental and non-governmental institutions. NanoBio&Med2017 will be the perfect place to get a complete overview into the state of the art in those fields and also to learn about the research carried out and the latest results. The discussion in recent advances, difficulties and breakthroughs will be at his higher level.

As in previous editions, an industrial forum will be organized to promote constructive dialogue between business and public leaders and put specific emphasis on the technologies and applications in the nanoBioMed sector.

We are indebted to the following Companies, Scientific Institutions and Government Agencies for their financial support: Institute for Bioengineering of Catalonia (IBEC), Bicosome, ThermoFisher Scientific, NANOMED Spain, Leica Microsystems and ICEX Spain Trade and Investment.

We would also like to thank the following companies for their participation: nanoLANE, nanoscale Biomagnetics, Neaspec and Bioinicia.

In addition, thanks must be given to the staff of all the organising institutions whose hard work has helped planning this conference.

Organising committee

- **Antonio CORREIA**

  President of the Phantoms Foundation (Spain)

- **Dietmar PUM**

  Deputy Head of the Biophysics Institute – BOKU (Austria)

- **Josep SAMITIER**

  Director of the Institute for Bioengineering of Catalonia – IBEC (Spain)

PHANTOMS foundation

BOKU Universität für Bodenkultur Wien
University of Natural Resources and Applied Life Sciences, Vienna

IBEC[R]
Institute for Bioengineering of Catalonia
EXCELENCIA SEVERO OCHOA

NANOMED SPAIN

Media Partner

biomimetics
an open access journal by MDPI

Sponsors

GOBIERNO DE ESPAÑA MINISTERIO DE ECONOMÍA Y COMPETITIVIDAD
iCEX España Exportación e Inversiones

IBEC[R]
Institute for Bioengineering of Catalonia
EXCELENCIA SEVERO OCHOA

ThermoFisher SCIENTIFIC

NANOMED SPAIN

bicosome®

Leica MICROSYSTEMS

exhibitors

Bioinicia Innovative Polymer Applications

nea spec see the nanoworld

nB nanoScale Biomagnetics Experts in Magnetic nanoHeating

nanolane EYES ENTERING THE NANOWORLD

Speakers list: Alphabetical order

Authors	Session	Page
Lorenzo Albertazzi (Institute for Bioengineering of Catalonia (IBEC), Spain) Nanoscopy for Nanomedicine: looking at nanomaterials in action one molecule at the time	Keynote Plenary Session	9
Giuseppe Battaglia (University College London, UK) Design principles in precision nano-medicine	Keynote Plenary Session	10
Ofra Benny (The Hebrew University of Jerusalem, Israel) Mechanical cues affecting interactions of nanoparticles with tumor cells	Keynote Plenary Session	11
Andrea Bernardos (Interuniversity Research Institute for Molecular Recognition and Technological Development IDM – UV/UPV, Spain) Senescent-associated nanoparticles as therapeutic derivatives	Oral Parallel Session	12
Gabriela Calderó (CIBER-BBN, Institut de Química Avançada de Catalunya, Spain) Nano-emulsions as Microbubble Precursors for Biomedical Applications	Oral Plenary Session	14
Julian Carrey (INSA-Toulouse, France)) Killing cancer cells using nanoparticles submitted to high- and low-frequency magnetic fields	Keynote Plenary Session	15
Carolina Carrillo Carrion (CIC biomaGUNE, Spain) Self-assembled nanoclusters of fluorinated quantum dots as delivery platform for enzymes	Oral Plenary Session	16
Kenneth Dawson (CBNI - University College Dublin, Ireland)Nanoscopy for Microscopic Molecular Foundations of nano particle interactions with living systems	Keynote Plenary Session	17
Massimo De Vittorio (CBN/IIT, Italy) Tapered optical probes and optrodes for optogenetics and neurophotonics	Keynote Plenary Session	18
Matilde Duran Lobato (Center for Research in Molecular Medicine and Chronic Diseases (CIMUS), Spain) Rational design of new oral peptide nanomedicines	Invited Plenary Session	19
Carlos Elvira (Institute of Polymer Science & Technology, CSIC, Spain) Design and synthesis of polymeric vectors improving transfection efficiency in gene therapy applications	Oral Parallel Session	20
Helena Florindo (Universidade de Lisboa, Portugal) Impact of multicomponent nano-vaccine on immune modulation against solid tumors	Oral Parallel Session	22
Giancarlo Franzese (Universitat de Barcelona - Institute of Nanoscience and Nanotechnology (IN2UB), Spain) Multiscale Approach for Water at Bio-Nano Interfaces	Oral Plenary Session	23
Christoph Geers (Adolphe Merkle Institute, Switzerland) Detection and characterization of nanoparticles in biological systems via stimuli-induced heating	Oral Plenary Session	24
Duncan Graham (University of Strathclyde, UK) Nanoparticle based analysis of biomolecules, cells and tissue	Keynote Plenary Session	25
Yannick Guari (Université de Montpellier, France) Biosafety of mesoporous silica nanoparticles	Keynote Plenary Session	26
Marilena Hadjidemetriou (The University of Manchester, UK) In vivo biomolecule corona onto clinically used blood circulating liposomes	Invited Plenary Session	28
Zvi Hayouka (The Hebrew University of Jerusalem, Israel) Development of novel antimicrobial agents for several applications	Keynote Plenary Session	29
Alba Hernández Bonilla (Universitat Autònoma de Barcelona, Spain) Synergistic role of nanoceria on the ability of tobacco-smoke to induce carcinogenic hallmarks in lung epithelial cells	Oral Plenary Session	30

Authors	Session	Page
Jurriaan Huskens (University of Twente, The Netherlands) General-purpose, functionalized poly-L-lysine polymers as bio-sensing layers, and their use in DNA detection	Keynote Plenary Session	32
Jagoba Iturri (BOKU, Austria) Atomic Force Microscopy as a tool for Studying Cell (and Cell Scaffold) Mechanics	Invited Plenary Session	33
Meder Kamalov (University of Vienna, Austria) Biomimetic Synthesis of Functionalized Silica Particles	Oral Plenary Session	34
Thorsten Knoll (Fraunhofer Institute of Biomedical Engineering, Germany) Multimodular in vitro platform for evaluating the effects of nanoparticles on the human body	Oral Parallel Session	35
Kostas Kostarelos (The University of Manchester, UK) Learning the pharmacology and toxicokinetics of biologically-relevant graphene materials	Keynote Plenary Session	37
Jose M. Lagaron (CSIC, Spain) Novel poly(ε-caprolactone)/gelatin wound dressings prepared by emulsion electrospinning with controlled release capacity of Ketoprofen anti-inflammatory drug	Oral Plenary Session	38
Anna Laromaine (ICMAB-CSIC, Spain) Bacterial cellulose, a natural polymer for biological applications	Invited Plenary Session	39
Laura Lechuga (ICN2, Spain) The potential of photonic point-of-care nanobiosensors for high-value diagnostics	Keynote Plenary Session	40
Seunghwan Lee (Technical University of Denmark, Denmark) Micro-to-Nanoscale Mechanical Properties of Pig Intestine and Gastric Mucus as Studied with Atomic Force Microscopy	Oral Parallel Session	41
David Limón (Universitat de Barcelona, Spain) Slow microscale coiling in bis-imidazolium supramolecular hydrogel fibres induced by release of a cationic serine protease inhibitor	Oral Parallel Session	42
Arben Merkoçi (ICN2, Spain) Health and environment diagnostics using paper-based nanobiosensors	Keynote Plenary Session	43
Thomas Moore (Adolphe Merkle Institute / University of Fribourg, Switzerland) Shoot it or dilute it: Administration method in cell culture alters particle-cell interaction	Oral Parallel Session	44
Silvia Muro (IBBR - University of Maryland - NIST, USA) Receptor-Targeted Drug Delivery: Biological Mechanistic and Applications	Keynote Plenary Session	45
Enrique Navarro (Bioinicia, S.L., Spain) Electrospinning and Electrospraying applications in pharma and in the BioSpace. Some real practical cases.	Oral Plenary Session	46
Solène Passemard (Intitute of Material Science of Barcelona-CSIC, Spain) Improvement of the Enzymatic Activity of α-Galactosidase Using Nanovesicles with application to Fabry Disease treatment	Oral Plenary Session	47
Tania Patiño (Institute for Bioengineering of Catalonia (IBEC), Spain) Unravelling fundamental aspects of enzyme-powered micro-&nanomotors: towards biomedical applications	Oral Plenary Session	49
Valery Pavlov (CIC BiomaGUNE, Spain) Optical and Electrochemical Bioassays Using Photo-catalytical Activity of Semiconductor Quantum Dots	Oral Parallel Session	50
Danny Porath (The Hebrew University of Jerusalem, Israel) Novel DNA-Based Molecules and Their Charge Transport Properties	Keynote Plenary Session	52
Francisco Porto (Leica Microsystems, Spain) The DMi8S: an open inverted microscopy platform	Invited Plenary Session	-
Marina Pöttler (University Hospital Erlangen, Germany) Magnetic tissue engineering of the vocal fold: generation of 3D cell constructs using superparamagnetic iron oxide nanoparticles	Oral Plenary Session	53
Veronique Preat (Université catholique de Louvain, Belgium) Nanomedicines for the local and targeted treatment of glioblastoma	Keynote Plenary Session	55
Archana Ramadoss (Nanolane, France) SEEC technology mediated label-free nano-biofilm characterization	Oral Plenary Session	57

Authors	Session	Page
Pilar Rivera Gil (Pompeu Fabra University, Spain) Theranostic nanocapsules for hyperthermia	Oral Parallel Session	58
Loris Rizzello (University College London, UK) Targeting mononuclear phagocytes for eradicating intracellular parasites	Oral Parallel Session	59
Laura Rodriguez-Lorenzo (Adolphe Merkle Institute, Switzerland) Quantification of CNT dose delivered to cell surfaces by UV-Vis-NIR spectroscopy.	Oral Plenary Session	61
Samuel Sánchez (IBEC, Spain)) Enzyme Catalysis to Power Nanovehicles Towards Nanomedicine	Keynote Plenary Session	62
Paola Sánchez-Moreno (Istituto Italiano di Tecnologia, Italy) Biotransformation and biological impact of graphene-related materials during simulated oral ingestion	Oral Plenary Session	63
Marcos Sanles-Sobrido (Pompeu Fabra University, Spain) Outstanding characterization of Tungsten nanoparticles to anticipate health harmfulness in case of nuclear reactor accident	Oral Plenary Session	64
Ronit Satchi-Fainaro (Tel Aviv University, Israel)) Identifying molecular signatures of tumor dormancy as a basis for the rational design of precision nanomedicines	Keynote Plenary Session	65
Philip Schäfer (neaspec GmbH, Germany) Exploring biological micro- and nanostructures using infrared nanospectroscopy (nano-FTIR)	Oral Plenary Session	66
Avi Schroeder (Technion, Israel) Barcoded nanoparticles for personalizing anti-cancer medicine in the primary tumor and metastasis	Keynote Plenary Session	68
Anna Scomparin (Tel Aviv University, Israel) Combination of Dendritic Cell-targeted Nano-vaccines with Immune Checkpoint Therapy for Melanoma	Oral Plenary Session	69
Dedy Septiadi (Adolphe Merkle Institute, Switzerland) 4D live cell imaging to study cellular interplay in a 3D lung model upon (nano)particle exposure	Oral Plenary Session	70
Orit Shefi (Bar-Ilan University, Israel) Magnetic Manipulations for Controlling Neuronal Engineering and Regeneration	Keynote Plenary Session	71
Oded Shoseyov (The Hebrew University of Jerusalem, Israel) Nanoscopy for Hybrid Nano Bio-fibers	Keynote Plenary Session	72
Álvaro Somoza (IMDEA Nanociencia, Spain) Smart Nanoparticles for the Treatment of Cancer	Keynote Plenary Session	73
Miguel Spuch-Calvar (Adolphe Merkle Institute, Switzerland) Nanoparticle Detection in Consumer Products	Oral Plenary Session	74
Kaori Sugihara (University of Geneva, Switzerland) Self-assembled lipid nanotubes	Oral Plenary Session	75
Fabrice Reuven Sultan (MERCK CHIMIE SAS, France) New very small magnetic microspheres in Medical Applications	Oral Parallel Session	77
Dionysia Tsoutsi (Universitat Pompeu Fabra, Spain) Hyperspectral microscopy for single and collective nanoparticle characterization in biological media	Oral Parallel Session	78
Alina Vasilescu (International Center of Biodynamics, Romania) Development of a SPR aptasensor: towards a robust tool for detecting traces of lysozyme dimer in oligomeric and aggregated mixtures	Oral Parallel Session	79
Martha Vázquez González (Bicosome, Spain) Smart drug delivery system that targets the epidermis and follicles	Oral Plenary Session	81
María J. Vicent (Príncipe Felipe Research Cente, Spain) Versatile Star-shaped Polypeptide Conjugates with Controlled Self-assembly as Single Agents and in Combination Therapy	Keynote Plenary Session	82
Clara Vilches (Institut de Ciències Fotòniques ICFO, Spain) In vivo optimization of plasmonic photothermal therapy for oncological medicine	Oral Plenary Session	83
Marija Vukomanovic (Bacterial Infections: Antimicrobial Therapies, IBEC, Spain) Arginine – Functionalized Gold Nanoparticles: Synthetic Analogues of Antimicrobial Peptides	Oral Plenary Session	84

Authors	Session	Page
Elisabet Xifre-Perez (Universitat Rovira i Virgili, Spain) Nanoporous Anodic Alumina for the Development of Molecular Gated Sensors	Oral Plenary Session	86
Yan Yan (CBNI - University College Dublin, Ireland) Biological Recognition of Nanoparticles	Keynote Plenary Session	87
Julia Xiaojun Zhao (University of North Dakota, USA) Graphene-based Nanomaterials for Biomedical Applications	Oral Plenary Session	88
Linda Angela Zotti (Universidad Autónoma de Madrid, Spain) Electron transport through peptides and blue-copper azurins	Oral Parallel Session	90

Nanoscopy for Nanomedicine: looking at nanomaterials in action one molecule at the time

Lorenzo Albertazzi,

Nanoscopy for Nanomedicine Group, Institute for Bioengineering of Catalonia (IBEC)
C\ Baldiri Reixac 15-21, Helix Building, 08028 Barcelona

lalbertazzi@ibecbarcelona.eu

Nanomaterials revolutionized the field of biomedicine introducing innovative approaches towards drug delivery, molecular imaging, regenerative medicine and biosensing. However, despite the large investments in nanotechnology the translation into clinical applications is still unsatisfactory. One of the main reasons is the lack of knowledge about the behavior of nanostructures in the biological environment that makes the rational design of effective materials extremely challenging.

The main aim of our group is to use advanced microscopy techniques to understand the interactions of nanomaterials with living matter and to exploit this information to design novel devices for biomedical applications with a particular focus on drug delivery. To this goal we employ innovative optical imaging techniques such as super resolution microscopy to visualize and understand the molecular interactions of nanomaterials with their cellular targets in unprecedented detail. Super resolution microscopy techniques such as stochastic optical reconstruction microscopy (STORM) and point accumulation for imaging in nanoscale topography (PAINT) offer nanometric resolution and multicolor ability, therefore they are ideal tools to study nano-sized multicomponent functional objects in vitro and in cells. This allows to get a closer "look" at the mechanisms of the key phenomena responsible for device performances such as particle stability, protein corona and targeting. The fundamental knowledge acquired will pave the way towards the "microscopy-guided" design of novel nanomaterials for drug delivery.

Design principles in precision nano-medicine

Giuseppe Battaglia

Deparment of Chemistry, University College London, 20 Gordon Street, WC1H 0AJ, London, United Kingdom

g.battaglia@ucl.ac.uk

As we advance our understanding of diseases and consequently our ability to design new drugs, we come to the realisation that effective therapy is only possible when drug development is combined with efficient delivery. Indeed, no matter how potent we design drugs, if these are not taken to their target or, even worse, left interacting with unwanted targets with consequent side-effects. Getting across biological barriers and deliver therapeutic cargo to the right site is indeed a very challenging task that requires the judicious combination of physiological information with carrier engineering. In the last decade, we have approached this problem, applying a constructionist approach where we mimic biological complexity in the form of design principles to produce functional bionic units from simple building blocks and their interactions. We combine synthetic and supramolecular chemistry to tune inter/intramolecular interactions and self-assembly processes to form dynamic soft materials. Among the different bionic efforts, we have focussed our attention to possibly one of the few that encompasses polymerisation, compartmentalisation and positional self-assembly in the same unit; Polymersomes. These are vesicles formed by the self-assembly of amphiphilic block copolymers in water [1]. We have equipped polymersomes with the critical elements to address the challenges for getting across biological barriers. They have surface engineered to control both attractive (binding) and repulsive (anti-fouling) interaction with proteins and receptors to create systems that can avoid opsonisation and yet target specific cell populations. We have engineered their mechanical properties so as to be flexible and able to penetrate dense tissues exploiting size-exclusion percolation patterns. We have equipped them with both asymmetric topology and enzymes to control their fluid-dynamics and diffusion so as to create chemotactic and active propulsion toward endogenous signalling molecules [2] **(Fig.1)**. Finally, we have engineered their shape and size to guide cellular endocytosis as well as to escape the endocytic sorting accessing and delivering cargo within the cell interior [3-4]. I will present our design effort discussing each structural and functional element as a function of the respective biological challenge, I will conclude presenting applications where these precision systems are being applied to address challenges in neurology [6], oncology [7], and immunology [8-9].

References

[1] L. Ruiz Perez, L. Messager, J. Gaitzsch, A. Joseph, L. Sutto, F. L. Gervasio and G. Battaglia *Science Adv.* 2016, e1500948

[2] A. Joseph, C. Contini, D. Cecchin, S. Nyberg, L. Ruiz-Perez, J. Gaitzsch, G. Fullstone, J. Azizi, J. Pre- ston, G. Volpe, G. Battaglia *Science Adv.* 2017, 3, 8, e1700362

[3] C. LoPresti, M. Massignani, C. Fernyhough, A. Blanazs, A. J. Ryan, J. Madsen, N. J. Warren, S. P. Armes, A. L. Lewis S. Chirasatitsin, A. Engler, G. Battaglia *ACS Nano* 2011, 5 (3),1775–1784

[4] J. D Robertson, G. Yealland, M. Avila-Olias, L. Chierico, O. Bandman, S. A Renshaw, G. Battaglia *ACS Nano,* 2014, 8, 4650–4661

[5] X. Tian, S. Nyberg, P. Sharp, J. Madsen, N. Daneshpour, S. P. Armes, J Berwick, M. Azzouz, P. Shaw, N. J. Abbott and G. Battaglia *Sci. Rep.* 2015, 5, 11990

[6] L. Simón-Gracia, H. Hunt, P. Scodeller, J. Gaitzsch, G. B. Braun, A. A. Willmore, E. Ruoslahti, G. Battaglia, and T. Teesalu *Mol. Cancer Ther.* 2016, 15 (4), 670-679

[7] L. Rizzello, J. D. Robertson, P. M Elks, A. Poma, N. Daneshpour, T. K Prajsnar, D. Evangelopoulos, J. Ortiz Canseco, S. Yona, H. M Marriott, D. H Dockrell, S. Foster, B. De Geest, S. De Koker, T. McHugh, S. A Renshaw, G. Battaglia *bioRxiv*, 2017, 10.1101/119297

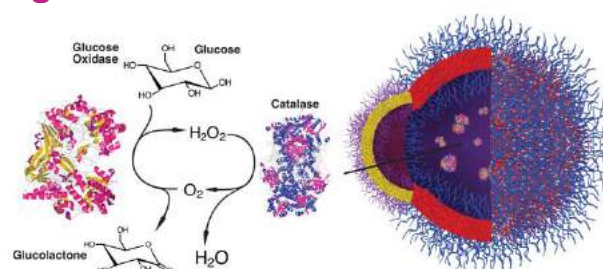[8] J. Robertsons, G. Battaglia and S. Renshaw *J. Immunol.* 2017, 198 (9) 3596-3604

Figures

Figure 1. Schematics of a glucose tactic polymersome

MECHANICAL CUES AFFECTING INTERACTIONS OF NANOPARTICLES WITH TUMOR CELLS

Stern T[1], **Kaner I**[1], **Shoval H**[1], **Brill-Karniely Y**[1], **Benny O**[1]

[1] Institute for Drug Research, School of Pharmacy, Faculty of Medicine, The Hebrew University, Jerusalem, Israel

ofrab@ekmd.huji.ac.il

Abstract

Drugs delivery into tumor tissue is one of the central challenges in cancer therapy. The ability to cross biological barriers is a critical parameter for success of treatment. Nanoparticles are being extensively studied as drug carriers which potentially can improve efficacy and selectivity of anti-cancer treatments. Polymer micelles composed of di-block polymers are a promising drug delivery system with markedly benefits including small dimension, ease of preparation, controlled drug release, drug targeting and reduction of side effects (1). However, as many other nanoparticle forms, the ability of polymer micelles to penetrate the core of solid tumor tissues is relatively low especially in poorly-vascularized tumors, such as pancreatic adenocarcinomas.

We addressed that issue and developed a novel form of highly penetrating particles which are based on Solidified Polymer Micelle (SPM). We showed that solely by changing the mechanical properties of the drug-carrier, without modifying its composition, the interactions with tumor cells is improved (2). Biodegradable polymer micelles composed of poly-ethylene glycol poly lactic acid (PEG-PLA) were tested in their solidified form vs. their "wet" elastic form. It has been shown that solid particles have better internalization into tumor cells, in addition to their ability to perform exocytosis, and they could penetrate into multi-layer cellular 3D culture which mimic the tumor microenvironment (3). This study suggests that transcytosis nanoparticle transport can provide an important mechanism for drug penetration into tumors, even when their stroma is dense and enhancing the exposure of the core to the chemotherapy. This work lay the ground for future rationale design of drug delivery systems, in respect to the vascular state of the tumor tissue.

References

[1] Abramov E, Cassiola F, Schwob O, Karsh-Bluman A, Shapero M, Ellis J, Luyindula D, Adini I, D'Amato RJ, Benny O. Nanomedicine. 2015 Nov;11(8):1993-2002

[2] Stern T, Kaner I, Laser Zer N, Shoval H, Dror D, Manevitch Z, Chai L, Brill-Karniely Y, Benny O. J Control Release. 2017 Jul 10;257:40-50.

[3] Shoval H, Karsch-Bluman A, Brill-Karniely Y, Stern T, Zamir G, Hubert A, Benny O. Sci Rep. 2017 Sep 5;7(1):10428.

Figures

Figure 1. Solidified Polymer micelles show higher penetration to 3D tissue-like multi cell culture (A) Schematic diagram of solidified polymer micelles (B) penetration of flexible" vs. rigid SPMs in tumor multicellular spheroids (red-cell cytoplasm, green-particles, blue- cell nuclei). (C) Two photon image of particles penetrating tumor 3D spheroid.
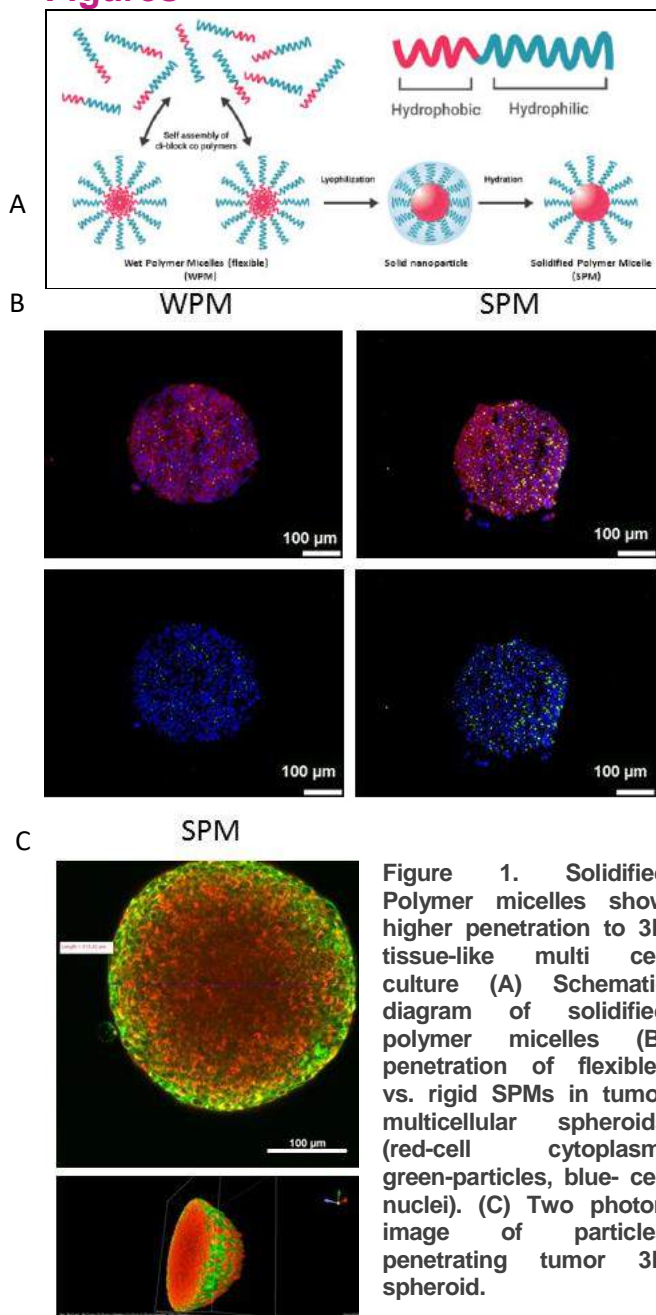
Senescent-associated nanoparticles as therapeutic derivatives

Andrea Bernardos[1,2],
Irene Galiana[1,2], Maria Alfonso[1,2], Beatriz Lozano-Torres[1,2,] Borja Diaz de Greñu[1,2], Daniel Muñoz[3], Miguel Rovira[3,4], José Ramón Murguía[1,2,5], Manuel Serrano[3,4,5], Timothy Cash[5], Marc Ramis[5], Ramón Martínez Máñez[1,2,5]

1 Interuniversity Research Institute for Molecular Recognition and Technological Development (IDM) Universitat Politècnica de València, Universitat de València, Camí de Vera s/n, 46022 Valencia, Spain.
2 CIBER- BBN (Bioengineering, Biomaterials and Nanomedicine), Spain.
3 Spanish National Cancer Research Centre, Melchor Fernández Almagro, 3, 28029 Madrid, Spain.
4 Institute for Research in Biomedicine, Carrer Baldiri Reixac, 10-12, 08028 Barcelona, Spain.
5 Senolytic Therapeutics SL, Carrer Baldiri Reixac 4, 08028 Barcelona, Spain.
anberba@upvnet.upv.es

It is known that cellular senescence is a state of permanent cell-cycle arrest that proliferating cells can adopt in response to cellular stresses as a measure to avoid the replication and proliferation of damaged cells. Thus, like apoptosis, senescence can be considered as an emergency defence system for elimination of unwanted cells. Senescent cells present several markers such as the absence of proliferative markers, senescence-associated β galactosidase (SA-β-Gal) activity, expression of tumour suppressors and cell cycle inhibitors and morphological changes.[1] Strategies to detect or remove senescent cells are so of fundamental interest both for basic research and clinical applications. However removal or replacement of senescent cells to treat aging-related conditions in humans are not available yet in the market and there are still very few studies in this area of research. An approach to achieve the goal of removing senescent cells is to develop selective delivery systems.

Recent advances in nanotechnology and in molecular and bio-molecular chemistry have resulted in the design of supramolecular and biologically inspired systems capable to show inventive related functions fuelling areas such as bio-engineering, bio-sensing and bio-nanotechnology into new horizons. In this field, one appealing application relates with the development of gated materials for controlled delivery. These gated materials usually contain a switchable "gate-like" ensemble capable of being "opened" or "closed" upon the application of certain external stimuli and a suitable inorganic porous support acting as nanocontainer.[2]

In this context, a gated mesoporous silica nanodevice (MSNs) loaded with a reporter and capped with a galacto-oligosaccharide (GOS) that are able to selectively deliver their cargo in senescent cells due to hydrolysis of the GOS cap by the β-galactosidase enzyme, which is overexpressed in senescent cells, was developed (see Figure 1).[3]

Following the same strategy, a galacto-hexasaccharide (GAL) nanodevice loaded with a reporter (rhodamine B) and doxorubicin (nano-dox) have been recently synthesized. This nanodevice is able to release their cargo under the specific presence of SA-β-Gal enzyme in senescent cells. β-galactosidase responding nanoparticles have been loaded both with rhodamine B and doxorubicin, and several assays have been performed in different cell lines to test the specific senescence-selectivity of the proposed nanodevices, for detection and therapeutic applications.

Furthermore, it has been recently demonstrated in a model of cancer chemotherapy, nanoparticles capped with GAL and loaded with doxorubicin target tumour cells undergoing chemotherapy-induced senescence and contribute to tumour xenograft regression. In addition, same nanoparticles (nano-dox) target senescent cells in the context of pulmonary fibrosis in mice, reducing collagen deposition and ameliorating pulmonary function (see Figure 2).

References

[1] D. Muñoz-Espín, M. Serrano, Nature Rev. Mol. Cell Biol. 15 (2014), 482.

[2] E. Aznar, M. Oroval, L. Pascual, J.R. Murguía, R. Martínez-Máñez, F. Sancenón. 116 (2016), 561.

[3] A. Agostini, L. Mondragón, A. Bernardos, R. Martínez-Máñez, M. D. Marcos, F. Sancenón, J. Soto, A. Costero, C. Manguan-García, R. Perona, M. Moreno-Torres, R. Aparicio-Sanchis and J. R. Murguía, Angew. Chem. Int. Ed. 51, (2012), 10556.

Figures
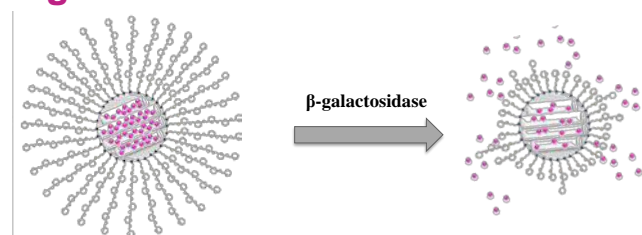
Figure 1. Schematic representation of the cargo release in the presence of β-galactosidase.
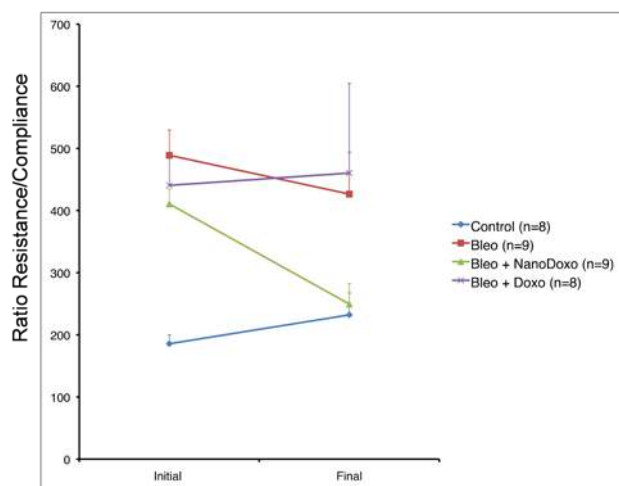
Figure 2. Male mice were subjected to a single intratracheal administration of PBS (control) or bleomycin. Beginning at day 10, mice were treated daily with free doxorubicin or with doxorubin loaded in MSNs and capped with GAL, for 14 days, that is, until day 24 post-bleomycin. Plethysmography, Computed tomography and histology were performed at the indicated days. Plethysmography (see figure) was used to determine the ratio between lung resistance (LR) and compliance dynamics (Cdyn) in the indicated groups before and after the indicated treatments. A remarkable restoration of pulmonary function was observed for mice treated with doxorubicin-loaded GAL-capped MSNs (nano-ox) in comparison with mice treated with free doxorubicin or untreated.

Nano-emulsions as Microbubble Precursors for Biomedical Applications

Gabriela Calderó[1],
Albert González[2], Marta Monge[1,2,3], Carlos Rodríguez-Abreu[2,1], María José García-Celma[3,1], Conxita Solans[2,1]

[1]CIBER-BBN, Barcelona, Spain
[2]Institut de Química Avançada de Catalunya (IQAC), CSIC. Jordi Girona 18-26, 08034 Barcelona, Spain
[3]Dept. de Farmàcia i Tecnologia Farmacèutica i Físicoquímica. Univ. de Barcelona. Unitat Associada d'I+D al CSIC. Av Joan XXIII, s/n, 08028 Barcelona, Spain

gabriela.caldero@iqac.csic.es

Biomedical microbubbles (MB) are colloidal gas globules dispersed in aqueous medium, with sizes typically below that of red blood cells, that is, smaller than 10 µm. One of their most interesting properties is their ability to respond to ultrasound stimuli. For this reason, they have attracted much interest in the biomedical field for a variety of applications, such as ultrasound imaging, targeted and triggered drug delivery, sonoporation, occlusive therapy, thermal therapy, blood brain barrier opening, lithotripsy, etc... However, the formulation of stable and monodisperse MB, capable of a uniform and predictable response to ultrasound stimuli is not straightforward. Although respiratory gases (O_2, CO_2, N_2) show high biocompatibility at suitable concentrations, their high solubility in aqueous media causes a short half-life in blood [1]. In this context, we propose the preparation of microbubbles from perfluorocarbon nano-emulsion templates. Perfluorocarbons show an extremely low solubility in aqueous medium, hindering their diffusion from the dispersed droplets into the body fluids. However, their low affinity for both, oil and aqueous media, and their high density make the preparation of stable colloidal systems a challenging issue. Due to the nanometric droplet size of perfluorocarbon nano-emulsion precursors, they could access easily capillaries or subcellular compartments [2,3]. Once they have reached their target, a phase shift of the liquid perfluorocarbon droplets to gas microbubbles may be triggered by appropriate stimuli (acoustic, optic, thermal, etc) (**Fig. 1**). The formation of polymeric perfluorocarbon nano-emulsions (NE) has been investigated in an aqueous solution / non-ionic surfactant / [polymer + perfluorocarbon + organic solvent] system in the presence and absence or an apolar low density oil. Fluorocarbon nano-emulsions have been obtained at high oil-to-surfactant ratios with hydrodynamic droplet sizes typically below 300 nm. It has been found that the colloidal stability of the obtained perfluorocarbon NE can be improved with the incorporation of an apolar low-density oil in the oil phase of the NE. Further, perfluorocarbon-loaded polymeric nanocapsules (NC) were obtained from the NE templates using a dialysis method. The as-obtained NC show globular shape and sizes below 250 nm by DLS. Successful perfluorocarbon encapsulation in the NC has been evidenced by spectral angle mapper classification of hyperspectral images of single NC. Preliminary cytotoxicity and vaporization assays suggest that the as-prepared perfluorocarbon NC are promising biomedical microbubble precursors.
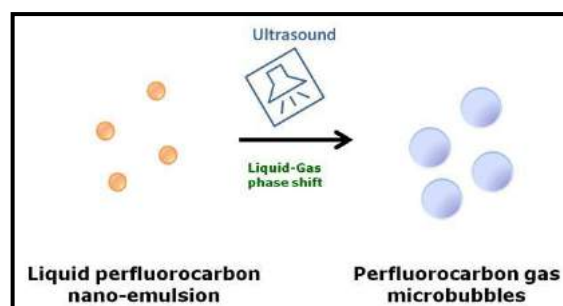
References

[1] Alvarez et al. Gastrointestinal Endoscopy J 2009; 69 (2): S71 – S77
[2] Sheeran et al. Biomaterials 2012; 33: 3262 - 3269
[3] Krafft MP. J Fluorine Chem 2015; 177: 19 - 28

Figures

Figure 1. Scheme of liquid perfluorocarbon nano-emulsion activation by ultrasound for microbubble formation.

Killing cancer cells using nanoparticles submitted to high- and low-frequency magnetic fields

J. Carrey,
B. Mehdaoui, R.P. Tan, N. Hallali, A. Meffre, L.-M. Lacroix, B. Chaudret, M. Respaud

Laboratoire de Physique et Chimie des nano-objets (LPCNO), CNRS, INSA, UPS, Université de Toulouse, 135, av. de Rangueil, 31077, Toulouse, FRANCE

julian.carrey@insa-toulouse.fr

Destroying cancer cells using magnetic nanoparticles and magnetic field can be done using two approaches : i) using the heat released by magnetic nanoparticles submitted to a high-frequency alternating magnetic field, a method known as magnetic hyperthermia, or ii) using the mechanical action generated by MNPs submitted to a low-frequency alternating or rotating magnetic field. In this presentation, we will first present an overview of these two approaches, including results from biology, chemistry and physics.

We will then present theoretical results obtained in our group on the conditions to maximize these effects: heating in magnetic hyperthermia and torque amplitude for the other approach. It will be shown that, in both case, a precise control of the size and magnetic properties of the nanoparticles is required. Experimental results obtained in our group permits to validate some of these experimental results, and will also be presented.

References

[1] R. P. Tan, J. Carrey and M. Respaud, Phys. Rev. B. 90, 214412 (2014), https://doi.org/10.1103/PhysRevB.90.214421
[2] J. Carrey and N. Hallali, Phys. Rev. B 94, 184420 (2016), https://doi.org/10.1103/PhysRevB.94.184420
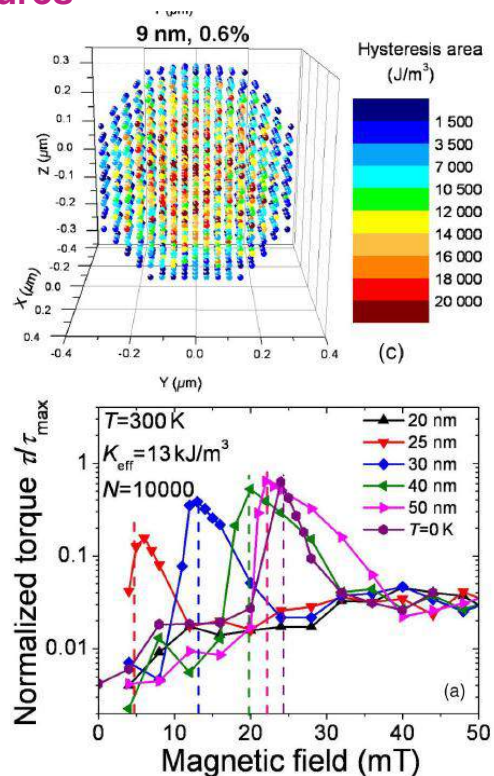
Figures

Figure 1. (up) : Heating power of an assembly of 9 nm MNPs, with a volume concentration of 0.6%, submitted to a high-frequency magnetic field. Each dot represents a MNP. The color scales is related to the heating power of the MNP. It is evidenced that the heating is much stronger in the middle of the assembly than on its periphery. (down) Torque undergone by non-interacting MNPs submitted to a low-frequency rotating magnetic field at room temperature as a function of the MNP diameter. In a given range of magnetic field, the torque is strongly enhanced

Self-assembled nanoclusters of fluorinated quantum dots as delivery platform for enzymes

Carolina Carrillo-Carrion[1],
Mona Atabakhshi-Kashi[2], Mónica Carril[1,3],
Khosro Khajeh[2], Wolfgang J. Parak[1,4]

[1]CIC biomaGUNE, Paseo Miramon 182, 20014 San Sebastian, Spain
[2]Tarbiat Modares University, 14115-175 Tehrān, Iran
[3]Ikerbasque, Basque Foundation for Science, 48011 Bilbao, Spain
[4] Philipps Universität Marburg Renthof 7, 35037 Marburg, Germany

ccarrillo@cicbiomagune.es

Self-assembled nanoparticles are considered as one of the most promising nanosystems to deliver drugs and biological molecules such as enzymes for therapeutic applications [1]. It is well-known that non-covalent hydrophobic interactions play an important role in the organization and stabilization of many types of assembled systems [1]. In particular, fluorine-fluorine interactions have demonstrated to form more stable self-assembled nanostructures [2-4] because such interactions are stronger than other non-covalent bonds due to the unique hydrophobicity and lipophilicity of the fluorine atoms [5]. The favorable interaction between fluorine atoms and proteins has also been a subject of intensive research [6].

Herein, inspired by the role of fluorine in self-assembly and its favorable interaction with proteins, we report a novel delivery platform for enzymes based on self-assembled nanoclusters of fluorinated quantum dots. Nanoclusters of ca. 50 nm diameter were formed by self-assembly of fluorinated quantum dots in aqueous medium through fluorine-fluorine interactions. These nanoclusters were able to encapsulate different enzymes with loading efficiencies ≥ 74 % and the encapsulated enzymes maintain their catalytic activity.
Under acidic environment mimicking the conditions of endosomal/lysosomal compartments, the nanoclusters were slowly disassembled allowing the release of encapsulated enzymes (Figure 1). The effective release of α-galactosidase (*i.e.,* a therapeutic enzyme for the treatment of the Fabry disease) demonstrated the feasibility of this nanoplatform to be used in enzyme replacement therapy for lysosomal storage diseases.

Moreover, the combination of high colloidal stability of these nanoclusters, effective enzyme loading and release, and fluorescence imaging potential make them very promising nanosystems for application in theranostics.

References

[1]   W. Cui, J. Li, G. Decher, Adv. Mater, 28 (2016) 1302.

[2]   S. D. Xiong, L. Li, J. Jiang, L. P. Tong, S. Wu, Z. S. Xu, P. K. Chu, Biomaterials, 31 (2010) 2673.

[3]   H. Wang, Y. Wang, Y. Wang, J. Hu, T. Li, H. Liu, Q. Zhang, Y. Cheng, Angew. Chem., 54 (2010) 11647.

[4]   K. Niikura, N. Iyo, T. Higuchi, T. Nishio, H. Jinnai, N. Fujitani, K. Ijiro, J. Am. Chem. Soc., 134 (2012) 7632.

[5]   V. Percec, M. Glodde, G. Johansson, V. S. K. Balagurusamy, P. A. Heiney, Angew. Chem., 42 (2003) 4338.

[6]   J. Pollock, D. Borkin, G. Lund, T. Purohit, E. Dyguda-Kazimierowicz, J. Grembecka, T. Cierpicki, J. Med. Chem, 58 (2015) 7465.

Figures
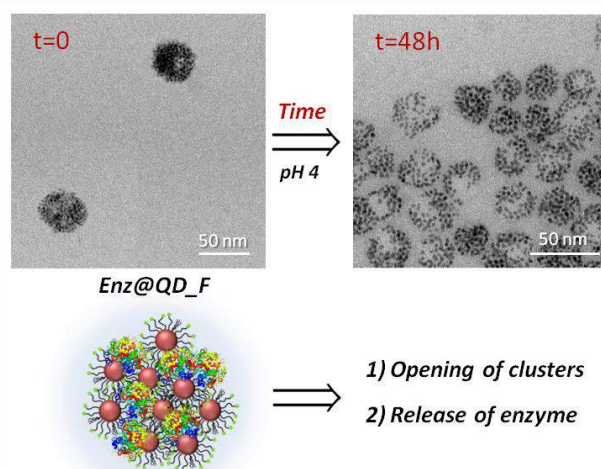
Figure 1. TEM images over time of nanoclusters with enzyme encapsulated (Enz@QD_F) under acidic conditions (acetate buffer 20 mM at pH 4), showing the opening of the nanoclusters which allows the realease of the enzyme.

Microscopic Molecular Foundations of nano particle interactions with living systems

Kenneth A. Dawson,

CBNI - University College Dublin, Ireland

kenneth.a.dawson@cbni.ucd.ie

It has been of interest to find guiding principles to help us understand how nanoscale objects interact with living organisms. Firstly, the nanoscale is unique in biology, and our capacity to engineer on that scale is transformative. The intrinsic machinery of biology is defined and operates on the nanoscale. This means that nanoparticles are also actively transported around cells and biological barriers all unlike small molecules which passively partition into biological compartments (cells, organs, etc.). Secondly, the power of being able to communicate with, and use those endogenous mechanisms of biology is potentially transformative in practical terms.

However, with this enormous potential power to engage with the machinery of organisms there are also challenges. To some degree, the challenge, of this field may have been underestimated, and only now are we beginning to face the need to invest in guiding principles and governing principles the whole arena.

We discuss progress being made in understanding how interactions between nanoscale objects and living organisms occur, and their governing principles. [2, 3] We argue that the future lies in pressing forward to develop a truly microscopic (molecular scale) understanding between the nanoscale and living organisms. [4]

References

[1] Nature nanotechnology, 2012, 7, 779-786
[2] Nature nanotechnology, 2012, 7, 62-68
[3] Nature Nanotechnology, 2015, 10, 472-479
[4] Nature Communications, 2016 (December)

Tapered optical probes and optrodes for optogenetics and neurophotonics

Massimo De Vittorio[1], Ferruccio Pisanello

[1] Center for Biomolecular Nanotechnologies, Istituto Italiano di Tecnologia, Via Barsanti, Arnesano (LE), Italy
[2] Dip. Ingegneria dell'Innovazione, Università del Salento, Via Monteroni, 73100 Lecce (LE), Italy

massimo.devittorio@iit.it

The combination of genetics, photonics, electronics and micromechanics is producing completely new technological approaches for physical and chemical sensors and actuators, which can be disposable, wearable or implantable in humans and animal models. These new approaches are opening the way to closed loop theranostics, i.e. device integrating diagnostic capabilities and therapeutic response.

In optogenetics, opsins, which are light-sensitive proteins, are genetically targeted into specific neurons types in an animal model (typically a mouse), making possible the activation or inhibition of brain neurons by light. The development of new devices to optically interface with the mammalian brain in vivo has represented a revolution for experimental neuroscience, allowing to identify the role of specific population of neurons within specific neural circuits.

Recent advances on technologies for in-vivo optical stimulation and inhibition of neuronal activity in optogenetic experiments will be reported. It will be shown that modal manipulation in tapered optical fibers makes possible an effective and minimally invasive light delivery in the mouse brain either for large brain volume excitation or for selective stimulation of multiple brain regions [1,2]. Nanomachining is also exploited for integrating arrays of microelectrodes and optical windows on tapered optrodes for combined extracellular electrophysiology and optogenetic stimulation.

References

[1] F. Pisanello, L. Sileo, I. A. Oldenburg, M. Pisanello, L. Martiradonna, J. A. Assad, B. L. Sabatini, and M. De Vittorio, "Multipoint-Emitting Optical Fibers for Spatially Addressable In Vivo Optogenetics," *Neuron*, vol. 82, no. 6, pp. 1245–1254, May 2014.

[2] F. Pisanello, G. Mandelbaum, M. Pisanello, I. A. Oldenburg, L. Sileo, J. E. Markowitz, R. E. Peterson, A. Della Patria, T. M. Haynes, M. S. Emara, B. Spagnolo, S. R. Datta, M. De Vittorio, and B. L. Sabatini, "Dynamic illumination of spatially restricted or large brain volumes via a single tapered optical fiber," *Nature Neurosci.*, vol. 20, no. 8, pp. 1180–1188, Jun. 2017.

Figures
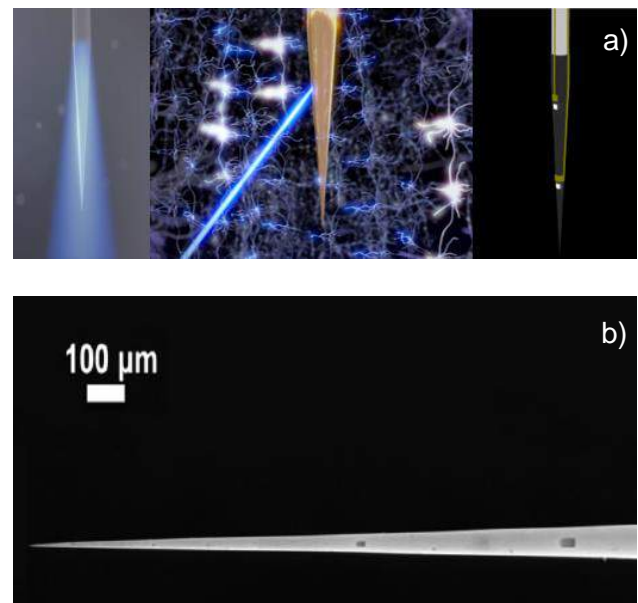
Figure 1. a) Schematics of tapered fibers for broad emission, site selective illumination and optrodes; b) SEM image of a focus ion beam nanomachined tapered fiber (courtesy of OptogeniX srl, www.optogenix.com).

Rational design of new oral peptide nanomedicines

Matilde Durán-Lobato,
María José Alonso

Dept. Of Pharmacy and Pharmaceutical Technology,
CIMUS Research Institute, University of Santiago de
Compostela, 15706 Campus Vida, Santiago de
Compostela, Spain
mariaj.alonso@usc.es

Objective

Injectable peptide and protein therapeutics are the main marketed treatment for important chronic and systemic diseases. Still, up to date they cannot be administered following the fashion that allows for the highest patient compliance: the oral route.

Our group has recently coordinated a large-scale integrating project within the 7th European Framework Programme, TRANS-INT. The overall objective of this consortium was the generation of cutting-edge knowledge on the interaction of nanomaterials with the GI barriers, which will help developing new oral nanomedicines for the treatment of high economic and social impact diseases.

To this aim, the rational design of delivery platforms based on safety, mechanistic, bioengineering and pharmaceutical technology criteria were clear and shared pillars among project partners.

Results

Among other partner labs expert on nanocarrier design, we participated in the design and evaluation of a wide array of nanocarriers, which followed a continuous screening, based on a defined Target Product Profile (TPP). Out of them, the most promising prototypes were optimized and explored for possible incorporation into a solid dosage form, i.e. an enteric capsule. From these, the best performing formulations were further tested for their quality properties after storage as solid dosage form for up to 3 months, under ICH conditions.

Expert partners on *in-vitro/in vivo* evaluation in terms of cytotoxicity and mechanistic issues tested screened prototypes either in the Caco-2 model, isolated human jejunal mucosae or in mouse/rat models. Toxicity assays provided positive information, while the mechanistic issues behind the behaviour of each prototype were widely variable and dependent on their composition. Some nanocarriers were highly distributed and retained along the intestinal mucosa, even reaching the intracellular space in some cases, whereas others were mainly retained in the mucus layer. Overall, a good correlation was found between the data obtained in rodents and in isolated human jejunal mucosae, although this was not always the case when compared with data obtained using the Caco-2 cell model. The lack of mucus in the Caco-2 model was identified as a potential reason for some discrepancies between models.

Finally, selected formulations based on their *in vitro*, *ex vivo* and/or preliminary *in vivo* performance were tested for PD / PK evaluation following intraintestinal injection to anesthetized or fully awake normoglycaemic and hyperglycaemic rats. Overall, among all the prototypes investigated, some of them elicited positive responses, especially in the diabetic rat model. However, there were discrepancies among the data obtained from the different models for the same prototypes. Finally, one prototype could be tested in a large animal model (pig model), and the results from this experiment showed a modest but promising response.

Conclusions

Overall, TRANS-INT provided a highly positive experience, which led to the generation of knowledge that will greatly impact the oral peptide delivery field in terms of the potential of nanotechnology.

Specifically for a pharmaceutical nanotechnology-based research team such as ours, TRANS-INT offered invaluable insight on the cooperation with industry, collaboration with partners' labs from complementary research fields and shared management of a large consortium. Furthermore, it offered the possibility for young PhD students and post-docs to gain relevant skills on medicine development and translation challenges associated, in the frame of a cross-disciplinary and challenging environment.

References

www.trans-int.eu

Grant Agreement Number: NMP4-LA-2012-281035

Design and synthesis of polymeric vectors improving transfection efficiency in gene therapy applications

Carlos Elvira[1], J.A. Redondo[1], D. Velasco[1], E. Martínez-Campos[2], R. Navarro[1], H. Reinecke[1], A. Gallardo[1], G. Corrales[3], A. Pandit[4], A. Fernández-Mayoralas[3].

[1] Department of Applied Macromolecular Chemistry, Institute of Polymer Science and Technology, ICTP-CSIC. Juan de la Cierva 3, 28006 Madrid, Spain.
[2] Institute of Biofunctional Studies (IEB), Tissue Engineering group, (UCM), Associated Unit to the Institute of Polymer Science and Technology (CSIC), Paseo de Juan XXIII 1, 28040 Madrid, Spain
[3] Institute of Organic Chemistry, IQOG-CSIC, Juan de la Cierva 3, 28006 Madrid, Spain
[4] Network of Excellence for Functional Biomaterials, National University of Ireland, Galway, Ireland

celvira@ictp.csic.es

Over recent years, significant efforts have been devoted to the synthesis of new polymeric cationic vectors that could become alternatives to viruses in gene therapy applications [1]. Such alternatives aim to obtain high transfection efficiency, and overcome virus drawbacks, as their potential immune responses in therapeutic settings or their high production costs. Most of the cationic polymeric vectors are polyamines containing secondary and tertiary amino groups that can participate in a phenomenon known as 'proton-sponge' hypothesis for endosomal escape. However, this net positive charge is also one of their main drawbacks, as it is directly associated to their high cytotoxicity. A strategy to modulate the properties and performance of these polyamines lay in their chemical modification with different entities, of differing biological significance, in order to reduce their positive charge.

This type of charge reduction may have consequences for biodistribution, cell-membrane interactions, cytotoxicity, and intracellular release, etc. Most of the chemical modifications reported in the literature are based on chain-end conjugation or post-polymerization functionalization. In previous studies, we have reported on an alternative, bottom-up approach, based on the radical copolymerization of the cationizable methacrylamide N-ethyl pyrrolidine methacrylamide (EPA) monomer [2] with neutral and hydrosoluble co-monomers, such as dimethylacrylamide (DMA) [3] or hydroxypropyl methacrylamide (HPMA) [4]. The statistical copolymers obtained exhibited enhanced cytocompatibility/transfection efficiency-balance compared to pure poly-EPA.

Improving transfection levels can be also achieved by incorporating chemical groups that interacts with the cellular membrane and making easier the cellular internalization of polymer-DNA complexes and consequently higher transfection. In this sense, sugars and cyclodextrines have been reported to interact with the surface of the cell membrane. In a recently published study [5], two complex styrenic structures, derived from the hydroxylated and permethylated forms of the cyclic oligosaccharide β-cyclodextrin (β-CD) [6], were chosen as the neutral co-monomer entities, as well as hydroxylated and permethylated forms of α-glucose [7], that were copolymerized with the cationic EPA monomer.

This communication presents the evolution in the chemical design of cationic polymers based on EPA as non-viral vector starting from EPA homopolymers and telomers (low molecular weight poly-EPA with primary amine chain end functionalization), EPA copolymers with hydrophilic monomers as DMA and HPMA in order to reduce charge density and therefore cytotoxicity, and finally EPA copolymers with monomers bearing non and permethylated α-glucose and β-cyclodextrines respectively, in order to improve cellular internalization.

All the prepared EPA polymer systems have been characterized by the conventional spectroscopic techniques (NMR, FTiR), determined their molecular weight by GPC and ionization constants by titration methods. Polymer-DNA complex formation were carried out at different N/P (polymer/DNA) ratios with the commercial plasmid pCMV-GLuc by using agarose gel electrophoresis, dynamic light scattering (DLS) and Zetamaster system to also determine polyplexes average size and complexes stability. Transfection experiments were performed using the luciferase gene encoded in the pCMV-GLuc plasmid as a reporter gene with mouse Swiss-3T3 fibroblasts and, in some cases, mouse melanoma cells B16 by following cell culture routine procedures. Polymer controls used were poly-lysine and PEI.

In the case of telomers and EPA-DMA copolymers polymer-DNA complexes were found, in most of the cases, to have appropriate sizes (lower than 200 nm). The telomers in all cases exhibited stable particles and higher transfection efficiency with respect to DMA copolymers. These oligomers give an attractive transfection values for serum-sensitive cell lines, which overcomes the limitations associated with the use of highly positively charged polymers.

The EPA-HPMA copolymers, with excess or equimolar amount of EPA, were able to complex DNA forming stable polyplexes with an average size between 50 and 200 nm. Cell viability was shown to depend on the EPA/HPMA molar ratio, exhibiting the equimolar copolymer poly-(EPA-HPMA) 50:50 a full cytocompatibility, similar to the HPMA-rich systems. This copolymer EPA50 has also shown significantly higher transfection levels than the systems with other compositions and the positive controls poly L-lysine (PLL) and poly EPA. This statistical equimolar

copolymer EPA50 has unique properties related to its composition and microstructure, which allows it to complex DNA, showing an excellent biocompatibility and high transfection efficiency.

On the other hand, copolymers of EPA with α-glucose (GLC) and permethylated α-glucose (MeGLC) units were characterized and found to complex DNA at N/P = 2/1 and higher ratios with the exception of GLC70 and MeGLC70, that contained comparatively lower amounts of the cationic EPA co-monomer. Average size, optimal polyplexes (around 200 nm) were found in most systems, with the exception of GLC at high N/P ratios, where sizes exceeded 300 nm. MeGLC copolymer transfection efficiency in Swiss cell line were higher than that of GLC and the MeGLC5 and MGLC10 systems showed also higher transfection efficiency than the PEI and PEPA controls, over all N/P ratios studied. Moreover, the MeGLC35 and MeGLC70 system transfection levels were significantly higher than the results obtained for MeGLC10. This high transfection efficiency is clearly related to the favourable cytocompatibility. MeGLC copolymers with the tumoral B16 cell culture showed very similar transfection results to those with Swiss fibroblasts, but notably MeGLC35 and MeGLC70 were found to be more toxic against the tumoral cell line.

Finally, we have observed that pendant hydroxylated or permethylated β-CD moieties distributed along the macromolecular poly (EPA-XCDSt) chains (where X = H or Me) influences in a strong and very dissimilar way the interaction with DNA and the performance of the polyplexes as gene carriers due to a different microstructure. Permethylated pendant MeCDs were found to decrease the complexation ability of the polycation in a composition-dependent manner, whereas hydroxylated moieties do not interfere. The permethylated structures were more cytocompatible even at high N/P ratios, which suggest that they confer complete cytocompatibility to the cationic polymer, and in terms of transfection efficiency the permethylated systems MeCD10 (Figure 1) showed significantly higher efficiency than the positive control PEPA, and similar to or higher than PEI, even at the highest N/P ratios studied. It is noteworthy that the results were found to be similar for the two cell lines tested (fibroblastic and melanoma), which indicates that the effect of the permethylation is not specific of a cell line. Cellular internalization analysis with fluorescent copolymers (Figure 1) was also studied showing proper polyplex internalization for the MeCD systems, but not for the hydroxylated poplyplexes.

As conclusion polymers chemical functionalization incorporating hydrophilic moieties and permethylated sugars or cyclodextrines improves transfection efficiency and cytocompatibility of poly-EPA based non-viral gene vectors.

Figures
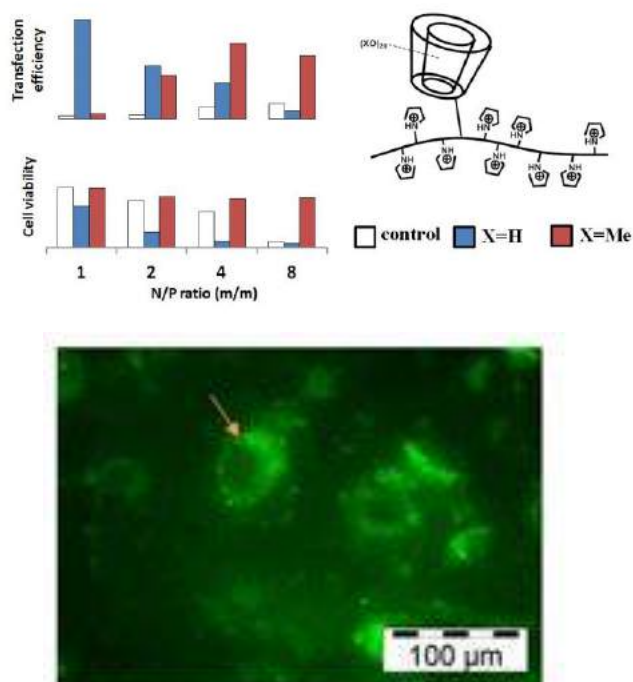
Figure 1. Transfection efficiency and cell viability versus N/P ratios for the EPA-CD10 and EPA-MeCD10 permethylated copolymers and poly-EPA control (upper Figure). EPA-MeCD10 (permethylated) with fluorescent linked group. Transfection at 24 h, showing a strong signal into cell cytoplasm (lower Figure).

References
[1] S.Y. Wong, J.M. Pelet, D. Putnam, Prog. Polym. Sci. 32 (2007) 799-837.
[2] D. Velasco, C. Elvira, J. San Román, J Mater Sci: Mater. Med. 19 (2008) 1453–1458.
[3] D. Velasco, E. Collin, J. San Román, A. Pandit, C. Elvira, European J. Pharmaceutics and Biopharmaceutics 79 (2011) 485–494.
[4] J. A. Redondo, D. Velasco, M. Pérez-Perrino, H. Reinecke, A. Gallardo, A. Pandit, C. Elvira. European J. Pharmaceutics and Biopharmaceutics 90 (2015) 38-43.
[5] J. A. Redondo, E. Martínez-Campos, R. Navarro, A. Pandit, H. Reinecke, A. Gallardo, J. L. López-Lacomba, C. Elvira. European J. Pharmaceutics and Biopharmaceutics, 93 (2015) 303-310.
[6] J. A. Redondo, E. Martínez-Campos, L. Plet, M. Pérez-Perrino, R. Navarro, G. Corrales, A. Pandit, H. Reinecke, A. Gallardo, J. L. López-Lacomba, A. Fernández-Mayoralas, C. Elvira, Macromol. Rapid Comm., 37 (2016) 575-583.
[7] J. A. Redondo, E. Martínez-Campos, M. Pérez-Perrino, R. Navarro, H. Reinecke, A. Gallardo, G. Corrales, A. Fernández-Mayoralas, C. Elvira, European J. Pharmaceutics and Biopharmaceutics, 117 (2017) 68-76.

Impact of multicomponent nano-vaccine on immune modulation against solid tumors

Helena F Florindo[1], E. Zupančič[1,2], V. Sainz[1], L. Moura[1], C. Curato[2], E. Yeini[3], S. Jung[2], Ronit Satchi-Fainaro[3]

[1]Research Institute for Medicines (iMed.ULisboa), Faculty of Pharmacy, Universidade de Lisboa, Lisbon, Portugal.
[2] Department of Immunology, The Weizmann Institute of Science, Rehovot, Israel
[3]Department of Physiology and Pharmacology, Sackler Faculty of Medicine, Tel Aviv University, Tel Aviv, Israel

hflorindo@ff.ul.pt

Immunotherapeutic approaches, in particular cancer vaccines, are between the most promising but also challenging alternative cancer treatments. Cancer vaccines, in comparison to other immunotherapeutic approaches, have the ability to trigger a memory immune response against cells presenting those antigens. Dendritic cell (DC) targeting has been used as a promising strategy for the development of vaccines and immune modulation [1]. Several studies have shown that aliphatic polyester-based biodegradable nanoparticles (NP) are potential vaccine delivery systems for cancer and infectious diseases, being suitable platforms for immune modulation [2].

We have developed different biodegradable aliphatic-polyester (poly(lactic-co-glycolic acid) (PLGA) NP with multiple combinations of tumor antigens, immune regulators (Toll-like receptor ligands (TLRI), and/or siRNA) to target complementary tumor progression-related pathways. We prepared mannose-grafted polymeric NP and hyaluronic acid-coated NP to deliver payloads to antigen-presenting cells (APC), such as DC and tumor cells, respectively. It involved the optimization of particle production parameters (size, surface charge, loading capacity, release profile), biodistribution profiles and *in vivo* immune therapeutic efficacy. Of particular interest was the elucidation of the effect of particle composition, surface properties and targeting ligands on immune cell activation and functionality, both *in vitro* and *in vivo*, using wild-type and solid cancer animal models (melanoma and breast carcinoma).

DC in the lymph nodes (LN) of animals immunized with our nanovaccine expressed significantly higher levels of the co-stimulatory molecule CD86 and MHCI. In addition, higher expression of the activation markers CD86, MHCI, MHCII, and CD80 was found on the surface of DC with internalized NP compared to DC that did not internalize those NP (Figure 1) [3]. Next, it was observed an increase secretion of IL-12 and IL-1β by those DC (Figure 2). These NP induced the most prominent long-lasting effector memory Cytotoxic T Lymphocytes (CTL),

even 8 weeks after a single immunization with the nanoparticulate vaccine entrapping the combination of antigen and the TLRI, suggesting an efficient cross-presentation and cross-priming that led to a broad and effective immune response pivotal for tumor rejections.

In melanoma and breast murine models, our nanovaccine demonstrated to significantly decrease tumor growth rate, especially when a combination of tumor-associated antigens and TLRI, with siRNA regulators or α-GalactosylCeramide (Natural killer T (iNKT) cell agonist), were delivered by a single NP. Our data reveals the impact of NP surface properties/composition on the type of immune response and overall anti-tumor effect. This deeper understanding on the NP-immune cell crosstalk can guide the rational development of nano-immunotherapeutic systems with improved and specific anti-tumor efficacy and safety, while avoiding off-target effects.
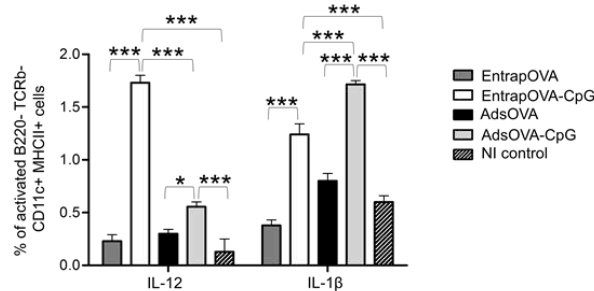
References

[1] Conniot J, et al., Front in Chemistry, 2 (2014) 1-27.
[2] Silva JM et al, J Control Release, 198 (2015) 91-103.
[3] Zupančič E et al, J Control Release 258 (2017) 182-195.

Figures
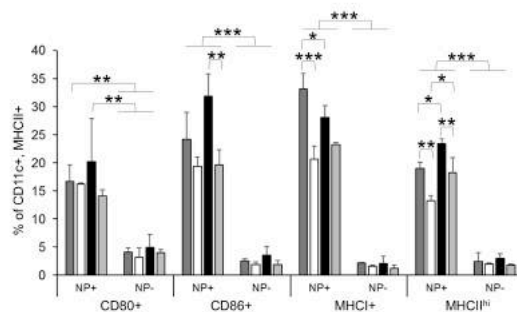
Figure 1. Expression of surface activation markers on DC, with and without internalized NP, in the same lymph nodes (LN), 16 h after immunization with different NP formulations. * p < 0.05; ** p < 0.01; *** p < 0.001.

Figure 2. Flow cytometry analysis of IL-12- and IL-1β-secreting DC in vivo (gated: B220-, TCRβ-, CD11c+, MHCII+) 16 h p.i. with different NP formulations (EntrapOVA: ovalbumin (OVA)-entrapped NP; EntrapOVA-CpG: OVA and CpG co-entrapped NP; AdsOVA: OVA adsorbed onto NP surface; AdsOVA-CpG: OVA adsorbed onto CpG-loaded NP). * p < 0.05; *** p < 0.001.

Multiscale Approach for Water at Bio-Nano Interfaces

Giancarlo Franzese

Secció de Física Estadística i Interdisciplinària–Departament de Física de la Matèria Condensada, & Institute of Nanoscience and Nanotechnology (IN2UB), Universitat de Barcelona, Marti i Franques 1, 08028 Barcelona, Spain

gfranzese@ub.edu

I will present recent simulations and theoretical results about the dynamics and structure of water at bio-interfaces (proteins and bio-membranes) and nano-interfaces (nanoparticles and graphene sheets). By all-atoms simulations I will analyze how hydrophobic and hydrophilic interfaces affect the properties of the vicinal water [1-3] and we will use the results in a multi scale approach to develop the Many-Body Model (MBM) for water [4,5] that allow us to extend our investigations to timescales and length-scales that would be unreachable in atomistic simulations [6,7]. We will consider applications to protein folding [8] and design [9], and self-assembly of nanoparticles-protein-corona [10].

References

[1] F. Martelli, H.-Y. Ko, C. Calero, and G. Franzese, Structural properties of water confined by phospholipid membranes, Frontiers of Physics 13, 136801 (2017).

[2] J. Martí, C. Calero, and G. Franzese, Structure and dynamics of water at carbon-based interfaces, Entropy 19, 135 (2017).

[3] C. Calero, H. E. Stanley and G. Franzese. Structural Interpretation of the Large Slowdown of Water Dynamics at Stacked Phospholipid Membranes for Decreasing Hydration Level: All-Atom Molecular Dynamics. Materials, 9, 319 (2016).

[4] V. Bianco, and G. Franzese, Critical behavior of a water monolayer under hydrophobic confinement, Scientific Reports 4, 4440 (2014).

[5] L. E. Coronas, V. Bianco, A. Zantop, and G. Franzese, Liquid-Liquid Critical Point in 3D Many-Body Water Model, arXiv:1610.00419 (2016).

[6] F. de los Santos, and G. Franzese, Relations between the diffusion anomaly and cooperative rearranging regions in a hydrophobically nanoconfined water monolayer, Physical Review E, 85, 010602(R) (2012).

[7] M. G. Mazza, K. Stokely, S. E. Pagnotta, F. Bruni, H. E. Stanley, and G. Franzese, More than one dynamic crossover in protein hydration water, Proceedings of the National Academy of Sciences of the USA 108, 19873 (2011).

[8] V. Bianco, and G. Franzese, Contribution of Water to Pressure and Cold Denaturation of Proteins, Physical Review Letters 115, 108101 (2015).

[9] V. Bianco, G. Franzese, C. Dellago, and I. Coluzza, Role of water in the selection of stable proteins at ambient and extreme thermodynamic conditions, Physical Review X, accepted (2017).

[10] O. Vilanova, J. J. Mittag, P. M. Kelly, S. Milani, K. A. Dawson, J. O. Rädler and G. Franzese, Understanding the Kinetics of Protein − Nanoparticle Corona Formation, ACS Nano 10, 10842 (2016).

Detection and characterization of nanoparticles in biological systems via stimuli-induced heating

Christoph Geers[1],
Lukas Steinmetz[1], Ana Milosevic[1], Barbara Rothen-Rutishauser[1], Alke Petri-Fink[1,2]

[1]Adolphe Merkle Institute, Chemin des Verdiers 4, Fribourg, Switzerland
[2]University of Fribourg – Chemistry Department, Chemin du Musée 9, Fribourg, Switzerland

christoph.geers@unifr.ch

One of the main challenges for the translation of nanomedicine is the complex analysis to predict behavior and fate of nanoparticles (NPs) in physiological environments (e.g. blood, cells, tissue). Phenomena like NP aggregation or dissolution render NP detection and analysis challenging in particular since typically used analytical methods have limitations:

Fluorescent microscopy, e.g. requires labelling of the NPs with fluorescent dyes, which can change the properties and behavior of NPs[1]. Other methods used to detect and quantify NPs or analyze their size, size distribution, and colloidal state in complex biological environments like *electron microscopy, dynamic light scattering* or *inductively coupled plasma mass or optical emission spectrometry* (ICP-MS/ICP-OES), require substantial sample preparation, are lacking spatial information, only analyze a small portion of the sample, or chemically digest the NPs for their quantification. *Darkfield hyperspectral imaging* is a very promising method for the analysis of NPs and their colloidal behaviour. However, when measuring NPs in complex fluids (i.e. protein crowded) or *in vitro* the method reaches its limitations quite rapidly, due to a large amount of parameters that can influence the recorded spectra[2].

A number of NPs have the ability to produce heat upon external stimulation (e.g. Magnetic NPs upon stimulation by an alternating magnetic field)[3], plasmonic NPs (e.g. gold (Au) NPs, silver (Ag) NPs) by absorbing and scattering light[4], or upon other mechanisms (e.g. carbon nanotubes)[5].

In this talk I will present a new technique based on lock-in-thermography (LIT) to measure and quantify the heat produced by NPs upon light stimulation. This heat can be recorded with an infrared camera and is processed by a specially developed LIT algorithm to yield 2D-images for detection of NPs and analysis of their properties (e.g. aggregation, dissolution).

This set-up allows very fast and accurate detection of NPs e.g. in biological environments like physiological fluids, cells or even tissues without requiring complicated sample preparation.

References

[1] L. Rodriguez-Lorenzo, K. Fytianos, F. Blank, C. Von Garnier, B. Rothen-Rutishauser, and A. Petri-Fink, "Fluorescence-encoded gold nanoparticles: Library design and modulation of cellular uptake into dendritic cells," *Small*, vol. 10, no. 7, pp. 1341–1350, 2014.

[2] G. A. Roth, S. Tahiliani, N. M. Neu-Baker, and S. A. Brenner, "Hyperspectral microscopy as an analytical tool for nanomaterials," *WIREs Nanomed Nanobiotechnol*, vol. 7, pp. 565–579, 2015.

[3] C. A. Monnier *et al.*, "A lock-in-based method to examine the thermal signatures of magnetic nanoparticles in the liquid, solid and aggregated states," *Nanoscale*, vol. 8, no. 27, pp. 13321–13332, 2016.

[4] K. Jiang, D. A. Smith, and A. Pinchuk, "Size-Dependent Photothermal Conversion Efficiencies of Plasmonically Heated Gold Nanoparticles," *J. Phys. Chem. C*, vol. 117, pp. 27073–27080, 2013.

[5] R. Singh and S. V Torti, "Carbon nanotubes in hyperthermia therapy," *Adv. Drug Deliv. Rev.*, vol. 65, no. 15, pp. 2045–2060, 2013.
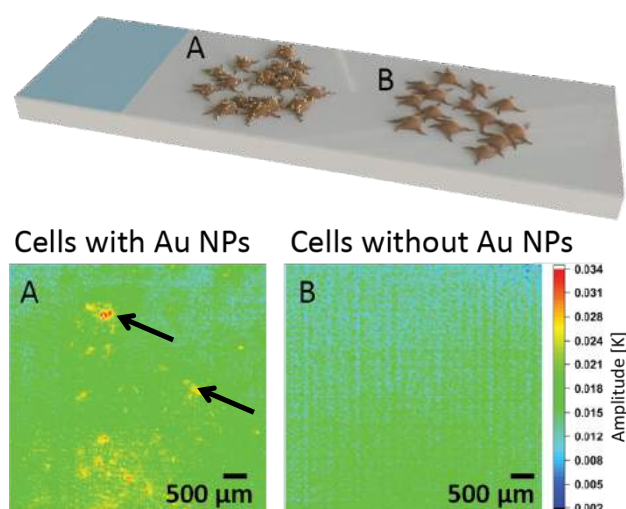
Figures

Figure 1. LIT measurement of cells with Au NPs (A) and without NPs (B). The red and yellow dots show NP accumulations in cells (see black arrows).

Nanoparticle based analysis of biomolecules, cells and tissue

Duncan Graham

Department of Pure and Applied Chemistry, University of Strathclyde, Glasgow, G1 1RD

Duncan.graham@strath.ac.uk

We are interested in the optical properties of metal nanoparticles and their potential application in a range of different biological studies. We can make use of the optical properties of nanoparticles in two ways.

1. The nanoparticle can act as an extrinsic label for a specific biomolecular target. The advantage of using the nanoparticle is its optical brightness and the lack of background vibrational signals.[1]

2. Nanoparticles can be designed to contain a specific recognition probe designed to cause a change in the aggregation status of the nanoparticles resulting in a discernible optical change when it interacts with its biomolecular target.[2]

To demonstrate the applicability of the two different approaches examples will be given on the use of nanoparticles for cell imaging in two and three-dimensions, imaging of nanoparticles in tissue and also their ability to report on biological molecules in vitro and in vivo.

References

[1] McQueenie, R., Stevenson, R., Benson, R., MacRitchie, N., McInnes, I., Maffia, P., Faulds, K., Graham, D., Brewer, J., Garside, P G.,
Detection of Inflammation In-Vivo by Surface-Enhanced Raman Scattering Provides Higher Sensitivity Than Conventional Fluorescence Imaging
Anal. Chem. 84, 14, 5968-5975, (2012)

[2] Guerrini, L., Graham, D.
Molecularly-mediated assembly strategies of plasmonic nanoparticles for Surface-enhanced Raman spectroscopy applications
Chem. Soc. Rev., 41 (21), 7085 – 7107, (2012).

Figures
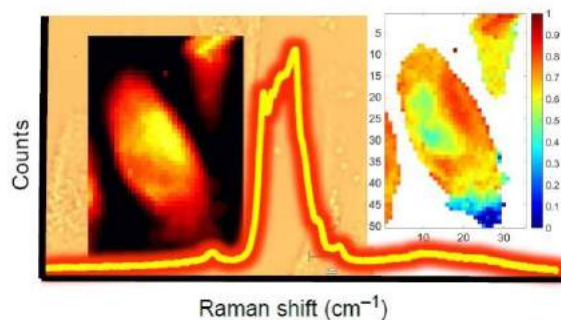
Figure 1. 2D Raman heat map of a cancer cell showing the lipid distribution

Biosafety of mesoporous silica nanoparticles

Yannick Guari[1],
Estelle Rascol,[1] Christophe Dorandeu,[1] Joël Chopineau,[1] Jean-Marie Devoisselle,[1] Clarence Charnay,[1] Cedric Pisani,[2] Jean-Claude Gaillard,[2] Jean Armengaud,[2] Odette Prat,[2] Marie Maynadier,[3] Magali Gary-Bobo,[3] Marcel Garcia[3]

[1]ICGM, Place E. Bataillon, Montpellier, France
[2]CEA-BIAM, Site de Marcoule, Bagnols-sur-Cèze, France
[3]NanoMedSyn, Avenue Charles Flahault, Montpellier, France

yannick.guari@umontpellier.fr

Numerous recent publications show that mesoporous silica Nps are presented on account of their sophisticated design and mode of action. Thanks to the silica chemistry, these Nps promise as new-generation smart drug nanocontainers due to their high stability, large surface areas, tunable pore sizes, and abundant surface functionalization sites. [1], [2]

Understanding the interactions of Nps with biological systems is clearly multidimensional. Nps display different shape, size, and can be decorated with a variety of functionality. Nps have increased surface area to volume ratios that dramatically increase their reactivity. The surface reactivity of Nps can, depending on the type of coating, cause different behavior and toxicological profile. In addition, the miniaturization of materials to the nanoscale has seen emergent properties due to their ultra-large surface, which have not been characterized before. Careful analysis of any new nanomedicine device or disposal should be undertaken to completely characterize the new product before application so that we can help avoid any unintended side effects.

Nps are generally covered by different layer depending on the desired function. A number of publications demonstrate that a PEO (polyethylene oxide) corona have several advantages like colloidal stability, inertia in biological media and higher circulation time of NPs. Moreover, this PEO grafting or coating can be easily applied to inorganic Nps. The presence of PEO creates a steric barrier enabling proteins to be adsorbed at the NPs surface. But whatever the efficiency of such functionalization, NPs are finally cleared from the circulation and taken-up by the reticulo-endothelial system. Another strategy consists in the deposition of a phospholipid bilayer at the inorganic Nps surface in order to create a biomimetic surface. Fusion of liposomes to a spherical, high-surface-area, nanoporous silica core improves capacity, selectivity and stability of NPs and enables their targeted delivery and controlled release within the targeted cells. Combinations of surface decoration are now described leading to high sophisticated nanocarriers that combines stealth property, imaging, targeting and controlled or triggered release.

There are an increasing number of nanotechnology-based drugs and we can anticipate that regulatory authorities might adapt the approval process for nanomedicine products due to safety concerns and e.g. request a more rigorous testing of the potential toxicity of Nps. *In vitro* studies at the molecular and cellular level allow for rapid knowledge generation before connecting to validate toxicological outcome *in vivo*. This approach could limit the extent, volume, and cost of animal testing. Actually, the challenge of the silica nanoparticles use as drug delivery systems lies on overcoming one major breakthrough, which is the lack of data on the toxicological profile of coated and non-coated silica Nps.

In this context, we proposed to study the influence of different functionalized mesoporous silica Nps (Fig. 1) [3] on the cellular uptake and in vivo behaviour.[4] The use of magnetic nanoparticles allows to efficiently separate the MSN from cell cultures with a simple magnet.[5] Our interest focused on the mechanism of interaction with model membranes, the adsorption of proteins in biological fluid (Fig. 2),[6] the quantification of uptake and the effect of such Nps on the transcriptomic profile of hepatic cells[7] that are known to be readily concerned by the Nps uptake *in vivo* especially in the case of an intravenous injection.

References

[1] J. Liu, S. Z. Qiao, Q. H. Hu, G. Q. Lu *Small* **2011**, 7, 425-443.

[2] M. Perrier, M. Gary-Bobo, L. Lartigue, D. Brevet, A. Morère, M. Garcia, P. Maillard, L. Raehm, Y. Guari, J. Larionova, J.-O. Durand, O. Mongin, M. Blanchard-Desce *J. Nanopart. Res.* **2013**, *15*, 1602-9.

[3] J. L. Nyalosaso, E. Rascol, C. Pisani, C. Dorandeu, X. Dumail, M. Maynadier, M. Gary-Bobo, J. Lai Kee Him, P. Bron, M. Garcia, J. M. Devoisselle, O. Prat, Y. Guari, C. Charnay, J. Chopineau *RSC Adv.* **2016**, *6*, 57275-57283.

[4] E. Rascol, M. Daurat, A. Da Silva, M. Maynadier, C. Dorandeu, C. Charnay, M. Garcia, J. Lai Kee Him, P. Bron, M. Auffan, W. Liu, B. Angeletti, J. M. Devoisselle, Y. Guari, M. Gary-Bobo, J. Chopineau *Nanomaterials*, **2017**, *7*, 162.

[5] C. Pisani, J. Gaillard, C. Dorandeu, C. Charnay, Y. Guari, J. C. chopineau, J. Devoisselle, J. Armengaud and O. Prat, *Nanoscale*, **2017**, *9*, 5769-5772

[6] C. Pisani, J.-C. Gaillard, M. Odorico, J. Nyalosaso, C. Charnay, Y. Guari, J. C. Chopineau, J.-M. Devoisselle, J. Armengaud, O. Prat *Nanoscale* **2017** *9*, 1840-1851.

[7] C. Pisani, E. Rascol, Ch. Dorandeu, J.-C. Gaillard, C. Charnay, Y. Guari, J. Chopineau, J. Armengaud, J.-M. Devoiselle, O. Prat *PLOS One* **2017**, 12(8), e0182906.

Figures

Figure 1. Magnetic Mesoporous Silica Nanoparticles nude (A), pegylated (B) and covered with a lipidic bilayer (C)

Figure 2. Representation of the corona interactome. Protein–protein interactions are represented in a network developed using the NetworkAnalyst software, based on InnateDB. The target represents the time scale (0.5 min to 7 days). Each protein (represented by its gene symbol) is placed according to its time of appearance within the corona. The colors symbolize the cluster membership. The grey lines represent the protein–protein interactions. Proteins that have a lot of interactions with other proteins are represented by a larger visual cue.

In vivo biomolecule corona onto clinically used blood circulating liposomes

Marilena Hadjidemetriou

Nanomedicine Lab
Faculty of Biology, Medicine & Health
The University of Manchester
Manchester M13 9PT, United Kingdom

marilena.hadjidemetriou@manchester.ac.uk

The adsorption of proteins and their layering onto nanoparticle surfaces, once in contact with biological fluids, has been termed the 'protein corona' and has been postulated as a determinant factor for their pharmacological, toxicological and therapeutic profile [1]. In our recent studies, we developed a protocol to investigate for the first time *in vivo* protein corona formation and its evolution onto clinically-used liposomes after their recovery from the blood circulation of mice [2, 3]. Overall, even though the total amount of protein adsorbed onto circulating liposomes *in vivo* was comparable with that observed from *ex vivo* incubations, the protein species that self-assembled onto the liposomes *in vivo* were considerably more, leading to a molecularly 'richer' protein corona (**Figure 1**).

Although *in vivo* models can significantly improve our understanding of protein corona formation under a more realistic setting, there is currently no published evidence of the existence of protein corona forming in humans *in vivo*. We will report for the first time our results from a clinical trial in collaboration Manchester Cancer Research Centre to thoroughly characterise the formation of *in vivo* protein corona in human patients injected with PEGylated, doxorubicin-encapsulated liposomes.

In addition, our studies explore the potential exploitation of *in vivo* protein corona to comprehensively analyse the blood circulatory proteome and facilitate thus the detection of previously unknown disease-specific molecules (**Figure 2**). Our results demonstrate, that liposomes are able to scavenge the blood pool of tumor-bearing mice and human patients and capture low molecular weight, low abundant plasma proteins that cannot be detected by plasma proteomic analysis.

We propose the use of clinically used nanoparticles (liposomes) as a platform to scavenge the blood pool for cancer biomarkers.

References

[1] M.Hadjidemetriou & K.Kostarelos, Nature Nanotechnology, 2017, 12, 288–290.
[2] M. Hadjidemetriou, Z. Al-Ahmady, M. Mazza, R. F. Collins, K. Dawson, K. Kostarelos, ACS Nano, 2015, 9, 8142.
[3] M. Hadjidemetriou, Z. Al-Ahmady, K. Kostarelos, Nanoscale 2016, 8, 6948-57.

Figures
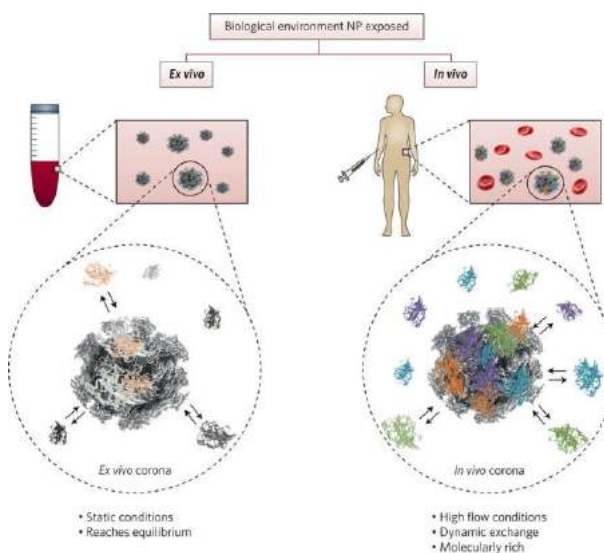
Figure 1. The main differences between the protein coronas formed on NPs after their incubation in plasma or administration in living organisms are illustrated. In a static *ex vivo* environment the protein corona rapidly adsorbs onto NPs and reaches equilibrium. *In vivo*, a molecularly richer protein corona is formed in flowing conditions within the blood circulation and by the dynamic exchange of proteins, it evolves over time.
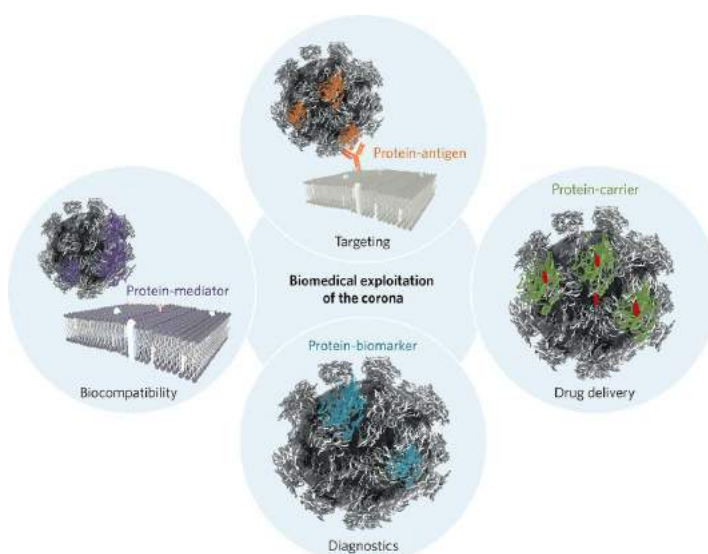
Figure 2. Potential exploitation of the biomolecule corona for improved NP biocompatibility and toxicity; cell targeting; increased drug payload NP capacity; and disease detection.

Development of novel antimicrobial agents for several applications

Zvi Hayouka,

Institute of Biochemistry, Food Science and Nutrition, The Hebrew University of Jerusalem, Rehovot, 76100, Israel

zvi.hayouka@mail.huji.ac.il

Pathogenic infections represent a persistent threat to human health. The rapid development of resistance to drug therapies creates a continuing need for developing new anti-infective agents. Host-Defense Peptides (HDPs) represent a potential source of inspiration for development of new antibacterial agents. HDPs are peptides naturally secreted by a variety of multicellular organisms as a protective mechanism from environmental influence, predators, or other threats to their survival. HDPs display a characteristic selectivity, favoring attack on prokaryotic membranes relative to eukaryotic membranes. This selectivity is thought to arise from the net cationic charge common to HDPs, since the external surfaces of prokaryotic cells typically have a larger net negative charge than do the external surfaces of eukaryotic cells. HDPs are rich in hydrophobic residues, which presumably mediate disruptive interactions with the hydrophobic interior of a lipid bilayer. The molecular diversity among HDPs in terms of sequences and structures is very broad. In my research we seek to understand if the specific sequences of the HDPs are crucial for their activity. To address this question, we employed solid-phase peptide synthesis in an unconventional way to generate peptide mixtures that contain one type of hydrophobic residue and one type of cationic residue. Each mixture was random in terms of sequence, but highly controlled in terms of chain length and stereochemistry. We showed that these compounds were highly active towards many types of bacteria and also were able to degraded bacterial biofilm structure [1, 2]. Recently, we showed that random peptide mixture that contain natural amino acids assemble into antimicrobial pores and also were hemolytic. By contrast, the peptide mixture that were generated with natural and non- natural amino acids attack bacterial membranes without forming visible pores. The results offer a mechanistic rationale for designing membrane-selective and amino acid sequence-independent antimicrobials [3].

References

[1] Hayouka, Z. Chakraborty, S. Liu, R. Gellman, H.S. J. Am. Chem. Soc. 2013, 135(32):11748-5.

[2] Stern, T.; Zelinger, E.; Hayouka, Z. Chem Commun (Camb) 2016, 52, 7102-7105.

[3] Hayouka Z, Bella A, Stern T, Ray S, Jiang H, Grovenor CRM, Ryadnov MG., Angew Chem Int Ed Engl. 2017, 6(28):8099-8103

Synergistic role of nanoceria on the ability of tobacco-smoke to induce carcinogenic hallmarks in lung epithelial cells

Alba Hernández[1,2],
Laura Rubio[1], Jordi Bach[1], Ricard Marcos[1,2]

[1]Grup de Mutagènesi, Departament de Genètica i de Microbiologia, Facultat de Biociències, Universitat Autònoma de Barcelona, Bellaterra, Spain
[2]CIBER Epidemiología y Salud Pública, ISCIII, Spain

alba.hernandez@uab.cat

The availability of Cerium as one of the most abundant rare earth oxides has prompted research on the synthesis and development of functional ceria nanoparticles. As a result, Cerium dioxide nanoparticles (CeO_2NP, nanoceria) are being increasingly used in a variety of industrial and commercial applications, as reviewed [1]. The inevitable increase in consumer and occupational exposures raises the need for a comprehensive toxicological characterization of nanoceria. Noteworthy, several companies and organizations have already identified nanoceria as a high priority material for toxicological evaluations [2]. Due to its demonstrated antioxidant properties, Nanoceria have been also proposed as a new promising agent in the treatment of diseases related with increasing levels of reactive oxygen species (ROS) [3], even as an antitumoral agent, since it is known that ROS contribute to cell transformation. However, several biosafety concerns need to be solved before this nanomaterial can be applied in biomedical applications with security, as i.e. there is no available data on the associated toxicological effects under realistic long-term exposure and co-exposure scenarios [4].

For all the above mentioned reasons, this work aim to evaluate the transforming effects of long-term exposure to nanoceria in lung epithelial BEAS-2B cells, along with the effects associated to a common plausible tobacco co-exposure. Thus, BEAS-2B cells continuously exposed to 2.5 µg/mL of nanoceria alone or in combination with 1 and 5 µg/mL of tobacco smoke condensate (CSC) for up to 6 weeks were monitored for intrinsic and extrinsic changes associated with the acquisition of an oncogenic phenotype. Alterations in cellular morphology, growth and differentiation status were measured through the exposure, matrix metalloproteinase (MMP) activities were measured by zymmography, colony formation and promotion were measured by soft agar assay, and cellular migration capacity was evaluated by wound healing assay.

Results evidence no transforming ability of nanoceria in exposed BEAS-2B cells. However, results support a synergistic role of nanoceria on CSC transforming ability, as cells co-exposed to nanoceria plus CSC, when compared to cells exposed to CSC alone, showed a more noticeable spindle-like phenotype, an increased proliferation rate, higher degree of differentiation status dysregulation, higher migration capacity, increased anchorage-independent cell growth and a secretome with higher levels of MMP 9 and cell growth promoting capability. When mRNA expression of FRA-1 was evaluated as a mechanism of tobacco-induced transformation, nanoceria co-exposure was again found to exacerbate the observed expression changes.

Our results highlight the need to study nanomaterials under mixed exposure scenarios likely to be found in the environment and/or at working place.

References

[1] Reed K, Cormack A, Kulkarni A, Mayton M, Sayle D, Klaessig F, Stadler B, Environ Sci Nano 1 (2014) 390-405.

[2] Organisation for Economic Co-operation and Development, Series on the safety of manufactured nanomaterials, Number 27 (2010) ENV/JM/MONO(2010)46

[3] Narayanan KB, Park HH, Adv Colloid Interface Sci 201-202 (2013) 30-42

[4] Yokel RA, Hussain S, Garantziotis S, Demokritou P, Castranova V, Cassee FR, Environ Sci Nano, 1 (2014) 406-28

Figures
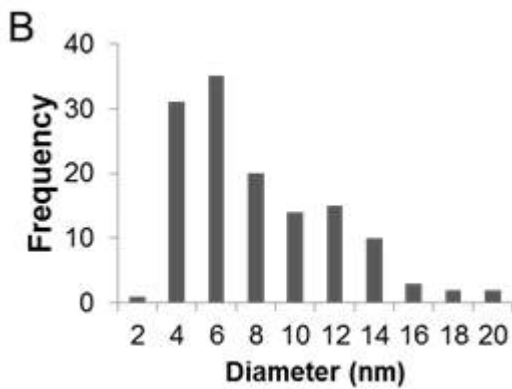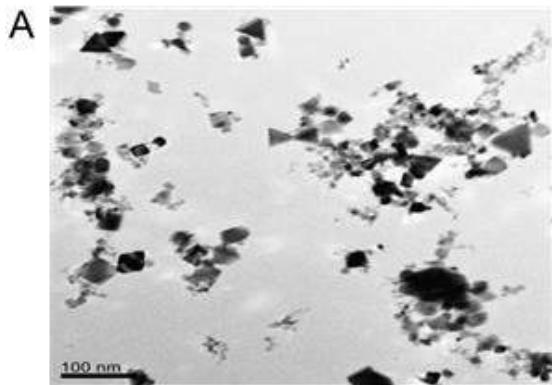
DLS, Average diameter: 93.17 ±5.10
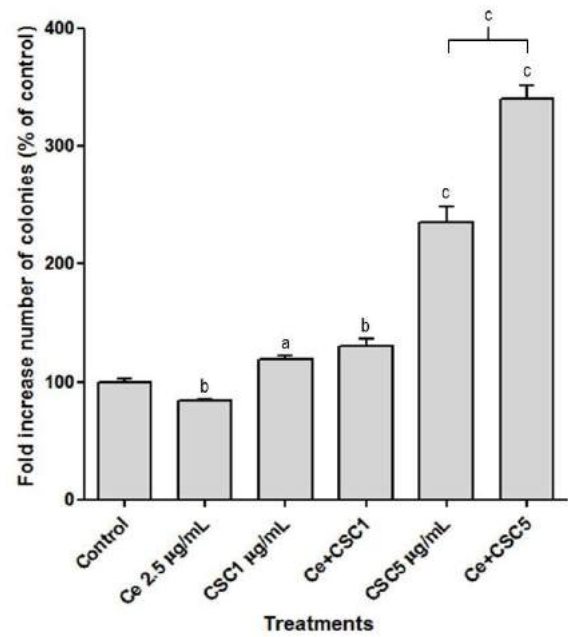DLS, PDI:0.562±0.029
LDV, Zeta potential:-10.6±1.3

Figure 2. Anchorage-independent cell growth capacity of BEAS-2B cells after 6 weeks of nanoceria and/or CSC exposure. Cells exposed to Ce+CSC1, CSC5 and Ce+CSC5 showed higher capacity to grow in soft-agar. Data are presented as mean values with time-matched controls set to 100% (n=3); error bars represent standard error of the mean; [a]$P<0.05$, [b]$P<0.01$, [c]$P<0.001$ compared with time-matched controls or between treatments, as indicated.

Figure 1. (A) TEM image of CeO_2-NP in pristine form. (B) Size distribution of CeO_2-NP over 100 particles showing an average of 9.52 ± 0.66 nm diameter; CeO_2-NP average size and charge in exposure medium by pre-wetting with 0.5% volume and steric stabilization using sterile-filtered 0.05% w/v BSA. Data represented as mean ± SEM.

General-purpose, functionalized poly-L-lysine polymers as bio-sensing layers, and their use in DNA detection

Jurriaan Huskens,
Jacopo Movilli, Salmeen Choudhury, Sander Koeman, Daniele di Iorio, Almudena Marti

University of Twente, MESA+ Institute for Nanotechnology, Enschede, The Netherlands

j.huskens@utwente.nl

Designing a biosensor needs to comply with several requirements. Its application, the specific analyte, the sample medium, and the desired physical signal determine the materials and molecules that constitute the bioreceptor and the transducer to form a properly functioning device. In particular the receptor and the transducer work synergistically to form a so-called "functional biointerface", where the recognition event takes place and is translated into a measurable signal. The functional biointerface is the core of the biosensor, affecting its overall sensitivity, selectivity and efficiency. Thus, controlling the physical and chemical properties of the biointerface will determine the performance of the whole sensing device. Thiol-based monolayers, EDC/NHS coupling chemistry, and silane-based chemistry are well known procedures to immobilize biomolecules on surfaces, but drawbacks exist in chemical instability, materials specificity, and others. Here, we present a new, quick method for surface modification based on functionalized poly-L-lysine (PLL) [1-3]. Due to its electrostatic interaction and the possibility of its easy functionalization with a large variety of functional groups, modified PLLs provide an interesting approach to develop biosensors, because the properties of the surface (such as the type of functional group, antifouling behavior and probe density) can be tuned at will. Here we will show the functionalization and successful detection of DNA with PLL-modified substrates on a variety of substrate materials.

References

[1]   X. Duan, L. Mu, S. D. Sawtelle, N. K. Rajan, Z. Han, Y. Wang, H. Qu, M. A. Reed, Adv. Funct. Mater. 25 (2015) 2279.

[2]   N.-P. Huang, J. Vörös, S. M. De Paul, M. Textor, N. D. Spencer, Langmuir 18 (2002) 220.

[3]   G. Zhen, D. Falconnet, E. Kuennemann, J. Vörös, N. D. Spencer, M. Textor, S. Zürcher, Adv. Funct. Mater. 16 (2006), 243.
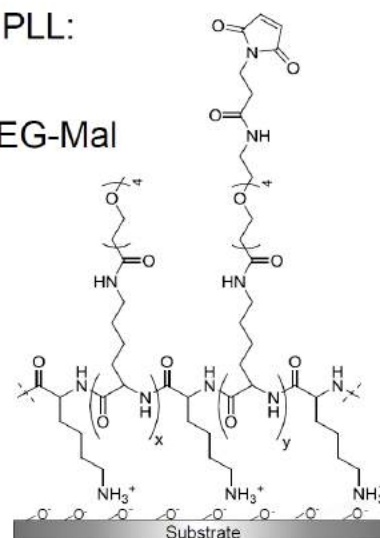
Figures
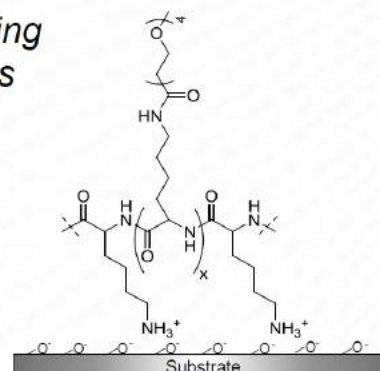
Figure 1. Functionalized PLL with both immobilization and anti-fouling properties (top) and with only anti-fouling properties (botttom).

Atomic Force Microscopy as a tool for Studying Cell (and Cell Scaffold) Mechanics

Jagoba Iturri,
José Luis Toca-Herrera[1]

Institute for Biophysics, Dept. of NanoBiotechnology, University of Natural Resources and Life Sciences, Muthgasse 11, 1190 Wien, Austria

jagoba.iturri@boku.ac.at

Atomic Force Microscopy (AFM) has become a very popular and useful tool to characterize matter at both the nano- and micro-scale levels. Through the years, together with its continuous evolution and technical implementation, AFM has shown high versatility and an almost on demand adaptive capability, thus contributing to its extended reputation and its presence in many (nano) biotechnology and materials science laboratories.

In terms of sample imaging, AFM has proven to be a solid alternative to other microscopy techniques (i.e., TEM & SEM) when investigating nano-scale structural features of (bio)materials, even under aqueous environments and at different temperatures [1,2]. However, these atomic force microscopes can be additionally used as a "mechanical" machine if operated in Force Spectroscopy mode, which enables studying mechanical properties of soft materials at the nanoscale, by sample indentation experiments [3].

This presentation will cover different examples of the mentioned mechanical applicability of AFM technique, such as the investigation of adhesion and surface forces, the quantification of ligand-receptor forces and, more extensively, the study of the mechanical properties of cells. Furthermore, the capability of an AFM to accurately manipulate samples at the microscale will be shown to permit direct quantification of cell–substrate adhesion forces by means of the so called "single-cell probe force spectroscopy", where a living cell is used as probe [4].

References

[1] A. Alessandrini and P. Facci. Meas. Sci. Technol., 16, R65–R92 (2005).
[2] S. Moreno-Flores and J.-L. Toca-Herrera, J.L. Hybridizing Surface Probe Microscopes: Toward a Full Description of the Meso- and Nanoworlds; CRC Press: Boca Raton, FL, USA (2013).
[3] H.-J. Butt, B. Cappella and M. Kappl. Surf. Sci. Rep., 59, 1 (2005).
[4] A. Moreno-Cencerrado, J. Iturri, et al. Microsc. Res. Tech., 80, 124 (2017).

Figures
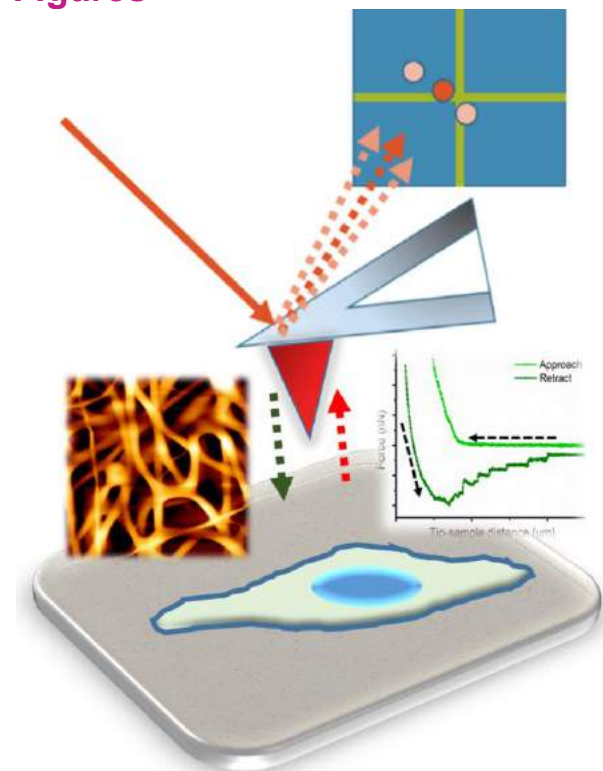
Figure 1. Scheme of an AFM operating on both a cell and its supporting scaffold. Examples of the different information that can obtained are: Topographical features (left) and distance-dependent tip-to-sample force variation.

Biomimetic Synthesis of Functionalized Silica Particles

Meder Kamalov[1],
Birgit Bräuer[1],
Cecile Echalier[2],
Gilles Subra[2],
Christian Becker[1]

[1]Universität Wien, Fakultät für Chemie, Institut für Biologische Chemie, Währinger Straße 38, Vienna Austria

[2]Université de Montpellier, Institut des Biomolécules Max Mousseron, 15 avenue Charles Flahault, 34093 Montpellier Cedex 05 France

meder.kamalov@univie.ac.at

Biomimetic methods for the synthesis of nanomaterials are attractive because they are especially mild and allow for incorporation of otherwise sensitive functional biomolecules. Biomimetic synthesis of silica particles can be accomplished by use of silaffin peptides that originally derive from proteins involved in silica deposition in the cell walls of diatoms [1]. Among silaffin peptides, the peptide R5 is particularly effective in precipitation of ordered silica particles from a solution of silicic acid at room temperature and neutral pH [2]. Use of R5 has enabled efficient encapsulation of bio-active substrates within the inner matrices of silica particles and resulted in syntheses of biologically functional silica materials [3]. In order to accomplish this, R5 peptide was linked to small molecules as well as recombinant proteins by using methods such as expressed protein ligation [4, 5]. Nevertheless, the non-covalent nature of the interaction between the cargo and silica means that it is challenging to control the retention and release of the cargo in a precise manner, with certain substrates continuously leaching out of the particles (Fig. 1A). While this property is valuable in some biomedical applications, a stronger covalent conjugation of biomimetic silica would be highly valuable as it would greatly stabilize the conjugated functional groups. Such covalent conjugation could also make it possible to synthesize multifunctional silica particles with functional groups attached both via the silaffin peptide and via the covalent bonds with silica.

We report on a new method of biomimetic synthesis of hybrid silica particles with covalently attached functional groups. The particles have been prepared by use of the R5 peptide at room temperature and neutral pH. The covalent functionalization was accomplished by use of a custom silylated building block [6]. It was possible to modify silica particles covalently in this manner with a fluorescent dye (Fig. 1B). The resulting particles retained spherical morphology and were observable by fluorescence microscopy. Use of these fluorescent particle conjugates enabled visualization of the uptake of silica particles by macrophages derived from the THP-1 cell line.

In addition, we demonstrated that the newly developed method can also be used in order to prepare multi-functional silica particles. It was possible to synthesize particles that have been simultaneously labeled by the cyanine and fluorescein dyes, where the former was loaded together with the R5 peptide and the latter was covalently linked to silica (Fig. 1C). The properties of the resulting materials, such as release kinetics of the cargo dyes, were carefully analyzed by electron and fluorescence microscopies as well as bio-analytical chemistry techniques.

The mild nature of this synthetic approach means that it is potentially applicable for a wide range of functional substrates, including proteins and nucleic acids. The use of this method can, therefore, have a significant impact in bio-medical research, as it enables easy access to hybrid bio-inorganic materials with highly tunable functionalities.

References

[1] N. Kröger, R. Deutzmann, M. Sumper, Science 286 (1999) 1129–1132.
[2] N. Kröger, R. Deutzmann, M. Sumper, J. Biol. Chem. 276 (2001) 26066–26070.
[3] C.C. Lechner, C.F. Becker, Mar. Drugs 13 (2015) 5297–5333.
[4] C.C. Lechner, C.F.W. Becker, Bioorg. Med. Chem. 21 (2013) 3533–3541.
[5] C.C. Lechner, C.F. Becker, Biomater. Sci. 3 (2015) 288–297.
[6] J. Ciccione, T. Jia, J.-L. Coll, K. Parra, M. Amblard, S. Jebors, J. Martinez, A. Mehdi, G. Subra, Chem. Mater. 28 (2016) 885–889.

Figures
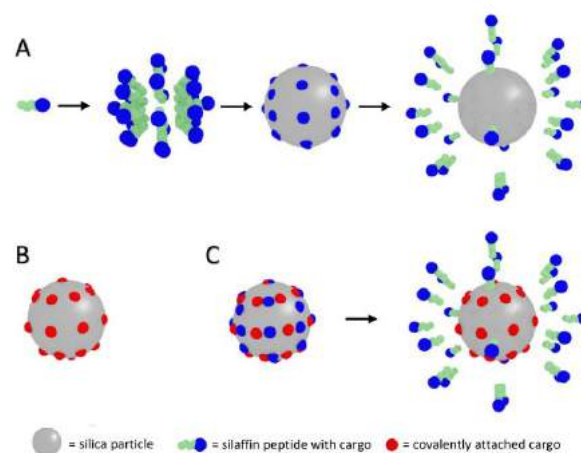
Figure 1. Silica particle fictionalization: A) biomimetic silica particles that release silaffin-cargo; B) silica particle covalently conjugated with cargo; C) multifunctional silica particles that release silaffin cargo but retain covalently attached cargo.

Multi-modular *in vitro* platform for evaluating the effects of nanoparticles on the human body

Thorsten Knoll
Yvonne Kohl, Michelle Hesler, Sylvia Wagner
Thomas Velten

Fraunhofer Institute for Biomedical Engineering
Joseph-von-Fraunhofer-Weg 1, Sulzbach, Germany

thorsten.knoll@ibmt.fraunhofer.de

Introduction

Synthetic nanomaterials are widely used for numerous applications in many areas of daily life like food production, cosmetics or medicine. Risk assessment and consequential regulatory measures for nanomaterials are of great importance, especially regarding the influence of nanoparticles on the human organism [1]. However, due to the lack of suitable models it is still difficult to estimate and predict the effects that are caused by nanomaterials. The physiologically based pharmacokinetic (PBPK) model, which is used in pharmaceutical research and drug industry for the mathematical prediction of kinetic profiles of medical compounds [2], yet has not been adequately adapted for corresponding studies of nanoparticulate substances and compounds.

We present a new *in vitro* platform with dynamic cell culture systems that enables the simulation of the pathway of nanoparticles through the human body. Data obtained with this platform can then be used for the development of a PBPK model for nanomaterials. The platform contains up to nine individual modules each of them representing either a barrier of the body, an organ or subcellular systems. The design of the microfluidic cartridge inside each module allows for the formation and investigation of a cell barrier layer or for the positioning and characterization of single cells. All modules can be operated individually or can be interconnected with each other in a flexible way. This set-up allows a realistic simulation of the situation *in vivo* and can further contribute to the replacement of animal testing procedures in risk assessment studies [3]. In parallel to the technological platform development new miniaturized *in vitro* systems are established to perform transport studies with nanoparticles on crossing biological barriers, as e.g. the lung or the gastrointestinal tract.

Materials and Methods

Each module of the *in vitro* platform comprises a fluidic system with valves, pumps, tubing and a microfluidic cartridge. The cartridge as the core component of the fluidic system contains a microfabricated silicon microwell and is employed as a miniaturized incubator. Cells are transported through a microchannel to the microwell and adhere on an optically transparent membrane from silicon nitride (Si_3N_4) [4] with 2.5 mm² cell culture area and 1.5 µm thickness (Figure 1). The membrane has a regular array of microholes with diameters smaller than 5 µm and a distance of 10 µm. For barrier transport studies the cell layer is cultivated on the nitride membrane without the need of a big lab incubator: each module comprises a temperature control system that maintains the temperature at $37 \pm 0.5 °C$. A peristaltic pump constantly supplies fresh culture medium to the cells in the microwell. Afterwards, the nanoparticle suspension is delivered through the upper microchannel until it reaches the cells in the microwell. At the end of the assay the nanoparticles crossing the barrier and the porous silicon nitride membrane and/or metabolites from the compartment above the barrier are transported from one module to the next.

Cells in the microfluidic cartridge are characterised optically and electrically during cultivation and their exposition to the nanoparticles. Embedded thin film electrodes in the two microchannels of the cartridge are connected with an impedance measurement set-up. They are used for transepithelial electrical resistance (TEER) measurement of the barrier layer or for the verification of the successful single cell positioning. Optical characterisation is performed by means of a compact imaging module that was specifically developed for the *in vitro* platform. It comprises a CMOS camera, a lens, LEDs for illumination and optical filters for bright-field and fluorescence imaging. The imaging module is mounted under the microfluidic cartridge and can be shifted from one module to the other. LED illumination for bright-field imaging is placed in the adapter with the temperature control system, which is on top of the cartridge.

The fluidic operation of the *in vitro* platform is controlled by a LabView program that enables the operation of one single module or the operation of several interconnected modules. The temperature control units of each module as well as the CMOS camera and the LED illumination are controlled electronically. In the end, the final platform comprises two individual but identical lines of interconnected modules that are run in parallel. The first line consists of the modules with the different cell cultures that are exposed to the nanoparticles whereas the reference cells, which are not exposed to nanoparticles, are cultivated in the second line.
An *in vitro* intestine co-culture model of two epithelial cell lines (Caco-2 and HT29-MTX-E12) was grown in a physiologic ratio on the porous membrane of the microwell. For system validation the co-culture model was cultured and differentiated in the microwell and in a standard Transwell® system. Functionality of the barrier was determined via TEER measurement. Human lung epithelial cells were used for the lung barrier.

Results

A first demonstrator module with fluidic circuit was assembled to prove the feasibility of the fluidic concept for cell cultivation in the microfluidic cartridge. Syringes without plunger served as reservoirs for the liquids (culture medium, cell suspension). Bubble traps in front of the inlet ports of the cartridge prevented air bubbles from entering the microchannels. After prefilling of the system with culture medium, Caco-2 cells were transported through the microchannels and successfully positioned on the porous membrane in the microwell of the cartridge (Figure 2). The operation of the imaging module was first tested separate from the platform module. The adapter with the temperature control system and the LED for bright-field imaging was positioned above the microfluidic cartridge. Figure 3 shows a picture of the imaging module and microscopic images of Caco-2 cells obtained with the imaging module in bright-field and in fluorescence mode. The staining of the cells with the green fluorescent dye Fluorescein diacetate (FDA) verified the viability of the cells after cultivation in the microwell for 48 TEER measurements of the differentiated intestine co-culture model in the Transwell® system verified the density of the intestine barrier. The TEER value of the *in vitro* model was between 180 and 200 Ω/cm^2. Experiments are ongoing to determine the TEER values of the intestine and lung *in vitro* models in the microwell.

Conclusion and outlook

With the first demonstrator of the new *in-vitro* platform we could show the function of the fluidic system in combination with the microfluidic cartridge. Cells were positioned on the porous microhole membrane and visualized by the imaging module. Electrical measurements will be performed soon to get first results about barrier density and interaction of cells with nanoparticles. Long-term cell cultivation and the interconnection of the presented demonstrator with two other modules will be established.

Acknowledgements

References

[1]   Savolainen et al., Toxicology, Vol. 269 (2010), pp. 92-104

[2]   Zhao et al., Clinical Pharmacology & Therapeutics, Vol. 89, Issue 2 (2011) pp. 259-267

[3]   Boverhof et al., Analytical and Bioanalytical Chemistry, Vol. 396, Issue 3 (2010) pp. 953-961

[4]   Kurz et al., Biosensors and Bioelectronics, Vol. 26, Issue 8 (2011), pp. 3405-3412

Figures
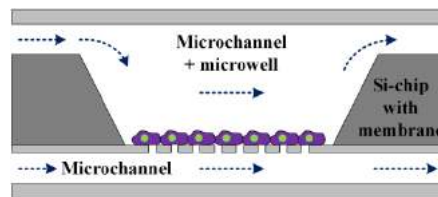
Figure 1. Cross-section drawing of microwell with porous membrane and microchannels.
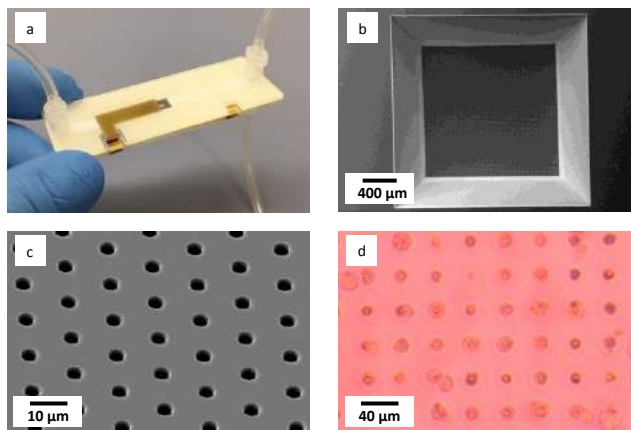
Figure 2. a) Microfluidic cartridge with electrodes, tubing and microwell for cell cultivation; b) SEM image of microwell; c) SEM image of microholes in the Si_3N_4 membrane; d) Caco-2 cells on microholes.
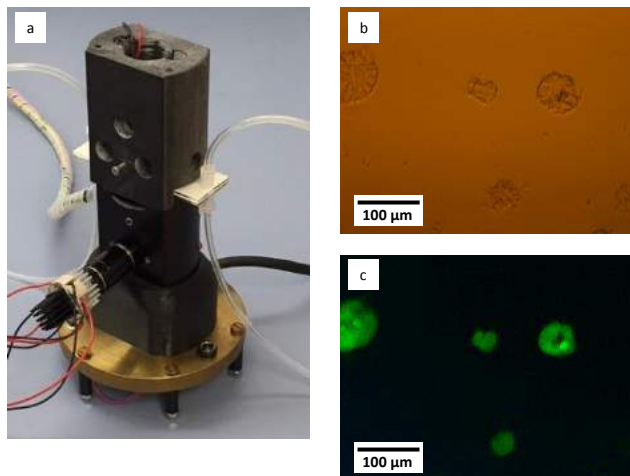
Figure 3. a) Imaging module with microfluidic module; b) Bright-field image of Caco-2 cells in the microwell; c) fluorescence image of FDA stained Caco-2 cells in the microwell.

Learning the pharmacology and toxicokinetics of biologically-relevant graphene materials

Kostas Kostarelos

Nanomedicine Lab
Faculty of Biology, Medicine & Health and
National Graphene Institute
The University of Manchester
Manchester M13 9PT, United Kingdom

kostas.kostarelos@manchester.ac.uk

The use of nanomaterials in medicine is growing at an unprecedented rate for a variety of therapeutic, diagnostic or combinatory applications. Graphene and other 2D materials possess properties that make them attractive materials for biomedical applications, however, their impact on the physiology of live organisms is still unexplored. What is needed today is the determination of the specific characteristics graphene and 2D materials should possess in order to determine the toxicological and adverse reaction risks following administration or implantation. This talk will illustrate how biological-grade graphene oxide (GO) sheets exhibit very interesting behaviour on interaction with tissues of living animals (*in vivo*). The pharmacokinetic and toxicokinetic profile of the GO sheets in correlation with their physicochemical characteristics (thickness, lateral dimensions) can allow the determination of the critical parameters that can allows their further development towards the clinic. Development of GO for therapeutic or diagnostic applications requires determination of the fundamental *in vivo* pharmacological parameters such as blood circulation half-life, tissue biodistribution, excretion rates, and kinetics of material biodegradation which will constitute the emerging research area of graphene pharmacology.

References

[1]   Jasim *et al.* **ACS Nano**, 2016
[2]   Jasim *et al.* **2D Materials**, 2016
[3]   Jasim *et al.* **Applied Materials Today**, 2016
[4]   Kostarelos, **Nature Reviews Materials**, 2016
[5]   Jasim *et al.* **Chemical Science**, 2015
[6]   Bussy et al. **Nanoscale**, 2015
[7]   Kostarelos & Novoselov, **Nature Nanotech**, 2014
[8]   Kostarelos & Novoselov, **Science**, 2014

Novel poly(ε-caprolactone)/gelatin wound dressings prepared by emulsion electrospinning with controlled release capacity of Ketoprofen anti-inflammatory drug

J.M. Lagaron[2],
A.O. Basar[1], S. Torres-Giner[2], S. Castro[3],
Turkoglu Sasmazel[1]

[1]Atilim University, Incek, Golbasi, Ankara, Turkey
[2]Novel Materials and Nanotechnology Group, CSIC,
Paterna (Valencia), Spain
[3]FluidnatekTM Applications Department, Bioinicia S.L.,
Paterna (Valencia), Spain

lagaron@iata.csic.es

In the present work, a single and double phase Ketoprofen-loaded mats of ultrathin fibers were developed by electrospinning and their physical properties and drug release capacity were analyzed. The single phase material was prepared by solution electrospinning of poly(ε-caprolactone) (PCL) with Ketoprofen at a weight ratio of 5 wt%. This Ketoprofen-containing PCL solution was also used as the oil phase in an emulsion with gelatin. The resultant stable oil-in-water (O/W) emulsion of PCL-in-gelatin, also containing Ketoprofen at 5 wt%, was electrospun to produce the double phase mat. Cross-linking was performed by means of glutaraldehyde vapor to prevent dissolution of the hydrophilic gelatin phase. The performed characterization indicated that Ketoprofen was successfully embedded in both electrospun mats, i.e. PCL and PCL/gelatin, and both mats showed high hydrophobicity. In vitro release studies interestingly revealed that, in comparison to the single phase PCL electrospun mat, the double phase PCL/gelatin mat significantly hindered Ketoprofen burst release and exhibited a sustained release capacity of the drug for up to 4 days. In addition, the electrospun Ketoprofen-loaded mats showed enhanced attachment and proliferation of L929 mouse fibroblast cells, presenting the double phase mat the highest cell growth yield due to its improved porosity. The here-developed electrospun materials clearly show a great deal of potential as novel wound dressings with an outstanding controlled capacity to release drugs.

References

[1]   Basar et al., Materials Science and Engineering: C, 2017
https://doi.org/10.1016/j.msec.2017.08.025

Bacterial cellulose, a natural polymer for biological applications

Anna Laromaine,
Soledad Roig-Sanchez, Irene Anton, Muling Zeng,
Jordi Floriach-Clark, Anna Roig

Nanoparticles and Nanocomposites
Group(www.icmab.es/nn)
Institut Ciencia de Materials de Barcelona (ICMAB-CSIC)
Campus UAB, 08193 Bellaterra, Spain

alaromaine@icmab.es

Looking towards green resources to fabricate advanced functional materials, cellulose seems to be a good candidate as it constitutes the most abundant renewable biosphere-produced polymer. Specially, nanocellulose is in the spotlight when designing new functional (bio)nanocomposites due to its characteristics: hydrophilicity, biodegradability, high porosity, transparency, high water holding capacity, chemical tunability and formation of semi-crystalline morphologies.

Cellullose can be synthesized by bacteria or obtained from plants, algae and fungi. In particular, bacterial cellulose (BC) does not contain lignin and hemicelluloses, potentials sources of toxicity present in plant cellulose. It also exhibits a higher degree of polymerization (DP 2000-8000) and better crystallinity (60%-90%). It presents a high elastic modulus (79GPa measured in a single fiber by AFM) and high tensile strength (200-300MPa). The highly porous matrix created by the nano-fiber gives to the material its large water holding capacity. Moreover, it offers the possibility to impact on its micro(nano)structuration and shape during its production.

Due to its properties, BC has an enormous potential in sectors as energy, health and catalysis therefore its investigations have been steadily increasing.
In this presentation will introduce how we can obtain novel bacterial cellulose nanocomposites with different types of nanoparticles for biomedical applications. The possibility to control the formation of the BC (in situ) and the modification after BC synthesis, ex situ, will be illustrated.

These innovative bacterial cellulose structures will provide the proof of concept for devices or products.

References

[1] Zeng et al. Journal of Materials Chemistry C (2014),2,6312-6318, DOI: 10.1039/c4tc00787e.
[2] Zeng et al. Cellulose (2014), 21, 4455–4469, DOI 10.1007/s10570-014-0408-y.

Figures
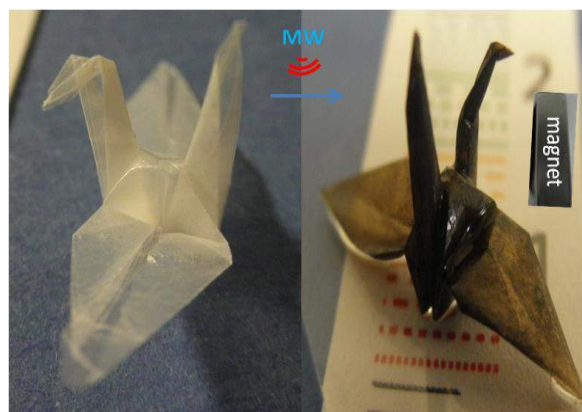
Figure 1. BC origami at the left which we composed with iron oxide nanoparticles to make it responsive to a magnetic field.
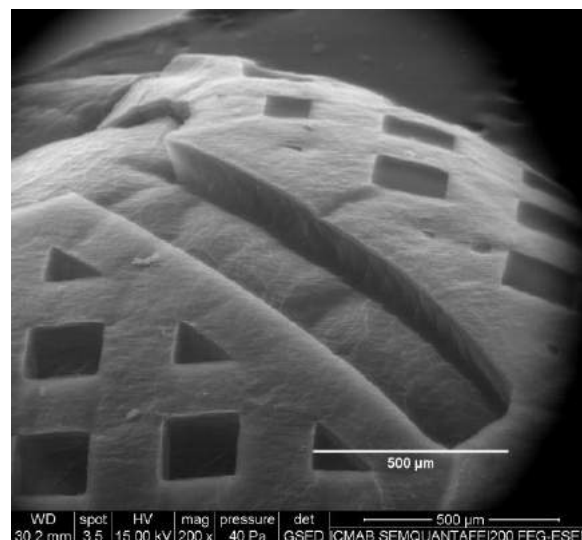
Figure 2. Topographic control of BC films in situ using microfluidic stamps.

The potential of photonic point-of-care nanobiosensors for high-value diagnostics

Laura M. Lechuga

Nanobiosensors and Bioanalytical Applications Group, Catalan Institute of Nanoscience and Nanotechnology (ICN2), CSIC and The Barcelona Institute of Science and Technology, CIBER-BBN, Campus UAB, Bellaterra, 08193 Barcelona, Spain

Laura.lechuga@icn2.cat

The need to monitor the human health in a fast and reliable way is one of the challenges faced by humanity in the 21st century. Modern diagnostics is demanding novel tools that could enable quick, accurate, sensitive, reliable and cost-effective results so that appropriate treatments can be implemented in time, leading to improved outcomes. Portable point-of-care (POC) devices, able to deliver an instant diagnostics, could become a reality soon thanks to the last advances in nanobiosensors, lab-on-a-chip, wireless and smart-phone technologies, which promise to surpass the existing challenges, opening the door to a global diagnostics access.

The driving force of our research is to achieve such ultrasensitive platforms for POC analysis using nanophotonic technologies and custom-designed biofunctionalization protocols, accomplishing the requirements of disposability and portability. We are using innovative designs of nanophotonic biosensors based on silicon photonics technology (bimodal waveguide nanointerferometers) or nanoplasmonics (gold nanostructures) and full microfluidics integration. We have demonstrated the suitability of our technology for the clinical diagnostics, with extremely sensitivity and selectivity and directly in human fluids, for the evaluation of infectious microorganisms (at few cfu/mL), early detection of colorectal cancer or the detection of microRNA biomarkers at aM level related to cancer progression, among others.

References

[1] J. Maldonado, A.B. González-Guerrero, C. Domínguez and L.M. Lechuga. Biosens & Bioelec., 85, 310-316. (2016)

[2] C. S. Huertas, D. Fariña and L.M. Lechuga. ACS Sensors, 1, 748–756 (2016)

[3] C. S. Huertas, S. Domínguez and L.M. Lechuga. Scientific Reports (Nature Publishing Group) 7, 41368 (2017)

[4] G.A. López-Muñoz, M.C. Estevez, E.C. Peláez-Gutierrez, A. Homs-Corbera, M.C. García-Hernandez, J. Ignacio Imbaud and L.M. Lechuga. Biosens. &Bioelec.96, 260–267. (2017)

[5] C. Szydzik, A.F. Gavela, S. Herranz, J. Roccisano, M. Knoerzer, P. Thurgood, K. Khoshmanesh, A. Mitchell, and L.M. Lechuga. Lab on a Chip 17, 2793 – 2804. (2017)

Figures
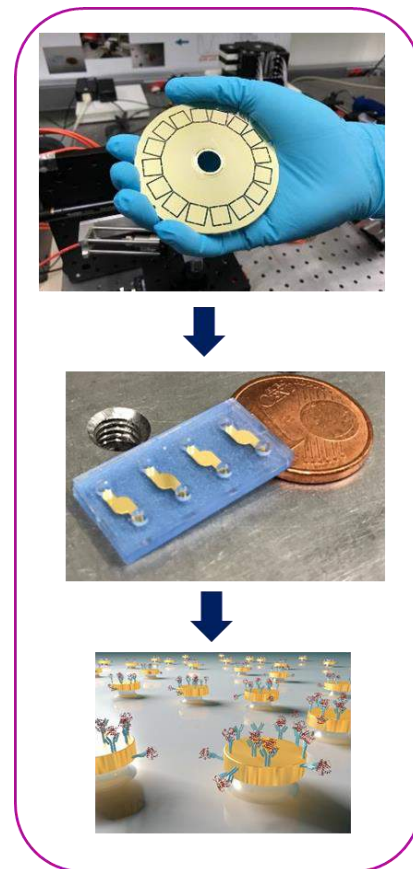
Figure 1. Multiplexed Nanoplasmonics biosensors
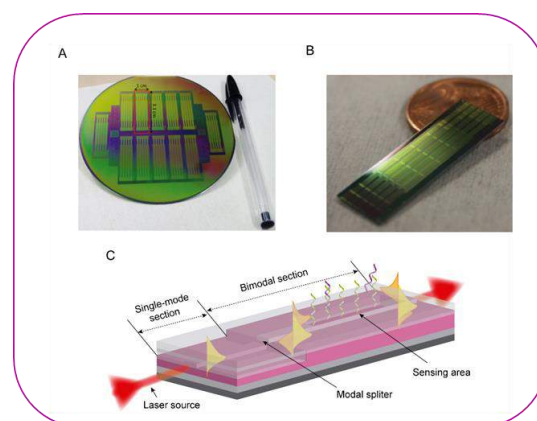
Figure 2. Nanophotonic waveguide interferometric biosensors for highly sensitive detection

Micro-to-Nanoscale Mechanical Properties of Pig Intestine and Gastric Mucus as Studied with Atomic Force Microscopy

Seunghwan Lee[1]
Nikolas Nikogeorgos[1]
[1]Department of Mechanical Engineering
Technical University of Denmark
Kgs. Lyngby, Denmark

seele@mek.dtu.dk

Mucus represents "first defense line" of all mucosal surfaces, such as gastrointestinal, cervical, ocular, respiratory lines against chemical, enzymatic, microbial, and mechanical insult [1,2]. Mucin over-production is a hallmark of chronic diseases of respiratory epithelia such as chronic obstructive pulmonary disease, asthma, and otitis media. While pathogenic colonization by microbes starts from adhesion on mucus surface, they have to overcome the mechanical integrity of mucus gels in order to reach the apical surface of epithelial cells. Ironically, this defensive behavior of mucus gels acts as physical barrier when it is needed to deliver drug molecules or functional foods to target cells or tissues [3,4]. When drug-loaded particles are administered, they are easily trapped by mucus gels via steric or adhesive contacts and eventually eliminated by mucociliary clearance. Mucoadhesive polymers [5] have been proposed as one of potent ways to enable the traverse of drug-loaded particles through mucus gel layers based on strong entanglement with mucin network. Nevertheless, it is often not sufficient to reach ultimate goal, i.e. delivery of drugs to target cells, due to relatively short turnover time (40 – 270 min. for intestinal mucus) and frequent clearance of mucus gels.

It is thus necessary to develop more effective means to engineer particles that can efficiently "penetrate through" the barrier for this purpose. Largely lacking to this end is the information on the mechanical properties of mucus gels, especially on nanometer scale. While rheological properties of mucus have extensively been studied to date [6,7], it is not certain to which extent macroscale rheological properties are relevant to penetration phenomena by microorganisms or drug/functional nutrients. In this context, we have employed atomic force microscopy (AFM) as an experimental approach/model to characterize the micro- to nanoscale mechanical properties of mucus gels and the interaction with microbes and drug/function nutrients (Figure 1). Mucus in this study was acquired from a freshly slaughtered pig's intestine and stomach by scraping and rinsing, and was reconstructed according to a standard procedure. Polyethylene (PE) or silica (SiOx) colloidal particles were attached to AFM probes, representing model microbes or drug molecules interacting with mucus layers. The AFM measurements were performed either in simulated intestine/gastric fluid, respectively, or dry air environment. In-depth discussion on the mechanical properties of pig intestine and gastric mucus, the influence of size and surface chemistry of the colloidal probe on the compression/penetration, as well as the force/energy required for a micro-sized particle to overcome and penetrate through the mucus layers will be provided.

References

[1] S.K. Linden, P. Sutton, N.G. Karlsson, M.A. McGuckin, Mucosal Immunology 1 (2008), 183-197.

[2] C.L. Hattrup, S.J. Gendler, Ann. Rev. Physiol. 70 (2008), 431-457.

[3] N.A. Peppas, Y. Huang, Adv. Drug. Delivery Rev. 56 (2004), 1675-1687.

[4] L.M. Ensign, R. Cone, J. Hanes, Adv. Drug Delivery Rev. 64 (2012), 557-570.

[5] J.O. Morales, J.T. McConville, Eur. J. Pharm. & Biopharm. 77 (2011), 187-199.

[6] A. Cone, Adv. Drug Delivery Rev. 61 (2009), 75-85.

[7] S.K. Lai, Y.-Y. Wang, D. Wirtz, J. Hanes, Adv. Drug Delivery Rev. 61 (2009), 86-100.

Figures
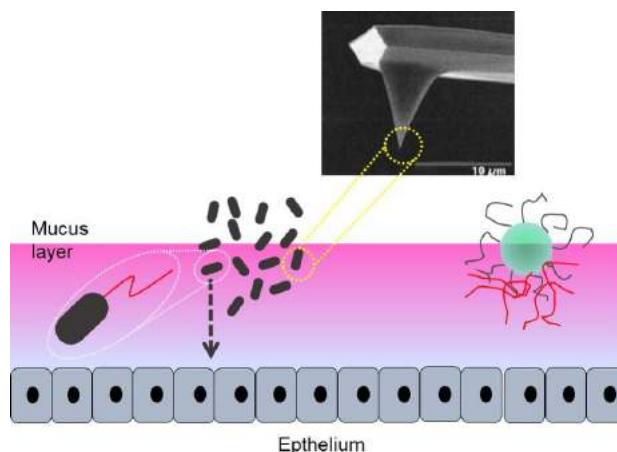
Figure 1. A schematic illustration for AFM probes as model microbes or drug molecules to interaction with mucus layers.

Slow microscale coiling in bis-imidazolium supramolecular hydrogel fibres induced by release of a cationic serine protease inhibitor

David Limón,[1,2]
Claire Jiménez-Newman,[1] Ana C. Calpena,[2,3]
Arántzazu González-Campo,[4] David B. Amabilino,[5,6]
and Lluïsa Pérez-García [1,2,*]

[1] Departament de Farmacologia, Toxicologia i Química Terapèutica, Universitat de Barcelona, Av. Joan XXIII, 27-31, 08028 Barcelona, Spain
[2] Institut de Nanociència i Nanotecnologia IN2UB, Universitat de Barcelona, 08028 Barcelona, Spain.
[3] Departament de Farmàcia, Tecnologia Farmacèutica i Fisicoquímica, Universitat de Barcelona, Av. Joan XXIII, 27-31, 08028 Barcelona, Spain.
[4] Institut de Ciència de Materials de Barcelona (ICMAB-CSIC). Campus de la UAB, 08193, Bellaterra, Barcelona, Spain.
[5] School of Chemistry, University of Nottingham, University Park, NG7 2RD, United Kingdom.
[6] The GSK Carbon Neutral Laboratories for Sustainable Chemistry, The University of Nottingham, Triumph Road, Nottingham NG7 2TU, United Kingdom.
*Corresponding author:
mlperez@ub.edu

Gels formed by a gemini dicationic amphiphile can incorporate the serine protease inhibitor 4-(2-aminoethyl)-benzenesulfonyl fluoride hydrochloride, which could be used in a new approach to the treatment of Rosacea. The presence of the drug strongly influences the gelation process in terms of time and temperature of gelation, as well as the thermodynamic events occurring. The drug is incorporated not only in the interstitial space but also within the gel fibres, affecting gel properties such as viscoelastic behavior, but most importantly, the morphology at the microscopic level: in gels containing a drug concentration above 3 mg/mL, a remarkable fibre coiling occurs as a result of the drug released from the fibres when the gel ages. The drug can be released from the gel in a suitable profile, and skin permeation experiments show that the drug can permeate and keep retained beneath the human skin, where it shows its therapeutic activity. These results show the potential of these gels for becoming a new approach in the treatment of Rosacea.

Acknowledgements

References

[1]   D. Limón, C. Jiménez-Newman, A. C. Calpena, A. González-Campo, D. B. Amabilino, and L. Pérez-García, Chem. Commun. 53 (2017) 4509-4512.

Figures
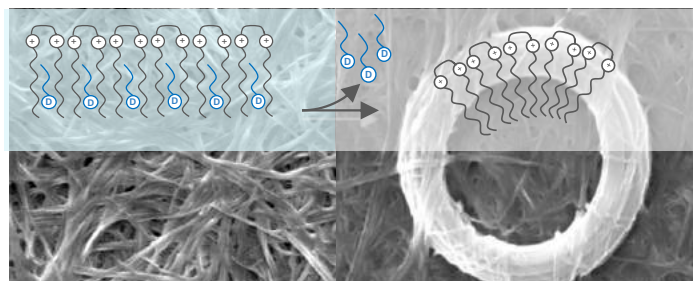
Figure 1. Bis-imidazolium supramolecular hydrogel fibres incorporating a serine protease inhibitor coil upon drug release.

Health and environment diagnostics using paper-based nanobiosensors

Arben Merkoçi

[1]Catalan Institute of Nanoscience and Nanotechnology (ICN2), CSIC and The Barcelona Institute of Science and Technology, Campus UAB, Bellaterra, 08193 Barcelona, Spain.
[2]ICREA - Institucio Catalana de Recerca i Estudis Avançats, 08010 Barcelona, Spain

arben.merkoci@icn2.cat

Biosensors field is progressing rapidly and the demand for cost efficient platforms is the key factor for their success. Physical, chemical and mechanical properties of cellulose in both micro and nanofiber-based networks combined with their abundance in nature or easy to prepare and control procedures are making these materials of great interest while looking for cost-efficient and green alternatives for device production technologies. Both paper and nanopaper-based biosensors are emerging as a new class of devices with the objective to fulfil the "World Health Organization" requisites to be ASSURED: affordable, sensitive, specific, user-friendly, rapid and robust, equipment free and deliverable to end-users. How to design simple paper-based biosensor architectures? How to tune their analytical performance upon demand? How one can 'marriage' nanomaterials such as metallic nanoparticles, quantum dots and even graphene with paper and what is the benefit? How we can make these devices more robust, sensitive and with multiplexing capabilities? Can we bring these low cost and efficient devices to places with low resources, extreme conditions or even at our homes? Which are the perspectives to link these simple platforms and detection technologies with mobile phone communication? I will try to give responses to these questions through various interesting applications related to protein, DNA and even contaminants detection all of extreme importance for diagnostics, environment control, safety and security. .

References

[1]   C. Parolo, A. Merkoçi, "Paper based nanobiosensors for diagnostics", Chem. Soc. Rev., 42, 2013, 450-457

[2]   D. Quesada-González, A. Merkoçi. « Nanoparticle-based lateral flow biosensors », Biosensors and Bioelectronics, 73, 2015, 47–63

[3]   E. Morales-Narváez, H.Golmohammadi, T. Naghdi, H. Yousefi, U. Kostiv, D. Horak, N. Pourreza, A.Merkoçi. "Nanopaper as an optical sensing platform ", ACS Nano, 9, 2015, 7296-7305

[4]   E. Morales-Narvaez, T. Naghdi, E. Zor, A. Merkoci, "Photoluminescent Lateral-Flow Immunoassay Revealed by Graphene Oxide: Highly Sensitive Paper-Based Pathogen Detection", Anal. Chem. 2015, 87, 8573−8577

[5]   L. Baptista-Pires, C. C. Mayorga-Martínez, M.M. Sanchez, H. Monton, A. Merkoçi, "Water Activated Graphene Oxide Transfer Using Wax Printed Membranes for Fast Patterning of a Touch Sensitive Device", ACS Nano 2016, 10, 853−860

[6]   A.M. López_Marzo, A. Merkoçi, "Paper-based sensors and assays: a success of the engineering design and the convergence of knowledge areas", Lab Chip, 2016, 16, 3150–3176

[7]   E.Morales-Narváez, L. Baptista-Pires, A. Zamora-Gálvez, A. Merkoçi, "Graphene-based biosensors: Going simple", Advanced Materials, 2017, 29, 1604905.

Shoot it or dilute it: Administration method in cell culture alters particle-cell interaction

Thomas L. Moore[1],
Dominic A. Urban[1], Laura Rodriguez-Lorenzo[1], Ana Milosevic[1], Miguel Spuch-Calvar[1], Sandor Balog[1], Barbara Rothen-Rutishauser[1], Marco Lattuada[2], Alke Petri-Fink[1,2]

[1]Adolphe Merkle Institute, University of Fribourg, Chemin des Verdiers 4, Fribourg, Switzerland
[2]Chemistry Department, University of Fribourg, Chemin du Musée 9, Fribourg, Switzerland

thomaslee.moore@unifr.ch

Nanotechnology was heralded as "the" emerging technology for biomedical applications in the last two decades; however, excitement has waned in recent years as nanoparticles (NPs) have proven difficult to translate from the benchtop into the clinic. Aside from the approval of liposomal drug formulations, polymer-drug conjugates, and a small handful of other particle-based drug delivery systems or magnetic hyperthermia mediators,[1,2] the expected windfall of improvements in medicine and imaging has not arrived. The reasons for this shortcoming are manyfold: technical difficulty of scaling the production of nanomedicines, lack of significant improvement in therapeutic efficacy compared to conventionally administered active pharmaceutical ingredients, and a lack of fundamental knowledge of particle-biology interactions and long-term particle fate.[3,4]

In vitro methodology is an important tool to assess the interactions of (newly) designed NPs with cells, and one seemingly (non)trivial aspect that may be overlooked could be differences in the way particles are pipetted in vitro to cells. For example, some experimental designs call for particles to be administered as a concentrated dose (e.g. with live cell imaging experiments) in order to minimize temperature fluctuations in sensitive setups. Otherwise, simple differences in training and personal preference may dictate how research personnel administer particles to cells. We hypothesized that such a change, a literal difference in the way particles are pipetted in vitro, could influence particle cell interactions and in fact observed a significant impact on NPs cellular uptake.

To test this hypothesis, we administered NPs to J774A.1 mouse monocyte/macrophages via a concentrated, mixed, or pre-mixed approach (Figure 1). We observed that the administration method had a significant effect on particle deposition on or uptake by the cells. Prior to cell experiments, NPs were characterized via electron microscopy, depolarized dynamic light scattering, and UV-Vis spectroscopy. NPs were found to be colloidally stable in complete cell culture media (DMEM supplemented with 10% FBS and 1% penicillin-streptomycin).

In order to explain the observed differences, we evaluated the relative amount of protein adsorbed onto the NPs surface based on administration method. It is apparent that administration method strongly correlates to the relative amount of adsorbed protein and in turn significantly impacts cellular uptake. Furthermore, we built upon the previously described in vitro sedimentation, diffusion and dosimetry model to describe the behavior of the particles in solution.[5]

These data show that in vitro methodology can have a significant impact on experimental outcomes vis-à-vis particle-cell interaction, and therefore necessitates at minimum an awareness and at most a standardization of experimental technique.

References

[1] von Roemeling C, et al., Trends in Biotechnology, 35 (2017) 159-171.
[2] Anselmo AC and Mitragotri S. Journal of Controlled Release, 190 (2014) 15-28.
[3] Venditto VJ and Szoka FC, Jr. Advanced Drug Delivery Reviews, 65 (2013) 80-88.
[4] Wilhelm S, et al. Nature Reviews Materials, 1 (2016) 16014.
[5] Hinderliter PM, et al., Particle and Fibre Toxicology, 7 (2010) 36.

Figures
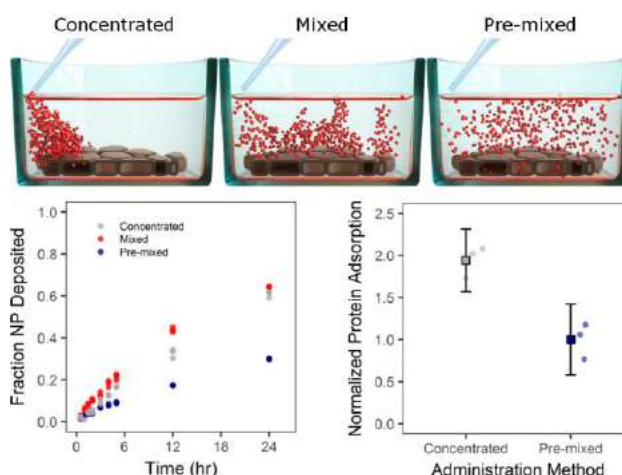
Figure 1. The method of administration in cell culture can have a significant impact on nanoparticle-cell interaction. Depending on the method, the fraction of initially administered nanoparticles that are deposited/taken up by cells can change and this is related to the initial adsorption of proteins on the particle surface.

Receptor-Targeted Drug Delivery: Biological Mechanistic and Applications

Silvia Muro,

Fischell Department of Bioengineering and Institute for Bioscience and Biotechnology Research, University of Maryland, College Park, MD, USA
&
Institució Catalana de Reserca i Studis Avançats and Institute for Bioengineering of Catalonia, Barcelona, Spain

muro@ibbr.umd.edu

The design of targeting and drug carrier strategies to enable delivery of therapeutic agents to areas of the body requiring intervention is an active research field. Therapeutic and diagnostic targets are often confined to specific regions or tissues in the body, where access may require active transport from the circulation into the subjacent tissue. In addition, once within the tissue or body compartment of interest, most targets of intervention relate to sub-cellular environments, e.g., the cell surface versus different intracellular compartments, further requiring strategies to achieve this goal. Using polymer nanocarriers functionalized with affinity moieties against single or combined cell-surface receptors, along with additional biological signaling moieties, my laboratory focuses on understanding the parameters that regulate transport of drug delivery vehicles across cellular barriers and into cells of subjacent tissues. We examine these aspects using cell culture models with subsequent validation in laboratory animals to correlate molecular/cellular mechanisms with in vivo outcomes. We investigate the influence exerted on targeting and uptake by drug carrier design parameters (size, shape, avidity, combination targeting, etc.) and parameters that are intrinsic to the physiological system (disease states, flow, receptor epitopes being targeted, modulation of regulatory molecules, etc.). The characterization of these complex physiological and design parameters, along with the understanding of the mechanisms governing the interaction of drugs carriers with the surrounding biological environment, are necessary steps toward achieving efficient drug delivery systems.

Electrospinning and Electrospraying applications in pharma and in the BioSpace. Some real practical cases.

Enrique Navarro[1]

[1]Bioinicia S.L., Valencia, Spain

enavarro@bioinicia.com

Figure 1. Electrospun pharma product. Patches for wound healing.

Electrospinning-Electrospraying technologies have been proven as one of the most powerful and versatile methods of manufacturing micro and nanostructured materials in fields such as pharma, biomedical and foodtech.

From drug-controlled delivery platforms to scaffolds, from medical devices to functional coatings or encapsulation of APIs, food ingredients or bioactives.

The aim of this presentation is to showcase to the audience some real examples of products made by electrospinning-electrospraying using Bioinicia's proprietary technology, including also Bioinicia's industrial facilities (GMP & ISO 13485 certified).

Figure 2. Electrospun medical device. Multi-layer scaffold for small intestine.

Improvement of the Enzymatic Activity of α-Galactosidase Using Nanovesicles with application to Fabry Disease treatment

Solène Passemard[1,2],
Elisabet González-Mira[1,2], Nathaly Segovia[1,2], Anna Lechado[2,3], Natalia Garcia Aranda[2,3], Ibane Abasolo[2,3], José Luis Corchero[2,4], Santi Sala[1,2,5], Daniel Pulido[2,6], Edgar Cristobal[2,6], Míriam Royo[2,6], Antonio Villaverde[2,4], Simó Schwartz[2,3], Jaume Veciana[1,2], Nora Ventosa[1,2]

[1]Institut de Ciència de Materials de Barcelona (ICMAB-CSIC), Campus UAB, Bellaterra, Spain
[2]CIBER de Bioingeniería, Biomateriales y Nanomedicina (CIBER-BBN), Bellaterra, Spain
[3]CIBBIM-Nanomedicine, Vall d'Hebron Institut de Recerca (VHIR), Universitat Autònoma de Barcelona, Barcelona, Spain
[4]Departament de Genètica i de Microbiologia, Institut de Biotecnologia i de Biomedicina, Universitat Autònoma de Barcelona, Bellaterra, Spain
[5]Nanomol Technologies SA, Mòdul de Recerca B, Campus Universitari de Bellaterra, Cerdanyola del Vallès, Spain
[6]Combinatorial Chemistry Unit, Barcelona Science Park, Barcelona, Spain

ventosa@icmab.es

Fabry disease is a rare inherited disease caused by loss of function of the enzyme α-Galactosidase A (GLA) [1]. Commercially available treatments are based on the intravenous administration of GLA demonstrating positive short-term effect, reducing the progression of the disease and improving the quality of life in patients. However, GLA replacement therapy exhibits drawbacks such as the degradation of the exogenously administered enzyme, its limited efficacy in patients with an advance stage of the disease and the extremely high cost of the treatment. In order to improve the delivery efficacy and the systemic circulation of the current treatment, nanoliposomes containing GLA were prepared as novel drug delivery systems (DDS). The incorporation of GLA in liposomes was obtained following the DELOS-SUSP process based on the use of compressed CO_2 [2] as co-solvent (**Figure 1**). Liposomes were constituted from phospholipids (DPPC) and cholesterol-based compounds. In addition, c(RGDfK) peptide ligand was incorporated in the membrane bilayer of the vesicles to enhance the targeting and the uptake efficiency of the GLA-loaded conjugates to the diseased cells. The conjugate was further characterized to obtain information on its physico-chemical characteristics and morphology entrapment efficiency and also biological efficacy and cell uptake. Through the DELOS-SUSP process, nanometric liposomes containing GLA were successfully prepared with an entrapment efficiency of about 40 %. *In vitro* efficacy studies in GLA deficient cells of Fabry KO mice showed that the GLA-nanoformulations were able to reduce lysosomal Gb3 deposits more efficiently than the free enzyme in agreement with a greater specific activity also encountered (**Figure 2**). This finding indicates that (i) such multifunctional nanovesicles are uptake by GLA deficient cells, (ii) the GLA-nanovesicles reach the lysosomal compartment, and (iii) the cargo (GLA) is efficiently released so that the GLA activity in the cells is restored. The results obtained prove the great potential of DELOS-SUSP method for the production of new nanomedicine candidates based on enzyme-nanovesicle conjugates. The development of these new GLA-nanoconjugates up to the end of the regulatory preclinical phase will be carried out under the frame of the European Smart-4-Fabry project (H2020-NMBP-2016-2017 GA 720942).

References

[1] Desnick, R. J.; *et al. Ann. Intern. Med.* 4 (2003) 338-346.
[2] Cabrera, I.; *et al. Nano Lett.* 13 (2013) 3766-3774.
[3] Cabrera, I.; *et al. Adv. Healthcare Mater.* 7 (2016) 829-40.

Figures
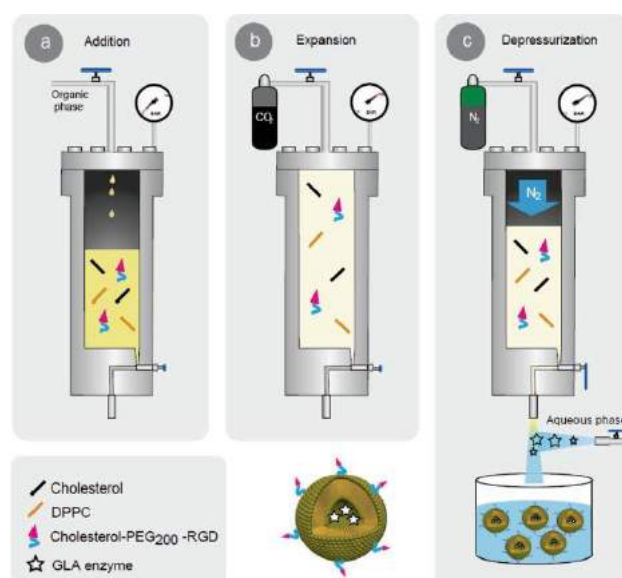
Figure 1. Nano-GLA multifunctional nanoformulation, manufactured by the DELOS-SUSP platform.
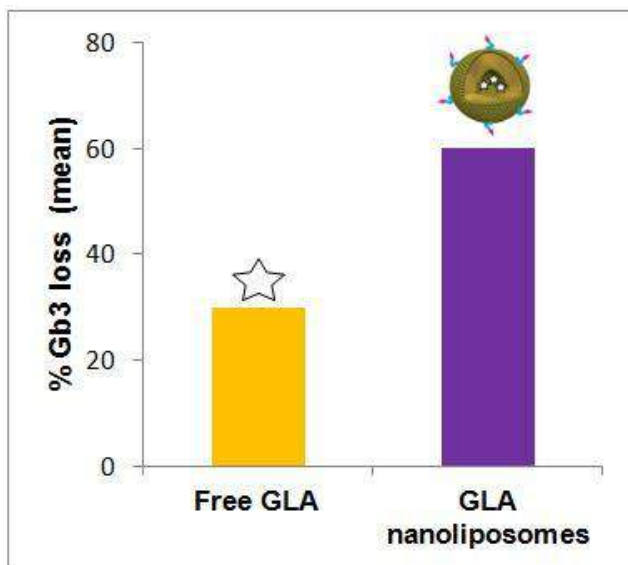
Figure 2. Effect of free GLA and GLA-Nanoliposomes in the reduction of Gb3 deposits in aortic endothelial cells of Fabry KO mice (right). Represented values correspond to mean.

Unravelling fundamental aspects of enzyme-powered micro-&nanomotors: towards biomedical applications

Tania Patiño[1,2],

Ana Hortelao[1,2], F. Xavier Arqué[1], Natalia Feiner[1], Lorenzo Albertazzi[1], Samuel Sánchez[1-3]

[1]Institute for Bioengineering of Catalonia, Barcelona, Spain.
[2] Max Planck Institute for Intelligent Systems, Stuttgart, Germany
[3]Institució Catalana de Recerca i Estudis Avançats (ICREA), Barcelona, Spain

tpatino@ibecbarcelona.eu, ssanchez@ibecbarcelona.eu

Inspired by nature, bio-hybrid micro- and nanomotors based on the use of enzymes as power sources has recently been achieved [1]. These systems are able to self-propel due to the catalytic conversion of a substrate into products [2]. Their unique properties, including biocompatibility, bioavailability and versatility, makes them excellent candidates for biomedical applications, where their active motion could improve current approaches based on passive micro- and nanodevices. However, a deeper and fundamental understanding on their structure and motion mechanism is still required for their implementation in biomedical applications. With the aim of exploring the versatility of such systems, we studied new enzymes as power sources for the self-propulsion of micromotors. Results showed that the motion behavior is strongly dependent on the enzyme type, being the catalytic constant a key parameter for the generation of active motion. In addition, the enzyme number and distribution might play a key role on their motion behavior. Traditionally, asymmetry has been claimed to be essential for the motion of catalytic micro-swimmers. Yet, other studies have reported that symmetrically enzyme coated particles present enhanced Brownian diffusion (self-propulsion) [3]. Nonetheless, enzyme distribution and origin of that symmetric-based motion was not reported. We investigated the effect of enzyme quantity as powering engines, as well as their distribution upon the motion behavior of urease-powered micromotors at a single-molecule resolution by using STORM imaging technique. Additionally, we explored the effect of self-propulsion on the doxorubicin anti-cancer drug release and intracellular delivery. We observed an enhanced drug release and cell uptake using active particles, when compared to their passive counterparts [4].

These results provide new insights into the design features of enzymatic micro- & nanomotors from the fundamental aspects towards efficient biomedical applications.

References

[1] Ma X., Jannasch A., Albrecht UR., Hahn K., Miguel-López A., Schäffer E., Sánchez S., Nano Lett, 15 (2015), 7043–7050

[2] Ma X., Hortelao A. Patino T., Sánchez S., ACS Nano, 10 (2016), 9111–9122

[3] Dey K., Zhao X., Tansi BM., Méndez-Ortiz WJ., Córdova-Figueroa UM., Golestanian R., Sen A., Nano Lett, 15 (2015), 8311-8315.

[4] Hortelao A., Patino T., Pérez-Jiménez A., Blanco A., Sánchez S., Adv Funct Mater, (2015) *In press.*

Figures
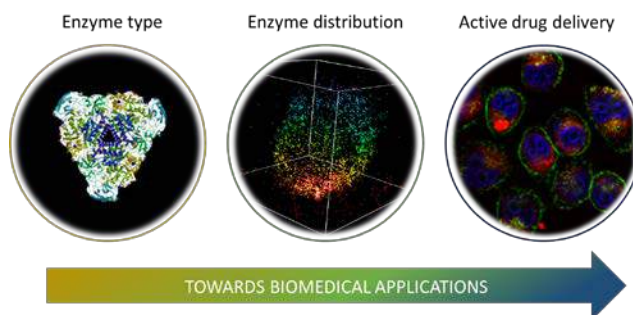
Figure 1. Schematic representation of the main aspects for the application of enzymatic motors in biomedicine.

Optical and Electrochemical Bioassays Using Photo-catalytical Activity of Semiconductor Quantum Dots

Valery Pavlov
Javier Barroso, Laura Saa, Biatriz Diez
CIC BiomaGUNE, Paseo Miramon, San Sebastian, Spain

vpavlov@cicbiomagune.es

Nanomaterials based analytical assays are becoming a promisinglow cost approach for the detection of analytes. Usually, nanomaterials like metal and semiconductor nanoparticles (SNPs) were employed in analytical systems as fluorescent and

electrochemical labels tethered to recognition elements such as antibodies and DNA oligomers, enhancers of raman scattering, fluorescence quenchers or tracers. Moreover, metal nanoparticles (NPs) can be generated *in situ* in the course of biocatalytic processes catalyzed by different enzymes. Unfortunately, metal NPs produced in situ in the above mentioned biocatalytical assays are not fluorescent thus the sensitivity of those assays is limited by the sensitivity of UV-Vis spectroscopy employed to follow the formation of gold and silver NPs. SNPs used in bioanalytical assays are fluorescent and demonstrate quantum effects. They emit photons of light upon photoexcitation hence they are referred to as quantum dots (QDs). QDs allow to use much more sensitive fluorescence spectroscopy and photoelectrochemistry to follow the readout signal. We pioneered bioassays in which analytes modulate the formation of CdS QDs *in situ*. Our early assays were applied to fluorogenic determination of enzymatic activities of enzymes such as acetylcholine esterase[1], horseradish peroxidase[2], glucose oxidase[3] etc.

We reported a new class of sensitive electrochemical assays employing generation *in situ* of QDs suitable for determination of analytes using affinity interaction and oxidative properties of metal cations. In our new immunno assay alkaline phosphatase conjugated to antibody calalyzes formation of CdS QDs[4]. Irradiation of QDs with the standard laboratory UV-illuminator results in photooxidationof 1-thioglycerol (TG) mediated by Os–PVP complex on the surface of graphite electrode at applied potential of 0.31 V vs. Ag/AgCl. (Figure 1).

We designed a new assay based on microbead linked enzymatic generation of CdS QDs (Microbead QD-ELISA) and employed it in optical and electrochemical affinity assays for the cancer biomarker superoxide dismutase 2 (SOD2) as shown in Figure 2. Biotinylated antibodies against SOD2 were immobilized on the surface of polyvinyl chloride microbeads bearing streptavidin. The analyte, SOD2 was captured on microbeads and labeled with alkaline phosphatase-conjugated antibody linked with mouse antibody against SOD2. Hydrolysis of para-nitrophenylphosphate by immobilized alkaline phosphatase triggered the rapid formation of phosphate-stabilized CdS QDs on the surface of microbeads. The electrochemical assay based on the detection with square-wave voltammograms of Cd^{2+} ions originating from immobilized CdS QDs showed linearity up to 45 ng mL^{-1}, and the limit of SOD2 detection equal to 0.44 ng mL^{-1} (1.96×10^{-11} M). This detection limit is lower by 2 orders of magnitude in comparison with that of other previously published assays for superoxide dismutase. The electrochemical assay was validated with HepG2 (Human hepatocellular carcinoma) cell lysate containing SOD2.

Cysteine (CSH) readily stabilizes CdS QDs that grow in aqueous buffered solutions. The oxidation of CSH by hydrogen peroxide (H_2O_2) at room temperature yields cystine (CSSC), which is less efficient in stabilizing CdS QDs compared to CSH. We have demonstrated that such oxidation causes a decrease in the formation rate of CSH-capped CdS QDs from Cd^{2+} and S^{2-} ions. For the first time, we combined the oxidation of CSH with the glucose oxidase (GOx)-assisted biocatalytic oxidation of D-glucose, which leads to a buildup of H_2O_2 in the reaction mixture. The enzymatically modulated *in situ* growth of CdS QDs was monitored using two techniques: fluorescence spectroscopy and photoelectrochemical (PEC) analysis. This system enables quantification of GOx and glucose in human serum[6].

We discovered that copper ions (Cu^{2+}) catalyze the oxidation of CSH by oxygen (O_2) to modulate the growth of CSH-capped CdS QDs .This new chemical process was applied to sensitive fluorogenic and photoelectrochemical (PEC) detection of Cu^{2+} ions in real samples of mineral and tap water using the photocatalytic activity of the resulting NPs. Disposable screen-printed electrodes (SPCEs) modified with electroactive polyvinylpyridine bearing osmium complex (Os-PVP) by cyclic voltammetry (CV) were employed for PEC analytical system. CdS NPs formed during the assay photocatalyze oxidation of 1-thioglycerol (TG) upon application of 0.3 V vs. Ag/AgCl to SPCEs. Os-PVP complex mediated the electron transfer between the electrode surface and CdS NPs. We proved that our assays did not suffer from interference from other ions accompanying Cu^{2+} and the sensitivity of our assays covers the European Union standard limit of Cu^{2+} ions in drinking water[7].

The other poison, methanol is frequently discovered in alcoholic beverages. We reported for the first time a new strategy for the detection of methanol using fluorescence spectroscopy and photoelectrochemical (PEC) analysis. The analytical system is based on the oxidation of CSH with hydrogen peroxide enzymatically generated by alcohol oxidase (AOx). H_2O_2 oxidizes capping agent CSH, modulating the growth of CSH-stabilized CdS QDs. Disposable screen-printed carbon electrodes (SPCEs) modified with a conductive osmium polymer (Os-PVP) complex were employed to quantify resulting CdS QDs. This polymer facilitates the

"wiring" of in situ enzymatically generated CdS QDs, which photocatalyze oxidation of 1-thioglycerol (TG), generating photocurrent as the readout signal. Likewise, we proved that our systems did not suffer from interference by ethanol. The PEC assays showed better sensitivity than conventional methods, covering a wide range of potential applications for methanol quantification.

Optical and electrochemical detection *strategies employing semiconductor growth of CdS QDs in situ* open up new opportunities for highly sensitive and selective determination of target analytes.

References

[1] L. Saa, A. Virel, J. Sanchez-Lopez,V. Pavlov, Chem. Eur. J. 16 (2010) 6187

[2] R. Grinyte, L. Saa, G. Garai-Ibabe, V. Pavlov, Chem. Commun. 51 (2015) 17152

[3] L. Saa, V. Pavlov, Small, 8 (2012) 3449

[4] J. Barroso, L. Saa, R. Grinyte, V. Pavlov, Biosens. Bioelectron. 77(2016) 323

[5] R. Grinyte, J. Barroso, M. Möller, L. Saa, V. Pavlov, ACS Appl. Mater. Interfaces, 8(2016) 29252

[6] R. Grinyte, J. Barroso, L. Saa, V. Pavlov, Nano Res. 10 (2017), 1932

[7] R. Grinyte, J. Barroso, B. Díez-Buitrago, L. Saa, M. Moller, V. Pavlov, Anal. Chim. Acta 986 (2017) 42-47.

[8] J. Barroso, B. Díez-Buitrago,L. Saa, M. Möller, N. Briz, V. Pavlov, Biosens. Bioelectron (2017) In press.

Figures

Figure 2. Microbead ELISA using biocatalytic formation of QDs for ultra high sensitive electrochemical detection.
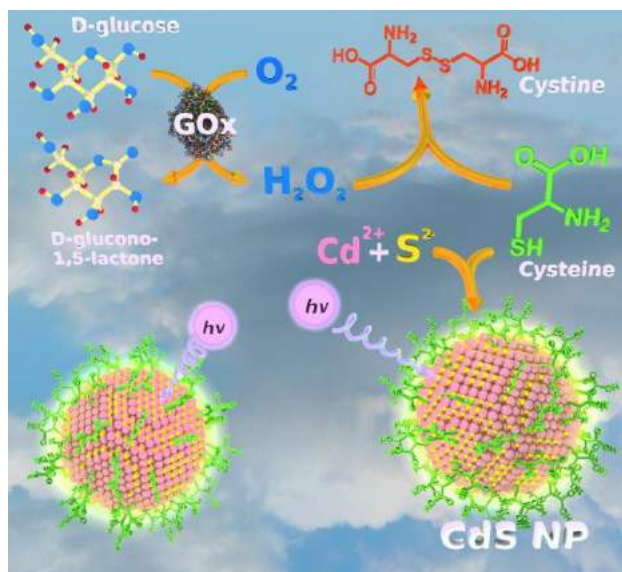
Figure 3. Fluorometric assay for glucose oxidase activity.

Figure 4. Photo-electrochemical bioassay for methanol.

Figure 1. Immunoassay using photoelectrochemical detection of enzymatically generated CdS QDs.

Novel DNA-Based Molecules and Their Charge Transport Properties

Danny Porath,

Institute of Chemistry and Center for Nanoscience and Nanotechnology, The Hebrew University of Jerusalem, 91904 Israel

danny.porath@mail.huji.ac.il

The DNA double-strand recognition, as well as the ability to manipulate its structure open a multitude of ways to make it useful for molecular electronics. Step by step we improve the synthesized constructs and the measurement methods of single DNA-based molecules. I will present new DNA-based molecules and report on our measurements of their properties. I will also present new and surprising results on dsDNA molecules.

References

[1]   "Direct measurement of electrical transport through DNA molecules", Danny Porath, Alexey Bezryadin, Simon de Vries and Cees Dekker, Nature 403, 635 (2000).

[2]   "Charge Transport in DNA-based Devices", Danny Porath, Rosa Di Felice and Gianaurelio Cuniberti, Topics in Current Chemistry Vol. 237, pp. 183-228 Ed. Gary Shuster. Springer Verlag, 2004.

[3]   "Direct Measurement of Electrical Transport Through Single DNA Molecules of Complex Sequence", Hezy Cohen, Claude Nogues, Ron Naaman and Danny Porath, PNAS 102, 11589 (2005).

[4]   "Long Monomolecular G4-DNA Nanowires", Alexander Kotlyar, Nataly Borovok, Tatiana Molotsky, Hezy Cohen, Errez Shapir and Danny Porath, Advanced Materials 17, 1901 (2005).

[5]   "Electrical characterization of self-assembled single- and double-stranded DNA monolayers using conductive AFM", Hezy Cohen et al., Faraday Discussions 131, 367 (2006). Cited 43 times

[6]   "High-Resolution STM Imaging of Novel Poly(G)-Poly(C)DNA Molecules", Errez Shapir, Hezy Cohen, Natalia Borovok, Alexander B. Kotlyar and Danny Porath, J. Phys. Chem. B 110, 4430 (2006).

[7]   "Polarizability of G4-DNA Observed by Electrostatic Force Microscopy Measurements", Hezy Cohen et al., Nano Letters 7(4), 981 (2007).

[8]   "Electronic structure of single DNA molecules resolved by transverse scanning tunneling spectroscopy", Errez Shapir et al., Nature Materials 7, 68 (2008).

[9]   "A DNA sequence scanned", Danny Porath, Nature Nanotechnology 4, 476 (2009).

[10]   "The Electronic Structure of G4-DNA by Scanning Tunneling Spectroscopy", Errez Shapir, et.al., J. Phys. Chem. C 114, 22079 (2010).

[11]   "Energy gap reduction in DNA by complexation with metal ions", Errez Shapir, G. Brancolini, Tatiana Molotsky, Alexander B. Kotlyar, Rosa Di Felice, and Danny Porath, Advanced Maerials 23, 4290 (2011).

[12]   "Quasi 3D imaging of DNA-gold nanoparticle tetrahedral structures", Avigail Stern, Dvir Rotem, Inna Popov and Danny Porath, J. Phys. Cond. Mat. 24, 164203 (2012).

[13]   "Comparative electrostatic force microscopy of tetra- and intra-molecular G4-DNA", Gideon I. Livshits, Jamal Ghabboun, Natalia Borovok, Alexander B. Kotlyar, Danny Porath, Advanced materials 26, 4981 (2014).

[14]   "Long-range charge transport in single G4-DNA molecules", Gideon I. Livshits et. al., Nature Nanotechnology 9, 1040 (2014).

[15]   "Synthesis and Properties of Novel Silver containing DNA molecules", Gennady Eidelshtein et. al., Advanced Materials 28, 4839 (2016).

Figures
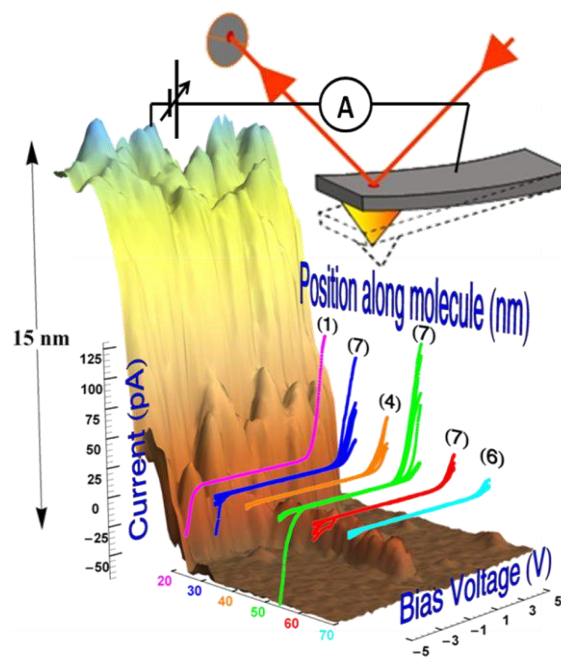
Magnetic tissue engineering of the vocal fold: generation of 3D cell constructs using superparamagnetic iron oxide nanoparticles

Marina Pöttler[1]

Eveline Schreiber[1], Anne Schützenberger[2], Michael Döllinger[2], Christoph Alexiou[1], Stephan Dürr[2]

[1]Department of Otorhinolaryngology, Head and Neck Surgery, Section of Experimental Oncology and Nano-medicine (SEON), Else Kröner-Fresenius-Stiftungsprofessor, University Hospital Erlangen, Germany
[2]Department of Otorhinolaryngology, Head and Neck Surgery, Section of Phoniatrics and Pediatric Audiology, University Hospital Erlangen, Germany
Marina.poettler@uk-erlangen.de

Introduction

The principles of biology and engineering are combined in tissue engineering to generate functional replacement for damaged tissue. Growing interest on new approaches, including nanotechnology, are promising solutions for overcoming the rejection of transplanted organs. Tissue engineering comprises the isolation of autologous cells from healthy tissue or stem cells, cultivation and proliferation of these cells and finally generation of 3D-structures resembling functional tissue structures. Even though expertise of these methods in tissue engineering has been established, there is still scope for enhancement. *In vivo* tissue has a complex cellular organization and defined arrangements of cells need to be established. Therefore, techniques to manipulate and remotely control cellular behaviour can deliver a powerful tool for tissue engineering. Such a tool bargains Magnetic Tissue Engineering (MTE) [3,4]. The underlying concept includes cellular uptake of magnetic nanoparticles and the usage of external magnetic fields to manipulate and remotely control magnetized cells and their behaviour. As the voice is the basic instrument of oral communication [1], tissue defects in this region lead to serious aggravation in quality of life. Briefly, voice is produced by vibrations of the vocal fold via an air flow from the lungs. Until now, no satisfactory possibilities for vocal fold replacement exist [2].
We aim for an establishment of a functional vocal fold transplant in a rabbit model by MTE using superparamagnetic iron oxide nanoparticles (SPION).

Methods

Rabbit vocal fold fibroblasts (VFF) were incubated for 24 h with different concentrations of SPIONs (20, 40 or 80 µg/cm^2). Vocal fold cell behaviour under SPION treatment was tested extensively for adhesion, spreading and migration, which are important for formation of 3D-structures. The possibility of magnetic guidance of SPION-loaded cells was tested in 2D. 1 x 10^5 SPION loaded VFFs were seeded in 6-well plates were a 24-well magnet-plate (Fig. 1, B) was positioned below. Cells were allowed to adhere for 24 h. To generate 3D VFF cell-constructs, 1 x 10^6 cells loaded with 20 µg/cm^2 SPIONs were placed in a 24- well plate with a magnet above to induce MTE (Fig. 2).

Results

The effects of SPIONs on cell behaviour were dose-dependent for adhesion, with good tolerability observed up to the nanoparticle concentration of 20 µg/cm^2, migration and spreading were not significantly influenced by SPION uptake up to 80 µg/cm^2 [6]. Magnetically guidance of cells loaded with SPIONs (20 and 40 µg/cm^2) was demonstrated in 2D with cells only growing in areas where a magnet is present [5,6] (Fig.1). To establish a 3D structure of VFFs, a magnet (0.7 T) was placed above the cell culture-plate and cells loaded with 20 µg/cm^2 were able to generate a 3D cell-construct after 24h. (Fig. 2)

Conclusion and Discussion

Here, we present first results of Magnetic Tissue Engineering (MTE) for voice rehabilitation. To develop 3D cell-structures, cell behaviour, which affects cell-cell interactions, must not be affected by SPION uptake. Therefore, cell features including adhesion, spreading and migration were proven to be intact after SPION treatment. As a proof of principle for magnetic cell guidance, SPION loaded vocal fold fibroblasts were allowed to "choose" either to grow on the side were a magnet or none was placed. Interestingly, 5 and 20 µg/cm^2 are sufficient to induce cell growth solitary at site of the magnet in 2D. Furthermore, magnetic cell guidance as only initiator for 3D cell-construct formation was proven to work with very low amounts of SPIONs 5 µg/cm^2). Next steps include the isolation of epithelial cells and establishment of functional multi-layered 3D co-cultures, as well as the proof of functionality in a flow channel model of the rabbit larynx. Our results will constitute a solid basis for a successful transfer of this technique into humans, in order to provide a functional and personalized vocal fold transplant. This is particularly important for patients, who suffer from dysphonia as a consequence of a vocal fold tissue defect, and will help to improve their quality of life.

References

[1] Rosanowski, F.; Grassel, E.; Hoppe, U.; Kollner, V. HNO 2009, 57, (9), 866-72.
[2] Ling, C.; Li, Q.; Brown, M. E., et al. Sci Transl Med 2015, 7, (314), 314ra187.
[3] Perea, H.; Aigner, J.; Heverhagen, J. T.; Hopfner, U.; Wintermantel, E. J Tissue Eng Regen Med 2007, 1, (4), 318-21.

[4] Horch, R. E.; Boos, A. M.; Quan, Y., et al. J Cell Mol Med 2013, 17, (10), 1197-206.

[5] Dürr S, Bohr C, Pöttler M, Lyer S, Frie-drich RP, Tietze R, Döllinger M, Alexiou C, Janko C. Anticancer Res. 2016 Jun;36(6):3085-91.

[6] Pöttler M, Fliedner A, Schreiber E, Janko C, Friedrich RP, Bohr C, Döllinger M, Alexiou C, Dürr S.Nanoscale Res Lett. 2017 Dec;12(1):284.
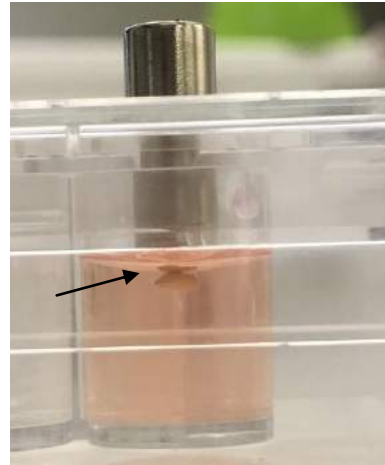
Figures

Figure 2, 3D VFF cell construct (arrow) in 48 well-plate after 24h. Magnet on top (outside of lid) retains magnet in well. Cells were incubated for 24 h with 20 µg/cm2 SPIONs. 1 x 10^6 cells were used for construct formation.
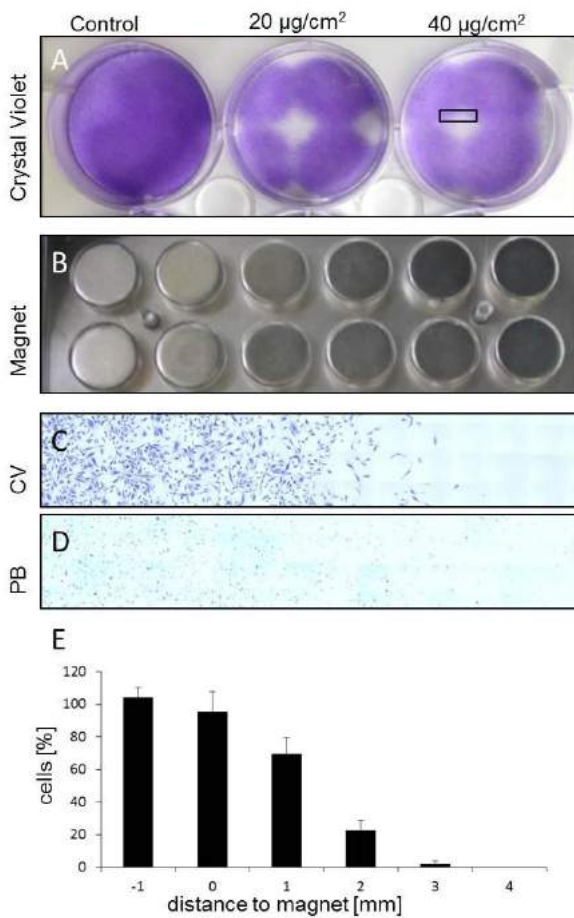
Figure 1. 2D cell-control: A: Magnetic field induced VFF cell-growth, control cells are not loaded with SPIONs, VFFs (SPION concentrations as indicated) only grow in magnetic zones. B: 24- well magnet-plate. C and D: magnification of A (rectangle) with cells stained with Crystal Violet (C) and Prussian Blue (iron) (D). F: Cell concentrations of magnetized VFFs in distance to magnet.

Nanomedicines for the local and targeted treatment of glioblastoma

Véronique Préat[1],
Chiara Bastiancich, John Bianco, Mengnan Zhao,
Pallavi Ganipineni, Fabienne Danhier,

[1]Université catholique de Louvain, Louvain Drug Research Institute, Advanced Drug delivery and biomaterials, avenue Mounier, 73 B1.73.12, 1200 Brussels, belgium,

veronique.preat@uclouvain.be

Abstract

Glioblastoma (GBM) treatment includes, when possible, surgical resection of the tumor followed by chemoradiotherapy but the survival remains low. The local and targeted systemic delivery of anticancer drug-loaded nanomedicines to treat GBM after surgical resection of the tumor could be a promising strategy.

Introduction

Among central nervous system tumors, glioblastoma (GBM) is the most common, aggressive and neurological destructive primary brain tumor in adults. Standard care therapy for GBM consists in surgical resection of the accessible tumor (without causing neurological damage) followed by radiotherapy and oral chemotherapy with an alkylating agent temozolomide (TMZ). However, recurrences quickly develop around the resection cavity borders leading to patient death. Despite the efforts of the scientific community to increase the long-term benefits of GBM therapy, at the moment GBM remains incurable. Several obstacles limit the effectiveness of GBM treatments: (i) the anatomical location of the tumor in the brain often impedes a complete surgical resection (ii) the central nervous system barriers such as the blood brain barrier (BBB) represent a challenge to the delivery of cytotoxic drugs at therapeutic concentrations at the tumor site (iii) GBM is highly heterogeneous at all levels (iv) the hallmark characteristics of GBM are uncontrolled cellular proliferation, propensity for necrosis and angiogenesis, resistance to apoptosis, high genomic instability and chemoresistance. GBM cells are able to extend their tendrils into the normal surrounding parenchyma infiltrating diffusely beyond the primary lesion in the early stages of tumor development [1].

In vitro and in vivo models of experimental glioma are useful tools to gain a better understanding of GBM and to investigate novel treatment strategies. However, the majority of preclinical models focus on treating solid intracranial tumours, despite surgical resection being the mainstay in the standard care of patients with GBM today. The lack of resection and recurrence models therefore led us to develop a novel orthotopic tumour resection and recurrence model that has potential for the investigation of local and systemic delivery strategies in the treatment of GBM. We showed that tumour resection is well tolerated, does not induce deleterious neurological deficits, and significantly prolongs survival of mice bearing U87MG GBM tumours. In addition, the resulting cavity could accommodate adequate amounts of hydrogels for local delivery of chemotherapeutic agents to eliminate residual tumour cells that can induce tumour recurrence [2].

Local delivery of nanomedicine

Among the strategies that have been adopted in the last two decades to find new and efficacious therapies for the treatment of GBM, the local delivery of chemotherapeutic drugs in the tumor resection cavity emerged [3]. We developed two formulation of anticancer nanomedicines that can be included perisurgically in the resection cavity of orthotopic GBM.

We hypothesized that a polyethylene glycol dimethacrylate (PEG-DMA) injectable hydrogel would provide a sustained and local delivery of TMZ. The hydrogel photopolymerized rapidly (<2min) and presented a viscous modulus (≈10kPa). The in vivo tolerability study showed that the unloaded hydrogel did not induce apoptosis in mice brains nor increased microglial activation. In vivo, the anti-tumor efficacy of TMZ-hydrogel was first evaluated on xenograft U-87MG tumor-bearing nude mice. The tumor weight of mice treated with the photopolymerized TMZ hydrogel drastically decreased compared with all other groups [4]. The photopolymerizable TMZ-loaded hydrogel was also tested in the resection model of U-87MG GBM. When combined with paclitaxel (PTX)-loaded nanoparticles, it significantly prolonged the mice survival compared to mice undergoing the resection (unpubished data).

Gemcitabine is a chemotherapeutic agent that has a different mechanism of action compared to alkylating agents and shows excellent radio-sensitizing properties. We developed an injectable gel-like nanodelivery system consisting in lipid nanocapsules loaded with anticancer prodrug lauroyl-gemcitabine (GemC12-LNC) in order to obtain a sustained and local delivery of this drug in the brain and to bypass the blood brain barrier, thus reaching high local concentrations of the drug. The GemC12-LNC formed a gel and showed a sustained and prolonged in vitro release of the drug over one month. GemC12 and the GemC12-LNC increased in vitro cytotoxic activity on U-87MG glioma cells compared to the parent hydrophilic drug. The GemC12-LNC hydrogel reduced significantly the size of a subcutaneous human GBM tumor model compared to the drug. Short-term tolerability studies showed that this system is suitable for local treatment in the brain. This proof-of-concept study demonstrated the feasibility, safety and efficiency of the injectable GemC12-LNC hydrogel for the local

treatment of GBM [5]. We then administered GemC12-LNC hydrogel for the local delivery of GemC12 in an orthotopic xenograft model of GBM. The GemC12-LNC hydrogel was well tolerated when injected in mouse brain. After intratumoral administration, GemC12-LNC significantly increased mice survival compared to the controls. Moreover, its ability to delay tumor recurrences was demonstrated after perisurgical administration in the GBM resection cavity. In conclusion, we demonstrate that GemC12-LNC hydrogel could be considered as a promising tool for the post-resection management of GBM, prior to the standard of care chemo-radiation [6].

Targeted delivery of nanomedicines

Targeted nanotheranostics are promising multifunctional system with nano-size, possibility of surface functionalization, diagnostic and therapeutic capabilities. Loss of BBB integrity is a characteristic of GBM that could justify the systemic treatment. Super Paramagnetic Iron Oxides (SPIO) have dual advantage of detection by magnetic resonance imaging (MRI) (reduction of relaxation times) and magnetic property for a targeting strategy using external magnet [7]. We hypothesized that PTX/SPIO loaded PLGA-based nanoparticles could be a potential nanotheranostic system to image and treat gliomas.

PTX/SPIO loaded PLGA-based nanotheranostic particles were prepared [7]. In vitro cellular studies U-87MG cell line confirmed that the cytotoxic effect was solely due to PTX. By investigating BBB disruption in U87MG glioma tumor model using MRI after intravenous injection of T1 contrast agent, we validated that the BBB was disrupted. In vivo biodistribution studies showed that NP did not cross the intact BBB in healthy mice whereas in GBM bearing mice, brain samples were traced with significant quantities of SPIO. Magnetic targeting increased the amount of SPIO detected. Preliminary in vivo efficacy results of PTX/SPIO-PLGA NP intracranial injection in orthotopic U-87MG GBM tumour showed significantly improved mice survival rate when compared to controls. Intravenous injection associated with magnetic targeting also increased mice survival. (unpublished data).

References

[1]   Bianco J, Bastiancich C, Jankovski A, des Rieux A, Préat V, Danhier F. Cell Mol Life Sci. 74 (2017) 2451-2466.

[2]   Bianco J, Bastiancich C, Joudiou N, Gallez B, des Rieux A, Danhier F.J Neurosci Methods. 284 (2017) 96-102.

[3]   Bastiancich C, Danhier P, Préat V, Danhier F.J Control Release. 243 (2016) 29-42

[4]   Fourniols T, Randolph LD, Staub A, Vanvarenberg K, Leprince JG, Préat V, des Rieux A, Danhier F.J Control Release. 210 (2015) 95-104.

[5]   Bastiancich C, Vanvarenberg K, Ucakar B, Pitorre M, Bastiat G, Lagarce F, Préat V, Danhier F. J Control Release. 225 (2016) 283-293.

[6]   Bastiancich C, Bianco J, Vanvarenberg K, Ucakar B, Joudiou N, Gallez B, Bastiat G, Lagarce F, Préat V, Danhier F. J Control Release. 264 (2017) 45-54

[7]   Schleich N, Po C, Jacobs D, Ucakar B, Gallez B, Danhier F, Préat V. J Control Release. 194 (2014) 82-91.

Figures
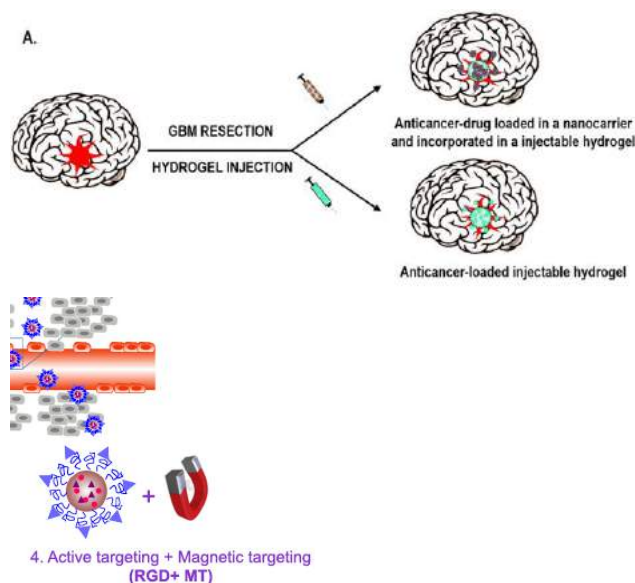
Figure 1. Strategies used for GBM treatment by nanomedicines A. local delivery of hydrogel containing nanomedicines B. Systemic delivery of nanomedicines targeted by RGD and/or magnetic targeting. (adapted from [3]and [7]).

SEEC technology mediated label-free nano-biofilm characterization

Archana Ramadoss[1],
A.Ducret[2], M.P.Valignat[2], F.Mouhamar[2], T.Mignot[2], and O.Theodoly[2]

[1]Nanolane, Pôle Novaxud, 57 Boulevard Demorieux, 72000 Le Mans, France
[2] Laboratory Adhesion & Inflammation, Aix-Marseille University; Inserm UMR 1067; CNRS, France

archana.ramadoss@eolane.com

Abstract:

Studies on molecular interactions are of immense interest in biological research. Label-free, real-time imaging of such interactions provides greater insights into such interaction studies. SEEC Microscopy offers highly enhanced contrast that permits live imaging and quantification of nanoscale samples such as thin films in solutions. The enhancement of optical contrast is attributed to specially designed substrate coatings in which multiple reflections and interferences yield dark background and very high contrast sensitivity to thin surface deposits. Using SEEC Microscopy, we show that we can perform live imaging and characterize the slime deposits during bacterial locomotion, at an unprecedented resolution.

Bacterial nanofilm, "the slime", is produced by bacteria during its locomotion such as gliding. Bacterial slime is implicated in its locomotion. Currently, techniques such as, Electron Microscopy (EM), Fluorescence Microscopy are employed to visualize the slime [1]. These methods do not permit simultaneous imaging and quantitative characterization of the slime produced during bacterial locomotion. However, aside from being invasive, Fluorescence techniques also result in sample photo bleaching. Therefore, limited studies have been performed so far to elucidate the importance of slime during such locomotion. SEEC Microscopy is a new generation technology that offers competitive edge for visualizing and quantifying dynamic nano-events. SEEC technology has been successfully employed to visualize molecular interactions such as enzyme induced substrate polymerization reaction, lipid-protein interaction studies [2, 3].

Our present work exploits the enhanced axial resolution of SEEC Microscopy to visualize and quantify nano-biofilms such as bacterial slime [1]. Live quantitation of bacterial slime production and topographical analysis of the nano-biofilm shows that bacterial slime thickness varies between 0 nm and 5 nm and the slime width varies between 300 nm and 900 nm.

Cumulative graphic summary of the slime trail deposition, as shown in Figure 1, suggests that the slime trail is not continuous but extends as discontinuous segments from patchy and scattered depositions. Further, these results show that the amount of slime deposition is directly correlated to time of residence of the bacterial cell at a given location.

Visualizing the slime, which is up to 1000-fold thinner than a bacterial cell, demonstrates the power of SEEC Microscopy to detect extremely tenuous dynamic biological films.

Reference

[1] Ducret, A., Valignat, M.P., Mouhmar, F., Mignot, T., and Theodoly, O., Proc Natl Acad Sci U S A. **109**(2012), 10036-10041.

[2] Egea, A., Metivier, M., Crogeunnoc, P., Remaud-Simeon, M., and Vieu, C., BioNanoScience. **4**(2014), 37-45.

[3] Gunnarsson, A., Bally, M., Jonsson, P., Médard, N., and Hook, F, Annal.Chem. 84(2012), 6538-6545.

Acknowledgements
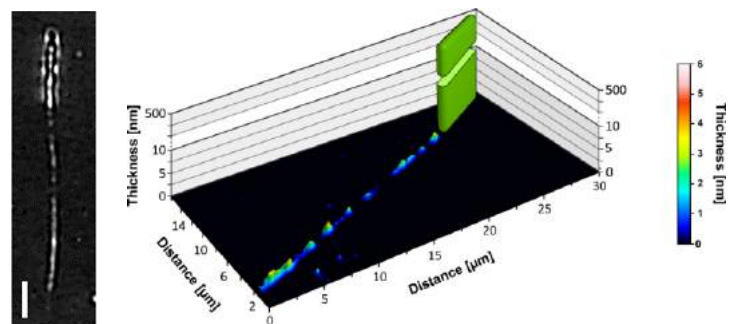
Figures

Figure 1. Real-time monitoring and topographical analysis of bacterial slime trail. Left. Representative SEEC image of slime. Right. Quantitative summary of the produced slime trail.

Theranostic nanocapsules for hyperthermia

Pilar Rivera Gil,

Department of Experimental and Health Sciences,
Pompeu Fabra University

pilar.rivera@upf.edu

Theranostics is a medical strategy combining diagnostics with therapeutics. Based on the results of diagnostic tests on patients, a targeted drug therapy is created; thus, giving rise to a more specialized medicine. In molecular theranostics, a tool of information (ion homeostasis, proteins, genes, etc) is required for the design of the most adequate therapy for a patient to avoid unnecessary treatment. By monitoring the response to the treatment, drug selection and efficacy can also be optimized. The requirements that such a theranostic tool must have are within others, (i) to be biocompatible and small enough to ensure outstanding biodistribution, (ii) to entrap a payload and protect it from the physiological milieu (also healthy tissue from the drug), (iii) to give a feedback from the treatment response or to detect analytes imbalances, etc. Nowadays there is no single material capable of performing all these actions and therefore, composite materials are required. By integrating various materials with different properties within a single matrix, all required functionalities can be combined in one single structure. Nanotechnology allows us playing Lego using nanoparticle building blocks with different physicochemical properties that are combined to create a multifunctional, composite material intelligent enough to perform and fulfill the requirements mentioned above. Our theranostic nanoplatform are plasmonic nanocapsules which are currently being characterized to perform diagnosis (sensing) and treatment. We have already proven the capacity of these capsules to monitor changes in the concentration of nitric oxide inside living cells (i.e. the lysosome) at real time and at the level of a single capsules. Now we are studying their ability for the hyperthermia treatment of tumor cells in 3D cultures. We will present current results on this topic.

Targeting mononuclear phagocytes for eradicating intracellular parasites

Loris Rizzello[1],
J.D. Robertson[1,2], P.M. Elks, A. Poma[3,4], N. Daneshpou[1], T.K. Prajsnar[2], D. Evangelopoulos[7], J.O. Caneseco[7], S.Yona[8], H.M. Marriott[3,6], D.H. Dockrell[3,6], S. Foster[5,6], B. De Geest[9,10], S. De Koker[11], T. McHugh[7], S.A. Renshaw[3,4,6], G. Battaglia[1,12]

1 Department of Chemistry, University College London, London UK
2 Department of Biomedical Science, University of Sheffield, Sheffield, S10 2TN, UK
3 Department of Infection, Immunity, and Cardiovascular Disease, University of Sheffield Medical School, Beech Hill Road, Sheffield, S10 2JF, UK
4 The Bateson Centre, University of Sheffield, Firth Court, Western Bank, Sheffield, S10 2TN, UK
5 Department of Molecular Biology and Biotechnology, University of Sheffield, Sheffield, S10 2TN, UK
6 The Florey Institute, University of Sheffield, Sheffield, S10 2TN, UK
7 Department of Clinical Microbiology, University College London, Royal Free Hospital, London, NW3 2PF, UK
8 Faculty of Medical Sciences, Division of Medicine, University College London, London, WC1 6JJ, UK
9 Department of Pharmaceutics, Ghent University, Ghent, Belgium
10 Cancer Research Institute Ghent, Ghent, Belgium
11 Department of Biomedical Molecular Biology, Ghent University, Belgium
12 Department of Chemical Engineering, University College London, London UK

l.rizzello@ucl.ac.uk

ABSTRACT

Mononuclear phagocytes such as monocytes, tissue-specific macrophages and dendritic cells are primary actors in both innate and adaptive immunity, as well as tissue homoeostasis.[1] They have key roles in a range of physiological and pathological processes, so any strategy targeting these cells will have wide-ranging impact. These phagocytes can be parasitized by intracellular bacteria, turning them from housekeepers to hiding places and favouring chronic and/or disseminated infection. One of the most infamous is the bacteria that cause tuberculosis, which is the most pandemic and one of the deadliest disease with one third of the world's population infected, and 1.8 million deaths worldwide in 2017.[2-4] Here we demonstrate the effective targeting and intracellular delivery of antibiotics to both circulating monocytes and resident macrophages, using pH sensitive nanoscopic polymersomes made of poly(2-(methacryloyloxy)ethyl phosphorylcholine)-co-poly(2-(di- isopropylamino)ethyl methacrylate) (PMPC-PDPA).[5] Polymersome selectivity to mononuclear phagocytes is demonstrated and

ascribed to the polymerised phosphorylcholine motifs affinity toward scavenger receptors. We subsequently explored the inherent affinity of PMPC-PDPA polymersomes towards phagocytes *in vivo* using mice as model organism. Upon intravenous (i.v.) tail injection, we measured the plasma PMPC-PDPA $Cp(t)$ polymersomes concentration as a function of time (**Figure 1a**). The plasma concentration decays according to two phases, ($Cp(t) = C1\mathrm{e}(-\lambda 1 t) + C2\mathrm{e}(-\lambda 2 t)$) where about 84.5% of the polymersomes are quickly eliminated from the plasma with a fast half-life of τF=ln2=0.4hr=25min, and $1/2$ $\lambda 1$ the remaining amount is removed with slow half-life of τS=ln2=20.5hr. We then measured the uptake of polymersomes in the different blood cell types by flow cytometry and observed a remarkable selectivity of PMPC-PDPA polymersomes for monocytes (Ly6C+ cells) with over 98% of these positive only 5min after i.v. injection (**Figure 1b**). This is in contrast to about 12% of B cells, 7% of T cells and 6% of neutrophils while red blood cells did not show any detectable level of polymersomes uptake. These are remarkable results considering monocytes make up only about 2% of the total blood cell population, strongly supporting the ability of PMPC-PDPA polymersomes to selectively target monocytes. The ability of polymersomes to distinguish sub-classes of monocytes including classical (Ly6C high) and non-classical monocytes (Ly6C low) was assessed. Classical monocytes internalised polymersomes more efficiently at early time points (after 10 minutes post injection, **Figure 1c**, red). However, 24 hours post injection, the non-classical monocytes more readily took up polymersomes (**Figure 1c**, blue)
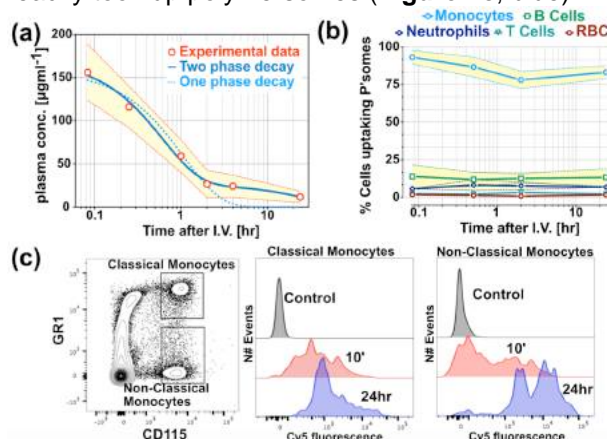
Figure 1. Bioavailability of polymersomes

We then demonstrated the PMPC-PDPA efficacy in delivering antimicrobials to reduce bacterial burden by using *S. aureus*, *M.bovis*-BCG, *M. tuberculosis*, and *M. marinum*. The encapsulation efficiency of vancomycin, gentamicin, lysostaphin, rifampicin, isoniazid was assessed (**Figure 2a**). Treatment with polymersomes loaded with rifampicin or gentamicin improved the drug efficacy and reduced the number of viable *S. aureus* in THP-1 cells compared with controls (**Figure 2b**). Encapsulation of lysostaphin or

vancomycin within polymersomes did not significantly improve or hinder drug efficacy. The enhancement of rifampicin and gentamicin at killing intracellular *S. aureus* compared to the same dose of free drugs can be ascribed to improved intracellular delivery and the consequent increase in drug reaching the intracellular pathogen. For both BTG and *M. tuberculosis*, we limited our screening to rifampicin and isoniazid either alone or in combination mirroring the most common therapeutical approach used for the treatment of tuberculosis. With respect to BCG infection, no significant differences were observed in CFU after 1 day of treatment (**Figure 4c**); only the free rifampicin was able to reduce the bacterial colonies. However, a signifi- cant difference was observed after 72 hours of treatment, where both rifampicin and isoniazid-encapsulated polymersomes elicited a clear reduction in bacteria compared to the free drug (**Figure 4c**). Notably, the ri- fampicin/isoniazid co-loaded polymersomes completely eradicated the intracellular BCG after 72 hours (no CFU detected). Similar results were observed with *M. tuberculosis* infected THP-1 cells (**Figure 4d**). In this case, after 24 hours of treatment, the multiple drug co-loaded polymersomes significantly reduced bacterial burden compared to the controls. Moreover, this drug formulation was also able to eradicate intracellular *M. tuberculosis* after 72 hours of treatment (**Figure 4d**).
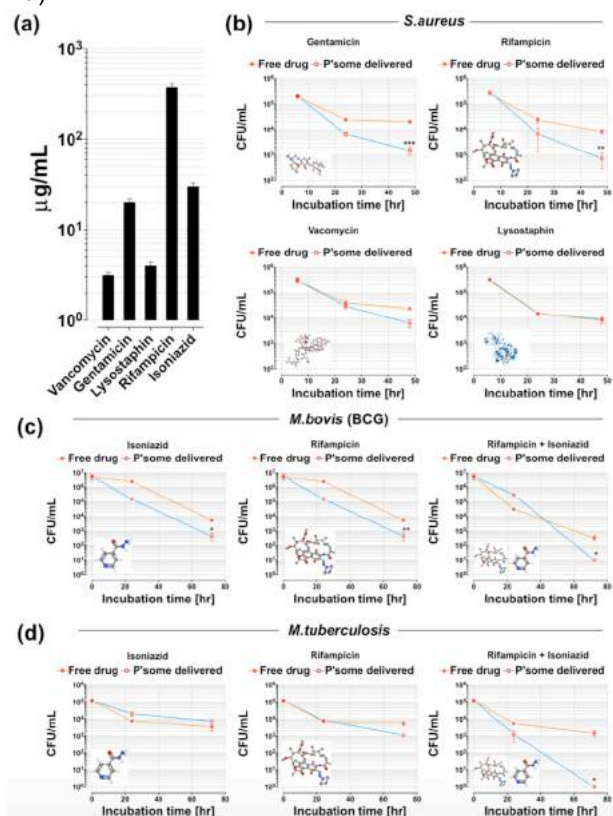
Figure 2. Polymersome mediated drug delivery in human macrophages.

To demonstrate the therapeutic impact of polymersomes in zebrafish, we tested the ability of polymersomes encapsulated antibiotics to reduce bacterial burden *in vivo*. Zebrafish embryos were infected with mCherry-expressing *M. marinum*, and with GFP expressing *S. aureus*. To compare the effect of encapsulated antimicrobials and free antimicrobials to treat *S. aureus* infection, zebrafish embryos (2 d.p.i.) were injected with *S. aureus* followed by a second injection of drug loaded polymersomes 20 hours later. We assessed the efficacy of the four drugs tested *in vitro*, lysostaphin, vancomycin, gentamicin and rifampicin (**Figures 3a-b**). In agreement with the *in vitro* results, only encapsulated rifampicin and gentamicin treatment improved the outcome of infection. Lysostaphin and vancomycin did not change the outcome of infection, with similar numbers to the control groups showing high numbers of bacteria (**Figure 3a**). The polymersomes-encapsulated rifampicin was the most effective treatment, resulting in a reduction in the bacterial CFU and preventing the fish from succumbing to overwhelming infections. Polymersomes did improve considerably the output with the rifampicin formulation getting very low CFU and with survival close to 100%. The efficacy of polymersomes delivered rifampicin was confirmed using a second *in vivo* model, the *M. marinum* infected zebrafish model of TB. In this case, mCherry-expressing fluorescent bacteria were microinjected, and 24 hours later an injection of the polymersomes-encapsulated drugs (or controls) was performed. As was the case for *S. aureus* infected zebrafish, rifampicin-encapsulated polymersomes signif- icantly reduced the *M. marinum* burden *in vivo*, compared to the same concentration of free drug (**Figures 3b**).
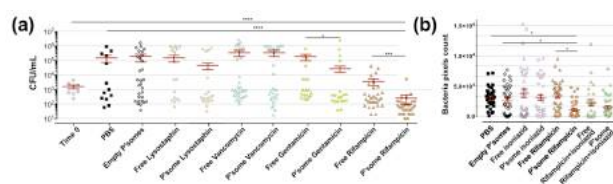
Figure 3. Commonly used antimicrobials encapsulated in polymersomes can be used to treat infection *in vivo*.

References

[1] F. Ginhoux *et al.* Nat. Rev. Immunol., 14 (2014) 392

[2] G. Ferrari, et al. Cell 97(1999) 435

[3] S. Kaufmann. Nat. Rev. Imm. 1 (2001) 20

[4] G. Weiss *et al. Imm. Rev.* 264 (2015) 182

[5] G. Battaglia *et al.* Nat. Mater. 4 (2005) 869

Quantification of CNT dose delivered to cell surfaces by UV-Vis-NIR spectroscopy.

L. Rodriguez-Lorenzo[1],
D. Septiadi[1], S. Balog[1], S. Chortarea[1], H. Barosova[1],
M. Spuch[1], A. Petri-Fink[1,2], B. Rothen-Rutishauser[1]

[1] Adolphe Merkle Institute, University of Fribourg, Chemin des Verdiers 4, 1700 Fribourg, Switzerland
[2] Department of Chemistry, University of Fribourg, Chemin du Musée 9, 1700 Fribourg, Switzerland)

laura.rodriguez-lorenzo@unifr.ch

The overt toxicity of carbon nanotubes (CNTs) is often assessed using *in vitro* methods,[1,2] but determining a dose-response relationship is still a challenge.[3] We demonstrate for the first time, to the best of our knowledge, an analytical approach to accurately determine the *in vitro* dosimetry of CNTs suspended in protein-rich cell culture media by UV-Vis-NIR spectroscopy to either monitor the decrease of CNTs concentration in the media suspension, or to directly measure the deposition of CNTs on cells grown on the bottom surface of a plastic well (Figure 1).[4] The presented approach is simple, inexpensive and requires a spectrophotometer fairly accessible to standard laboratories working with nanomaterials. We have shown that the optimized protocol is independent of the dispersion method or cell culture medium, thereby making it applicable to CNT suspensions ranging from well-dispersed to poorly defined and very heterogeneous dispersions derived from CNT powders. Furthermore, neither extensive CNT physicochemical characterization nor modelling are required, thus minimizing the potential for systematic errors. Moreover, this approach could also be adapted for other types of carbon-based nanomaterials (*e.g.*, graphene) or exposure techniques (*e.g.*, air liquid interface exposure).

References

[1] Donaldson K, Aitken R, Tran L, Stone V, Duffin R, Forrest G, et al. *Toxicol Sci*, 92 (2006): 5-22.
[2] Madani SY, Mandel A, Seifalian AM. *Nano Reviews,* 4 (2013): 21521
[3] DeLoid G, Cohen JM, Darrah T, Derk R, Rojanasakul L, Pyrgiotakis G, et al. *Nat Commun,* 5 (2014): 3514.
[4] Septiadi D, Rodriguez-Lorenzo L, Balog S, Chortarea S, Barosova H, Spuch M, et al. Submitted.

Figures
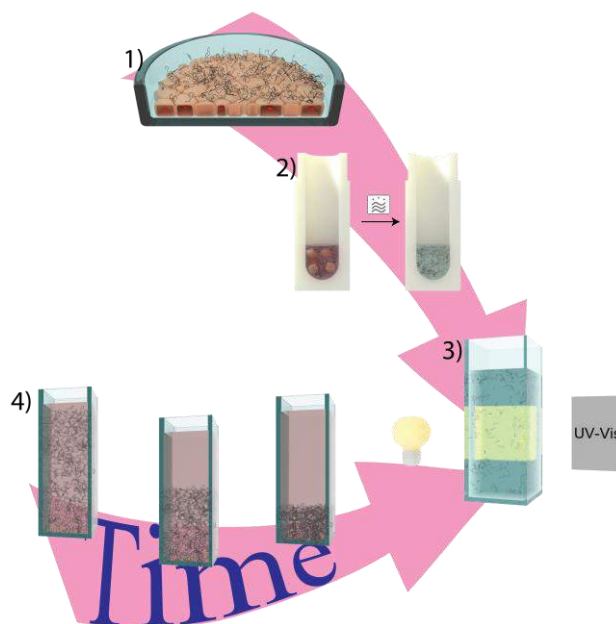
Figure 1. A schematic illustration of the experimental steps to determine the delivered dose of CNTs onto the surface of cells grown on the bottom of a plastic flask including (1) incubation of CNTs in complete cell culture media, (2) microwave-assisted acid digestion and oxidation treatment the CNT incubated cells, and (3) UV-Vis-NIR spectroscopy analysis to determine the cell associated CNT fraction. The step 4) shows the indirect method to quantify of the delivered dose through the monitoring of the CNTs depletion (*e.i.* the decrease of CNTs concentration in the suspension) as function of time *in situ*.

Enzyme Catalysis to Power Nanovehicles Towards Nanomedicine

Samuel Sánchez[1,2,3],

[1]Institute for Bioengineering of Catalonia (IBEC), The Barcelona Institute of Science and Technology, Barcelona Spain
[2]Max Planck Institute for Intelligent Systems Institution, Stuttgart, Germany
[3] Institució Catalana de Recerca i Estudis Avancats (ICREA), Barcelona, Spain

ssanchez@ibecbarcelona.eu

Engineering tiny bots that can be applied in life science is opening many avenues in fields such as robotics, biosensing, nanomedicine, on-chip microfluidics and more [1]. One example could be the active and direct transport of drugs to specific locations enabled by hybrid micro-nano-bots, which are powered by highly efficient enzymatic catalytic reactions. [2]

Here, I will present our recent developments in the field of bio- and nano-engineering systems that can be autonomously swim and perform complex tasks. We fabricate nano-bots from mesoporous silica nanoparticles [3], microcapsules[4], and nanotubes [5]. Our types of hybrid Nano-bots combine the best from the two worlds, biology and nanotechnology providing remote control with biocompatible fuels. We recently demonstrated the motion of nanomotors in glucose and urea fuel, overcoming the limitations of former systems where toxic fuels were employed. Current results are devoted into the internalization of nanomotors into living cells and their motion in 3D bioenginnered complex media.

References

[1]   S. Sanchez, Ll. Soler and J. Katuri. Angew.Chem.Int.Edit. 2015, 54,1414-1444
[2]   X. Ma, A. C. Hortelao, T. Patiño, S. Sanchez. ACS Nano 2016 10 (10), 9111-9122
[3]   X. Ma, A. Jannasch, U-R Albrecht, K. Hahn, A. Miguel López, E. Schäffer and S. Sanchez. Nano Lett. 2015, 15, 7043–7050.
[4]   X. Ma, X. Wang, K. Hahn, S. Sanchez. ACS Nano. 2016, 10, 3597–3605
[5]   X. Ma, A. C. Hortelao, A. Miguel-López and S. Sánchez. J. Am.Chem.Soc. 2016, 138 (42), 13782-13785

Biotransformation and biological impact of graphene-related materials during simulated oral ingestion

Paola Sánchez-Moreno [1],
Daniela Guarnieri[1], Antonio Esau Del Rio Castillo[2], Francesco Bonaccorso[2], Francesca Gatto[1,3], Giuseppe Bardi[1], Cristina Martin[4,5], Ester Vázquez[4,5], Tiziano Catelani[6], Stefania Sabella[7], and Pier Paolo Pompa[1]

[1] Nanobiointeractions&Nanodiagnostics, Istituto Italiano di Tecnologia (IIT), Via Morego, 30 – 16163 Genova, Italy
[2] Graphene Labs, Istituto Italiano di Tecnologia, Via Morego, 30 – 16136 Genova, Italy
[3] Department of Engineering for Innovation, University of Salento, Lecce, Italy
[4] Departamento de Química Orgánica, Facultad de Ciencias y Tecnologías Químicas, Universidad de Castilla-La Mancha, 13071 Ciudad Real, Spain
[5] Instituto Regional de Investigación Científica Aplicada (IRICA), Universidad de Castilla-La Mancha, 13071 Ciudad Real, Spain
[6] Electron Microscopy Facility, Istituto Italiano di Tecnologia, Via Morego 30 – 16163 Genova, Italy
[7] Drug Discovery and Development Department, Istituto Italiano di Tecnologia, Via Morego, 30 – 16136 Genova, Italy.

paola.sanchez@iit.it

Graphene is endowed with superb properties that make it potentially applicable in many technological and biomedical fields. Therefore, the potential for widespread human exposure to graphene-related materials (GRMs) raises safety concerns[1]. For this reason, studying the behavior of GRMs in a biological context is crucial to assess any possible impact on human health[2,3]. In this work, we investigated the biotransformation of few layer pristine graphene (FLG) and graphene oxide (GOx) and their biological effect following the ingestion route. We used a dynamic *in vitro* digestion assay to mimic the passage of FLG and GOx through the different gastro-intestinal (GI) tract environments (salivary, gastric and intestinal)[4], schematically represented in Figure 1. The assay is part of a standard operating procedure (SOP) developed in the EU project NANoREG (A common European approach to the regulatory testing of nanomaterials. http://www.nanoreg.eu/). A detailed characterization by Raman spectroscopy was carried out to assess the impact of each step of the *in vitro* digestion (including strong pH variations, degradative enzymes, ions and other organic molecules) on GRM physical-chemical properties. Moreover, the effect of digested GRMs on an *in vitro* model of intestinal barrier was also determined following a second NANoREG SOP method. In particular, the impact on integrity and functionality as well as the inflammatory response were studied. Raman observations indicated that FLG and GOx flakes do not undergo significant biodegradation processes, suggesting their possible biodurability in the GI tract. Furthermore, digested nanomaterials did not affect intestinal barrier integrity and were not associated to inflammation and cytotoxicity, though possible long-term adverse effects cannot be predicted due to the observed biopersistence. In conclusion, the outcomes presented in this work have important implications in the risk assessment of GRMs upon ingestion and pave the way to address their possible bio-applications.

References

[1] Bianco, A. Angewandte Chemie International Edition 2013, 52 (19), 4986-4997.
[2] Sánchez, V.C.; Jachak, A.; Hurt, R. H.; Kane, A. B., Chemical research in toxicology 2011, 25 (1), 15-34.
[3] Kostarelos, K.; Novoselov, K. S., Science 2014, 344 (6181), 261-263.
[4] Bove, P.; Malvindi, M. A.; Kote, S. S.; Bertorelli, R.; Summa, M.; Sabella, S. Nanoscale 2017, 9, 6315-6326.

Figures
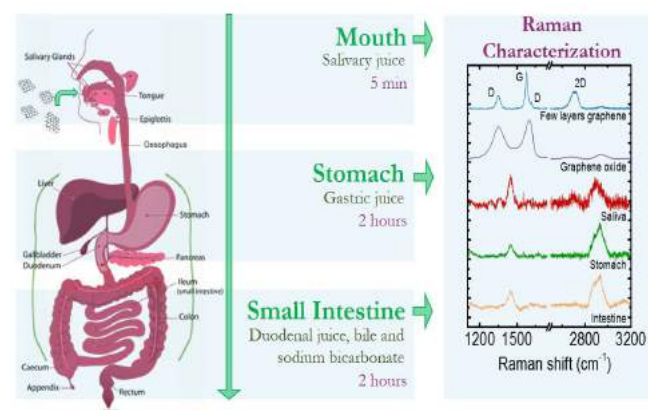
Figure 1. Schematic representation of the dynamic *in vitro* digestion assay. Along the passage through the different digestive compartments (mouth, stomach and small intestine), FLG and GOx were physically-chemically characterized by Raman spectroscopy. Representative Raman spectra (@514 nm) of GRMs and digestive juices are shown on the right. FLG and GOx are reported in blue and purple respectively. Red, green and yellow correspond to Raman spectra of saliva, stomach and intestine.

Outstanding characterization of Tungsten nanoparticles to anticipate health harmfulness in case of nuclear reactor accident.

M. Sanles-Sobrido[1,2,3],
I. Georges[4], E. Bernard[5], F. Jambon[4], D. Vrel[6], C. Uboldi[7], T. Orsiere[7], V. Malard[8], B. Rousseaue[4], C. Grisolia[12,13], A. Cabot[2], P. Rivera Gil[1] J. Rose[3].

[1]Pompeu Fabra University, Dr. Aiguader, 88, 3rd Floor, Lab Nr 62.312.10, Barcelona, Spain.
[2]Catalonia Institute for Energy Research, Jardins de les Dones de Negre, 1, 2ª pl., 08930 Sant Adrià de Besòs, Barcelona, Spain.
[3]Aix-Marseille Université, CNRS, IRD, Collège de France, INRA, CEREGE UMR34, Aix en Provence, France
[4]CEA Saclay, iBiTec-S, Building 547, 91191 Gif-sur-Yvette, France
[5]CEA, IRFM, F-13108 Saint Paul lez Durance, France
[6]LSPM, UPR 3407 CNRS, 93430 Villetaneuse, France
[7]Faculté de Médecine Timone, IMBE, F-13005 Marseille, France
[8]CEA, IBEB, Bagnols-sur-Cèze F-30207, France
[12]Univ Paris Saclay, CEA, Den Serv Corros & Comportement Mat Environm SCCME, F-91191 Gif Sur Yvette, France
[13]National Research Nuclear University "MEPhI", Moscow, 115409 Russian Federation

marcos.sanles@UPF.edu
rose@cerege.fr

Experimental Reactors prototypes used for nuclear fusion energy production usually operate with carbon refractory material as plasma facing components. Refractory material nature is huge important because it helps to minimize the unprecedented high fluxes produced during plasma operation. Therefore the selection of the adequate refractory material is one of the biggest drawbacks that must be solved to produce energy in a safe way.

Currently research is done in Tungsten metal as refractory material[1], essentially because of its low tritium retention property compared with Carbon material.

Metallic Tungsten particles of variable sizes and high specific surface areas will be present in the vacuum vessel due to Tungsten blocks-plasma interactions.

In case of a breakdown of the first protection barrier (as LOVA (Lost Of Vacuum Accident)), they could be dispersed in the close environment. Under normal operating conditions, they can also be released in the open air in very small quantity when passing through High Efficiency Particulate Air (HEPA) filters used to purify the atmosphere. Indeed, considering the HEPA filters characteristics, it has been shown experimentally and theoretically confirmed that the collector efficiency (trapping efficiency) decrease in the particle size range between 100-300 nm[2]. Also, recently published results[3] showed adverse Tungsten and Tungsten compounds effects in biological media and in the environment that could lead to toxic effects.

The current objective of this research is to address the physical-chemical evolution of Tungsten nanoparticles in several aqueous media and determine their potential toxicological effects to anticipate health harmfulness.

References

[1] Pitts et al., Journal of Nuclear Materials, 438 (2013) S48-S56.
[2] Steffens and Coury, Separation and Purification Technology, 58,1, (2007), 99-105.
[3] Strigul et al., Ecotoxicology and Environmental safety, 73, (2010), 164-171.

Figures
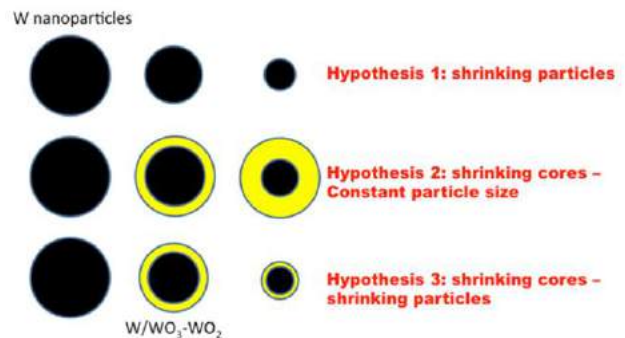
Figure 1. Possible mechanism modes of Tungsten dissolution in media.

Identifying molecular signatures of tumor dormancy as a basis for the rational design of precision nanomedicines

Prof. Ronit Satchi-Fainaro, Ph.D.

Head, Cancer angiogenesis and Nanomedicine Laboratory; Chair, Department of Physiology and Pharmacology, Sackler Faculty of Medicine, Tel Aviv University, Tel Aviv 69978, Israel

ronitsf@post.tau.ac.il

Tumor progression is dependent on a number of sequential steps, including initial tumor-vascular interactions and recruitment of blood vessels, as well as established interactions of tumor cells with their surrounding microenvironment and its different immune, endothelial and connective cellular and extra-cellular components. Failure of a microscopic tumor, either primary, recurrent or metastatic, to complete one or more of these early stages may lead to delayed clinical manifestation of the cancer. Micrometastasis, dormant tumors, and minimal residual disease, contribute to the occurrence of relapse, and constitute fundamental clinical manifestations of tumor dormancy that are responsible for the majority of cancer deaths. However, although the tumor dormancy phenomenon has critical implications for early detection and treatment of cancer, it is one of the most neglected areas in cancer research and its biological mechanisms are mostly unknown.

To that end, we created several models of patient-derived cancer models mimicking pairs of dormant *versus* fast-growing, primary *versus* metastatic and drug-sensitive *versus* drug-resistant cancers using cutting-edge techniques of patient-derived xenografts, 3D printing and genetically-modified mouse models. We investigated the molecular changes in tumor-host interactions that govern the escape from dormancy and contribute to tumor progression. Those led to the discovery of novel targets and provided important tools for the design of novel cancer nano-sized theranostics (***thera***peutics and diag***nostics***) (1-3). Our libraries of precision nanomedicines are synthesized as highly controlled micellar, nanogels, coiled or globular particulated supramolecular structures consisting of linear, hyperbranched or dendritic polymers based on polyglutamic acid (PGA), polyethyleneglycol (PEG), poly(N-(2-hydroxypropyl)methacrylamide) (HPMA) copolymer, polyglycerol, poly(lactic-coglycolic acid) (PLGA) and hybrid systems (4-9).

We hypothesize that the acquired knowledge from this multidisciplinary research strategy will revolutionize the way we diagnose and treat cancer (Figure 1).

References

[1] Tiram G, *et al.* ACS Nano, 10, 2028-2045, (2016).
[2] Ferber S*, Tiram G*, *et al.* eLife, in press, (2017).
[3] Gibori H, *et al.*, Nature Communications, in press (2017).
[4] Baabur-Cohen H, *et al.* J Control Release, 257,118-131 (2017).
[5] Ofek P, *et al.* Nanomedicine, 12, 2201-2214 (2016).
[6] Polyak D, *et al.* J Control Release, 257:132-143 (2017).
[7] Scomparin A, *et al.* J Control Release, 208, 106-120 (2015).
[8] Shatsberg Z, *et al.* J Control Release, 239, 159-168 (2016).
[9] Markovsky E, *et al.* J Control Release, 249, 162-172 (2017).

Figures
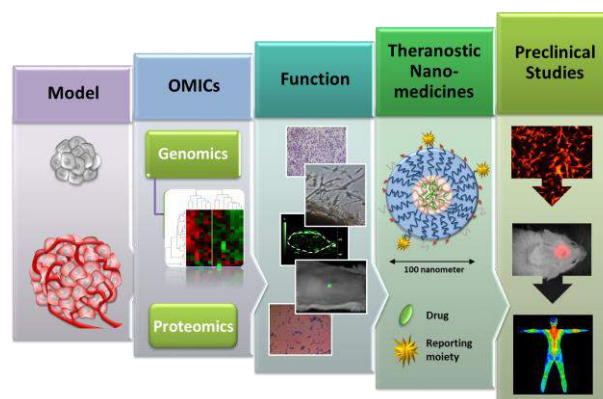
Figure 1. A comprehensive approach to address tumor dormancy- from bed-site to bench and back.

Exploring biological micro- and nanostructures using infrared nanospectroscopy (nano-FTIR)

Dr. Philip Schäfer

neaspec GmbH, Bunsenstraße 5, D-82152 Martinsried, Germany

philip.schaefer@neaspec.com

Scattering-type scanning near-field optical microscopy (s-SNOM) has emerged to the forefront of key technologies to study the optical and electronic properties of plasmonic, electronic and dielectric materials as well as the chemical composition of synthetic and biological materials, not on the macroscopic scale but on the 10nanometer length scale – far beyond the diffraction limit of light [1]. s-SNOM employs a sharp metallic AFM tip which is externally-illuminated to create a nanoscale optical hot-spot at the tip apex. The light within the optical hotspot interacts with the sample surface below the tip and is modified by the local dielectric properties (e.g. absorption, reflection) of the sample material. Detection of the elastically tip-scattered light simultaneous to AFM imaging yields nanoscale resolved near-field images [2] and broadband near-field spectra (nano-FTIR) with <20nanometer spatial resolution. Utilizing broadband laser sources like a mid-IR supercontinuum laser for tip illumination enables near-field spectroscopic measurements at nanoscale spatial resolution with unprecedented signal quality.

In the scope of bio-nano measurements and microscopy, we demonstrate acquisition of nanoscale resolved material-specific nano-FTIR absorption spectra of biomaterials at unmatched spatial resolution and sensitivity. Structural analysis and mapping of individual protein complexes in the mid-IR spectral range are shown. To demonstrate that nano-FTIR can probe protein secondary structure on the nanometer scale and with sensitivity to individual protein complexes, the amide bands of individual tobacco mosaic viruses (TMVs) and ferritin complexes for their well-defined, robust and dominantly α-helical protein structure, insulin aggregates for exhibiting β-sheet structure and purple membranes (PMs) due to well-defined orientation of the transmembrane α-helices were studied [3]. Investigating a mixture of TMV and insulin aggregates on silicon using nano-FTIR enabled unambiguous identification of the respective structures. Imaging with neaSNOM and recording absorption spectra with nano-FTIR (Figure 1a & 1b) revealed a clear contrast. The red spectrum exhibits the absorption maximum at 1,660 cm^{-1}, which corresponds to the amide I resonance frequency of α-helices. The shape fits well to the infrared spectrum of TMV. This permits to identify this rod-like structure as a TMV particle. In contrast, the green spectrum significantly differs from the red, exhibiting two peaks at 1,660 and 1,634 cm^{-1}, which can be attributed to the presence of α-helices and β-sheets, respectively. Thus, this particle can be identified as an insulin aggregate, as its nano-FTIR spectrum agrees with the conventionally recorded FTIR spectrum of a pure insulin sample. Next to the topography image (Figure 1c) an adapted spectrum-thresholding allowed to depict a conclusive map of color-coded TMV (pink) and insulin (yellow) (Figure 1d).

In the case of the broadband infrared studies on a single ferritin complex nano-FTIR indicated its sensitivity to about 4,000 amino acids, corresponding to about 5,000 C=O and N-H bonds, respectively. Most importantly, the amide I band in the nano-FTIR spectra could be analyzed and interpreted in the framework of standard infrared spectroscopy. The studies established a solid foundation for infrared nanobiospectroscopy, which is a prerequisite for highly impactful future nano-FTIR applications in biochemical and biomedical research.

Similar results of nanoscale variations of the secondary structure could be obtained for single collagen fibrils as can be seen in Figure 3. The D-banding structure gets clearly evident [4].

The exceptional signal to noise ratio obtained even for polymeric and biological samples provides the basis to reduce measurement times by orders of magnitude to acquire characteristic near-field spectra in the 100-200 millisecond time scale. This allows hyperspectral imaging on reasonable timescales. Consequently, a precise map of chemical information on the nanometer scale can be realized.

Here we show an *in-situ* analysis of native melanin in the human hair medulla [5]. An enhanced infrared absorption of the cuticle and cortex regions compared with the resin, owing to the strong amide I absorption of the hair proteins (α-keratin microfibrils) is observed (Figure 3a). Within the cortex region disk-shaped areas of about 300nm diameter, where the infrared absorption is reduced (the protein content is reduced) become visible. From the hyperspectral data cube (Figure 3b) spectra at different positions (Figure 3c) can be extracted. Within the cortex region (position C) the well-known amide I and II bands being typical for protein (α-keratin) appear. For particle A four distinct peaks that are characteristic for melanin are identified. This demonstrates non-invasive nanoscale resolved material identification and analysis of the secondary structure of biological specimens.

Besides non-invasive nanoscale resolved material identification or analysis of the secondary structure of biological specimens, nano-FITR enables quantitative measurements of dielectric values for

polymers or the determination of free carrier concentration and mobility in low-dimensional structures.

References

[1] F. Keilmann, R. Hillenbrand, Phil. Trans. R. Soc. Lond. A 362, 787 (2004)

[2] C. Westermeier, et al., Nature Comm. 5, 4101 (2014)

[3] I. Amenabar, et al. Nature Comm. 4, 2890 (2013)

[4] R. Wiens, et al., Faraday Discuss. 187, 555 (2016)

[5] I. Amenabar, et al., Nature Comm. 8, 14402 (2017)

Figures
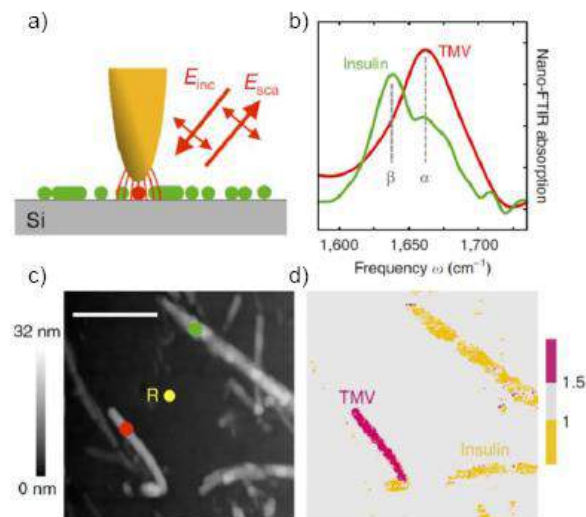
Figure 1. Nanoscale mapping of α-helical and β-sheet secondary structure. (a) Scheme of tip-induced nano-hotspot showing incident and scattered propagating electric fields for nano-scale IR-spectroscopy on insulin and TMV on a Si-substrate. (b) Recorded insulin and TMV nano-FTIR spectra with clear α-helical and β-sheet absorption bands. (c) Topography of a mixture of TMV and insulin aggregates on silicon. Red and green dots in the topography image mark the positions where the nano-FTIR spectra were taken. The position marked by the yellow dot and R indicates where the reference spectrum was recorded. Scale bar: 500 nm; (d) Concluded map of TMV (purple) and insulin (yellow) aggregates. [3]
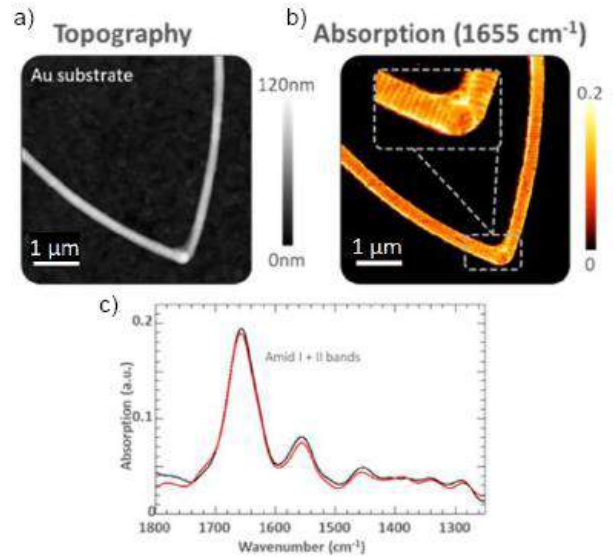
Figure 2. (a) Topography and (b) optical absorption image of a single collagen fibril. The typical periodic substructure of the collagen is resolved in the AFM and in the IR-absorption image. (c) nano-FTIR spectra of the collagen fibril feature clear Amid I + II bands.
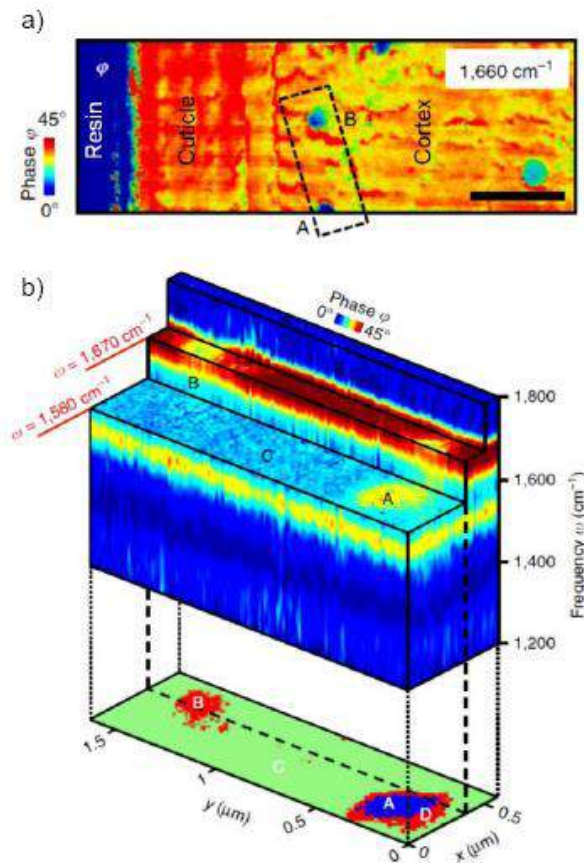
Figure 3. In situ hyperspectral infrared nanoimaging of native melanin in human hair medulla. (a) Infrared near-field phase image φ at 1,660cm-1. Scale bar: 1 μm. (b) Hyperspectral infrared data cube with a spectral resolution of 35 cm-1 partially cut at different frequencies ω. It shows the phase of the tip-scattered light as a function of position (x, y) and frequency ω. The dashed black rectangle in a shows the area where the data cube was recorded.

Barcoded nanoparticles for personalizing anti-cancer medicine in the primary tumor and metastasis

Avi Schroeder, PhD

Dept. of Chemical Engineering, Technion – Israel Institute of Technology, Haifa 32000, ISRAEL

avids@technion.ac.il

Abstract

The field of nanomedicine is taking its first steps towards personalized care. Our research is aimed at predicting how a cancer patient will respond to treatment, before the actual medication program begins. In fact, at least 30% of cancer patients are prescribed a medication that fails to affect the tumor; these numbers greatly increase when dealing with a metastatic or recurrent disease. To address this need, we developed liposomes that target tumor and metastasis, where they gauge the activity of medicines in a personalized manner. Specifically, **we developed a liposomal diagnostic system for predicting the therapeutic potency of anti-cancer drugs inside the patient's tumor in a safe manner**. The system is similar by concept to an 'allergy test', screening the potency of miniscule doses of multiple medicines directly inside the patient's tumor, before beginning a treatment cycle. Based on the screen, a patient-specific drug potency chart is constructed, rating the activity of the different medicines for each individual patient. Furthermore, the system predicts the activity of drugs in various cellular subsets of the tumor microenvironment and in the metastasis.

In pre-clinical trials we found the system is accurate in predicting the response of triple-negative tumors to medication.

The clinical implications of these approaches will be discussed.

Figure 1. Barcoded nanoparticles, each loaded with miniscule doses of different anti-cancer drugs, are used to simultaneously determine the potency of each of the drugs inside the patient's tumor. In a process similar to an 'allergy test' the patient specific activity of each of the drugs is recoded.

References

[1] Yaari, Nature Communications, 7 (2016) 13325
https://www.nature.com/articles/ncomms13325
[2] Goldman, Nanotechnology, 28 (2017) 43LT01
http://iopscience.iop.org/article/10.1088/1361-6528/aa8a3d/meta

Combination of Dendritic Cell-targeted Nano-vaccines with Immune Checkpoint Therapy for Melanoma

Anna Scomparin[1]

J. Conniot[1;2], C. Peres[2], E. Yeini[1], S Pozzi[1], E. Zupancic[3], S. Jung[3], Ronit Satchi-Fainaro[1], Helena F Florindo[2]

[1]Department of Physiology and Pharmacology, Sackler Faculty of Medicine, Tel Aviv University, Tel Aviv, Israel
[2]Research Institute for Medicines (iMed.ULisboa), Faculty of Pharmacy, Universidade de Lisboa, Lisbon, Portugal
[3]Department of Immunology, The Weizmann Institute of Science, Rehovot, Israel

anna.scomparin@gmail.com

Immune checkpoint therapy significantly improved the clinical outcome of melanoma treatment compared to standard therapy. However, results are far from the initially expected. In fact, Programmed cell death protein-1 (PD-1) antibody monotherapy induced effective and durable responses in 30-40% of advanced melanoma patients [1]. Monoclonal anti-OX40, an immune checkpoint stimulator, member of the tumor necrosis factor (TNF) receptor family, has shown modest monotherapy outcomes in clinical trials [2]. Poor clinical results have been associated with complex mechanisms behind anti-tumor immunity. Currently, it is widely accepted that melanoma therapy will benefit from integrated complementary approaches, which can inhibit tumor immunosuppressive pathways and enhance immunity in an orchestrated manner. We hypothesized that combinatorial therapy with anti-PD-1/anti-OX-40 – to inhibit tumor immunosuppression and to boost T-cell activity, respectively – could be improved by cancer vaccination, which will increase tumor-associated antigen recognition, internalization, processing and presentation to those T cells (Fig. 1).

Mannose-poly(lactic-co-glycolic acid)/poly(lactic acid) (PLGA/PLA) were produced as mannosylated dendritic cell (DC)-targeted nanoparticle (NP) vaccine, containing major histocompatibility complex (MHC) class I and MHC class II melanoma MART-1 peptide antigens (Fig. 2A). The physico-chemical characterization of the NP demonstrates their potential as *in vivo* vaccine delivery systems for antigens and immune potentiators, with an average size of ~170 nm and a slightly negative ζ potential (~ -2 mV). The spherical morphology of the NP was evaluated via Transmission and Scanning Electron Microscopy (TEM, Fig. 2B and SEM, Fig. 2C) and Atomic Force Microscopy (AFM) (Fig. 1D). The NP presents high entrapment efficiency (>80%) and >40% loading capacity, calculated via fluorescence spectroscopy. The NP and man-NP are biocompatible, not inducing red blood cell lysis *in vitro*, and are efficiently internalized by JAW SII DC.

Male C57BL/6 mice were immunized by 3 weekly subcutaneous injections. Seven days after the last immunization, the mice were inoculated with Ret melanoma cells, and 9 days after the inoculation, PD-1 and OX40 antibodies were administered intraperitoneally at 10 mg/kg. Compared to anti-PD-1/anti-OX-40 alone, treatment with this combination of animals previously immunized with our DC-targeted vaccine induced maximal tumor inhibition with minimal systemic toxicity, leading to 100% of mice surviving 42 days after tumor inoculation, in contrast to 20% surviving following treatment with anti-PD-1/anti-OX-40 only. In this group, 50% of the animals were still alive two months after tumor inoculation, presenting infiltrating lymphocytes within tumors.

References

[1] Topalian SL, et al.,The New England journal of medicine. 2012;366:2443-54.
[2] Melero I, et al., Clinical cancer research 2013; 19:997-1008.

Figures
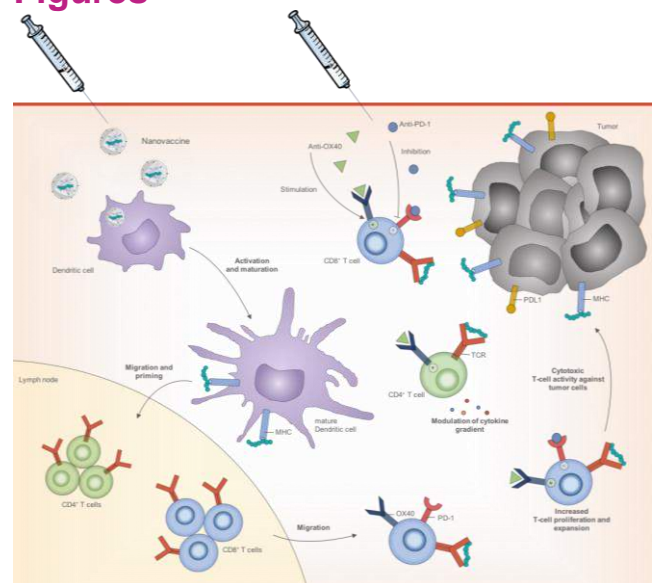
Figure 1. Proposed model for the combinatorial therapeutic strategy with PD-1/OX40 and man-NP.
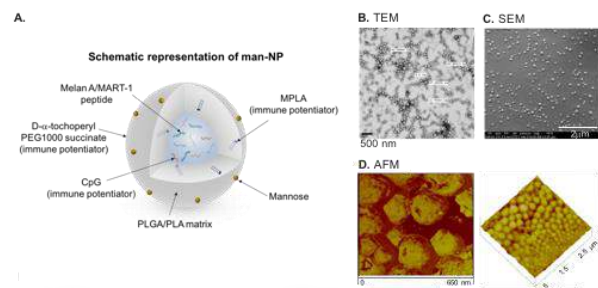
Figure 2. A. Schematic representation of DC-targeted mannose-PLGA/PLA nanoparticles (man-NP). B. TEM image of spherical man-NP. C. SEM image of spherical man-NP. D. AFM images of spherical man-NP, showing narrow size polydispersity.

4D live cell imaging to study cellular interplay in a 3D lung model upon (nano)particle exposure

D. Septiadi[1],
J. Bourquin[1], E. Durantie[1], A. Fink[1,2],
B. Rothen-Rutishauser[1]

[1]Adolphe Merkle Institute, University of Fribourg, Chemin des Verdiers 4, 1700 Fribourg, Switzerland
[2]Department of Chemistry, University of Fribourg, Chemin du Musée 9, 1700 Fribourg, Switzerland

dedy.septiadi@unifr.ch

Figures

Figure 1. A) Schematic and **B)** confocal micrograph of *in vitro* 3D lung model consisting macrophages (red), epithelial cells (cyan) and dendritic cells (green). **C)** Selected time-frame 4D live cell images showing kinetics and dynamics of cellular uptake and translocation of 200 nm rhodamine-labeled silica particles (yellow). Black arrows denote translocated particles. Dendritic cells in basal side of panel C was colored red.

Simplicity of *in vitro* three dimensional (3D) co-culture systems for mimicking human tissues has brought a tremendous impact in biotechnology and biomedical research.[1] However, limitations on current light microscopy imaging setup especially for live cells/tissues and time-lapse purpose has hampered the possibility to understand the dynamics of cells grown on a 3D co-culture configuration by means of conventional fluorescence microscopes which generally provide limited resolution and produce blurry images especially for thicker samples. Herein, we developed a specific sample holder optimized for permeable membrane inserts and combined this with a simple time-lapse fluorescence confocal imaging technique -which we refer as 4D live cell imaging- allowing a direct visualization of a live 3D co-culture lung model consisting three cell types (e.g. epithelial cells and macrophages on the apical and dendritic cells on the basolateral side of permeable inserts[2] over several hours up to one day (**Figure 1A and 1B**). We further extend our approach to monitor kinetics and dynamics of cellular uptake of fluorescently-labeled (nano)particles by macrophages and epithelial cells and particle translocation to the dendritic cell sites (**Figure 1C**). The developed system is robust and it can provide a useful platform to study many cellular processes of 3D cell models including cell adhesion, transmigration, wound healing, etc. in the presence of (nano)particles.

References

[1]   Edmondson et al., Assay Drug Dev. Technol. 12, 207–218 (2014)
[2]   Rothen-Rutishauser et al., Am. J. Respir. Cell. Mol. Biol. 32, 281-289 (2005)

Magnetic Manipulations for Controlling Neuronal Engineering and Regeneration

Orit Shefi[1,3],
Merav Antman-Passig[1,3], Michal Marcus[1,3], Naor Vardi[2,3], Amos Sharoni[2,3]

[1]Faculty of Engineering, Bar Ilan University, Ramat Gan, Israel
[2]Physics Department, Bar Ilan University, Ramat Gan, Israel
[3]Institute of Nanotechnologies and Advanced Materials, Bar Ilan Univeristy, Ramat Gan, Israel

Orit.shefi@biu.ac.il

Controlling cell navigation, organization and growth has great importance in tissue engineering and regeneration, for a wide range of tissues. In this talk I will present our recent studies of magnetic-based manipulations for nerve regeneration and for controlled drug delivery.

Neurons rely on physical topographical cues. Techniques to control cell growth include bio-mimetic scaffolds, nano-fibrous constructs, structured gels, etc., offering a mechanical guide to the regenerating cells. We have developed a novel approach of injectable hydrogels combined with magnetic nanoparticles (MNPs), to be incorporated directly into the injured site. We show that gel fiber structure can be aligned in situ dynamically and remotely in response to an external magnetic field. Neurons embedded within the aligned gel demonstrated polarized growth pattern. We show a directed and effective neuronal regeneration for neurons embedded in the aligned gels in vitro and ex-vivo. This platform is now examined as a novel method to direct neuronal growth and to bridge gaps efficiently post trauma.

In addition, we functionalized the MNPs by coating them with nerve growth factor, presenting a 'smart' delivery system of biomolecules, together with integral guidance cues. The enrichment of the gel platform with biomolecules conjugated MNPs promoted differentiation and elongation.

As physical mechanical forces play a key role in neuronal morphogenesis, we used magnetic nanoparticles (MNPs) as mediators to apply forces locally on neurons throughout their migration and organization. Following incubation, the MNPs accumulated in the cells, turning the cells sensitive to magnetic stimulation. Applying magnetic fields with controlled magnetic flux densities led to pre-designed cellular movement and to organized networks. Growing neurons loaded with MNPs under magnetic fields has affected the pattern of dendritic trees. With this method we could control drug distribution and delivery as well. Our study presents an emerging magneto-chemical approach for promoting tissue regeneration.

References

[1]   Antman-Passig et al., Tissue Eng., 2017
[2]   Antman-Passig and Shefi, Nano Letters, 2016
[3]   Marcus et al., J NanoBioTech., 2016
[4]   Alon et al., Lab on Chip, 2015

Figures
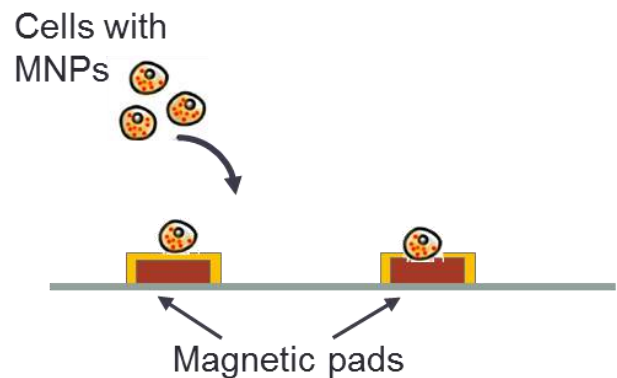
Figure 1. Organizing neural networks by controlled magnetic fluxes. Cells are uploaded with MNPs turned into magnetic elements.
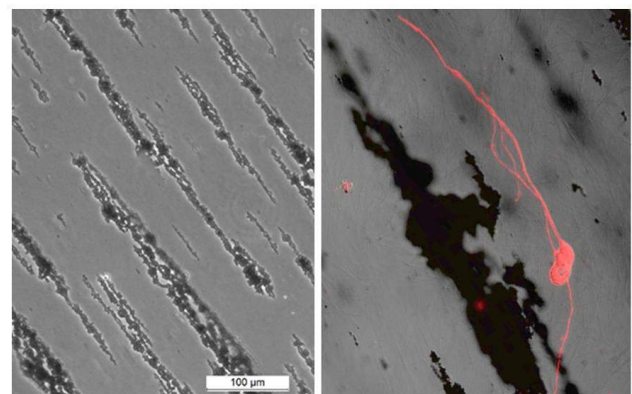
Figure 2. Collagen gel embedded with aligned aggregates of MNPs (Left). PC12 cell (red) is polarized within the magnetically aligned gel (Right).

Hybrid Nano Bio-fibers

Oded Shoseyov,

The center for Nanoscience and Nanotechnology. The Robert H. Smith Faculty of Agriculture, Food and Environment, the Hebrew University of Jerusalem, P.O.B. 12 Rehovot 76100, Israel. Tel: +972-54-2341863

Shoseyov@agri.huji.ac.il

Bringing together the toughness of cellulose nano-fibers from the plant kingdom, the remarkable elasticity and resilience of resilin that enables flees to jump as high as 100 times their height from the insect kingdom combined with Human Recombinant Type I collagen produced in tobacco plants; These are the materials of the future; Nature's Gift. Resilin is a polymeric rubber-like protein secreted by insects to specialized cuticle regions, in areas where high resilience and low stiffness are required. Plant cell walls also present durable composite structures made of cellulose, other polysaccharides, and structural proteins. Plant cell wall composite exhibit extraordinary strength exemplified by their ability to carry the huge mass of some forest trees. Inspired by the remarkable mechanical properties of insect cuticle and plant cell walls we have developed novel composite materials of resilin and Crystalline Nano-Cellulose (resiline-CNC) that display remarkable mechanical properties combining strength and elasticity. We produced a novel resilin protein with affinity to cellulose by genetically engineering a cellulose binding domain into the resilin. This CBD-Resilin enable, interfacing at the nano-level between the resilin; the elastic component of the composite, to the cellulose, the stiff component.

As a central element of the extracellular matrix, collagen is intimately involved in tissue development, remodeling, and repair and confers high tensile strength to tissues. Numerous medical applications, particularly, wound healing, cell therapy, and bone reconstruction, rely on its supportive and healing qualities. Its synthesis and assembly require a multitude of genes and post-translational modifications. Historically, collagen was always extracted from animal and human cadaver sources, but bare risk of contamination and allergenicity and was subjected to harsh purification conditions resulting in irreversible modifications impeding its biofunctionality. A tobacco plant expression platform has been recruited to effectively express human collagen, along with three modifying enzymes, critical to collagen maturation. The plant extracted recombinant human collagen type I forms thermally stable helical structures, fibrillates, and demonstrates bioactivity resembling that of native collagen. Today in greenhouses all over Israel farmers grow transgenic tobacco plants producing human recombinant collagen that is used for the production of medical implants that have already in clinical use. Combining collagen at the nano-scale with resilin to produce fibers resulted in super-performing fibers with mechanical properties which exceed that of natural fibers.

Figures

Figure 1. Transparent conductive composite CNC-CNT films
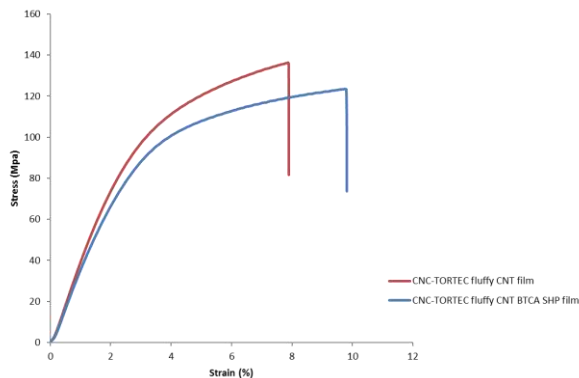
Smart Nanoparticles for the Treatment of Cancer

Álvaro Somoza,

IMDEA Nanociencia, Faraday 9, Madrid, Spain

alvaro.somoza@imdea.org

Nanomaterials are having a significant impact in biomedical applications since they can overcome some limitations of traditional approaches for the detection and treatment of diseases [1].

Notably, the treatment of diseases using nanocarriers has led to a significant reduction of toxicity and an increased efficacy due to the EPR effect [2]. This has been the case for Doxil and Abraxane. However, despite these improvements, further developments are desirable to tackle such diseases with precision nanomedicines. For instance, it is desirable that the therapeutics transported by the nanostructures remain inactive till the target area is reached. In this sense, we are exploring different nanomaterials as carriers of a variety of therapeutic molecules, which are covalently bound to the nanoparticle [3, 4]. This approach has allowed us to include multiple active molecules in a given nanostructure, which are released under different internal stimuli, such as low pH or high concentration of reductive molecules (Figure 1).

The diseases we are investigating include breast and pancreatic cancer and Uveal Melanoma and the nanostructures employed are mainly in our preparations are: gold, iron oxide, and albumin-based nanoparticles.

In the case of gold nanoparticles, we are studying the effect of nucleic acids (aptamers and antisense) and chemotherapeutics in Uveal Melanoma (UM). Currently, there is not an effective treatment of metastatic UM and it is usually detected when the disease has reached other organs, mainly the liver. At this point, the patients usually die in few months (6-18 months) [5].

In addition to gold nanoparticles, we are exploring albumin-based nanostructures for the treatment of UM and other cancers. These nanostructures are very promising due to their excellent stability and lack of toxicity.

References

[1]   M. Björnmalm, K. J. Thurecht, M. Michael, A. M. Scott, F. Caruso, *ACS Nano* **2017**, acsnano.7b04855.

[2]   O. C. Farokhzad, R. Langer, *ACS Nano* **2009**, *3*, 16–20.

[3]   A. Latorre, P. Couleaud, A. Aires, A. L. Cortajarena, Á. Somoza, *Eur. J. Med. Chem.* **2014**, *82*, 355–362.

[4]   A. Latorre, C. Posch, Y. Garcimartín, A. Celli, M. Sanlorenzo, I. Vujic, J. Ma, M. Zekhtser, K. Rappersberger, S. Ortiz-Urda, et al., *Nanoscale* **2014**, *6*, 7436–42.

[5]   B. Álvarez-Rodríguez, A. Latorre, C. Posch, Á. Somoza, *Med. Res. Rev.* **2017**, *37*, 1350–1372.

Figures
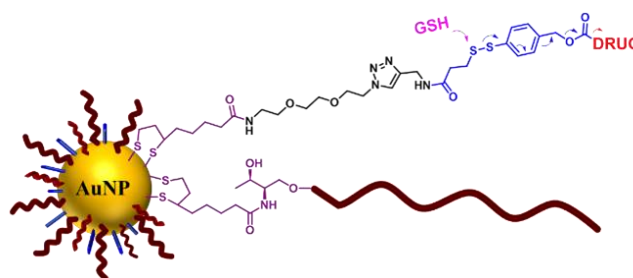
Figure 1. Drug release promoted by the presence of glutathione (GSH)

Nanoparticle detection in Consumer Products

Miguel Spuch-Calvar[1],
Laura Rodriguez-Lorenzo[1], Barbara Rothen-Rutishauser[1], Alke Petri-Fink[1,2]

[1]Adolphe Merkle Institute, Chemin des Verdiers 4, Fribourg, Switzerland
[2]Université de Firbourg, Chemin du Musée 9, Fribourg, Switzerland

miguel.spuch-calvar@unifr.ch

In 2011 the European Commission has decided that "all ingredients present in the form of engineered nanoparticles must be clearly indicated in the list of ingredients, followed by the word 'nano' in brackets for consumer products" [1].

This guideline is already implemented for cosmetic products and is currently under extensive discussion to be applied for food and other consumer products in the near future. So far, however, no standardised and validated methods are available to identify and quantify nanoparticles in complex matrices.

So what particles are found in which food (or consumer product) for what reason and at which concentration?

This question is almost impossible to answer to date: The identification/detection, characterization and quantification of engineered nanoparticles pose tremendous challenges including e.g. (i) the low concentration (0.1-5 wt. %) of the nanoparticles in the food matrix, (ii) the complexity and variability of the matrix (including powders, solids, oils etc.), (iii) the presence of organic molecules, proteins, lipids which can interact with the particles, or (iv) the change of nanoparticle composition (e.g. dissolution), dispersion state (i.e. agglomeration), or surface chemistry.

Over the past years, an increasing number of studies in this field have appeared in the literature. However, the thorough characterization of nanoparticle polydispersity and nanoparticle aggregation in the sample still remains a major issue in the field.

Therefore, we have developed a protocol to extract and characterize silicon dioxide (SiO_2) and/or titanium dioxide (TiO_2) nanoparticles, their size and size distribution including the aggregation state, from a large variety of products ranging from powders (e.g. spice mixes) and pastes (e.g. ketchup), to solids (e.g. M&Ms, Chewing Gum).

Results:

All tested samples contained one or both of the above mentioned materials and particulate form.

Food matrix digestion protocols were developed and reproducible. After the digestion of the food matrix the remaining SiO_2 and TiO_2 nanoparticles formed stable aggregates in extracted suspension as shown by dynamic light scattering allowing to determine the hydrodynamic diameter and polydispersity. The TiO_2 nanoparticles were additionally studied by electron microscopy (Scanning and transmission electron microscopy) to investigate shape, composition and size of the nanoparticles. Some of the tested products included highly anisotropic particles, i.e. titania coated silica platelets.

References

[1]   Art 18 (3), EU's 2011 Regulation on Food Information to Consumers (1169/2011).
[2]   B. Franze, I. Strenge, C. Engelhard, J. Anal. At. Spectrom., 27 (2012) 1074
[3]   R. Peters, Z. Herrera-Rivera, A. Undas, M. van der Lee, H. Marvin, H. Bouwmeester, S. Weigel, J. Anal. At. Spectrom., 30 (2015) 1274
[4]   F. Aureli, M. D'Amato, A. Raggi, F. Cubadda, J. Anal. At. Spectrom, 30 (2015) 1266

Figures

Figure 1. Full process to separate the nanomaterial from the food product: a. product selection; b. sample preparation; c. matrix digestion; d. characterization. TEM image: SiO_2 nanoparticles extracted from Doritos.

Self-assembled lipid nanotubes

Kaori Sugihara[1]

[1]University of Geneva, 30 quai Ernest Ansermet, 1211 Geneva, Switzerland

kaori.sugihara@unige.ch
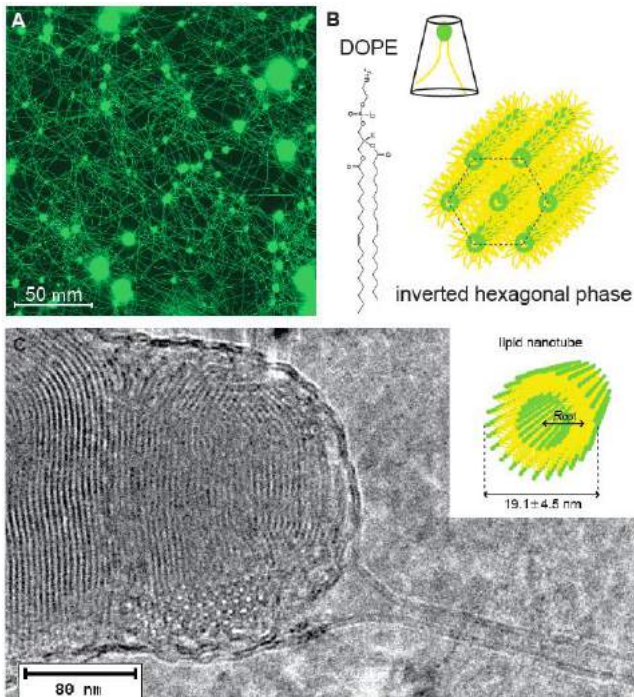
Figure 1: Directed self-assembly of lipid nanotubes from inverted hexagonal structures. (A) A fluorescent image of the surface-assembled lipid nanotubes. (B) The chemical structure of DOPE lipid and a scheme of the inverted hexagonal phase. (C) A cryoTEM image of the lipid nanotube protruding from the inverted hexagonal lipid block.[1]

Previously, we have discovered a new type of lipid nanotube self-assembly made of the main lipid component of bacterial cell membranes, 1,2-dioleoyl-sn-glycero-3-phosphoethanolamine (DOPE, Figure 1A).[1] The assembly starts with formation of inverted hexagonal lipid blocks in physiological buffer solution. DOPE is a conical lipid that prefers the inverted hexagonal phase, where the inverted micelle tubes are bundled into a hexagonal pattern, constructing a densely-packed three-dimensional architecture (Figure 1B).[2] These inverted hexagonal lipid blocks adhere onto polyelectrolyte coated glass substrates (e.g. PEI, PLL) intact. When there is a fluctuation in the solution such as turbulence flow created by pipettes or lamellar flow induced by microfluidic systems, a part of the lipid block moves while the other part is kept attached to the substrates, pulling out a tube as shown in the cryo-transmission electron microscopy (cryoTEM) image in Figure 1C.

In our group, we have been attempting to explore possible applications of these self-assembled lipid nanotubes in bio-nanofabrication, sensing, or as a model system for fundamental studies.
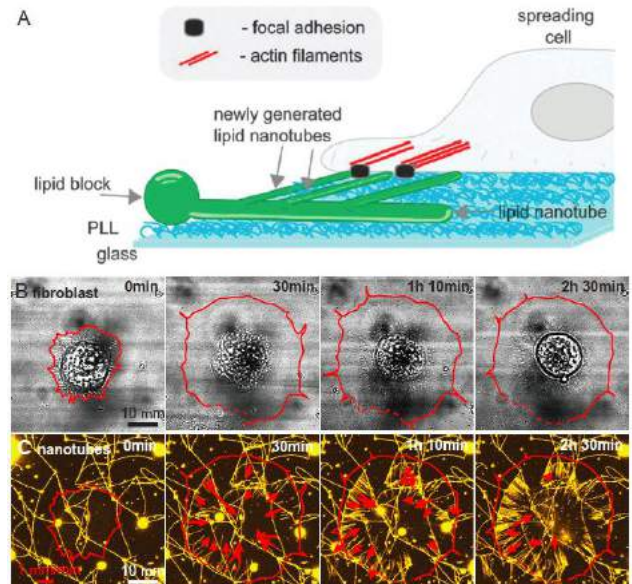
Figure 2: Label-free detection of cell-contractile activity with lipid nanotubes. (A) A scheme showing the new lipid nanotube formation directed by cell forces. (B) Bright field and (C) fluorescent images from a movie where the interaction between a fibroblast and lipid nanotubes was monitored.[3]

These surface-assembled lipid nanotubes can be used to study cell contractility. A fibroblast was seeded on top of Rhodamine-stained lipid nanotubes, and its initial spreading was monitored by fluorescence microscopy.[3] Figure 2BC are the snapshots from the bright field and the Rhodamine channel respectively. As the cell spreads, new lipid nanotubes came out from the edge of the cell. It looks as if the cell grabbed the existing lipid nanotubes and is pulling them towards the cell center. We found that these new lipid nanotubes are nucleated between focal adhesions (anchors that cells make to firmly attach substrates). Inhibition of the actin-myosin affinity by blebbistatin suppressed it. All the evidences suggest that this phenomenon is linked to the cell contractility. When initial small focal contacts try to make an anchor to the substrate, sometimes they attach to nanotubes instead of the solid substrate. Upon application of forces, these focal contacts slip because lipids are very soft, resulting in the nucleation of new lipid nanotube branches (Figure 2A). In other words, cells are applying a point load to the lipids via focal contacts, somewhat similarly how we do by micropipettes. From the fundamental studies, we know that the minimum force required to start pulling lipid nanotubes in our system is around 90 pN,[1] which corresponds to 20-30 myosin motors (single myosin exceeds 3-4 pN).[4] Using this approach, we studied

the cell force activity of different types and conditions of cells in a label-free manner. For example, malignant cells typically have low contractility, which was visualized by absence of the nucleation of new lipid nanotubes, while endothelial cells pulled the lipid nanotubes intensively, presenting a high level of contractility.
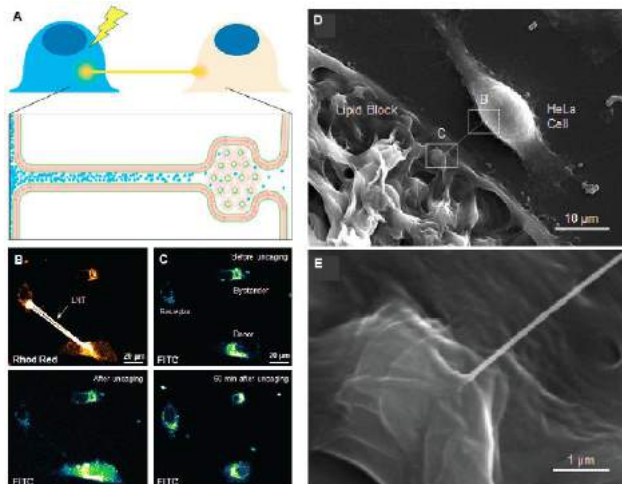
Figure 3: Artificial tubular connections between cells based on synthetic lipid nanotubes.[5]

Lipid nanotubes can be also used as a model system for studying tunneling lipid nanotubes (TNT) between living cells. TNTs are means for inter-cellular communication discovered in 2004.[6] Research over the last decade has revealed that TNTs are universal communication tools for many types of cells that have diverse structures and functions. Currently, TNTs are being studied with either in-vivo or in-vitro cell models. However, such traditional biological approaches often suffer from the complexities and a lack of controllability in the connection.

We demonstrated a simple approach to create a direct tubular connection between cells based on the self-assembled lipid nanotubes. The technique requires only a micromanipulator and a fluorescence microscope for controlling the LNT positioning and the connection to the cells (Figure 3). The diffusion of water-soluble dye was monitored from one cell to the connected cells, demonstrating the cytosol connections between two cells (Figure 3BC). The SEM images visualized the diameter of the lipid nanotubes after fusing to cell membranes, which matches with the time scale of the dye transport we observed by fluorescence microscopy.

Another use of the lipid nanotubes is as a template for fabricating solid structures. As a proof of concept, we fabricated gold nanowires with the lipid nanotube templates by attaching gold nanoparticles to the lipid nanotubes, fixing them chemically, removing the template through oxygen plasma cleaning, and annealing.[7] Gold nanoparticles were attached to the lipid nanotubes, using streptavidin-biotin interaction

(Figure 4A). Both cryoTEM (Figure 4B) and atomic force microscopy (Figure 4C) showed successful adhesion of gold nanoparticles to the template. Electrical conductivity was observed only after the oxygen plasma treatment for removing the organic template (Figure 4D). The approach exploits the self-assembled organic template for the high-throughput nanostructure fabrication. The same strategy can be used to align other particles and biomolecules.
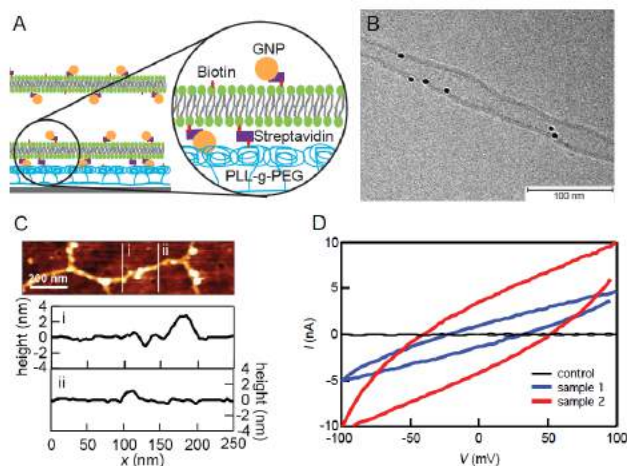
Figure 4: Gold nanowire fabrication with surface-attached lipid nanotube templates. (A) A scheme describing the strategy of gold nanoparticle attachment to the lipid nanotubes. (B) A cryoTEM image of gold nanoparticle attached lipid nanotubes. (C) An AFM image of gold nanoparticle adhered lipid nanotubes after chemical fixing. The cross sections correspond to the white lines in the image. (D) *I-V* curve from the fabricated gold nanowires.[7]

References

1. Sugihara, K.; Chami, M.; Derenyi, I.; Voros, J.; Zambelli, T., *ACS nano* **2012,** *6* (8), 6626-32.
2. Sugihara, K.; Stucki, J.; Isa, L.; Vörös, J.; Zambelli, T., *J. Colloid Interface Sci.* **2012,** *386* (1), 421-427.
3. Sugihara, K.; Delai, M.; Mahnna, R.; Kusch, J.; Poulikakos, D.; Voros, J.; Zambelli, T.; Ferrari, A., *Integrative biology : quantitative biosciences from nano to macro* **2013,** *5* (2), 423-30.
4. Finer, J. T.; Simmons, R. M.; Spudich, J. A., *Nature* **1994,** *368* (6467), 113-119.
5. Kozintsev, A.; Sugihara, K., *Rsc Adv* **2017,** *7* (33), 20700-20708.
6. Rustom, A.; Saffrich, R.; Markovic, I.; Walther, P.; Gerdes, H. H., *Science* **2004,** *303* (5660), 1007-1010.
7. Jajcevic, K.; Chami, M.; Sugihara, K., *Small* **2016**, DOI: 10.1002/smll.201600431.

New very small magnetic microspheres in Medical Applications

Fabrice Reuven

MERCK CHIMIE SAS

fabrice.sultan@merckgroup.com

The use of magnetic beads in cell biology, quantitative lateral flow, biosensor or biochip technologies is becoming very common. Several sophisticated systems are under development and the immunoassays are much more complex to develop. In order to meet the changing needs and to reach higher sensitivity, ease of use and low price, we have initiated several R&D projects to significantly reduce the size of existing Superparamagnetic Microspheres.

In standard immunoassay applications, the gold standard is a magnetic microsphere of 1µm in size COOH or Tosyl-modified in surface and containing 35-45% of magnetic pigment.

In a first step, we have reached small magnetic microspheres with a nominal size of 300-350 nm and finally a new process allowed us to reach 150-200 nm size beads. These very small magnetic microspheres offer great surface area, increased assay sensitivity, very low sedimentation rate, high ferrite content and good magnetic signature. Our very small beads are now used with success in various biological applications such as cell sorting, immuno-precipitation, biosensor, microfluidics and of course, quantitative lateral flow assays.

Hyperspectral microscopy for single and collective nanoparticle characterization in biological media

Dionysia Tsoutsi[12],
Paula Zamora Perez[12],
Pilar Rivera Gil[12]

[1] Department of Experimental and Health Sciences, Universitat Pompeu Fabra, Doctor Aiguader 88, Barcelona, Spain
[2] Parc de Recerca Biomèdica de Barcelona (PRBB), Aiguader 88, Barcelona, Spain

dionysia.tsoutsi@upf.edu

Enhanced darkfield microscopy with hyperspectral imaging capability arises as a potent tool in modern bioanalysis. This technique permits real-time optical imaging of biologicals, nanoscale materials, or a combination of both, based on the detection of light that is elastically scattered by the sample. This enables fast and easy optical observation of nanoscale objects in solution, biological media, at live cells and tissues, without additional contrast agents.

Moreover, this technique can resolve individual nanoparticles and therefore, changes in the surface chemistry and other physicochemical properties affecting the scattering efficiencies will be monitored at real-time without processing the sample. In this context, plasmonic nanometric scatterers are advantageous as they highly increase the sensitivity of the method and particles with sizes down to few nanometers can be identified.

This constitutes a unique tool for tracking how the biological milieu (growth media, cell environment, blood, etc.) changes the nanoparticles. The results are at the level of single and collective particles. To shed light upon these processes, we engage particles of different shapes and compositions in single or multiparticle configurations.

Development of a SPR aptasensor: towards a robust tool for detecting traces of lysozyme dimer in oligomeric and aggregated mixtures

Alina Vasilescu[1],
Szilveszter Gaspar[1], Sorin David[1] , Ana Maria Titoiu[1], Cristina Purcarea[2], Medana Zamfir [2]

[1]International Center of Biodynamics,1B Intrarea Portocalelor, 060101 Bucharest, Romania
[2]Institute of Biology of the Romanian Academy, 296 Splaiul Independentei, 060031 Bucharest, Romania

avasilescu@biodyn.ro

Protein aggregates formed in various steps during the manufacturing or storage of therapeutic proteins affect the quality, safety and efficacy of biopharmaceutics[1]. While various methods have been developed to assess oligomers and aggregates of different sizes, the methods applicable for detecting aggregates under 50 nm have some limitations. Aggregates' analysis is complicated by the existence of many of oligomers and conformers with different properties[2], moreover physical aggregates elude separation-based methods. For peptides and proteins undergoing amyloid-type aggregation various antibodies and aptamers have been developed recognizing with high selectivity either the monomeric, the oligomeric or the fibrillar form. Antibody or aptamer-based methods may complement well the current separation-based procedures for aggregate detection, in particular when combined with label-free detection methods such as Quartz Crystal Microbalance[3] or Surface Plasmon Resonance. Working towards developing a sensitive method that will allow detecting low amounts of oligomers in concentrated monomeric protein solutions, we hereby report the optimization of an SPR aptasensor[4] for the detection of lysozyme dimer, chosen here as model of protein oligomers. Lysozyme is a 14.3 kDa enzyme found in the human body as well as in plants, bacteria and animals. Lysozyme was widely used as a model for enzyme catalysis, protein structure, function and interactions, including protein aggregation, moreover was employed as a model in pharmaceutical applications, e.g. drug delivery, novel treatment strategies etc. The method described here exploits the differences in binding kinetics and affinity between the lysozyme monomer and dimer, to an aptamer developed for the monomeric form. In previous works we have optimized an aptasensor for the detection of monomeric lysozyme. The aptasensors design is based on coating the Au interfaces with a self-assembled monolayer of a thiol containing ethylene glycol groups and having carboxylic end groups, that allowed to further

immobilize neutravidin by amine coupling. A lysozyme aptamer with the sequence 5'-/5-Biosg_TTT TTT TTT TTT TTT TTT GCA GCT AAG CAG GCG GCT CAC AAA ACC ATT CGC ATG CGG C-3', biotynilated at the 5' end was attached next by affinity. The experimental setup included a detection system based on a Spreeta SPR2K23 SPR sensor (Texas Instruments, TX, USA), with a fitted 2-channel PDMS flow cell and a PC interface for signal acquisition. This aptasensor and setup were also used to study the self-association of lysozyme, where high non-specific adsorption of aggregated protein samples was observed[5]. Advancing from this, in this report we show that by changing the ionic strength, pH and composition of testing buffer the non-specific adsorption is minimized and the aptamer's binding to a covalent lysozyme dimer is exacerbated in certain experimental conditions compared to the binding of monomer (Fig.1). Aiming to achieve quantitative evaluations of aggregates present in the protein sample, we produced intentionally a covalent lysozyme dimer by cross-linking with dimethylsuberimidate, we purified it by size-exclusion chromatography and we used it as standard. The aptasensor detected 1.4 nM lysozyme dimer at pH 7.4. Next, sensorgrams recorded for mixtures of monomer and dimer revealed different features compared to those for either monomer or dimer in individual solutions. Chemometric methods were applied to obtain qualitative and quantitative information regarding the composition of the analyzed mixtures. Seven features of the sensorgrams, representing areas under the curve for specific time intervals were selected as variables to describe the SPR signal for monomer-dimer mixtures. Based on these variables, Principal Components Analysis allowed observing groups of samples with the same dimer content and a relatively good separation between groups with different concentrations of dimer. Additionally, Multiple Regression analysis enabled to establish quantitative correlations between features of the sensorgrams and the dimer concentration in the samples (Fig.2). The amounts of dimer estimated by MR analysis of sensorgrams recorded with the aptasensor were very similar to the theoretical concentrations. By this approach the SPR aptasensor allowed determining 0.1-1% dimer in solutions of lysozyme monomer without any separation. This concentration range corresponds to the typical levels investigated with regards to degradation products and related compounds in pharmaceutical products, as the corresponding maximum allowed limits per compendia or manufacturer specifications are generally set in this range. The aptasensor was furthermore applied to observe the variations in lysozyme oligomer amounts during the aggregation of lysozyme solutions at 60°C and pH 2.
However, the thiol-coated SPR interfaces are not very advantageous for aggregated sampled as tightly binding oligomers mean that the sensor

needs to be regenerated in more stringent conditions, which shortens its lifetime. As an alternative to the thiol-coated interfaces we explored graphene-coated surfaces deposited via layer-by-layer and functionalized with lysozyme aptamer[6]. First, clean Au interfaces were coated with poly(allyldiethylammonium) (PDDA), a polycationic polymer, followed by immersion in graphene oxide(GO) solution for 15 minutes. The procedure was repeated to deposit successive layers and the deposition process was followed both by SPR, by following the increase in the SPR angle with the number of PDDA/GO layers and by cyclic voltammetry, using the redox probe $[Fe(CN)_6]^{3-}$, whose oxidation and reduction current decreased with the increase in the deposited PDDA/GO layers.

The optimum number of layers was found to be two and neutravidin was immobilized on the surface by amine coupling with the carboxylic groups on the GO. Finally the biotynilated lysozyme aptamer was bound by affinity on the neutravidin-functionalised surface (Fig.3). The aptasensor thus obtained was compared to the previous one based on a thiolated interface and displayed similar stability in buffer, slightly lower aptamer coverage but increased sensitivity with a detection limit of 0.7 nM for monomeric lysozyme at pH 6. The application of this aptasensor for monitoring the aggregation of lysozyme is also described.

The study is a starting point for aptasensors as novel analytical tools for the sensitive detection of small oligomers in therapeutic proteins, for which specific aptamer exists. The versatile aptasensor can be tuned, by simply adjusting the experimental conditions, for the sensitive and specific detection of either the monomer or the dimer, as per the desired application.

References

[1]   Vázquez-Rey, M., Lang, D.A., Biotechnol.Bioeng., 108 (2011),1494–1508

[2]   Pivato, M., De Franceschi, G., Tosatto, L., Frare, E., Kumar, D., Aioanei, D., Brucale, M., Tessari, I., Bisaglia, M., Samori, B., Polverino de Laureto, P., Bubacco, L., PloS ONE 7 (2012),12, e50027

[3]   Zurdo, J., Michael, R., Stallwood, Y., Hedman, K., Aastrup, T., 2011. Innov. Pharma. Technol. 37(2011), 34-40

[4]   Vasilescu A., Purcarea C., Popa E., Zamfir M., Mihai I., Litescu S., David S., Gaspar S., Gheorghiu M, Marty J-L,Biosens Bioelectron, 83 (2016), 353-360

[5]   Vasilescu, A., Gaspar,S., Mihai, I., Tache, A., Litescu, S., Analyst, 138 (2013), 3530–3537

[6]   Vasilescu A, Vezeanu A, David S, Gaspar S, in Maria Zaharescu, Horia Chiriac, Dan Dascalu (eds), Nanomaterials, nanoparticles, nanodevices, Series on Micro and Nanoengineering vol 24 (2016), p.145-160,

Figures
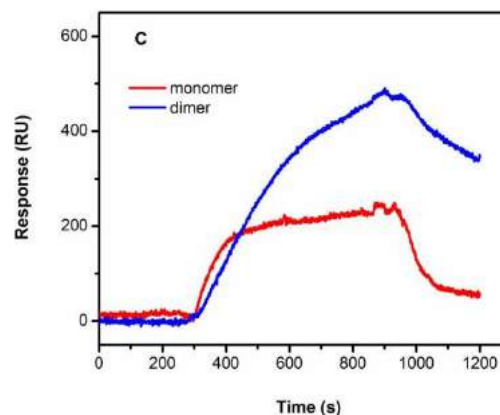
Figure 1. Sensorgrams recorded with the aptasensor for lysozyme monomer (3.5 µM, red curves) and lysozyme dimer (35 nM, blue curves), respectively in 20 mM TRIS buffer pH 7.4 with 100 mM NaCl and 5 mM $MgCl_2$ 0.05% Tween-20.
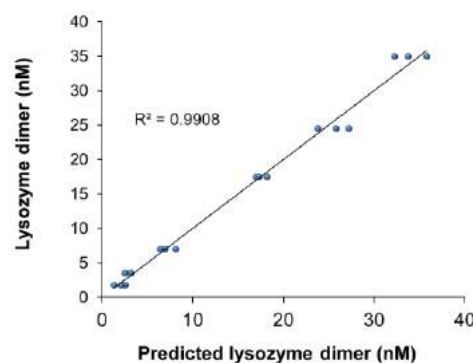
Figure 2. Analysis mixtures by Multiple Regression of the SPR data recorded for monomer-dimer mixtures.
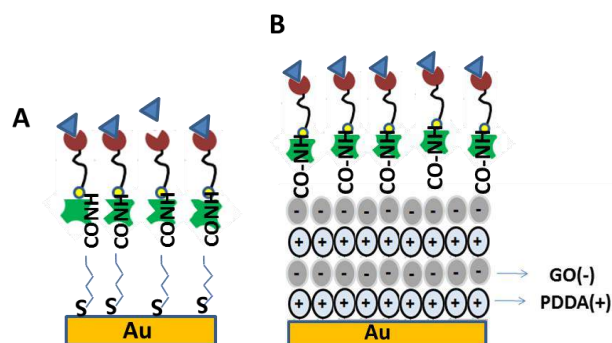
Figure 3. The design of lysozyme aptasensors based on (A) thiol-coated interfaces and (B) surfaces coated with PDDA and GO via layer-by-layer. On both interfaces, neutravidin is covalently linked to carboxylic groups on the surface, followed by the binding of a biotynilated lysozyme aptamer .

Smart drug delivery system that targets the epidermis and follicles

Martha Vázquez[1],
Rosana Saldaña[1], Mercedes Cócera[1],
Gelen Rodríguez[1], Lucyanna Barbosa-Barros[1] and
Olga López[2]

[1]Bicosome SL, Barcelona, Spain
[2]IQAC-CSIC, Barcelona, Spain

martha.vazquez@bicosome.com

Although drug delivery through the skin offers advantages over other administration routes, there are big challenges on target delivering actives in specific skin layers. Several strategies have been developed during the last decades attempting to overcome the skin barrier, however the technologies able to accomplish these tasks are still limited. The development of a topical delivery system requires a clever management of the actives and the interaction with the skin tissue. Bicosome is an innovative lipid system formed by smart biocompatible nanostructures enclosed in a lipid bilayer. These smart structures are able to penetrate through the narrow intercellular spaces of the stratum corneum, and once there, they are able to deliver the actives to the specific layer of the skin required.

This study describes the development of a bicosome system that targets the epidermis and follicles to effectively deliver a sebostatic active compound and potentiate its effects in order to prevent the development of the Acne.

The results observed in this study evidence the capacity of bicosomes to penetrate the epidermis and follicles (fig.1) and potentiate the effects of the sebostatic active ingredient (Fig.2) decreasing the presence *P Acnes* in the sin surface (Fig. 3).

References

[1] Fernández E, Rodríguez G, Hostachy S, Clède S, Cócera M, Sandt C, et al. Colloids Surfaces B Biointerfaces. 131 (2015)102–7.
[2] Shahmoradi Z, Iraji F, Siadat AH, Ghorbaini A. J Res Med Sci. 18 (2013) 115–7.
[3] Araviiskaia E, Dréno B. J Eur Acad Dermatology Venereol. 30 (2016) 926–35.

Figures
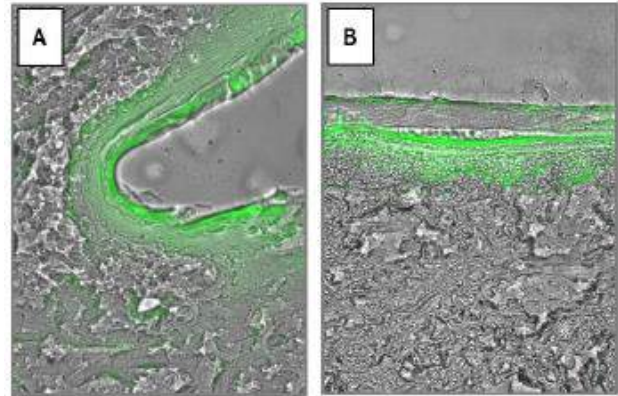
Figure 1. Fluorescence microscopy images of skin samples treated with the bicosome system containing the sebostatic agent, labelled with a fluorescent probe. The green areas show the penetration in the epidermis and follicle.
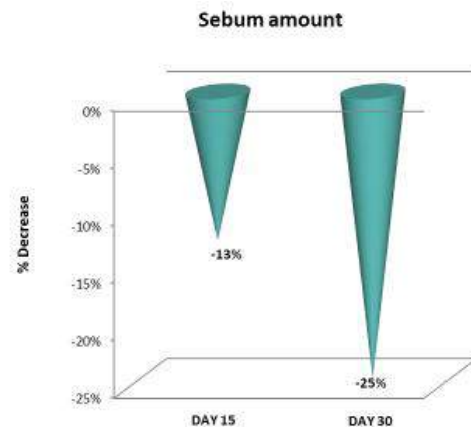
Figure 2. Decrease of sebum amount in the face of 20 volunteers treated with the bicosome system containing the sebostatic agent on Day 0 and Day 30 of the treatment . The sebum amount was determined with a Sebumeter® SM 815 (p value = 0,00).
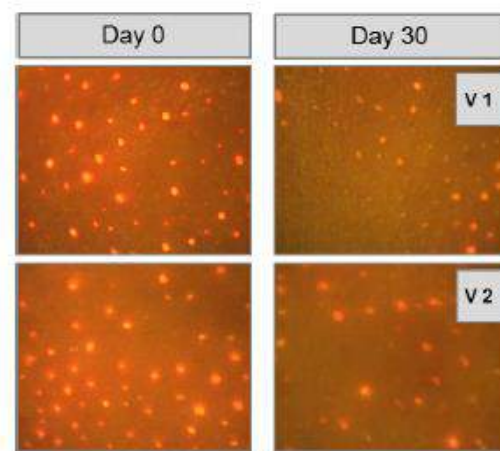
Figure 3. Visiopor® photographs of the face of two volunteers treated with bicosome system containing the sebostatic agent, showing the fluorescence in the pores, which indicates presence of P Acnes, on Day 0 and Day 30 of the treatment.

Versatile Star-shaped Polypeptide Conjugates with Controlled Self-assembly as Single Agents and in Combination Therapy

María J. Vicent

Polymer Therapeutics Lab. Centro Investigación Príncipe Felipe. Av. Eduardo Primo Yúfera 3, 46012, Valencia, Spain

mjvicent@cipf.es

Polypeptides are already playing a major role on a number of different relevant areas such as nanomedicine [1]. The physico-chemical parameters of a polypeptide-conjugate, and hence its biological performance, are defined by an intricate interplay of multiple structural factors. This highlights the need for detailed structure-activity relationship studies to develop the hierarchical strategies of polypeptide conjugate design. However, structural complexity also represents a unique opportunity, since small changes at the structural level might endow nanomedicines with outstanding and unexpected biological performance [2].

In our group, we have overcome the main classical limitations for the synthesis of defined polypeptides using precise controlled reactions followed by an adequate characterization yielding to well-defined polypeptidic architectures (including stars, graft and block-copolymers) by NCA polymerization techniques [3]. In addition, post-polymerization techniques allow us the introduction of a variety of functionalities yielding a set of orthogonal reactive attachment sides [4]. Using these techniques and following a bottom-up strategy we have been able to obtain star-based polypeptide architectures with the capacity to self-assemble yielding supramolecular nanostructures with interesting properties [5].

Star-shaped polypeptides with different cores and varied length of arms have been studied. We observed two different mechanism that control the self-assembling behaviour of these polymers. For compounds with short arms we observed formation of supramolecular polymers driven by hydrophobic interactions and hydrogen bonding. For bigger polymers we observed core-independent self-assembly. Supramolecular polymers and polyions with transition state formed distinct morphological structures - fibrillar and spherical, respectively. Interestingly enough, for some molecules we also observed an intermediate mechanism. Many compounds were found to be ionic strength and temperature dependent that directly correlated with the reported mechanism of self-assembly.

This strategy enabled *in vitro* and *in vivo* evaluation, revealing a lack of toxicity, an enhanced *in vitro* cell internalization rate and significantly greater terminal and accumulation half-life *in vivo* together with a significant lymph node accumulation [5].

These results allow us to envisage these systems as promising nanocarriers for therapeutic or diagnostic applications, especially in anti-cancer treatments. Additionally, further studies to identify the mechanism for the significant accumulation found in the lymph nodes will open up a wide range of opportunities for the currently unsuccessful clinical approaches to target lymph node metastasis, imaging of sentinel lymph node and cancer immunotherapy.

References

[1] Duro-Castano A., Conejos-Sánchez I., Vicent M.J. Polymers 2014, 6, 515-551.

[2] Zagorodko O., Arroyo-Crespo, J.J., Nebot, V.J., and Vicent, M.J. Macromolecular Bioscience 2017, 17, 1600316-n/a.

[3] a) Duro-Castano A., England, R.M., Razola, D., Romero, E., Oteo-Vives, M., Morcillo, M.A., and Vicent, M.J. Molecular Pharmaceutics 2015, 12, 3639-3649; b) Conejos-Sánchez I. Duro-Castano, A., Birke, A., Barz, M., and Vicent, M.J. Polymer chemistry 2013, 4, 3182-3186.

[4] Barz M., Duro-Castano A., Vicent M.J. Polymer Chemistry 2013, 4, 2989-2994

[5] Duro-Casaño Nebot, V. J., Niño-Pariente, A., Armiñán, A., Arroyo-Crespo, J. J., Paul, A., Feiner-Gracia, N., Albertazzi, L. and Vicent, M. J. Advanced Materials 2017, doi. 10.1002/adma.201702888

Acknowledgements

In vivo optimization of plasmonic photothermal therapy for oncological medicine

Clara Vilches[1],
Jordi Morales-Dalmau[1], Miguel Mireles[1], Mar Martínez-Lozano[2], Vanesa Sanz[1], Ignacio de Miguel[1], Oriol Casanovas[2], Turgut Durduran[1], Romain Quidant[1]

[1]ICFO – Institut de Ciències Fotòniques, The Barcelona Institute of Sciences and Technology, 08860, Castelldefels, Spain
[2]Catalan Institute of Oncology, Bellvitge Biomedical Research Institute – IDIBELL, 08908, L'Hospitalet de Llobregat, Spain

Clara.Vilches@icfo.eu

Nanomedicine is an emerging field where cutting-edge advances in nanotechnology, biology and medicine are constantly converging. During the last decades, the use of organic and inorganic nanoparticles has been increasing in several biomedical areas. Specifically in oncology, nanoparticles have become promising agents in the research of new strategies for cancer screening and therapy [1]. Among all different types of existing nanostructures, gold nanoparticles (AuNPs) have attracted special attention given their heating efficiency and light absorption tunability in the near-infrared region due to their localized surface plasmon resonance, which makes them very versatile in nanomedicine [2]. These plasmonic properties of AuNPs, along with their ease of surface functionalization and biocompatibility, are at the basis of the so called plasmonic photothermal therapy (PPTT). In this technique, laser light illumination is used to enhance cell destruction in cancerous tissue decorated with AuNPs from heat generation. When tissue is under laser irradiation, the absorbed light from accumulated nanoparticles leads to an exchange of energy resulting in an increase of temperature, triggering cell death mechanisms and, ultimately, tumour shrinkage [1]. The local enhanced permeability and retention effect shown by tumors allow the passive accumulation of nanoparticles in target cancer tissues, thus minimizing the impact of the PPTT in healthy tissue [2]. However, and as in other therapies, PPTT requires a tight control of all actors involved, from the surface chemistry and toxicity of AuNPs, to the amount of generated heat and its physiological effect to the tumor.

Here, we present our first results in the optimization of PPTT with gold nanorods (AuNRs) both *in vitro* and *in vivo* in an orthoxenograft mouse model of clear renal cell carcinoma. First, and through a systematic *in vitro* study, we have defined the optimal surface chemistry of the AuNRs in order to maximize cell internalization with low toxicity and high heating efficiency. Then, these results have been validated *in vivo*, determining AuNR biodistribution, tumor accumulation and long-term toxicity at working concentration in the mentioned murine model. To study the influence of external treatment factors in PPTT, mice with renal carcinoma have been treated under different irradiation power and exposure time of the laser. Together with changes in physiological parameters, experimental light conditions have been correlated with final skin temperature, macroscopic dermal lesion and tumor damage. In addition, and for the first time, two diffuse optics techniques –diffuse correlation and diffuse reflectance spectroscopy (DCS and DRS, respectively [3])- have been used to non-invasively determine the evolution of hemodynamic parameters, such as tissue oxygen saturation, total haemoglobin concentration, and AuNRs concentration. The monitorization of all these tumor hemodynamic parameters are crucial to understand the efficacy of the PPTT treatment.

Altogether, we have set the bases of PPTT and characterized all variables to, in a near future, establish a feedback system that integrates light treatment conditions, AuNP concentration, and physiology of the tumour, allowing the modulation and personalization of this therapy for different tumour types.

References

[1] Wilhelm S *et al.*, *Nature Reviews Materials*, 1 (2016).
[2] Abadeer N and Murphy C, *Journal of Physical Chemistry C*, 120 (2016), pp 4691-4716.
[3] Farzam P *et al.*, *Biomedical Optics Express*, 5 (2017), pp 2563-2582.

Arginine – Functionalized Gold Nanoparticles: Synthetic Analogues of Antimicrobial Peptides

Marija Vukomanovic[1,2],
Eduard Torrents[1]

[1]Bacterial Infections: Antimicrobial Therapies, Institute for Bioengineering of Catalonia, c/ Baldiri Reixac 15-21, Barcelona, Spain
[2]Advanced Materials Department, Institute Jozef Stefan, Jamova 39, Ljubljana, Slovenia

mvukomanovic@ibecbarcelona.eu

As a part of the innovative strategies recently developed to cope with the urgent global issue associated with antimicrobial resistance and consequent decreasing of the efficiency for some of the major antimicrobial therapeutics, antimicrobial peptides (AMPs) are studied as one of the most perspective choices [1]. Originally, a class of antimicrobials which belongs to AMPs corresponds to a small oligopeptides with 5-100 amino acids in length characterized by positive net charge and amphiphilic nature which are considered to be critical for their solubility and mechanism of action [2]. They are prone for intensive interactions with negatively charged bacterial cell wall and capable for changing the permeability of their membrane which may cause leaking the cytosol out the cell (leading directly to death) or increasing permeability and opening the pathways for getting antimicrobials inside bacteria (enabling their interference with bacterial metabolism, replication and growth) [2]. As natural-sourced antimicrobials, AMPs are originally found and isolated from the metabolism of both prokaryotes (bacteria) and eukaryotes (fungi, plants, insects, animals) and are a part of the innate immune system used against infection [3]. Following the natural models, a number of different strategies have been developed to design synthetic analogues capable to mimic the structure and biological function of natural AMPs mainly based on polymerization of monomers with critical functional groups responsible for antimicrobial activity (i.e. poly-arginine) or post-polymerization modification of the polymers (structure re-arrangements and surface chemistry) [2]. The main issues associated with practical applications of AMPs are associated with high cost, low biological stability (inactivated by small structural changes and especially sensitive to enzymes) and low bioavailability [2]. Currently the main attempts directed to resolving these issues consider using nanotechnological approaches, including application of drug delivery systems (encapsulation of AMPs within polymeric nanoparticles/micelles) and/or formulation of nanoparticles made of AMPs. The second approach has found to be particularly efficient especially in the case of self-assembly of AMPs into nano-formulations (shown to increase the therapeutic index against *Staphylococcus aureus* infection in mice model) [4] as well as functionalization of the surface of gold (Au) nanoparticles (shown to extend activity of nisin peptide, characterized by activity to Gram-positive bacteria, to a number of Gram-negative strains including *Pseudomonas aeruginosa*, *Escherichia coli*, *Salmonella enteritidis*, *Bacteroides fragilis* and amp-C *Enterobacter cloacae* (antibiotic-resistant strain)) [5].
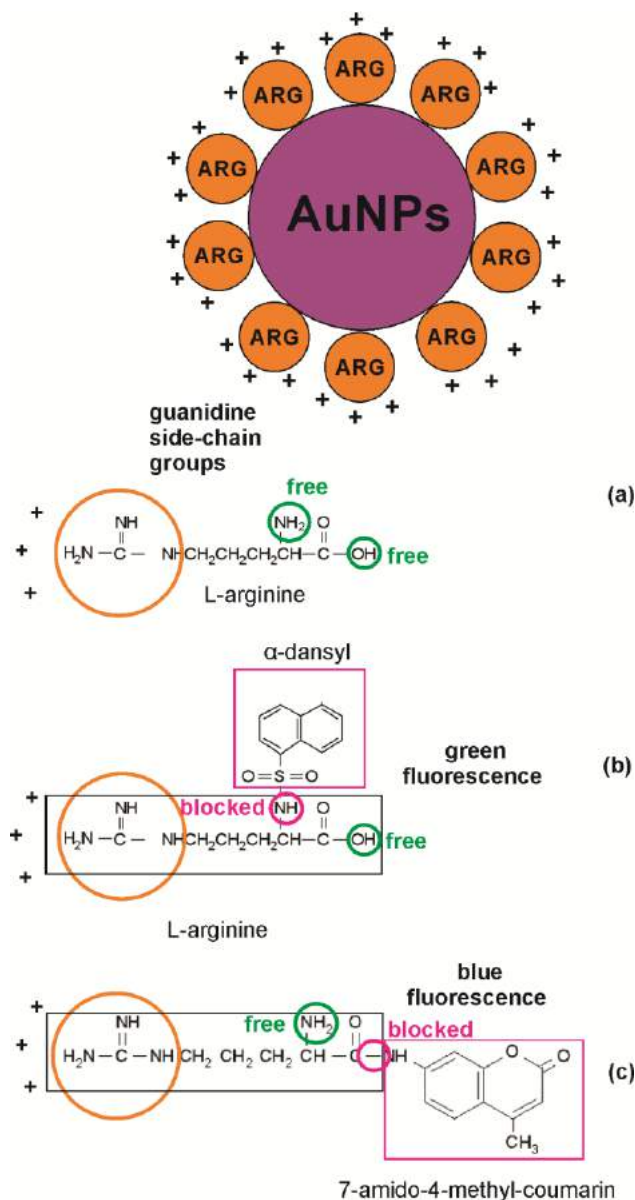
Figure 1. Illustration of the structural analogues of AMPs formed of positively charged Au NPs functionalized with: (a) arginine with free NH_2 and COOH groups, (b) α-dansyl-arginine (arginine with blocked NH_2 groups) and (c) 7-amido-4-methylcoumarin (arginine with blocked COOH groups).

Recently it has been shown that biological function of AMPs could be achieved also by mimicking their structure in highly simplified manner. The approach considered formulation of arginine-functionalized Au NPs deposited to apatite template [6] containing

arginine as cationic, Au NPs as hydrophobic and apatite as hydrophilic components. The main advantages of designed structure, entitled as structural analogue of AMPs, is in its potential to provide significant improvement in stability and bioavailability. It has been assumed that NH_2 functional groups in these structures are responsible for bonding to Au NPs, COOH groups are responsible for stabilization of Au NPs (preventing aggregation and ingrowth by providing boding to the template) while side-chain groups (containing positively/charged guanidinum functional group) are a source of antimicrobial activity. Considering the potential these structures hold and their perspective in designing innovative antimicrobial therapies, we performed comprehensive investigation of their properties including detailed testing of antimicrobial potential and investigation of the functional groups with the critical role in achieving antimicrobial activity of these nano-systems. Following this concept we synthesized a series of similar structural analogues of AMPs with three types of functionalization: arginine, *L*-arginine-7-amido-4-methylcoumarin and dansyl-*L*-arginine. All of them contained the same side-chains with positively charged guanidinum. In contrast to arginine (with free carboxylic (COOH-) and amine (NH_2-) groups), *L*-arginine-7-amido-4-methylcoumarin is with blocked COOH- (bonded with 7-amido-methylcoumarin- group) while dansyl-*L*-arginine is with blocked NH_2- (bonded with dansyl-group). The chemistry of the groups selected for functionalization of the surface of Au NPs is illustrated in Fig. 1 while the summary of the antimicrobial properties including minimal inhibitory concentrations (MICs) and their log reduction capacities as well as their comparison to ciprofloxacin used as a reference is provided in Table 1. Results confirmed that arginine-Au NPs were able to provide susceptibility in *E. coli* (MG1655), *S. aureus* (ATCC 12600) and *P. aeruginosa* PAO1 (ATCC 15692). The activity of the arginine/Au NPs, with free COOH and NH_2 groups, was most efficient in *E. coli* and it was decreased for *S. aureus* and *P. aeruginosa*. When NH_2 groups were blocked, activity against all three types of bacteria drastically decreased. Opposite happened in the case when COOH group was blocked by replacing OH- with larger, aromatic group resulting in significantly enhanced activity against all three types of bacteria. Accordingly we confirmed that free COOH groups in arginine-Au are responsible to provide stabilization of Au NPs while free NH_2 groups have a role to enable bonding to Au NPs. In this case when functionalization of Au NPs, which takes place through N-Au bonding, was prevented instead of stable conjugation, functionalizing molecules were probably remained absorbed forming the structures which were not able to provide efficient antimicrobial activity. On the other hand replacing OH groups with larger, aromatic group (with much higher possibility for steric interactions) provided more efficient stabilization of Au NPs which resulted in better antimicrobial activity. Both chemical stability of the surface functionalization as well as morphological stability of the Au NPs are found to be highly relevant for antimicrobial activity of these AMPs structural analogues. This finding reveal important parameters responsible for antimicrobial activity of structural analogues of AMPs and open the new toolbox for further exploring of their antimicrobial properties and ability for interactions with bacteria.

Au NPs with:		Microbiological strains		
		Escherichia coli (MG1566)	Staphylococcus aureus (ATCC 12600)	Pseudomonas aeruginosa PAO1 (ATCC 15692)
arginine	*MIC$_{50}$	0.4 mg/ml	0.5 mg/ml	0.4 mg/ml
	**MIC$_{>90}$	1.0 mg/ml	2.0 mg/ml	1.5 mg/ml
	log-reduction	90% (9x10^5 cfu/ml) (0.6 mg/ml) >99.9% (<5x10^3 cfu/ml) (1.0 mg/ml)	99% (9.5x10^4 cfu/ml) (2 mg/ml)	90% (4.1x10^8 cfu/ml) (2 mg/ml)
L-arginine-7-amido-4-methyl coumarin	MIC$_{50}$	0.2 mg/ml	0.2 mg/ml	<0.1 mg/ml
	MIC$_{>90}$	0.5 mg/ml	2.0 mg/ml	1.0 mg/ml
	log-reduction	99.9% (5x10^3 cfu/ml) (0.6 mg/ml) >99.9% (<5x10^3 cfu/ml) (1.0 mg/ml)	90% (3.4x10^6 cfu/ml) (1.5 mg/ml) 99.99% (<5x10^3 cfu/ml) (2 mg/ml)	99% (3x10^7 cfu/ml) (1 mg/ml) 99.99% (8.6x10^5 cfu/ml) (2 mg/ml)
dansyl-L-arginine	MIC$_{50}$	1.0 mg/ml	0.35 mg/ml	1.0 mg/ml
	MIC$_{>90}$	/	/	2.0
	log-reduction	/	90% (4.5x10^6 cfu/ml) (2 mg/ml)	/
cipro-floxacin reference	MIC$_{50}$	0.5 µg/ml	0.5 µg/ml	0.5 µg/ml
	log-reduction	>99.9% (<5x10^3 cfu/ml) (0.5 µg/ml)	99% (5.7x10^5 cfu/ml) (0.5 µg/ml)	99.9% (1.1x10^6 cfu/ml) (0.5 µg/ml)

Table 1. Summary of the antimicrobial properties of arginine-based structural analogues of AMPs.
*MIC$_{50}$ –minimal inhibitory concentration of the material which enabled dead of 50% of bacteria.
**MIC $_{>90}$ –minimal inhibitory concentration of the material which enabled dead of more than 90% of bacteria.

References

[1] L. S. Tavares, C. S. F. Saliva, V. C. de Souza, V. L. da Saliva, C. G. Diniz, M. O. Santos, Front. Microbiol.. 4 (2013) 412.

[2] A. Ficai, A. M. Grumezesku (Eds.), Nanostructures for Antimicrobial Therapy, Elsevier 2017.

[3] A. A. Bahar, D. Ren, Pharmaceuticals (Basel) 2013, 6(12) 1543.

[4] L. Liu, K. Xu, H. Wang, J. P. K. Tan, W. Fan, S. S. Venkatraman, L. Li and Y.-Y. Yang, Nat. Nanotechnol., 4 (2009) 457.

[5] M. Vukomanovic, V. Zunic, S. Kunej, B. Jancar, S. Jeverica, R. Podlipec, D. Suvorov, Sci. Rep., 7 (2017) 4324.

[6] M. Vukomanovic, M., Logar, S. D. Skapin, D. Suvorov, J. Mater. Chem. B, 2 (2014) 1557.

Nanoporous Anodic Alumina for the Development of Molecular Gated Sensors

E. Xifre-Perez[1],
A. Ribes[2,3], E. Aznar[2,3], F. Sancenón[2,3],
R. Martínez-Mañez[2,3], L.F. Marsal[1]

[1]Departament d'Enginyeria Electrònica, Elèctrica i Automàtica, Universitat Rovira i Virgili, Avda. Països Catalans 26, 43007, Tarragona, Spain
[2]Instituto Interuniversitario de Investigación de Reconocimiento Molecular y Desarrollo Tecnológico (IDM). Universitat Politècnica de València,, Camino de Vera s/n, 46022, Valencia, Spain.
[3]CIBER de Bioingeniería, Biomateriales y Nanomedicína (CIBER-BBN)

lluis.marsal@urv.cat, rmaez@qim.upv.es

Nanoporous anodic alumina (NAA) is a cost-effective material that presents an ordered distribution of pores. Its well-known electrochemical fabrication techniques allow for the precise control of pore diameter, interpore distance, pore length, and pore geometry [1]. Moreover, NAA is stable, biocompatible, and does not degrade in aqueous solutions [2], which has contributed to its successful use in a wide array of medical and biological applications like orthopedic prosthetics, dental and coronary stents, cell culture scaffolds, and biomolecular filtration [3,4].

The high effective surface area of NAA makes it a versatile and interesting platform for loading active agents like drugs or molecules as pores are used as nanocontainers [5]. In this context, we present here the use of NAA to develop gated materials for sensing applications. The biosensors proposed consist of a NAA support where the pores are loaded with a fluorophore and blocked by selected molecules able to recognize selectively a certain target analyte. The presence of the analyte unblocks the pores resulting in a selected delivery of the entrapped reporter.

These gated-NAA based biosensors have high potential for the selective and sensitive detection of molecules that currently require complex and/or long processing. Are very simple to prepare, easy to handle, reusable, and do not require trained personnel.

References

[1] Xifre-Perez, E.; Ferré-Borrull, J.; Pallarès, J.; Marsal, L. F. Microporous Mesoporous Mater. 239 (2017) 363.
[2] Xifre-Perez, E.; Ferré-Borrull, J.; Pallarès, J.; Marsal, L.F., Mesoporous Biomaterials, 2 (2015) DOI: 10.1515/mesbi-2015-0004.
[3] Losic, D.; Simovic, S., Expert Opin. Drug Deliv. 6 (2009) 1363.
[4] Swan, E.E.L.; Popat, K.C.; Grimes, C.A.; Desai, T.A., J. Biomed. Mater. Res. Part A 72 (2005) 288.
[5] Porta-i-Batalla, Xifré-Pérez, E.; M.; Eckstein, C.; Ferré-Borrull, J.; Marsal, L.F. Nanomaterials 7 (2017) 227.

Figures
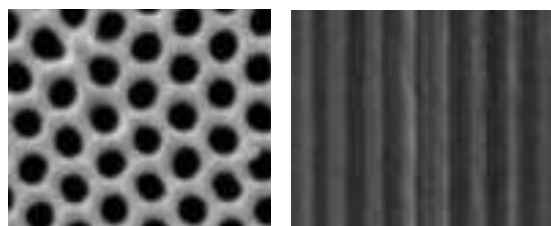
Figure 1. Scanning Electron Microscopy image of porous anodic alumina: top view (left) and transversal cut (right).
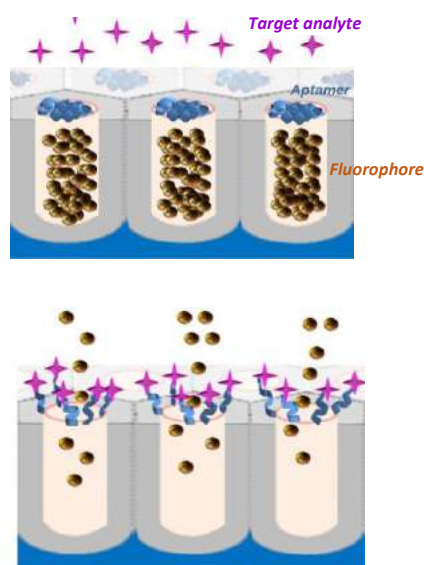
Figure 2. Schematic representation of capped porous anodic alumina (top) and the selective delivery of the fluorophore due to the presence of the target analyte (bottom).

Biological Recognition of Nanoparticles

Yan Yan,

Centre for BioNano Interactions, University College Dublin, Ireland

yan.yan@cbni.ucd.ie

It has been of interest to find guiding principles to help us understand how nanoscale objects interact with living organisms. Firstly, the nanoscale is unique in biology, and our capacity to engineer on that scale is transformative. The intrinsic machinery of biology is defined and operates on the nanoscale. This means that nanoparticles are also actively transported around cells and biological barriers all unlike small molecules, which passively partition into biological compartments (cells, organs, etc.). Secondly, the power of being able to communicate with, and use those endogenous mechanisms of biology is potentially transformative in practical terms. It is clear, and is often discussed how transformative could be the contribution of nanoscience to medicine, diagnostics, and new kinds of cell therapies. However, with this enormous potential power to engage with the machinery of organisms there are also challenges. In this presentation, we discuss progress being made in understanding how interactions between nanoscale objects and living organisms occur, and their governing principles. We argue that the future lies in pressing forward to develop a truly microscopic (molecular scale) understanding between the nanoscale and living organisms.

Graphene-based Nanomaterials for Biomedical Applications

Julia Xiaojun Zhao[1],
Xu Wu[1], Min Wu[2], and David Pierce[1]

[1]Department of Chemistry, University of North Dakota, Grand Forks, ND 58202, USA
[2]Department of Biomedical Sciences, University of North Dakota, Grand Forks, ND 58202, USA

julia.zhao@und.edu

Graphene, one of the most attracting two-dimensional nanomaterials, has demonstrated a broad range of applications because of its excellent electronic, mechanical, optical and chemical properties. We have developed a few new graphene-based nanomaterials, including graphene-based fluorescent quantum dots, reduced graphene oxide (RGO)/metal (oxide) (*e.g.* RGO/Au, RGO/Cu$_2$O, and RGO/Ag) nanocomposties, graphene-silica core-shell nanostructures, and 3-D graphene scaffold. In this presentation, the methods of making these new graphene-based materials will be introduced. A series of characterizations of these nanomaterials using STEM, FE-SEM, EDS, UV-vis absorption spectroscopy, XRD, FT-IR and Raman spectroscopy will be discussed. Finally, the applications of these nanomaterials in the fields of biomedical study will be reported including fluorescence imaging using graphene quantum dots, , cell culture using 3D graphene, anti-bacterial applications of graphene-metal nanocomposite, and photothermal therapy and drug delivery of the graphene nanostructures.

The first example is the graphene quantum dots. a facile bottom-up method for the synthesis of highly fluorescent graphene quantum dots (GQDs) will be discussed using a one-step pyrolysis of a natural amino acid, L-glutamic acid, with the assistance of a simple heating mantle device. The developed GQDs showed strong blue, green and red luminescence under the irradiation of ultra-violet, blue and green light, respectively. Moreover, the GQDs emitted near-infrared (NIR) fluorescence in the range of 800-850 nm with the excitation-dependent manner. This NIR fluorescence has a large Stokes shift of 455 nm, providing significant advantage for sensitive determination and imaging of biological targets. The fluorescence properties of the GQDs, such as quantum yields, fluorescence life time, and photostability, were measured and the fluorescence quantum yield was as high as 54.5 %. The morphology and composites of the GQDs were characterized using TEM, SEM, EDS, and FT-IR. The feasibility of using the GQDs as a fluorescent biomarker was investigated through *in vitro* and *in vivo* fluorescence imaging. The results showed that the GQDs could be a promising candidate for bioimaging. Most importantly, compared to the traditional quantum dots (QDs), the GQDs is chemically inert. Thus, the potential toxicity of the intrinsic heavy metal in the traditional QDs would not be a concern for GQDs. In addition, the GQDs possessed an intrinsic peroxidase-like catalytic activity that was similar to the graphene sheets and carbon nanotubes. Coupled with 2,2'-azino-bis(3-ethylbenzothiazoline-6-sulphonic acid) (ABTS), the GQDs can be used for the sensitive detection of hydrogen peroxide with a limit of detection of 20 µM.

The second example is the graphene oxide. We explored potential biomedical applications of graphene-based nanomaterials by systematically studying antibacterial capacity of graphene oxide (GO) in both macrophages and animal models. Three types of bacteria, including *Klebsiella pneumoniae* (*Kp*), *Escherichia coli* (*E. coli*) and *P. aeruginosa* (*Pa*) were used for *in vitro* study. *Kp* was also selected as a representative multidrug resistant (MDR) bacterium for *in vivo* study. In *in vitro* study, GOs effectively eradicated *Kp* in agar dishes and thus protected alveolar macrophages (AM) from *Kp* infection in the culture (Figure 1). In the *in vivo* evaluation, GOs were introduced intranasally into mouse lungs followed by testing, organ tissue damage including lung, liver, spleen, and kidneys, polymorphonuclear neutrophil (PMN) penetration, bacterial dissemination, and mortality in Kp-infected mice. We found that GO can contain and eradicate the growth and spread of *Kp* both *in vitro* and *in vivo*, resulting in significantly increased cell survival rate, less tissue injury, subdued inflammatory response, and prolonged mice survival. These findings indicate that GO could be a promising biomaterial for effectively controlling MDR pathogens.

The third example is the reduced graphene oxide (RGO)/metal (oxide) (*e.g.* RGO/Au, RGO/Cu2O, and RGO/Ag) nanocomposties. It was developed using glucose as the reducing agent and the stabilizer. The glucose not only reduced GO effectively to RGO, but also reduced the metal precursors to form metal (oxide) nanoparticles on the surface of RGO. Moreover, the RGO/metal (oxide) nanocomposites were stabilized by gluconic acid on the surface of RGO. The developed RGO/metal (oxide) nanocomposites were characterized using STEM, FE-SEM, EDS, UV-vis absorption spectroscopy, XRD, FT-IR and Raman spectroscopy. Finally, the developed nanomaterials were successfully applied as an electrode catalyst to simultaneous electrochemical analysis of L-ascorbic acid (L-AA), dopamine (DA) and uric acid.

Figures
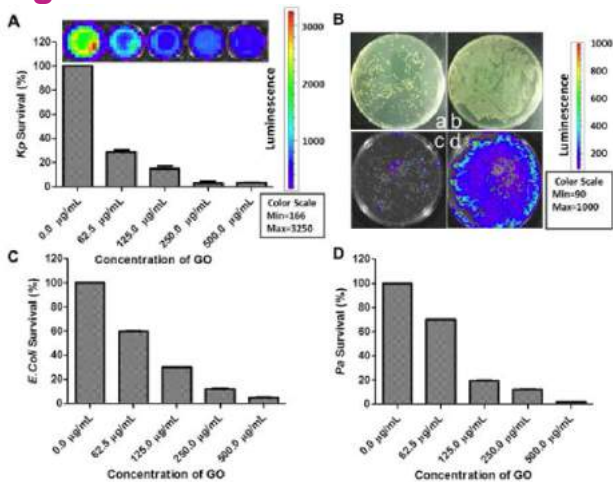
Figure 1. Concentration-dependent antibacterial property of GO. (A) Kp survival rate after treatment with different concentrations of GO. Inset: Bioluminescence images of Kp bacteria after incubation with different concentrations of GO. From left to right: 0, 62.5, 125.0, 250.0, and 500.0 µg/mL of GO. (B) Representative photographs (a and b) and bioluminescence images (c and d) of Kp bacterial colonies treated with 250.0 µg/mL of GO (a and c) and without GO (b and d) formed on LB-agar plates. (C) The *E. coli* survival rate after treatment with different concentrations of GO. (D) Pa survival rate after treatment with different concentrations of GO. The survival rate was calculated by measuring the OD600.

Electron transport through peptides and blue-copper azurins

Linda Angela

1Universidad Autónoma de Madrid,
Cantoblanco, Madrid, Spain

linda.zotti@uam.es

Inspired by recent experiments [1], we present a theoretical study of the electron transport through heptapeptides based on alanine, glutammic acid, lysine and tryptophan. For them all, we found very low conductance values and we ascribed them to the high localization of their frontier orbitals [2].

We also show a combined experimental and theoretical work on the transport through a bluecopper azurin and a mutant; we found that the conductance channels in the single-protein electrical contact can be finely tuned by performing point-site mutations in the outer protein structure [3].

References

[1] Sepunaru, L.; Refaely-Abramson, S.; Lovrincic, R.; Gavrilov, Y.; Agrawal, P.;Levy, Y.; Kronik, L.; Pecht, I.; Sheves, M.; Cahen, D. J. Am. Chem. Soc. 2015, 137,9617

[2] L. A. Zotti, S. Refaely-Abramson,L. Kronik and J. C. Cuevas, in preparation.

[3] M. P. Ruiz, A. C. Aragonés, N. Camarero, J. G. Vilhena, M. Ortega,L. A. Zotti, R. Peréz, J. C. Cuevas, P. Gorostiza, I. Diez Pérez, submitted

Figures
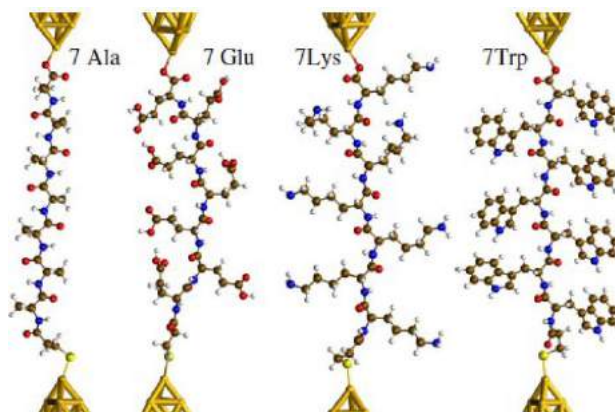
Figure 1. Junctions embedding four kinds of heptapeptides held between gold electrodes.

authors	country	topic	poster title	student senior	page
Acero, Josep Lluís Carmen Bermudo, Teresa Mairal, Ciara K. O'Sullivan, Ian Riley, Ioanis Katakis	Spain	Integrated Systems / Sensors	Development of an automated system for the analysis of cell-free fetal DNA from maternal plasma for non-invasive pre-natal diagnostics	Senior	**95**
Acosta Capilla, Laura Karen Elisabet Xifré-Perez,Josep Ferré-Borrull and Lluis F. Marsal	Spain	Nanomaterials for Bio and Medical Applications	Stacked Periodic Nanoporous Anodic Alumina Structures for Sensing Applications	Student	**96**
Arqué, Francesc Xavier Tania Patiño, Samuel Sánchez	Spain	Bio-Inspired nanotechnologies	Exploring Enzymatic Reactions to Power Biocompatible Silica-Based Micromotors	Student	**98**
Barguilla, Irene Laura Vila, Laura Rubio, Balasubramanyam Annangi, Alba García-Rodríguez, Ricard Marcos, Alba Hernández	Spain	Nanotoxicology	Frozen dispersions of nanomaterials are a useful operational procedure in nanotoxicology	Student	**99**
Bellassai, Noemi Almudena Marti Morant, Jurriaan Huskens and Giuseppe Spoto	Italy	Bio-nanofabrication	Nanostructured antifouling polymer for DNA detection	Senior	**101**
Cabal Tato, Alexandre Aïda Varea Espelt, Albert Cirera Hernández	Spain	Bioelectronics	A Gold-based Inkjet-Printed Substrate for Physioelectric Research on Neurons	Student	**102**
Casanellas, Ignasi Anna Lagunas, Iro Tsintzou, Yolanda Vida, Daniel Collado, Ezequiel Pérez-Inestrosa, Cristina Rodríguez, Joana Magalhaes, Josep Samitier	Spain	Nanomaterials for Bio and Medical Applications	RGD dendrimer-based nanopatterns promote chondrogenesis and intercellular communication for cartilage regeneration	Student	**104**
Cheong, Yuen-Ki Xiuyi Yang, Rory M. Wilson, Sai Li and Guogang Ren	United Kingdom	Nanomaterials for Bio and Medical Applications	Structure activity relationship of antimicrobial nanoparticles to selective microbes	Senior	**105**
Chodara, Agnieszka Sylwia Kuśnieruk, Tadeusz Chudoba, Jacek Wojnarowicz, Witold Łojkowski	Poland	Nanomaterials for Bio and Medical Applications	Synthesis of nanohydroxyapatite using microwave energy	Student	**107**
Cortés, Constanza Laura Vila, Alba García-Rodriguez, Ricard Marcos, Alba Hernández	Spain	Nanotoxicology	Interaction of silver nanoparticles with differentiated Caco-2 cells monolayers	Senior	**108**
Dabrowska, Sylwia Jacek Wojnarowicz, Tadeusz Chudoba, Agnieszka Chodara, Andrzej Majcher, Witold Łojkowski	Poland	Nanomaterials for Bio and Medical Applications	The new generation of microwave reactors for hydro- and solvothermal synthesis	Student	**110**

authors	country	topic	poster title	student senior	page
Ene, Vladimir-Lucian Georgeta Voicu, Bogdan Stefan Vasile, Alexandru Grumezescu, Ecaterina Andronescu	Romania	Nanomaterials for Bio and Medical Applications	Nanostructured magnetic materials used in cancer treatment	Student	111
Escorihuela Marti, Laura Benjami Martorell, Alberto Fernandez	Spain	Nanotoxicology	Computational Toxicology descriptors for Metal oxide Nanoparticles	Student	113
Escudero, Pedro Rosa Villa, Mar Alvarez	Spain	Integrated Systems / Sensors	Nanomechanical Sensing with 2D Colloidal Diffraction Gratings	Student	114
Feiner-Gracia, Natalia Michaela Beck, Sílvia Pujals, Sébastien Tosi, Tamoghna Mandal, Christian Buske, Mika Linden, Lorenzo Albertazzi	Spain	Bio-nano measurement and microscopy	Super-resolution microscopy study of protein corona composition and evolution in single nanoparticles	Student	115
Hortelão, Ana C. Tania Patiño, Ariadna Perez-Jiménez, Ángel Blanco and Samuel Sánchez	Spain	Nanomaterials for Bio and Medical Applications	Urease Powered Nanobots for Drug Delivery Applications	Student	116
Ioniță, Mariana Teddy Tite, Luisa Pilan, George Mihail Vlăsceanu, Adi Ghebaur, Jorge S. Burns	Romania	Bio-nano measurement and microscopy	Graphene-based electrochemical biosensors for DNA detection in healthcare diagnosis	Senior	117
Khanal, Dipesh Alexey Kondyurin, Iqbal Ramzan, Kee Woei Ng, Wojciech Chrzanowski	Australia	Bio-nano measurement and microscopy	Probing the corona formation on nanodiamonds- its dynamics and biological consequences	Student	119
Kubíčková, Lenka Jaroslav Kohout, Ondřej Kaman, Petr Brázda, Pavel Veverka, Tomáš Kmječ, Karel Závěta, Petr Dvořák, Vít Herynek	Czech Republic	Nanomaterials for Bio and Medical Applications	Relaxivity of ε-Fe$_{2-x}$Al$_x$O$_3$ Nanoparticles	Student	120
Lado Touriño, Isabel Arisbel Cerpa Naranjo, Piedad Ros Viñegla, Paloma Ballesteros García, Sebastián Cerdán, García-Esteller	Spain	Nanomaterials for Bio and Medical Applications	Molecular Dynamics Simulations of Surfactants Adsorption on Carbon Nanotubes Surfaces	Senior	122
Lopes, Daniela Rita M. Pinto, Catarina Seabra, Sofia Lima, Bruno Sarmento, Cristina Martins, Cláudia Nunes, Salette Reis	Portugal	Drug Delivery	Amoxicillin-loaded lipid nanoparticles: towards a therapeutic approach for Helicobacter pylori infections	Student	123
Madden, Olena	Ireland	Bio-nanofabrication	Microfabrication of Gold colloids, size control, biomedical conjugation applications	Senior	124
Magalhães, Joana Alexandre C. Vieira, Sónia Rocha, Marcos S. Cardoso, Susana G. Santos, Margarida Borges, Marina Pinheiro, Salette Reis	Portugal	Drug Delivery	Rifampicin-loaded lipid nanoparticles to improve tuberculosis treatment: an active targeting approach	Student	126
Magrì, Davide Paola Sánchez-Moreno, Gianvito Caputo, Athanassia Athanassiou, Pierpaolo Pompa, Despina Fragouli	Italy	Nanotoxicology	In vitro toxicity of Polyethylene terephthalate nanoparticles in a Caco-2 model of intestinal barrier	Student	127

authors	country	topic	poster title	student senior	page
Melguizo, Consolación Laura Cabeza, Raul Ortiz, Julia Jiménez-Lopez, Gloria Perazzoli, Octavio Caba, Ana R. Rama, Celia Velez, Maria Carmen Leiva, Jose Carlos Prados	Spain	NanoMaterials for Medicine	Poly(ε-caprolactone) nanoparticles loading doxorubicin: effect in lung cancer	Senior	128
Mena Mollá, Salvador	Spain	Nanobioanalysis in vitro	miRNA sensing for disease monitoring	Senior	129
Mestre, Rafael Rafael Mestre, Tania Patino, Ariadna Pérez-Jiménez, Samuel Sánchez	Spain	Far Future Challenges	3D Bioprinting of Skeletal Muscle Tissue for the Development of Soft Bio-Robotic Systems	Student	130
Murillo, Nerea Samuel Sánchez	Spain	Nanomaterials for Bio and Medical Applications	Confinement of biomolecules to enhance the efficacy of enzyme-powdered micro/nanomotors	Senior	131
Neacsu, Ionela Andreea Patricia Medeşan, Florin Iordache, Vladimir Ene, Ecaterina Andronescu, Anton Ficai	Romania	NanoMaterials for Medicine	Leflunomide delivery for Rheumatoid arthritis therapy by folic acid-enhanced PEG-coated magnetic nanoparticles	Student	132
Neves Borgheti-Cardoso, Livia Xavier Fernàndez-Busquets	Spain	Drug Delivery	Extracellular vesicles derived from Plasmodium-infected red blood cells: Characterization and drug encapsulation studies	Senior	134
Nicoara, Adrian Ionut Patricia Medeşan, Ionela Andreea Neacşu, Bogdan Vasile, Florin Iordache, Ecaterina Andronescu, Anton Ficai	Romania	Drug Delivery	Folic acid-enhanced polyethylene glycol-coated Fe_3O_4 for Methotrexate delivery	Student	136
Pamplona Pagnossa, Jorge Pedro H. S. Cesar; Tamara L. dos Santos; Juliano E. de Oliveira; Eduardo Alves; Roberta H. Piccoli; Silvana Marcussi	Brazil	Nanomaterials for Bio and Medical Applications	Antimicrobial PVA/Alginate macroporous foam scaffold for wound dressing	Student	138
Paulo Mirasol, Sofia Santi Gene, Roger Mallol, Emilio Palomares	Spain	Nanomaterials for Bio and Medical Applications	Colloidal Quantum dots@SiO_2 as platform for enzymes detection	Student	139
Perlman, Or Iris S. Weitz, and Haim Azhari	Israel	NanoMaterials for Medicine	Potential Medical Applications of Ultra Small Copper Oxide Nanoparticles	Student	141
Pletsa, Vasiliki Ioanna Theochari, Vassiliki Papadimitriou, Dimitrios Papahatjis, Aristotelis Xenakis	Greece	Drug Delivery	Nanodispersions as carriers of novel bioactive compounds - Biological Applications	Senior	142
Pol Aira, Laura L.K. Acosta, A.J. Ferré-Borrull, L.F. Marsal	Spain	Nanomaterials for Bio and Medical Applications	Interferometric real time monitoring Streptavidin bioconjugation in Nanoporous Anodic Alumina	Student	143
Porta-i-Batalla, Maria Elisabet Xifré-Pérez, Chris Eckstein, Josep Ferré-Borrull and Lluis F. Marsal	Spain	Drug Delivery	Nanoporous Anodic Alumina Three-Dimentional Structures for Drug Delivery	Student	145

authors	country	topic	poster title	student senior	page
Prados, Jose Carlos Maria Carmen Leiva, Rafael Contreras-Cáceres, Amelia Díaz, Miguel A. Casado-Rodríguez, Jose M. Baeyens, Gloria Perazzoli, Laura Cabeza, Julia Jiménez-Lopez	Spain	NanoMaterials for Medicine	Paclitaxel loading Poly(4-vinylpyridine) and Tripalmitin Nanoparticles for Breast Cancer Therapy	Senior	147
Sayed Hanafy, Amira	Egypt	Far Future Challenges	Nanocarriers for Alzheimer's disease treatment: from bench to bedside	Senior	148
Serrà, Albert José García-Torres, Elisa Vallés	Spain	Bio-nanofabrication	Magnetically controlled cells movement after internalization of synthesised metal nanostructures	Senior	149
Spasojevic, Vojislav I. Spasojevic, M. Ognjanovic, M. Mirkovic, M. Radovic, S. Vranjes Djuric, T. Stanojkovic, Z. Prijovic and B. Antic	Serbia	NanoMaterials for Medicine	Preparation and evaluation of multifunctional (Mg, Fe)$_3$O$_4$ nanoparticles designed for cancer therapy	Senior	151
Steinmetz, Lukas Christoph Geers, Laura Rodriguez-Lorenzo, Mathias Bonmarin, Barbara Rothen-Rutishauser, Alke Petri-Fink	Switzerland	Nanomaterials for Bio and Medical Applications	Determination of nanoparticle batch reproducibility via stimuli-induced heating	Student	152
Suarez Zamora, Edgar Fernando Miguel Angel Gomez Lim	Mexico	Bio-nanofabrication	Towards targeted drug delivery: A highly efficient system for production and functionalization of Hepatitis C virus like particles employing transient expression in plants.	Senior	153
Vilela Garcia, Diana M.M. Stanton, Ana C. Hortelao, S.Sanchez	Spain	Drug Delivery	Mesoporous silica microtubes as promising chassis for micromotor medical applications	Senior	154
Yang, Xiuyi	United Kingdom	NanoMaterials for Medicine	Structural characterisation of antimicrobial Copper oxides and its leaching study using inductively coupled plasma optical emission spectrometry (ICP-OES)	Student	156
Zahmanova, Gergana Valentina Toneva and Ivan Minkov	Bulgaria	Bio-Inspired nanotechnologies	Hepatitis E virus-like particles (VLPs) produced in plants as nanoparticle-based bivalent vaccine	Senior	158
Zamora, Paula Dionysia Tsoutsi, Ruixue Xu, Pilar Rivera Gil	Spain	Nanomaterials for Bio and Medical Applications	Enhanced dark-field optical microscopy with high resolution hyperspectral imaging for nanoscale bioimaging and analysis	Student	159
Zhang, Yajie Irene Anton Sales, Alba Grayston, Ignasi Barba, Anna Rosell, Anna Roig	Spain	Drug Delivery	Multifunctional Platform of Nanocapsules as Drug Carrier for Angiogenic Therapies	Student	160

Development of an automated system for the analysis of cell-free fetal DNA from maternal plasma for non-invasive pre-natal diagnostics

Josep Lluís Acero[1],
Carmen Bermudo[1], Teresa Mairal[1], Ciara K. O'Sullivan[1,2], Ian Riley[3], Ioanis Katakis[1]

[1]Universitat Rovira i Virgili, Av. Països Catalans 26, Tarragona, Spain.
[2]Institució Catalana de Recerca i Estudis Avançats, Pg. Lluís Companys 23, Barcelona, Spain.
[3]Labman Automation Ltd., Seamer Hill, Seamer, Stokesley, North Yorkshire TS9 5NQ, UK

joseplluis.acero@urv.cat

The analysis of circulating cell-free (cf) DNA from plasma, serum or urine, has the potential to serve as non-invasive approach to detect and monitor targets associated with certain diseases. In 1997 the presence of fetal DNA in the plasma and serum of pregnant women was demonstrated [1]. This opened new perspectives in field of non-invasive pre-natal diagnostics since the analysis of cell-free fetal (cff) DNA can provide information about pregnancy related disorders (pre-eclampsia, pre-term labour), chromosomal aberrations (e.g. aneuploidies), and genetic disorders (e.g. cystic fibrosis, thalassaemia, Huntington's disease) [2].

We report on the development of an automated and integrated modular system for the isolation, amplification and detection of cffDNA from maternal plasma for non-invasive pre-natal diagnostics. The system consists of a first module for the cfDNA isolation from plasma based on silica-coated magnetic beads technology. Subsequently, the cfDNA obtained is introduced to a second module which is based on a polymeric microsystem containing a capillary electrophoresis step for the size separation of the fetal DNA from maternal DNA. Finally, the cffDNA is transferred to the amplification/detection module. This module consists of PCB (Printed Circuit Board) electrode arrays functionalized with surface immobilised primers for the multiplexed isothermal recombinase polymerase DNA amplification (RPA) and electrochemical quantitative detection of specific genetic sequences.

The developed technology is of generic and flexible nature allowing its' facile modification to other targets of interest in clinical diagnostics and thus the developed platforms can also be exploited for analysis of circulating nucleic acids in oncology and multiple other disorders.

References

[1] Lo Y.M., Corbetta N., Chamberlain P.F., Rai V., Sargent I.L., Redman C.W., Wainscoat J.S. Lancet, 9076 (1997) 485-7.

[2] Daley R., Hill M., Chitty L.S. Arch Dis Child Fetal Neonatal, 5 (2014) 426-30.

Stacked Periodic Nanoporous Anodic Alumina Structures for Sensing Applications

L. Karen Acosta

Elisabet Xifre-Perez, Josep Ferré-Borrull, and Lluis F. Marsal

Departament d'Enginyeria Electrònica, Elèctrica i Automàtica, Universitat Rovira i Virgili, Avinguda Països Catalans 26, 43007 Tarragona, Spain

lluis.marsal@urv.cat

Nanoporous Anodic Alumina (NAA) is a material with growing interest in nanotechnology and for biological and medical applications [1-2]. It is a cost-effective nanostructured material obtained by the electrochemical etching of aluminum in acidic electrolytes at the adequate conditions of applied voltage or current, temperature and electrolyte composition. It consists of a network of longitudinal pores self-arranged on an aluminum oxide matrix, and perpendicular to their surface, with diameters and interpore distances that can be tuned between 30 nm and 500 nm. Furthermore, the pore geometry can be varied by different methods to obtain different functionalities such as funnels [2-3], branched pores [4] and even structures with remarkable optical properties such as Distributed Bragg Reflectors[5].

One interesting structure can be obtained by NAA pore engineering: rugate filters (RF-NAA): it is obtained by applying a sinusoidal anodization current, what results in a continuous modulation of the pore diameter along its length. This periodic pore diameter modulation confers the RF-NAA the structure of a one-dimensional photonic crystal [6] with a modulation of the refractive index along the pore direction and a photonic stop band.]. In previous works, RF-NAA have been proposed as platforms for biosensing [7]. Furthermore, if multiple periodic currents are overlapped and applied as anodization current, it is possible to obtain multiple stop bands on the same porous structure. This has been applied to encode optical information within the nanostructure [8-9].The fabrication of such overlapped multiple periodic structures poses several drawbacks such as it has only been demonstrated for sulphuric acid electrolytes and that the stop bands are narrow and with low reflectance due to the small index contrast that can be obtained.

In this work we propose an alternative fabrication method for NAA-based periodic structures: the multiple periodic currents are applied sequentially instead of simultaneously. In this case, the different periodic structures are stacked on the same structure. This permits to use a bigger current contrast in the current variations and using electrolytes with different composition. In this work we study the possibility to obtain such stacked structures in oxalic acid electrolyte. We will also evaluate the sensitivity of the structure to changes in refractive index of the medium filling the pores with real-time spectroscopy method. Stacked structures were prepared by anodization of a high-purity aluminum chip in 0.3 M oxalic acid electrolyte at 5 ºC. The applied current is illustrated in Figure 1: an average current $I_0 = 4$ mA was applied and a three sinusoidal currents with amplitude of $I_1 = 2$mA were sequentially stacked to this average current. These three sinusoidal currents had different periods, $T_1 = 150$s, $T_2 = 175$s and $T_3 = 200$ s. All the sinusoidal currents were applied for $N = 100$ periods. Figure 1a shows a part of each of the three applied anodization currents while Figure 1b shows the corresponding measured anodization voltage. It can be seen that the obtained anodization voltage follows the sinusoidal variations of the applied anodization current with a certain delay.

Furthermore, it is remarkable that the average value and amplitude of the measured voltage depends of the period of the applied current. This indicates that the porous layer growth has a dynamic behavior governed by a characteristic reaction time. Figure 1c shows the ESEM cross-section picture of a sample obtained in the described conditions, while the inset corresponds to the top view for the same sample. The straight pores can be recognized in the cross section, but not the pore diameter modulations.

Figure 2 shows the reflectance spectrum of the described sample after removing the remaining aluminum. As it can be seen, the three successive sinusoidal currents give rise to the formation of three stop bands. The height of these stop bands reaches between 20 % and 40 % while its widths are between 21 nm and 26 nm. It can be observed that there is a direct relationship between the period of the anodization current and the corresponding central wavelength, $\lambda_1 = 518$ nm of $T_1 = 150$ s, $\lambda_2 = 619$ nm of $T_2 = 175$ s, $\lambda_3 = 704$ nm of $T_3 = 200$ s.

Finally, the ability to detect a change in refractive index of the medium filling the pores has been investigated by real-time spectroscopy. To this end, the sample is mounted in a sealed cell with a transparent window that permits the measurement of the reflectance spectrum by a fiber mini spectrometer as different fluids are injected to the

cell and fill the staked structure NAA pores. Figure 3 shows a plot of the peak wavelength for each stop band in the sample as a function of time, as different glucose solutions of increasing concentration are injected. It can be seen that the peak wavelength shifts linearly towards higher values for increasing glucose concentrations, with a lower limit of detection of 0.025 M. In conclusion, in this work we demonstrate the possibility to fabricate NAA-based periodic structures in stack configuration by the application of successive sinusoidal anodization currents with different period. The central wavelength of the obtained photonic stop bands is directly related with the period of each of the different applied successive sinusoidal currents. Further research will be carried out to determine the relation between these two magnitudes. We also demonstrated the ability of such stacked periodic structures to detect a change in the refractive index of the fluid filling the pores by means of real-time spectroscopy. With this method, it is possible to sense glucose in a concentration as small as 0.025 M.

References

[1] W.Lee, S.J Park, Chemical Reviews, 114, (2014) 7487-7556.

[2] W.J.Stepniowski, A.N.Stepniowska, M. Michalska, M. Norek, T. Czuijko, Z. Bojar. Polish Journal of Chemical Technology, 16, (2014) 63-69.

[3] A. Santos, P. Formentín, J.Pallarés, J. Ferré-Borrull, L.F. Marsal. Journal of Electroanalytical Chemistry (2011) 73-78.

[4] A. Santos,T. Kumeria, Y. Wang, D. Losic, Nanoscale, 6 (2014) 9991.

[5] J. Ferre-Borrull, E. Xifre-Perez, J. Pallares, L.F. Marsal. Science Vol. 219 (2015).

[6] M. Mahbubur Rahman, L.F. Marsal, J. Pallarès, J. Ferré-Borrull, Applied Materials and Interfaces, 5 (2013) 13375-13381.

[7] G. Macias, J. Ferré-Borrull, J. Pallarès, L.F. Marsal, Nanoscale Research Letters, 9 (2014) 315

[8] J.D. Joannopoulos, S.G. Johnson, J.N. Winn, R.D.Meade. Priceton University Press (2011).

[8] A. Santos, C. Suwen Law, T.Pereira. D.Losic Nanoscale, 8 (2016) 8091.

[9] A. Santos, J.H. Yoo, C. Vashisth, T. Kumeria, Y. Wang, D. Losic, Nanoscale, 8 (2016) 1360.

Figures
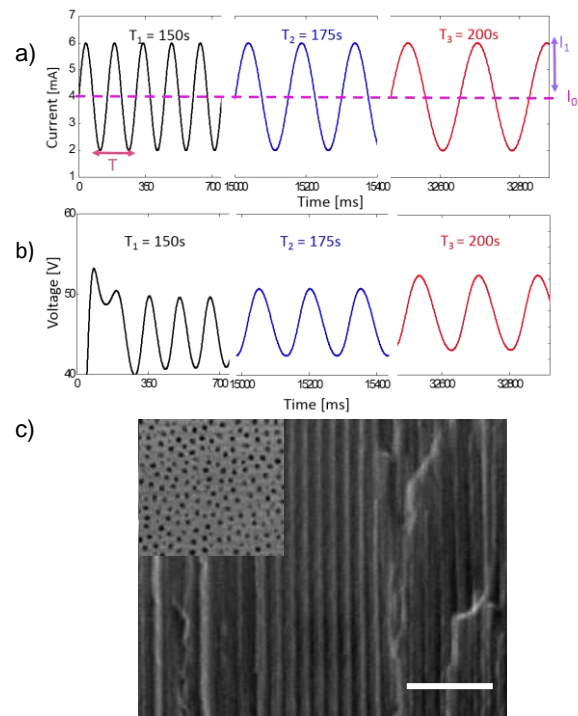
Figure 1. a) sample of applied anodization current for the indicated periods; b) resulting anodization voltage; c) cross-section SEM picture of the obtained stached sugate filter and top view (inset). The white bar corresponds to 1μm and both pictures are at the same scale.
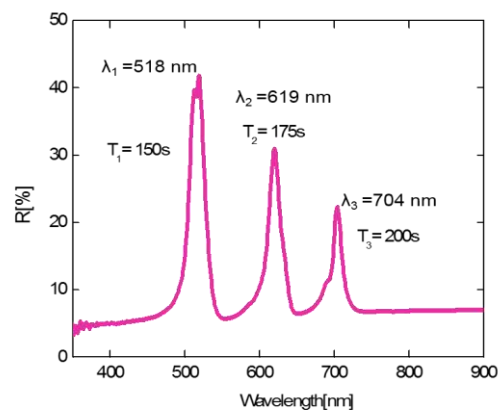
Figure 2. Reflectance spectrum of the stacked rugate filter obtained as specified in the text.
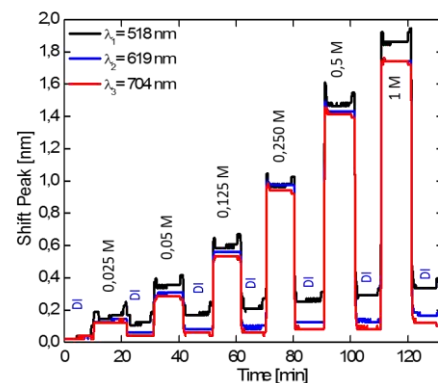
Figure 3. Peak wavelength shift as a function of time for the three photonic stop bands of the stacked structure, as glucose solutions with the indicated concentration are injected in the flow cell.

Exploring Enzymatic Reactions to Power Biocompatible Silica-Based Micromotors

F. Xavier Arqué[1],
Tania Patiño[1,2], Samuel Sánchez[1,2,3]

[1]Insitut de Bioenginyeria de Catalunya (IBEC), Baldiri i Reixac 10-12, Barcelona, Spain.
[2]Institució Catalana de Recerca i Estudis Avançats (ICREA), Pg. Lluís Companys 23, Barcelona, Spain.
[3]Max Planck Institute for Intelligent Systems Institution, Heisenbergstraße 3, Stuttgart, Germany.

xarque@ibecbarcelona.eu

In the past years, there has been a growing interest in the field of micro-/nanomachines for its promising and diverse applications. Among these, the research has been specially focused on seeking efficient and biocompatible enzyme-powered micro-/nanomotors[1] for novel biomedical applications promoted by active motion, such as targeted delivery, sensing, surgery and detoxification.[2,3]

These encouraging projects rely only on some types of micro-/nanomotors and not more than a few enzymes have been proven to be able to produce self-propulsion.[4] Hence, an expansion of our understanding on the mechanisms of active motion generation at this scale is required before its implementation. The possible aspects playing a role are: local gradients of temperature or products produced by the catalysis, and the conformational changes and binding-unbinding processes experienced by enzymes when interacting with the substrate.[4]

To address this, the approach of this project is based on the selection of four enzymes to cover the surface of Hollow Silica Microparticles (HSMP) and determine their capabilities of propulsion. Due to the biocompatibility properties and the easy surface modification that silica offers, this platform has been chosen to attach urease, glucose oxidase, aldolase and acetylcholinesterase, since their differences in turnover number (k_{cat}) allow to suggest the relevance of this property by comparing their motion. Aldolase and acetylcholinesterase have never been used for this purpose, which raise promising new micro-/nanomotors, able to navigate in different environments and encouraging new applications.

During the process of fabrication, a detailed characterization is performed to confirm the optimal fabrication in terms of topography, shape, size, composition and presence of enzymes on the Hollow Silica Micromotors (HSMM). Next, their motion is studied for different substrate concentrations and the highest active motion of each micromotor is compared. While aldolase and glucose oxidase micromotors don't show significant active motion, acetylcholinesterase micromotors reach a velocity of 0.43 µm/s, and the maximum speed is achieved by micromotors with urease as a power source, swimming at 2.07 µm/s (Figure 1).

These results correlate with the k_{cat} magnitude of each enzymes (Figure 1), suggesting that the driving mechanism is the generation of local gradients of products, known as diffusiophoresis. On the other hand, the heat production is greater for glucose oxidase than for urease, so the temperature gradient generation is not enough, by itself, to achieve self-propulsion. Other factors, such as conformational changes and binding-unbinding processes undergone by the enzymes could be playing a role. In this direction, urease and acetylcholinesterase micromotors are exposed to competitive reversible inhibitors and no active motion is detected.

With this approach, some light is shed on the fundamental aspects of active motion generated by enzymes while the field is expanded with new enzymes able to produce active motion, such as acetylcholinesterase. This leads to promising novel biomedical applications when acetylcholine presence or excess causes harmful effects, such as in cholinergic crisis, hypercholinergic depression, some types of cancer and other diseases.[5]

References

[1] Ma, X.; Wang, X.; Hahn, K.; Sánchez, S. ACS Nano, 10, 3597-3605 (2016)

[2] Hortelão, A. C.; Patiño, T.; Pérez-Jimenez, A.; Blanco, A.; Sánchez, S. Adv. Funct. Mat. (2017) *in press*

[3] Li, J.; Esteban-Fernández de Ávila, B.; Gao, W.; Zhang, L.; Wang, J. Sci. Robot. 2, eaam6431 (2017)

[4] Ma, X.; Hortelão, A. C.; Patiño, T.; Sánchez, S. ACS Nano, 10, 9111-9122 (2016)

[5] Beckmann, J.; Lips, K. S. Pharmacology, 92, 286-302 (2013)

Figures
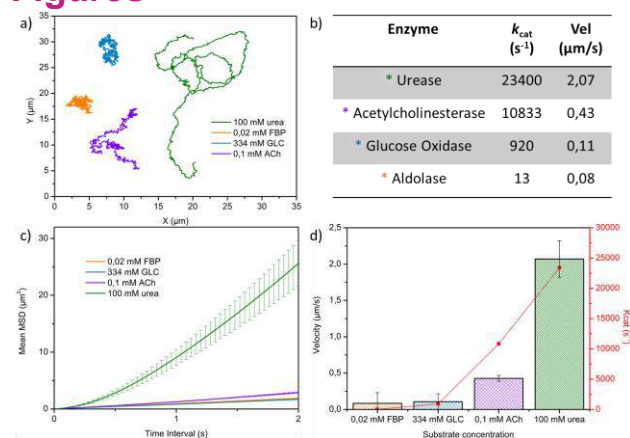
Figure 1. Comparison of motion dynamics of HSMM. (a) Representative tracking trajectories of each HSMM. (b) Table of k_{cat} of each tested enzyme and velocity of their HSMM. Representation of (c) the mean MSD over time and (d) the velocities of each HSMM, exposed to the best substrate concentration in terms of self-propulsion. (for panels c and d, 20 microparticles are analyzed, and the error bars in the panel d represent the standard error of mean, N = 20)

Enzyme	k_{cat} (s^{-1})	Vel (µm/s)
* Urease	23400	2,07
* Acetylcholinesterase	10833	0,43
* Glucose Oxidase	920	0,11
* Aldolase	13	0,08

Frozen dispersions of nanomaterials are a useful operational procedure in nanotoxicology

Irene Barguilla[1],
Laura Vila[1], Laura Rubio[1], Balasubramanyam Annangi[1], Alba García-Rodríguez[1], Ricard Marcos[1,2], Alba Hernández[1,2]

[1]Grup de Mutagènesi, Departament de Genètica i de Microbiologia, Universitat Autonoma de Barcelona, Bellaterra, Spain
[2]CIBER Epidemiología y Salud Pública, ISCIII, Spain

irene.barguilla@uab.cat

The potential advantages of the physicochemical properties of nanomaterials (NM) make them desirable for different applications such as electronics, biomedicine, cosmetics and food packaging [1]. The increasing development of the NM related industry has raised serious concerns about the potential harmful effects of these materials in human health. In the development of experimental approaches focused on the study of the biological effects of nanoparticles (NP), their dispersion has arisen as a determinant factor for their toxicological properties [2]. However, there is an intrinsic variability to the dispersion processes between and within laboratories. Most of the *in vitro* studies carried out to assess the toxic and genotoxic effects of NM involve acute treatments with high doses of the compound. Nonetheless, long-term treatments with low doses are a more realistic model in terms of human exposure and the assessment of the carcinogenic potential of NM [3]. Both at short- and long-term, the dispersion-related variability could be responsible for the disparities in the biological effects shown in the literature [4]. Moreover, the development of high-throughput screening methodologies is also limited as the preparation of fresh NM dispersions acts as a bottleneck, preventing the application of these approaches.

The freezing of aliquots from a NM stock dispersion in liquid nitrogen and their posterior storage at -80ºC would overcome the dispersion-related limitations regarding reproducibility and could simplify the procedures. However, no studies have explored the impact of freeze-thawing cycles of samples on the physicochemical and biological properties of NM. Therefore, this work aims to compare freshly-prepared and frozen MWCNT, ZnO-, Ag-, TiO_2- and CeO_2-NP dispersions as models.

We analyzed different endpoints to test the suitability of the proposed procedure. NP characterization was performed by TEM (size and morphology analysis) and the hydrodynamic size and zeta potential were also studied. Viability comparisons were determined in BEAS-2B cells. Cellular NP uptake and induced reactive oxygen species (ROS) production was assessed by TEM and flow cytometry, respectively.

The figures illustrate the obtained results for TiO_2-NP as a representative example of the results obtained for all the NP studied. The size distribution and morphology were very similar between the fresh and frozen samples of the different NP and no significant differences were found with the NP characterization procedures. Regarding the biological effects, while the cellular uptake of nanoparticles, the toxicity and the intracellular ROS production was different depending on the studied NP, all showed the same effect when comparing fresh and frozen samples.

Therefore, this study is the first to demonstrate that there is no scientific evidence to dismiss the use of frozen NP, offering the chance of carrying out of short- and long-term experiments with higher consistency, accuracy and reproducibility in a much shorter time and using a simplified procedure.

Figures
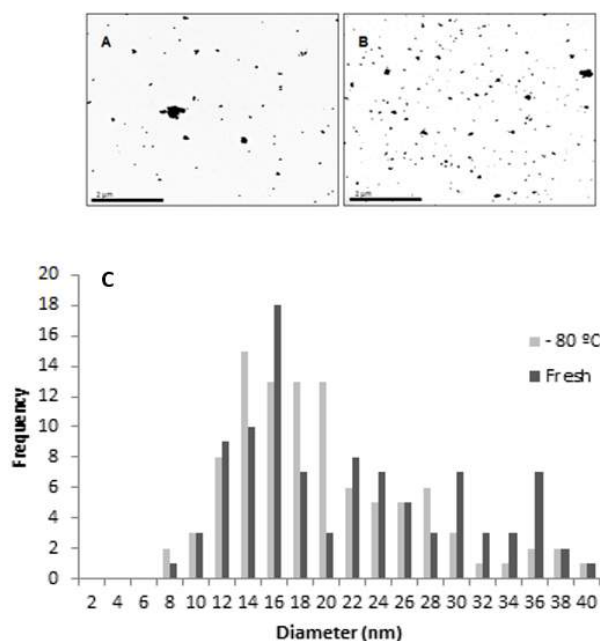
Figure 1. (A, B) TEM image of TiO_2 in dried form. The left side (A) corresponds to the freshly-prepared dispersions and the right side (B) to the thawed dispersions from frozen samples. **(C) Size distribution of TiO_2.** Analysis of over 100 randomly selected particles for both the freshly-prepared and the thawed dispersions from frozen samples.
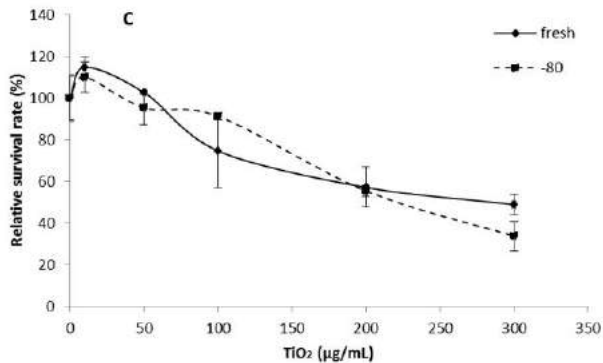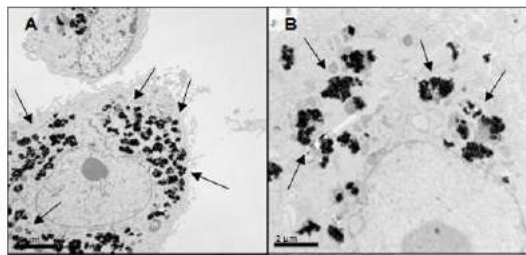
Figure 2. (A, B) TEM images of BEAS-2B cells treated with TiO$_2$-NP. The images show the NP cellular uptake after a 24h treatment with 100µg/ml of fresh (A) or frozen (B) TiO$_2$-NP. The arrows indicate nanoparticles or nano-agglomerates in cellular vacuoles. **(C) Cell viability of BEAS-2B cells treated with various concentrations of freshly-prepared or frozen samples of TiO$_2$-NP**. Data show the percentage of viable cells with respect to controls and are represented as mean ± SEM (n=3); *$p<0,05$, **$p<0,01$, ***$p<0,001$.

References

[1]   Roco MC, Hersam MC, Mirkin CA, J Nanopart Res 13 (2011), 897-919

[2]   Jiang J, Oberdörster G, Biswas P, J Nanopart Res 11 (2009) 77-89

[3]   Annangi B, Bach J, Vales G, Rubio L, Marcos R, Hernández A, Nanotoxicology 9 (2015), 138-47

[4]   Cohen J, DeLoid G, Pyrgiotakis G, Demokritou P, Nanotoxicology 7 (2013), 417-31

Nanostructured antifouling polymer for DNA detection

Noemi Bellassai[1,2],
Almudena Marti Morant[3], Jurriaan Huskens[3] and
Giuseppe Spoto[2,4]

[1]Consorzio Interuniversitario di Ricerca in Chimica dei Metalli nei Sistemi Biologici, c/o Dipartimento di Scienze Chimiche, Università degli Studi di Catania, Catania, Italy.
[2]Dipartimento di Scienze Chimiche, Università degli Studi di Catania, Viale Andrea Doria 6, 95125 Catania, Italy.
[3]Molecular NanoFabrication Group, MESA+ Institute for Nanotechnology, University of Twente, P.O. Box 217, 7500 AE Enschede, The Netherlands.
[4]Consorzio Interuniversitario Istituto Nazionale Biostrutture e Biosistemi, c/o Dipartimento di Scienze Chimiche, Università degli Studi di Catania, Catania, Italy.

noemi.bellassai@gmail.com

Figures

Figure 1. Schematic representation of PLL-Mal$_{y\%}$ - CEEEEE.

Antifouling surfaces are required for many biotechnological applications to prevent the non-specific protein/cell adhesion and select biological targets, such as cancer biomarkers, in complex natural media (e.g., blood) [1].

It has been suggested that a nanoscale homogenous mixture of balanced charged groups from polyzwitterionic systems is the key to control the non–fouling properties [2,3].

A new approach of nanostructured zwitterionic polymer has been performed using the combination of a cationic polyelectrolyte and an anionic oligopeptide structure. The polymeric system investigated consisted of a poly (L-lysine) (PLL) structure grafted with maleimide-NHS ester chains in different percentage (y%) of maleimide (PLL – Mal$_{y\%}$, from 26% to 13%). The anionic oligopeptide sequence included five glutamic acids (E) and one cysteine (C) (oligo CEEEEE) has been attached to a PLL – Mal$_{y\%}$ polymer through the thiol – maleimide "click" reaction. The final zwitterionic layer has overall charge neutrality, as a result of the balance between the positive charges of PLL–Mal$_{y\%}$ and the negative charges of CEEEEE peptide.

The antifouling surfaces have been characterized by Water Contact Angle and Polarization Modulation Infrared Reflection-Absorption Spectroscopy (PM-IRRAS). Data analysis indicated the successful formation of the layers. Their antifouling properties have been assessed in adsorption studies using Quartz Crystal Microbalance with Dissipation (QCM-D) using Bovine Serum Albumin (BSA) aqueous solutions as the standards. The best antifouling properties for PLL-Mal$_{y\%}$ have been obtained when 26% and 22% of maleimide were used with gold and silicon oxide sensors, respectively. Furthermore, preliminary data have been also collected for PLL – Mal$_{y\%}$ functionalized surfaces using diluted (5%, 10%, 33%) human plasma.
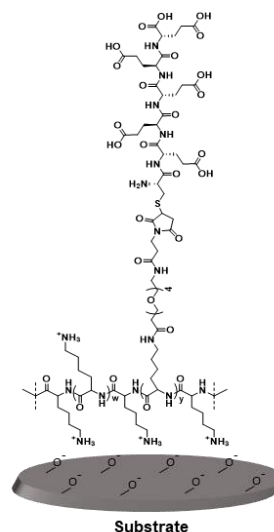
References

[1] C. Blaszykowski, S. Sheikh, M. Thompson, Chem. Soc. Rev. 41 (2012) 5599–5612.
[2] M.C. Sin, S.H. Chen, Y. Chang, Polym. J. 46 (2014) 436-443.
[3] H. Ye, L. Wang, R. Huang et al., ACS Appl. Mater. Interfaces 7 (2015) 22448-22457.

A Gold-based Inkjet-Printed Substrate for Physioelectric Research on Neurons

Alexandre Cabal Tato

Aïda Varea Espelt, Albert Cirera Hernández

MIND (Micro and Nanotechnologies and nanoscopies for Electronic and Electrophotonic Devices), Faculty of Physics, IN2UB-University of Barcelona, Barcelona, Spain

acabalta7@alumnes.ub.edu

Inkjet Printing (IP) is a low-cost and contactless technique which allows low material waste of electronic components using only a digital design and thereby with no need for masks. In addition, the versatility that inkjet printing provides due to the variety of biocompatible printable materials (such as metals [1], polymers [1, 2], or even neurons [2]) can be applicable for biological systems interfacing. Then, IP becomes a good candidate for the manufacturing of several devices for biological applications. Our aim is to provide a neural activity monitoring system, by simultaneously employing calcium imaging [3] and electrical measurement [4 - 7]. The key is the use of transparent substrate and walls, which allows the use of both measurement techniques. The reason is that transparency enables the use of high resolution optical microscope for calcium imaging. In this way, neural electrical spikes can be correlated with chemical traces. In particular, the deposition of gold electrodes onto glass substrates for physio-electric research on neurons is presented here. First of all, the study of an experimental organometallic gold ink is developed; results (viscosity, contact angle and thermogravimetric analysis) show that the ink is suitable to be printed. The deposit optimization is achieved varying the different printer parameters (drop spacing, temperature, nozzle voltage, etc) in order to obtain homogeneous gold tracks that become conductive after a thermal sintering process. In order to protect the gold contacts and to limit the working areas, either SU-8 walls are deposited by a spin-coating process or a PDMS layer adhered to the substrate with the aid of an autoclave is performed. The layer is erased in certain areas of interest for neuron culture purposes (windows); so that the liquid medium, where the neurons will be placed during the measurements, will be limited to this created cavity [Figure 1]. The properties of the electrodes are characterized. The porosity is examined by scanning electron microscopy technique (SEM), the roughness and thickness are both measured with a profilometer and the conductivity of the electrodes is determined using the 2-probe method. Once the device windows are made, Poly-L-Lysine (PLL) is also strategically deposited by IP or electrospray above the gold electrodes; this allows us to control the spatial distribution of the population of mice or rat cortical neurons [Figure 2b)]. In conclusion, an operational device such as the one depicted here could manage to dynamically analyze neuron populations and their connections, giving insight on the functions of the existent communication.

References

[1] Cummins, G., & Desmulliez, M. P. (2012). Inkjet printing of conductive materials: a review. Circuit World, 38(4), 193-213.

[2] Sanjana, N. E., & Fuller, S. B. (2004). A fast flexible ink-jet printing method for patterning dissociated neurons in culture. Journal of Neuroscience Methods, 136(2), 151-163.

[3] Orlandi, J. G., Soriano, J., Alvarez-Lacalle, E., Teller, S., & Casademunt, J. (2013). Noise focusing and the emergence of coherent activity in neuronal cultures. Nature Physics, 9(9), 582-590.

[4] Marom, S., & Shahaf, G. (2002). Development, learning and memory in large random networks of cortical neurons: lessons beyond anatomy. Quarterly Reviews of Biophysics, 35(1), 63-87.

[5] Massobrio, P., Massobrio, G., & Martinoia, S. (2016). Interfacing cultured neurons to microtransducers arrays: a review of the neuro-electronic junction models. Frontiers in Neuroscience, 10.

[6] Kim, R., Joo, S., Jung, H., Hong, N., & Nam, Y. (2014). Recent trends in microelectrode array technology for in vitro neural interface platform. Biomedical Engineering Letters, 4(2), 129-141.

[7] Spira, M. E., & Hai, A. (2013). Multi-electrode array technologies for neuroscience and cardiology. Nature Nanotechnology, 8(2), 83-94.

Figures
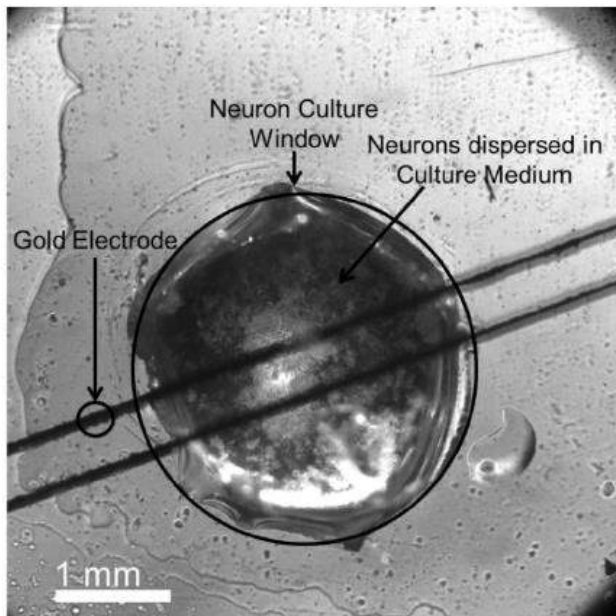
Figure 1. Neuron culture inside PDMS window, on top of gold electrodes.
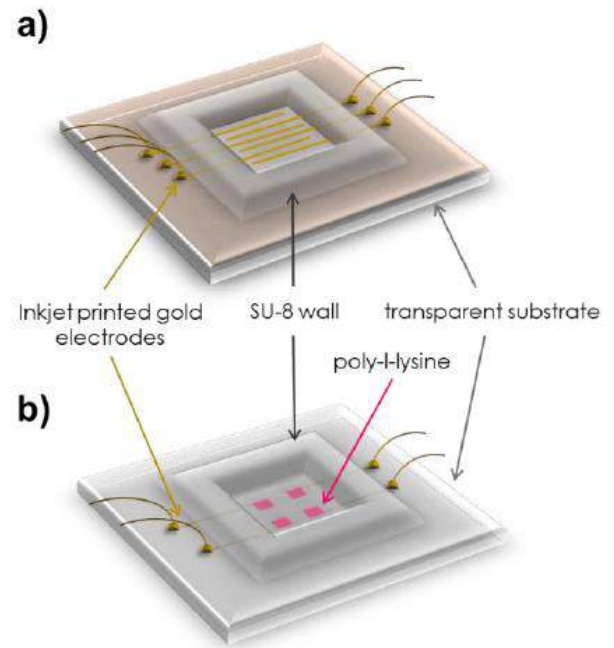
Figure 2. Device architecture employing SU-8 window. a) IPNeuron1.0 and b) IPNeuron 2.0 devices.

RGD dendrimer-based nanopatterns promote chondrogenesis and intercellular communication for cartilage regeneration

Ignasi Casanellas[1,2]

Anna Lagunas[3,1,*], Iro Tsintzou[1], Yolanda Vida[4,5], Daniel Collado[4,5], Ezequiel Pérez-Inestrosa[4,5], Cristina Rodríguez[6], Joana Magalhães[3,6], Josep Samitier[1,3,2]

[1] Institute for Bioengineering of Catalonia (IBEC), Barcelona, Spain
[2] Department of Engineering Electronics, University of Barcelona (UB), Barcelona, Spain
[3] Networking Biomedical Research Center (CIBER), Madrid, Spain
[4] Instituto de Investigación Biomédica de Málaga (IBIMA), Department of Organic Chemistry, Universidad de Málaga (UMA), Málaga, Spain
[5] Andalusian Centre for Nanomedicine and Biotechnology-BIONAND, Málaga, Spain
[6] Instituto de Investigación Biomédica de A Coruña (CHUAC), Sergas ,Universidade da Coruña (UDC), Coruña, Spain

icasanellas@ibecbarcelona.eu

Stem-cell based regenerative therapies to treat widespread cartilage damage have proved challenging, as direct stem cell implantation into affected joints leads to several complications, including heterotopia. Therefore, there is a need to precondition stem cells *in vitro* before implantation. We have previously shown that nanopatterns based on arginine-glycine-aspartate (RGD) dendrimers allow to locally control cell-substrate adherence at the nanoscale[1] and influence stem cell differentiation towards chondrogenesis[2]. Cartilage is an avascular tissue in which intercellular communication is maintained mainly by passive diffusion or through gap junctions (GJs), and the formation of this communication network is imperative for the development of new cartilage tissue. We here demonstrate that nanopatterns also promote intercellular communication through GJs containing connexin 43 (Cx43). This is an important milestone for the development of a cell carrier with nanofeatures that promote chondrogenic differentiation, ensuring an accurate reproduction of the native tissue structure and connectivity. Since nanopatterns are fully biocompatible, they allow implantation of the resulting cell construct into the damaged cartilage areas.

References

[1] Lagunas, A., Castaño, A. G., Artés, J. M., Vida, Y., Collado, D., Pérez-Inestrosa, E., Gorostiza, P., Claros, S., Andrades, A., Samitier, J. *Nano Res.* **2014**, 7(3): 399-409

[2] Lagunas, A., Tsintzou, I., Vida, Y., Collado, D., Pérez-Inestrosa, E., Rodriguez Pereira, C., Magalhaes, J., Andrades, A., Samitier, J. *Nano Res.* **2017**, 10(6): 1861-1871

Figures
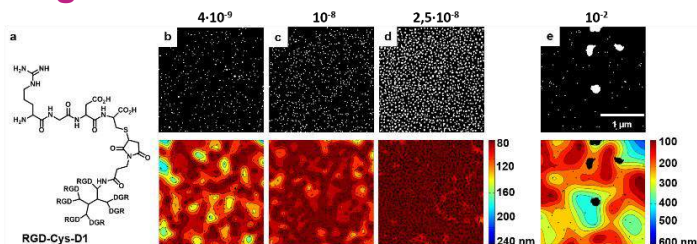
Figure 1. Dendrimer nanopatterning of (a) PAMAM G1-derived dendrimers containing the cell-adhesive moiety of RGD (RGD-Cys-D1). (b)–(e) Representative AFM image thresholds of the nanopatterns on PLLA obtained from initial aqueous solutions of various dendrimer concentrations, $4 \cdot 10^{-9}$ %, 10^{-8} %, $2.5 \cdot 10^{-8}$ %, and 10^{-2} % w/w, respectively, and the corresponding minimum interparticle distance probability contour plots, showing high-density RGD regions in dark red (dendrimers and dendrimer aggregates are plotted in black).
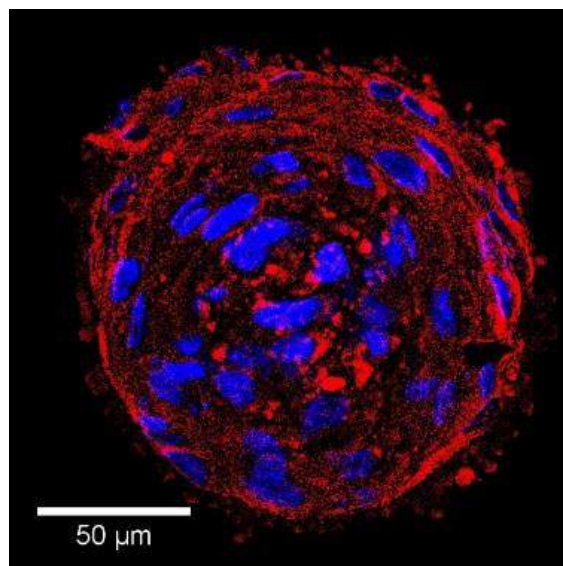
Figure 2. Representative confocal fluorescence microscopy image of a cell condensate after 6 days of culture on a nanopattern obtained from a 10^{-2} % w/w aqueous solution, stained for cell nuclei (Hoechst, blue) and Cx43 (red).

Structure activity relationship of Antimicrobial Nanoparticle Formulations to selective microbes

Yuen-Ki Cheong[1],
Xiuyi Yang[1], Rory M. Wilson[2], Sai Li[3]
and Guogang Ren[1]

[1]School of Engineering and technology, University of Hertfordshire, College Lane, Hatfield AL10 9AB, UK
[2]Materials Research Institute, Queen Mary University of London, London E1 4NS, UK
[3]Oxford Particle Imaging Centre, University of Oxford, Oxford OX3 7BN

y.cheong2@herts.ac.uk

Antimicrobial nano-metals/ metal oxides and their carbon based metallic formulations engineered using Tesima™ thermal plasma technology (Qinetic, Materials, Farnborough, UK) have shown effectively counteract a wide spectrum of pathogens, such as SARS coronavirus, Avian influenza virus (H5N1) and other deadly viruses. [1] The morphology and chemical structures of these antimicrobial nanoparticles (AMNP1 and AMNP2) were investigated in order to understand interactions between the powders and selective microbes. [2] Preliminary results obtained from cryogenic TEM imaging (Fig. 1) shows an example of how the surface of Uukuniemi viruses [3] were damaged and subsequently deactivated in the presence of AMNP2. However, more sophisticated studies are still to be performed to allow explorations of possible mechanisms involved during microbial inactivation in molecular levels.
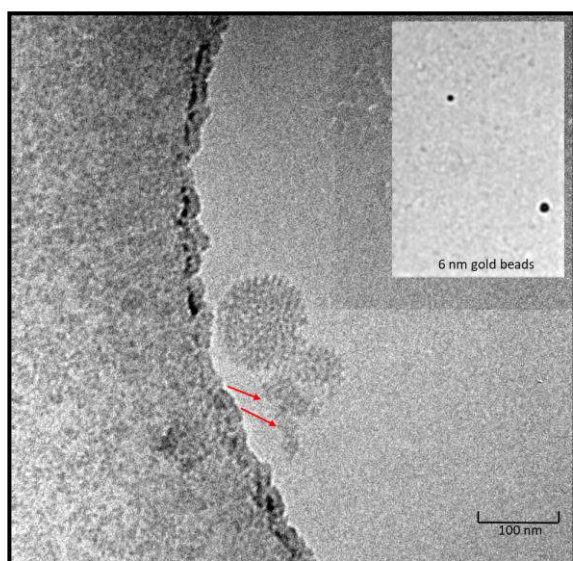
Figure 1. Cryogenic TEM image shows surface destruction of UUK virus envelopes caused by interaction with AMNP 2.

With an aim to promote the application of such antimicrobial nanoparticles and their formulations, polymeric-AMNP hybrids were produced in fibre forms using high pressure gyration process [4]. This study showed AMNPs were able to retain antimicrobial functions after incorporation into Poly(methyl methacrylate) PMMA.

More varieties of nano-metals were recently investigated, these include AMNP Ag and AMNP Cu, which were both engineered by the same manufacturer as previously mentioned. Interestingly, AMNP Ag was found to have selective inhibitory effects against *P. aeruginosa* (Gram –ve), while AMNP Cu was found to selectively inhibit growth of *S. aureus* (Gram +ve).[†] SEM image (Fig. 2 Left) shows AMNP Ag appeared as rod-shaped particles, which is similar to the shape of *P. aeruginosa*. Likewise, the spherical particles found in AMNP Cu also appear to match the spherical shaped *S. aureus*. Although we cannot draw conclusion with mechanistic interactions between the nanoparticles and the microbes. These morphology results certainly suggest a level of structure activity relationship in AMNP Ag and AMNP Cu with regards to their selectivity of microbe inhibitions.
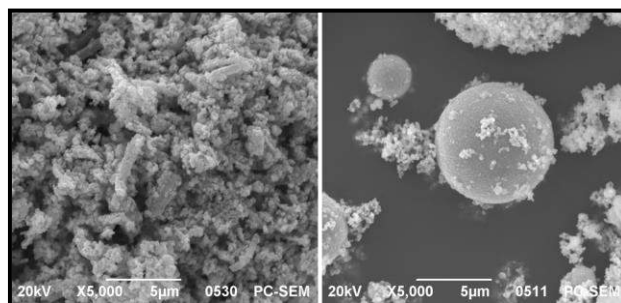
Figure 2. SEM images of engineered AMNP Ag (left) and Cu spheres (right) by Tesima™ thermal plasma technology.

In order to understand the chemistry and to determine the exact compositions present in the AMNP Ag and AMNP Cu, different analytical techniques were performed to characterise these antimicrobial particles. As shown in figure 3, X-ray photoelectron spectra (XPS) of the corresponding AMNP Ag and AMNP Cu show the expected binding energies exhibited from Ag3d (370 eV) and Cu2P (930 eV) orbitals, which were measured in high Ag and Cu elemental ratio as desired. A rather complex Raman spectra (not shown here) was obtained from AMNP Ag, which suggested this sample did not contain a single Ag component, hence it was a composite.
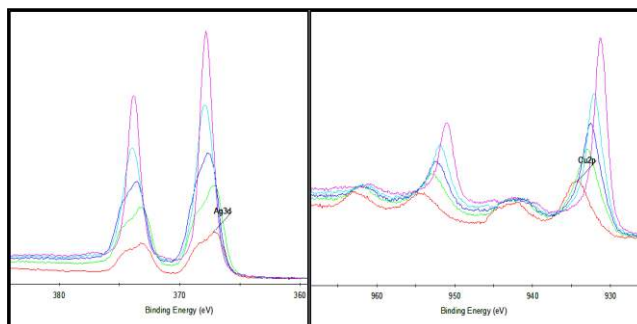
Figure 3. XPS analyses of AMNP Ag (top) and AMNP Cu (bottom)

An UV-vis absorbance (Fig. 4) was measured at 418 nm, which is associated with the presence nano-size silver present in the AMNP Ag suspension, as only nano-silver gives such distinctive Surface Plasmon Resonance (SPR). The short wavelength (418 nm) measured also indicated that particles sizes of this aqueous AMNP Ag sample were less than 70 nm and there is no doubt that nano sizes particles as such would anticipate microbial inhibitions. Aggregation of Ag particles was also observed, this can be seen as absorbance signals gradually broadened over the period of 5 days with sample being suspended in aqueous form.
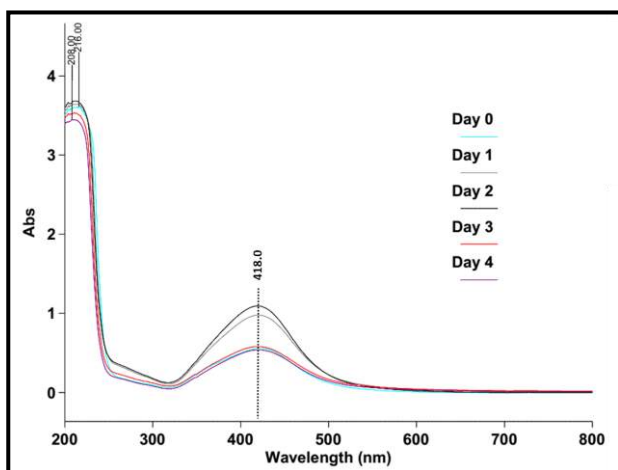
Figure 4. UV-vis spectrum shows Surface plasmon resonance (SPR) exhibited by AMNP Ag.

Finally, X-ray diffraction (XRD) of AMNP Ag and AMNP Cu has revealed the major chemical components present in both nano-powder. Table 1 summarizes all visible compounds identified in each AMNP along with their individual crystal details, estimated sizes and fraction ratio found in the compositions.

Sample	AMNP Ag			AMNP Cu	
Identified compounds	Ag	AgNO$_2$	AgNO$_3$	Tenorite (CuO)	Copper (Cu)
Crystal System	Cubic	Orthorhombic	Orthorhombic	Monoclinic	Cubic
Space Group	Fm-3m	Imm2	Pbca	C2/c	Fm-3m
Cell Volume (Å^3)	68.2274	112.74	518.64	82.3	47.24
Weight Fraction	0.44052	0.32395	0.23553	0.55397	0.44603
Particle Size (Å)	843.88028	2074.01028	2034.80585	112.5891	896.960450

Table 1. Table of XRD analysis of AMNP Ag and AMNP Cu.

The complexity of Raman spectra observed in AMNP Ag can be explained using the corresponding XRD results. This is associated with the three different silver components being found in this composite, they were identified as elemental Silver (Ag), Silver Nitrite (AgNO$_2$) and Silver nitrate (AgNO$_3$). We believe that the antimicrobial effect observed in *P. aeruginosa* was attributed by the water soluble component AgNO$_3$ in the AMNP Ag, as silver nitrate is long known to have generic antimicrobial activity. Although this does not explain why such effect was excluded from *S. aureus* and most viruses (i.e. PRRS animal virus) that we have investigated.[†]

On the other hand, AMNP Cu was found to contain almost 55% of copper oxide (CuO) and 44% of elemental Copper (Cu). We can be certain that the large spherical particles observed in the SEM image (Fig. 2 Left) was respected to elemental copper. Perhaps, the peculiar selective inhibitory effects observed in *S. aureus* was anticipated by the presence of heavy copper spherical metal.

To extend the scoop of this research, we were able to optimize antimicrobial effects to successfully counteract both *P. aeruginosa* and *S. aureus* using correct ratio of AMNP Ag and AMNP Cu to form a super-formulation.[†] Preliminary antimicrobial results obtained from this serial of formulations suggested microbe inactivation may have been caused by Cu/Ag ion ratio manipulations, which affected functions of protein channels within bacterial cell membrane. The majority of this work is to study a wide range of nanoparticles and composites to allow production of custom made formulations, which has selective or generic antimicrobial functions.

References

[1] G. Ren, J. S. Oxford and P. W. Reip. U. S. patent 2013/0091611 A1 (2013).

[2] Y.-K. Cheong and G. Ren *et al*, *Nanomaterials*, 152 (2017) doi:10.3390/nano7070152.

[3] D. Bitto and J. T. Huiskonen *et. al.*, Journal of Biological Chemistry (2016) doi: 10.1074/jbc.M115.691113.

[4] U. E. Illangakoon and L. Ciric *et. al. Mat. Sci. Eng. C*, 74 (2017) doi.org/10.1016/j.msec.2016.12.001.

† Minimum inhibitory concentration at 0.05 wt/v %. Detail is available at conference poster session or for further discussion please contact corresponding author.

Acknowledgements

Synthesis of nanohydroxyapatite using microwave energy

Agnieszka Chodara,
Sylwia Kuśnieruk, Tadeusz Chudoba,
Jacek Wojnarowicz, Witold Łojkowski

Laboratory of Nanostructures, Institute of High Pressure Physics, Polish Academy of Sciences, Sokolowska Street 29/37, 01-142 Warsaw, Poland

chodara.agnieszka@gmail.com

Hydroxyapatite (HAp) with the chemical formula of $Ca_{10}(PO_4)_6(OH)_2$ is an inorganic component of hard tissues such as bones and teeth. Hydroxyapatite possesses exceptional biocompatibility and bioactivity properties with respect to bone cells and tissues, probably due to its similarity with the hard tissues of the body. It has been used extensively for biomedical applications, because of osteoinductive and osteoconductive properties and biocompatibility with human body. Hydroxyapatite is using in regenerative medicine e.g. bone implants for regeneration of bone defects.

Nanohydroxyapatite were synthesized by hydrothermal synthesis using microwave reactor MSS2 (Microwave Solvothermal Synthesis). We used calcium hydroxide $Ca(OH)_2$ and orthophosphoric acid H_3PO_4 as substrates to obtain ceramic nanoparticles. The water is the only by-product. Microwave energy allows easily and precisely control the grain size of nanoparticles. Obtained nanoparticles were in the range of 8 - 45 nm grain size. Phase purity was checked using X-ray diffraction. Scanning electron microscopy (SEM) gave information about the morphology of produced nanohydroxyapatite. The skeleton density and specific surface area was determined using respectively helium pycnometry and Brunauer–Emmett–Teller (BET) method.

We obtained six types of hydroxyapatite GoHAP™ with different crystallinity degree and grain size by changing the synthesis parameters. Crystallinity and grain size is higher with increasing synthesis time. Wide variety of GoHAP™ can be used in many applications (e.g. implants, scaffold layers).
The Laboratory of Nanostructures is able to synthesize innovative nanoparticles similar to the natural hydroxyapatite. Thanks to a wide variety of grain size crystallinity it can be used in different application depending on desired resorption time of hydroxyapatite. GoHAP™ could be a perfect component of the medical implants.

References

[1] S.Kuśnieruk, J.Wojnarowicz, A.Chodara, T.Chudoba, S.Gierlotka, W.Łojkowski, Beilstein J Nanotechnol. 7 (2016) 1586–1601

[2] H. Alobeedallaha, J. L. Ellis, et al. Trends Biomater. Artif. Organs, 25, (2011), 12-19.

Figures
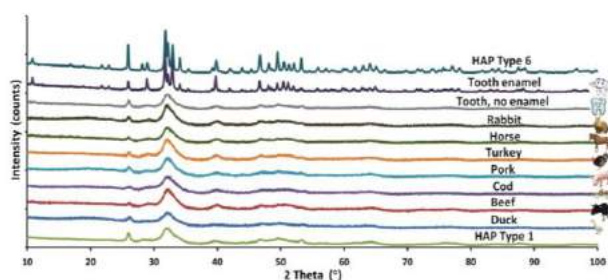
Figure 1. XRD patterns of bioapatite, as well as HAp Type 1 and Type 6 nanopowders.

Interaction of silver nanoparticles with differentiated Caco-2 cells monolayers

Constanza Cortés[1],
Laura Vila[1], Alba García-Rodríguez[1],
Ricard Marcos[1,2], Alba Hernández [1,2]

[1] Grup de Mutagènesi, Departament de Genètica i de Microbiologia, Facultat de Biociències, Universitat Autònoma de Barcelona, Bellaterra, Spain.
[2] CIBER Epidemiología y Salud Pública, ISCIII, Spain.

Constanza.cortes@uab.cat

The use of engineered nanomaterials (ENMs) such as nanoparticles (NPs) has increased dramatically over recent years in many consumer goods [1]. Among metal-based NPs, silver NPs (AgNPs) are gaining interest for their antimicrobial properties and, currently, there is an increasing number of consumer and industrial products containing AgNPs. Consequently, the increased human exposure, mainly via ingestion, could have important toxicological implications [2]. The goal of our work has been to investigate these potential effects.

To date, few data exist on the toxicokinetic and toxicodynamic processes taking place upon oral exposure to AgNPs, particularly those used as food additives/complements. Different dose-dependent animal toxicity findings report death, weight loss, hypoactivity, altered neurotransmitter levels, altered liver enzymes, altered blood values, enlarged hearts and immunological effects as AgNPs ingestion effects [3]. In addition, it has also been reported that ingested AgNPs cause adverse health effects due to differential effects on mammalian gut microbiota [4]. Nevertheless, conflicting data are usually reported owing to the complexity of *in vivo* models. To overcome this issue, we have evaluated the possible effects caused by AgNPs oral exposure using an *in vitro* model of the intestinal barrier. For this model, the human colon adenocarcinoma Caco-2 cell line is extensively used due to its capability to undergo a spontaneous differentiation process, leading to the formation of a cell monolayer which mimics the small intestine's mature enterocytes morphologically and functionally [5]. The use of Caco-2 cells monolayers (CCM) has grown greatly in the past decade as a standard permeability-screening assay since permeability through CCM correlates well with in vivo absorption in humans [6].

To increase our knowledge of the effects caused by the interaction of AgNPs with the intestinal barrier, different parameters such as toxicity, monolayer integrity and permeability (analysed morphologically and by changes in gene expression), internalization (uptake), translocation and induction of DNA damage (breaks and oxidative DNA damage) were evaluated. Results indicate that differentiated cells become more resistant to the toxic effects of AgNPs than undifferentiated Caco-2 cells. No significative effects on the monolayer's integrity/permeability were observed, although an important cell uptake was demonstrated by using confocal microscopy. Nevertheless, no translocation of AgNPs to the basolateral chamber was observed, in spite of the different experimental approaches used. The genotoxic effects evaluated using the comet assay indicate that, although AgNPs were not able to induce direct DNA breaks, the exposure to this NPs induces significant increases in the levels of oxidative DNA damage.

References

[1] Nel A, Xia T, Mädler L, Li N. Science, 5760 (2006). 311:622-7.
[2] Wijnhoven S, Peijnenburg W, Herberts C, Hagens W, Oomen A, Heugens E et al. Nanotoxicology, 2 (2009) 109-138.
[3] Hadrup N, Lam HR. Regul Toxicol Pharmacol. 68 (2014) 1-7.
[4] Fröhlich EE, Fröhlich E. Int J Mol Sci. 17 (2016) 509.
[5] Carr KE, Smyth SH, McCullough MT, Morris JF, Moyes SM. Prog Histochem Cytochem. 46 (2012) 185-252.
[6] Artursson P, Palm K, Luthman K. Adv Drug Deliv Rev. 46 (2001) 27-43.

Figures
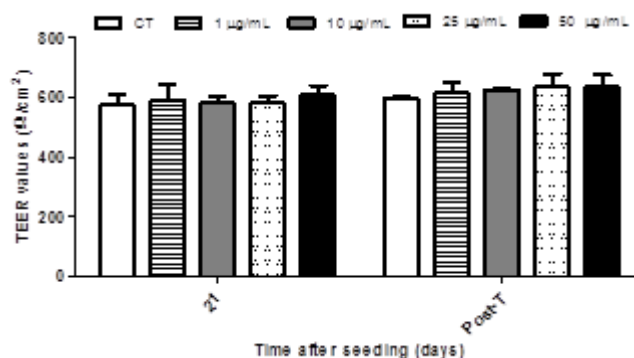
Figure 1. TEER values of the CCM evaluated before and after 24 h of AgNPs treatment. Data represented as mean ± SEM. ***P<0.001.
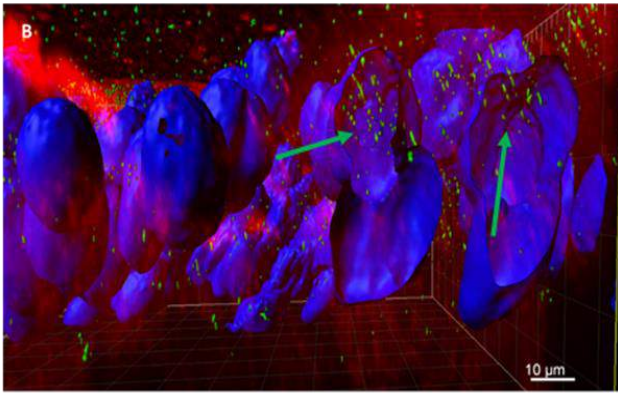
Figure 2. Confocal images from differentiated Caco-2 cells treated with 50 µg/mL of AgNPs. Cellular uptake was measured 24 h after treatment. Nucleuses are stained in blue, cell membranes in red, and AgNPs in green. Arrows indicate the localization of AgNPs in the cells.

A

B
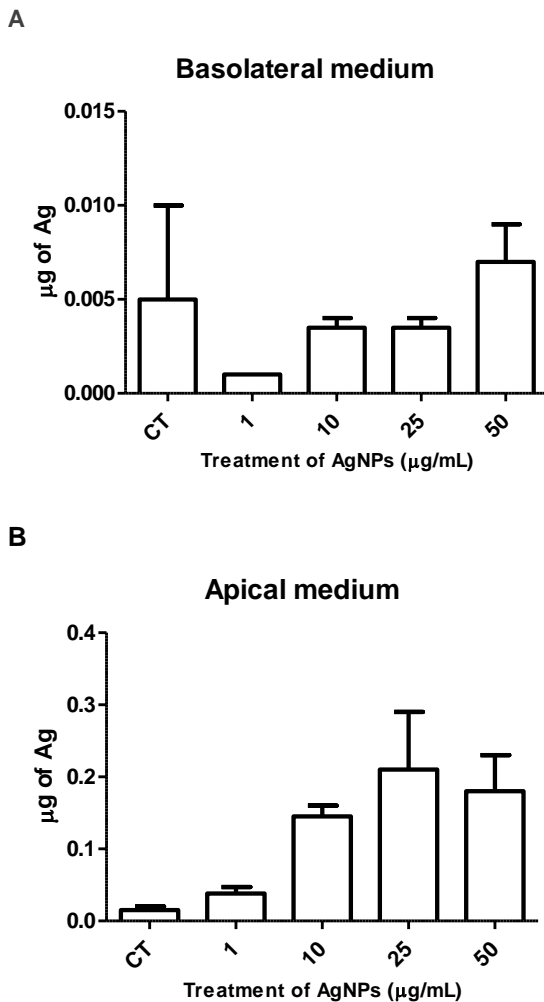
Figure 3. Translocation studies of AgNPs through Caco-2 monolayer. The basolateral extract was analyzed after 24h of AgNPs exposure by using ICP-MS: A (µg of Ag in the basolateral chamber)and B (µg of Ag in the apical chamber).

A

B
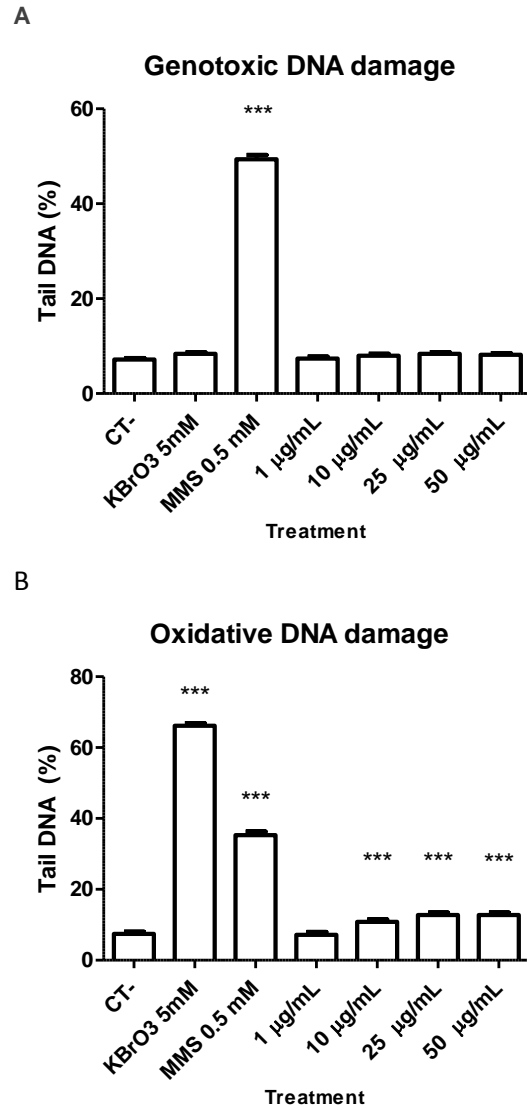
Figure 4. Analysis of genotoxic (A) and oxidative DNA damage (B) after 24h of AgNPs exposure. Data represented as mean ± SEM. ***P<0.001.

The new generation of microwave reactors for hydro- and solvothermal synthesis

Sylwia Dąbrowska[1,2],
Jacek Wojnarowicz[1], Tadeusz Chudoba[1], Agnieszka Chodara[1,2], Andrzej Majcher[3], Witold Łojkowski[1]

[1] Laboratory of Nanostructures, Institute of High Pressure Physics PAS, Sokolowska 29/37, Warsaw 01-142, Poland,
[2] Warsaw University of Technology, Faculty of Materials Science and Engineering, Warsaw, Poland
[3] Institute for Sustainable Technologies NRI, Pułaskiego 6/10, Radom 26-600, Poland

Contact: s.dabrowska@labnano.pl

Nowadays more and more bioactive materials are used in orthopedic and dental applications, which can support bone ingrowth and osseointegration. Bioactive hydroxyapatite (HAP) is one of the inorganic component of hard tissues, which is manufactured in The Institute of High Pressure Physics of the Polish Academy of Sciences (IHPP PAS) and it is called GoHAP™. The morphology, grain size and specific surface area of the nanopowder can be controlled by the microwave reactor and the high pressure consolidation technology for ceramic materials.

Microwave solvothermal synthesis (MSS) is an example of microwave assisted wet chemical synthesis process and nowadays it is counted as one of the most popular chemical methods of obtaining nanomaterials, like HAP, ZnO, ZrO_2 and other.

Microwave heating enables a better control of the reaction time, fast heating and reducing the thermal gradients. This results in a better crystallinity of the nanoparticles comparing to the precipitation process. An additional advantage is a reduced synthesis temperature, so no powder calcination is needed.

At the Laboratory of Nanostructures, IHPP PAS, we have been developing new type microwave reactors for nanomaterials synthesis for more than 10 years. The use of the microwave radiation and the unique design of the reactor permit precise pressure control during the quick synthesis processes, controlled with the accuracy of even one second. (Figure 1 and 2). The reactor also presents a control system which allows for an automatic operation in the stop flow mode or use the batch (closed vessel) mode. [1]

The MSS2 reactor was constructed as a part of the CePT project, reference: POIG.02.02.00-14-024/08, financed by the European Regional Development Fund within the Operational Programme "Innovative Economy" for 2007–2013.

References

[1]   A. Majcher, J. Wiejak and et al. Int. J. Chem. Reactor Engineering 2013, 11, 361-368.
[2]   S. Kusnieruk, J. Wojnarowicz and et al. Beilstein J. Nanotechnol. 2016, 7, 1586-1601.

Figures

Figure 1. The view of MSS2 reactor [2]

Figure 2. MSS2 reactor with Labview software

Nanostructured magnetic materials used in cancer treatment

Vladimir Lucian Ene[1],

Georgeta Voicu[1], Bogdan Stefan Vasile[1], Alexandru Grumezescu[1], Ecaterina Andronescu[1]

[1]University Politehnica of Bucharest, Faculty of Applied Chemistry and Materials Science, 1-7 Gheorghe Polizu Street, Bucharest, Romania

Vladimir.l.ene@gmail.com

Nanometric sized biomaterials assure a series of advantages which have greatly contributed to the advancements made in the biomedical field. First of all, these materials manifest chemical and structural similarities with tissues found in biological systems. Second, the size of nanobiomaterials is comparable with biomolecules and biomicrostrctures, allowing researchers to detect, maneuver and mediate such biocomponents. The last but not the least, from synthesis to processing, nanostructures can be easily adapted in order to tune important surface properties [1].

Magnetic nanoparticles are often used as a core which is covered by a biocompatible layer, determining a core-shell structure that can be used in the transport of bioactive components [2] [3].

Magnetite (Fe_3O_4) is a mineral that belongs to the iron oxide class and crystalizes in a face-centered cubic structure with 32 oxygen ions closely ordered on the (111) direction. Magnetite differs from the rest of the iron oxides by the fact that it contains both divalent (Fe^{2+}) and trivalent (Fe^{3+}) iron ions. It is found under an inverse spinel structure where all Fe^{2+} ions occupy half of the octahedral positions and Fe^{3+} ions are uniformly distributed at the rest of the octahedral positions and on the tetrahedral ones [1][4].

The present study is focused on the development of magnetite based nanostructures functionalized with cytostatics (paclitaxel - MP, carboplatin - MC, irinotecan - MI, aminoglutetimidă - MA, doxorubicină - MD, gemcitabine - MG) by coprecipitation method. The chosen precursors are $FeCl_3$ și $FeSO_4$, in stoichiometric proportions, and NH_3 is the compound set for assuring the alkaline environment.

For characterizing the obtained materials, a set of techniques were used, among which X-ray diffraction, Complex Thermal Analysis, FT-IR spectrometry, Scanning electron microscopy, Transmission electron microscopy (TEM, HRTEM, STEM, SAED, EDS) and gas adsorption analysis. The study also proposed the characterization of the antitumor effects of the synthetized materials by *in vitro* analysis of tumor cell cultures (HCT8) in controlled release in the absence of external magnetic field.

From the correlation of the mass loss analysis with the specific surface area and X-ray diffraction, it results that the magnetite particles possess amounts of hydrophilic cytostatics, and transmission electron microscopy shows the embedding of the particles by these molecules (figures 1 - 4).

From cell cycle analysis (Figure 5) it was demonstrated that Fe_3O_4 and Fe_3O_4-aminoglutethide hybrids, Fe_3O_4-paclitaxel, did not interfere significantly with normal cell cycle progression for HCT8 cells. In contrast, the Fe_3O_4-carboplatin hybrid material significantly affects cell cycle progression, Fe3O4-carboplatin increasing the percentage of cells under the G1 stage, generally in which non-viable cells or low metabolic activity are found, and Fe_3O_4-irinotecan causes growth of the percentage of cells in step G2 / M, in which cells are dividing.

References

[1]   M. Arruebo, R. Fernandez-Pacheco, M. R. Ibarra, and J. Santamaria, Nano Today, 2007, 22–32;

[2]   S. Laurent, D. Forge, M. Port, A. Roch, C. Robic, E. L. Vander, R.N. Muller, Chem. Rev. 2008, 2064-2110;

[3]   W. Wu, Z. Wu, T. Yu, C. Jiang, W.-S. Kim, Sci. Technol. Adv. Mater., 2015, 23501.

[4]   G. Unsoy et al., Curr. Top. Med. Chem., 2015, 1622–1640.

Figures
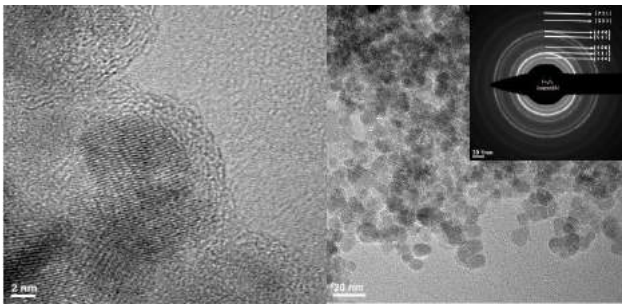
Figure 1. HRTEM, TEM and SAED of aminoglutetimide functionalized magnetite
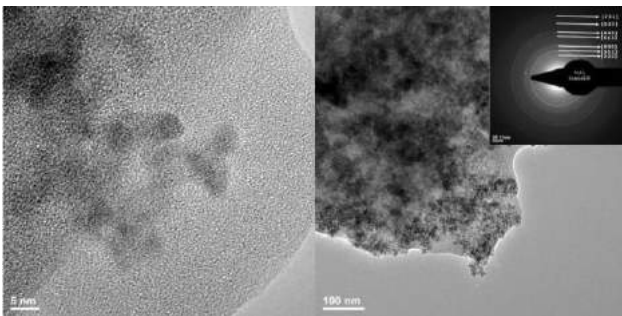
Figure 2. HRTEM, TEM and SAED of irinotecane functionalized magnetite
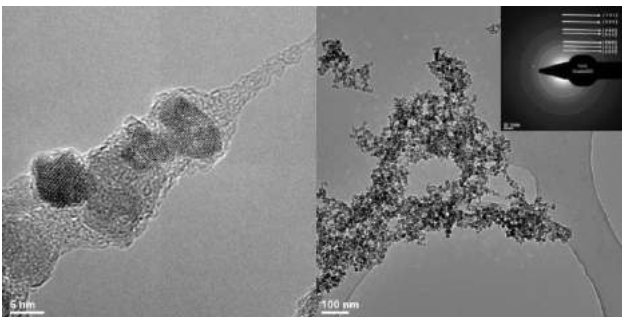
Figure 3. HRTEM, TEM and SAED images of gemcitabine functionalized magnetite
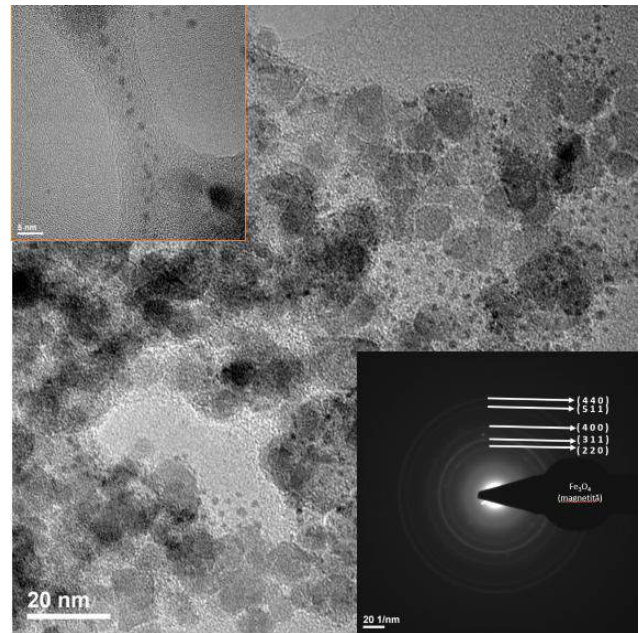
Figure 4. HRTEM, TEM and SAED of carboplatine functionalized magnetite
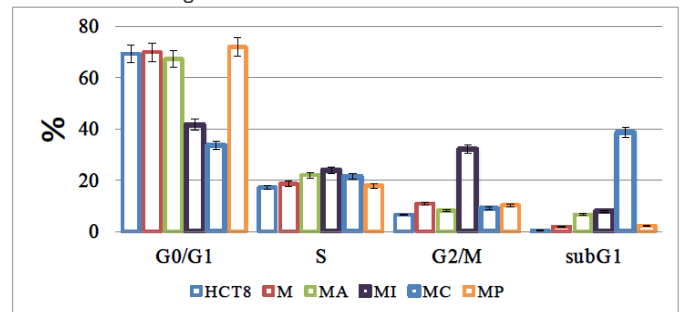
Figure 5. Cell cycle analysis

Computational Toxicology descriptors for Metal oxide Nanoparticles

Laura Escorihuela Martí[1],
Benjamí Martorell[1], Alberto Fernández[1]

[1]Universitat Rovira i Virgili, Tarragona, Spain.

laura.escorihuela@urv.cat

As widely stated in literature, the physico-chemical properties of metal oxide nanoparticles (MeO NPs) are size dependent. Relative to bulk materials, NPs below 5 nm in diameter are extremely changing in their properties due to the high ratio of atoms exposed on the surface. In contrast, NPs in the range of 15 to 90 nm are more similar to the bulk [1]. The use of QSAR/QSPR models for hazard screening helps significantly reducing time and cost of elaborate in vivo laboratory tests. For instance, the experimental determination of the band gap and its correlation with toxicity for 24 MeO nanoparticles has been obtained successfully. However, when the electronic energy levels do not correlate with the toxicity of some metal oxides, such as ZnO or CuO, the solubility can explain this toxicity [2]. Therefore, better understanding and mapping of the toxicity and the understanding of the relationship between size and NP properties is fundamental to establish safe-by-design strategies and the building of models representing the relationship between properties and size of NPs will avoid many of the experimental efforts. In this frame, the *in silico* methods developed nowadays can effort this challenge and furthermore.

For new nanomaterials, a set of nanodescriptors (i.e., physical and chemical properties) must be calculated a priori to develop these models and use them for ulterior predictions. ENMs (Engineered NanoMaterials) are extensively used given their novel/valuable chemical, electrical, magnetic properties that arise from their small size and structural features. Using the most advanced developments of quantum chemistry tools based on Density Functional Theory, one can nowadays obtain those descriptors without requiring extensive laboratory sampling and simultaneously reducing the need of in vivo experiments. Thus, basic studies of physical and chemical properties on nanoparticles provide the clue for their reactivity mechanism. Computational methods can focus to determine the lowest-energy geometry, physical properties, interactions, etc.

Our study compares two methodologies for the determination of ZnO and TiO_2 NPs electronic structure-related properties, solubility and band gap, properties correlated with the toxicity of NPs in cell media [3]. Using the Density Functional Theory (DFT) at GGA and GGA+U levels and Density Functional – Tight Binding (DFTB), the formation energies, band gaps and solubility of several ZnO low-dimensionality structures were evaluated.

Computer simulation results in vacuum showed the difference between ZnO at bulk, which is a semiconductor (band gap of 3.2 eV), relative to ZnO low-dimensionality structures, which became more conductor (band gap <1.5 eV) or slightly less conductor (<4 eV) in a few cases, depending on the crystal structures, what matches with previously published results. Afterwards, filling that vacuum with water molecules, we observed the effect of the aqueous environment in the electronic properties of the NP. Moreover, making use of DFTB methodology, our group was able to evaluate the solubility of NPs up to 3nm [4] of diameter (see Fig.1 for the molecular model) directly, and using the Ostwald-Freundlich equation we could extrapolate our results to larger NPs.

Using the aforementioned electronic descriptors, small structures were scaled up and, together with experimental toxicity data serve to develop structure-property (QSPR) and structure-activity (QSAR) relationships for larger NPs that ultimately will contribute to the computational design of NPs optimised for specific applications.

References

[1] A. Gajewicz, T. Puzyn, B. Rasulev, D. Leszczynska and J. Leszcynski, Nanosci. Nanotechnologt-Asia 1 (2011) 53.

[2] R. Liu, H.Y. Zhang, Z.X. Ji, R. Rallo, T. Xia, C.H. Chang, A. Nel and Y. Cohen. Nanoscale 5 (2013) 5644.

[3] A. B. Djurisic, Y. H. Leung, A. M. C. Ng, X.Y. Xu, P. K. H. Lee, N. Degger and R. S. S. Wu, Small 11 (2015) 26.

[4] L. Escorihuela, A. Fernández, R. Rallo and B. Martorell, Food and Chemical Toxicology (2017) DOI: 10.1016/j.fct.2017.07.038

Figures
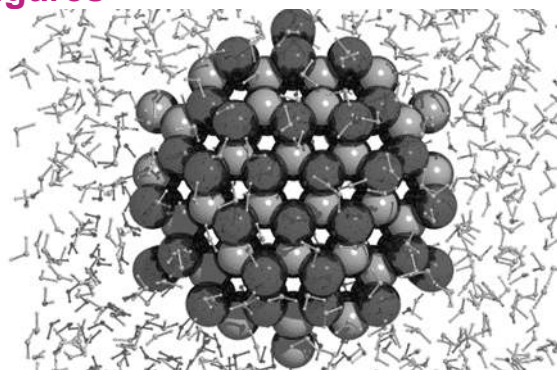
Figure 1. Nanoparticle of 2 nm in an aqueous medium.

Nanomechanical Sensing with 2D Colloidal Diffraction Gratings

P. Escudero[1],
R. Villa[1,2] and M. Alvarez[1+]

[1]Instituto de Microelectronica de Barcelona (IMB-CNM, CSIC).), Campus UAB, 08193 Bellaterra, Barcelona, Spain.
[2]Biomedical Research Networking Center in Bioengineering, Biomaterials and Nanomedicine (CIBER-BBN), Zaragoza, Spain

mar.alvarez@csic.es

Abstract

In the last years, nanomechanical sensors have become an emerging and promising technology for sensing and biosensing applications, due to their small size, fast response, high sensitivity and their compatible integration into "lab-on-a-chip" devices[1]. These properties make nanomechanical sensors an especially interesting tool for the diagnosis of diseases where the simultaneous detection of several analites is mandatory to achieve an appropriate diagnosis and treatment. However the multiplexed capability for monitoring several nanomechanical transducers (each one associated with the detection of a specific compound) still present some limitations related mainly with the integration of the read-out methodology when working with an array of transducers (alignment, power,…).

To solve this limitation, we propose the colorimetric detection of nanomechanical bending[2]. We present the development of polymeric nanomechanical biosensors (membranes or microcantilevers) with integrated diffraction gratings based on 2D colloidal crystals[3]. We explore and exploit the white light diffraction to achieve a power-free array of membranes that change their reflective colour depending on the surface stress change (bending) produced on each sensor. The transducer bending will induce a change on the angle of incident of light and a deformation of the grating (increase or decrease of the pitch for large bending).

We performed a study of the optimum membrane dimensions to maximize both the mechanical response and the colour change associated, when a surface stress-strain change is produced. Polymeric materials, besides being cheap and easily nanostructured, present a much lower Young's Modulus compare with standard nanomechanical materials such as silicon, which will increase the bending response. Experimentally, the arrays of membranes were fabricated by infiltrating 2D colloidal crystals of polystyrene nanoparticles with Polydimethylsiloxane (PDMS). The membranes were fixed and integrated into a microfluidic system. The colour of each membrane, due to the light scattering, was analyzed by UV-visible spectrometry and image analysis looking to develop an integrated multidetección system based on a smartphone reading. We demonstrate the suitability of this approach for the detection of nanomechanical bending induced by the adsorption of elements on the sensor surface.

References

1   M. Alvarez and L. M. Lechuga, *The Analyst*, 2010, 827–836.
2   P. Escudero, J. Yeste, R. Villa and M. Alvarez, 2017, 102460P.
3   T. Karrock and M. Gerken, *Biomedical Optics Express,* 2014, **6**, 392–399.

Figures
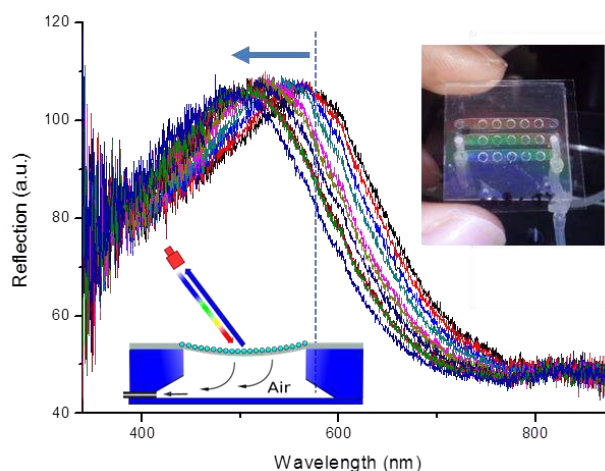
Figure 1. Membrane color change under deformation fabricated device (inset).

Super-resolution microscopy study of protein corona composition and evolution in single nanoparticles

Natalia Feiner-Gracia[1], Michaela Beck [2], Sílvia Pujals[1], Sébastien Tosi[3], Tamoghna Mandal[4], Christian Buske[4], Mika Linden[2], Lorenzo Albertazzi[1]

[1]Institute for Bioengineering of Catalonia (IBEC). The Barcelona Institute of Science and Technology. Baldiri Reixac 15-21. Barcelona, Spain
[2]Inorganic Chemistry II, Ulm University, Albert-Einstein-Allee 11, D-89081 Ulm, Germany
[3]Advanced Digital Microscopy Core Facility (ADMCF), Institute for Research in Biomedicine (IRB Barcelona). The Barcelona Institute of Science and Technology, Barcelona, Spain
[4]Institute of Experimental Cancer Research, University Hospital Ulm, Albert-Einstein-Allee 11, D-89081 Ulm, Germany

nfeiner@ibecbarcelona.eu

The formation of the protein corona when nanoparticles are introduced into the blood stream alters their interactions with the target cells, affecting their functionality and performances *in vivo* [1]. Therefore, to improve the design of effective nanoparticles it is important to understand the composition and temporal evolution of the protein corona. In the present work we use super-resolution optical microscopy (SRM) to study the protein corona growing on mesoporous silica nanoparticles. SRM enables us not only the imaging but the quantification of single proteins [ref]. Interestingly, we observed a significant heterogeneity in protein absorption between individual nanoparticles which was only possible to detect thanks to the high resolution of the technique and its ability to image in a particle-by-particle basis. We studied the role of the surface chemistry in the corona formation and the role of the degradability in the corona evolution in time. Moreover, we investigate the consequences of protein corona formation on selective cell targeting which provide us a detailed understanding of corona-activity relations. The present methodology is widely applicable to a variety of nanostructures and complements the existing ensemble approaches to further investigate protein corona phenomenon.

References

[1] Lazarovits J., Chen Y. Y., Sykes E. A., Chan W. C. W., Chem. Commun, 51 (2015) 2756.
[2] Walkey, C. D.; Chan, W. C. W. Chem. Soc. Rev., 41 (2012), 2780.
[3] Feiner-Gracia, N.; Beck, M.; Pujals, S.; Tosi, S.; Mandal, T.; Buske, C.; Linden, M.; Albertazzi, L. Small (2017)

Figures
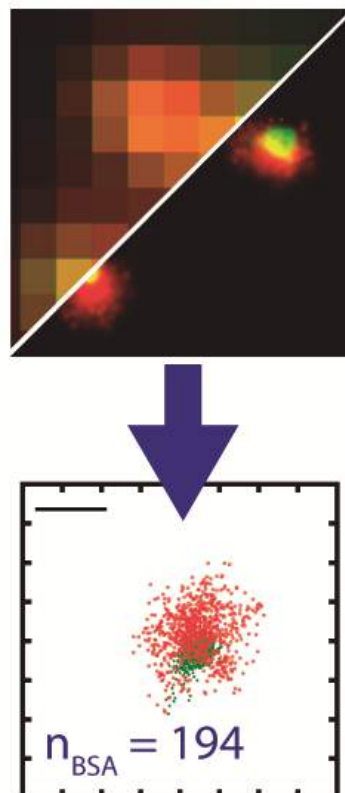
Figure 1. Super resolution imaging and quantification of protein corona formation on mesoporous silica nanoparticles incubated with 10%BSA/FBS v/v compared to conventional fluorescence imaging.

Urease Powered Nanobots for Drug Delivery Applications

Ana C. Hortelão[1,2],
Tania Patiño[1,2], Ariadna Perez-Jiménez[1], Àngel Blanco[1] and Samuel Sánchez[1,2,3]

[1]Institute for Bioengineering of Catalonia (IBEC), The Barcelona Institute of Science and Technology, Baldiri Reixac 10-12, 08028 Barcelona Spain
[2]Max Planck Institute for Intelligent Systems Institution, Heisenbergstraße 3, 70569 Stuttgart, Germany.
[3]Institució Catalana de Recerca i Estudis Avancats (ICREA), Pg. Lluís Companys 23, 08010, Barcelona, Spain

ahortelao@ibecbarcelona.eu
ssanchez@ibecbarcelona.eu
tpatino@ibecbarcelona.eu

Figures

Figure 1. Enhanced Doxorubicin release and delivery efficacy to cancer cells by urease powered nanobots.

The development of micro- and nanostructures capable of self-propulsion has opened new ventures for wastewater treatment,[1] bio-sensing,[2] and biomedical applications.[3,4] In this regard, the use of enzymes as biological engines to power nanomotors provides a versatile library of relevant and biocompatible fuels that can be tailored to the target application.[5] In this work, we present urease powered nanobots for the loading of Doxorubicin (Dox), fuel-dependent release and efficient delivery to cancer cells. These nanobots consist in a core-shell mesoporous silica structure and are able to propel in ionic media, as demonstrated by dynamic light scattering and optical tracking. Furthermore, it is observed a four-fold increase on drug release of Dox from active nanobots in the presence of fuel compared to their passive counterparts leading to an improved anti-cancer efficiency towards cancer cells. This effect arises from a synergistic effect of the boosted release and the ammonia produced by urea breakdown. Urease powered nanobots may hold potential for their use in future applications, namely the fuel-triggered drug release in target locations.

References

[1]   Parmar, J.; Vilela, D.; Pellicer, E.; Esqué-de los Ojos, D.; Sort, J.; Sánchez, S., *Adv. Funct. Mater.,* 26 (2016), 4152–4161.
[2]   Esteban-Fernández de Ávila, B.; Martín, A.; Soto, F.; Lopez-Ramirez, M. A.; Campuzano, S.; Vásquez-Machado, G. M.; Gao, W.; Zhang, L.; Wang, J., *ACS Nano*, 9 (2015), 6756–6764
[3]   Hortelao, A. C.; Patiño, T.; Perez-Jimenez, A.; Blanco, A; Sanchez, S., *Adv. Funct. Mater., In press*
[4]   Katuri, J.; Ma, X.; Stanton, M. M.; Sánchez, S., *Acc.Chem.Res*, 50 (2017), 2-11
[5]   Ma, X.; Hortelao, A. C.; Patiño, T.; Sanchez, S., *ACS Nano,* 10 (2016), 9111–9122.

GRAPHENE-BASED ELECTROCHEMICAL BIOSENSORS FOR DNA DETECTION IN HEALTHCARE DIAGNOSIS

Teddy TITE[1],
Luisa PILAN[1],
George Mihail VLĂSCEANU[1], Adi GHEBAUR[2]
Jorge S. BURNS[1], Mariana IONIȚĂ[1,2]

[1]Faculty of Medical Engineering, University Politehnica of Bucharest, Gh Polizu 1-7, 011061, Bucharest, Romania
[2]Advanced Polymer Materials Group, University Politehnica of Bucharest, Gh Polizu 1-7, 011061, Bucharest, Romania

titedfr@yahoo.fr

Quantification of biological processes is of utmost importance for biomedical applications. Biosensors have truly brought a revolution in diagnosis and preventive healthcare by detecting chemical or biological molecules of uninfected and infected cells using a biorecognition element and a transducer. Commonly, the specific interaction between an analyte (proteins, biomarkers, enzymes, nucleic acid, *etc.)* and the bioelement (substrate) is detected and converted into a measurable signal using the transducer. Electrochemical biosensors based on graphene materials are modern and future approaches to healthcare diagnosis, presenting more sensitive, selective, practical and less labor-intensive detection protocols compared to the conventional methods such as real-time polymerase chain reaction (RT-PCR) [1]. Remarkable and unique physiochemical properties of graphene that are advantageous for biosensor development include its large surface to volume ratio, excellent electrical conductivity, strong mechanical strength, good chemical stability and easy surface functionalization. Today, the use of glassy carbon electrode (GCE) as a substrate for graphene biosensors is well established [2]. Recently, screen-printed electrode (SPE) has received increasing attention as a means of achieving some essential requirements for advanced biosensor developments, such as low cost, ability to be mass-produced, and perhaps the most fundamental of all, simplicity [3].

In this work, we propose to develop robust electrochemical graphene biosensors by taking into account the versatility of graphene for DNA detection, molecules which play key roles in the regulation of gene expression (Figure 1). Versatility will be investigated using commercial multilayer graphene (Ml-G), graphene oxide (GO), commercial reduced graphene oxide (RGO), home-made electrochemically reduced graphene oxide (ERGO), as well as functionalized GO with carboxyl and amines group. Both GCE and SPE will be used and compared. The impact of graphene versatility upon the electrochemical detection of DNA molecules is still an open question.

Electrochemical measurements were performed with a potentiostat/galvanostat Autolab model Pgstat 204 (Nova 2 software) at room temperature (25°C) and a cell consisting of graphene modified GCE or SPE as working electrode, an Ag/AgCl reference electrode (in KCl 3 mol. L^{-1}) and a platinum wire as counter electrode. Experiments were carried out in 0.1 M KCl, or with 1mM [Fe(CN)$_6$]$^{3-/4-}$ redox probe (1:1) in 0.1 M KCl. Electrochemical reduction of GO was performed in one-step and two-step (drop-casting) approaches in various electrolytes [4], such as GO dispersion with PBS solution and alkaline solution. The structure, chemistry and morphology of graphene electrodes was investigated by optical microscopy, Raman spectroscopy (DXR Thermofisher and Renishaw Invia), and X-ray diffraction (XRD) (Neslab, Thermoflex 1400). In this study, detection of single strand DNA probes with the sequence 5'TTTCAACATCAGTCTGATAAGCTATCTCCC-3' and complementary target with the following sequence 5-GGG AGA TAG CTT ATC AGA CTG ATG TTG AAA-3' have been investigated by non-covalent functionalization after being drop-casted on the surface of electrode at different concentrations.

Figure 2 shows the XPS survey of graphene materials with various degree of oxidation. The C/O atomic ratio was 35.8, 3.9, 2.7 and 2 for Ml-G, ERGO, RGO and GO respectively. Graphene oxide samples show intense bands in C1s deconvolution at ~286.5 eV and ~288 eV attributed to C-O/C=O and O-C-O/O=C-OH groups, respectively in comparison to Ml-G. Detection of DNA probes were investigated on GO film modified GCE (Figs. 3&4). DNA probes were successively deposited at various concentrations on the surface of the electrode. A continuous decrease in the CV signal (Fig. 3) and increase in the charge transfer resistance in the Nyquist plot (Fig. 4) were observed upon the DNA deposition with good sensitivity (down to 25nM). The decrease of the current and increase of resistance were explained by the repellence of [Fe(CN)$_6$]$^{3-/4-}$ ions with the negatively charged DNA molecules [5]. Detection of DNA probes were also investigated on commercial Ml-G and RGO on SPE. In comparison to Ml-G, RGO samples presented abundant structural defects that were clearly evidenced by a higher I(D)/I(G) ratio (Figs. 5(a) and 6(a)). Upon DNA deposition, the intensity of CV curves decreases for RGO but not for Ml-G. The result was attributed to a better adsorption and anchoring of DNA molecules on RGO due to Van der Waals and π-π* interaction helped by surface specificities and defects sites [6]. RGO sample detect DNA at a concentration as low as 25 nM DNA. Our results show high promise for graphene oxide biosensor for healthcare diagnosis.

References

[1] P. Bollella et al., Biosensors and Bioelectronics, 89 (2017) 152
[2] P. Abdul Rasheed et al., Biosensors and Bioelectronics, 97 (2017) 226
[3] A. Hayat et al., Sensors, 14 (2014) 10432
[4] S. Y. Toh et al., Chemical Engineering Journal, 251 (2014) 422
[5] A. Benvidi et al., Talanta, 137 (2015) 80
[6] V. Georgiakilas et al., Chem. Rev., 112, (2012) 6156

Figures

Figure 4. Nyquist plots of GO/GC upon DNA deposition
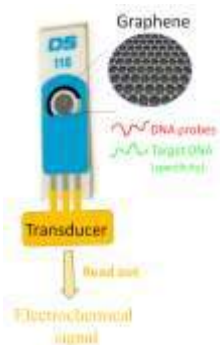
Figure 1. Graphene-based SPE biosensor
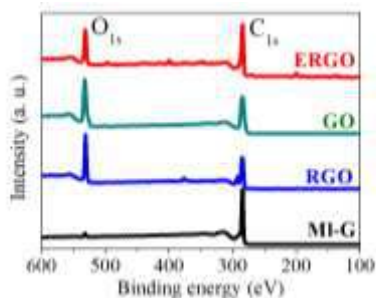
Figure 2. XPS spectra of SPE, GPH, RGPHOX, GO
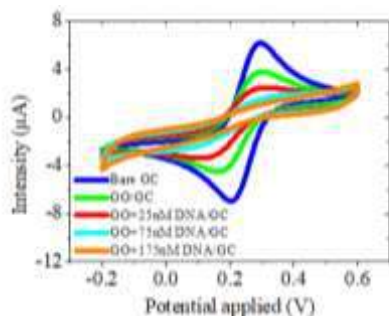
Figure 3. CV curves of GO/GC upon DNA deposition
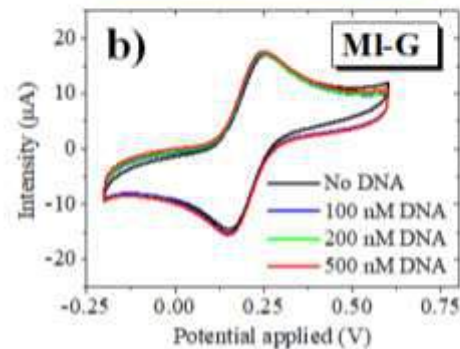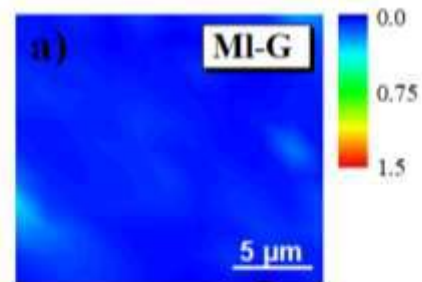
Figure 5. Raman mapping of I(D)/I(G) (a) and CV curves upon DNA deposition (b) of Ml-G
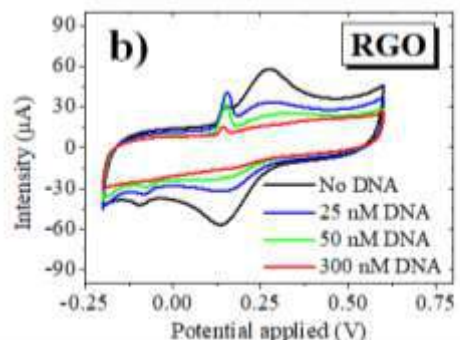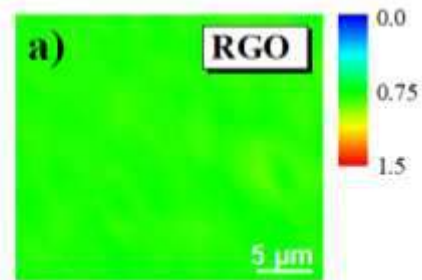
Figure 6. Raman mapping of I(D)/I(G) (a) and CV curves upon DNA deposition (b) of RGO

Probing the corona formation on nanodiamonds- its dynamics and biological consequences

Dipesh Khanal,[1, 2]
Alexey Kondyurin,[2] Iqbal Ramzan,[1] , Kee Woei Ng,[3]
Wojciech Chrzanowski[1,2]

[1]Faculty of Pharmacy, The University of Sydney, NSW 2006, Australia
[2]Australian Institute for Nanoscale Science and Technology, The University of Sydney, NSW 2006, Australia
[3]School of Materials Science & Engineering, Nanyang Technological University, 50 Nanyang Avenue, Singapore 639798, Singapore

dipesh.khanal@sydney.edu.au

When a nanoparticle enters the body, biomolecules (proteins, lipids, metabolites and sugars) coat the surface of nanoparticle to form a 'corona' which critically affects the fate of nanoparticle i.e. the aggregation tendency, uptake by the cell and toxicity. Since, physiological systems are highly dynamic and multiple classes of proteins exist, there is 'competition' within the proteins to get adsorbed onto the nanoparticle, therefore it is critical to obtain time-resolved knowledge of protein-corona formation. Here, for the first time combination of nano isothermal calorimetry, SDS Page and Matrix assisted laser ionization/deionization time of flight spectrometry was used to demonstrate the formation of corona on nanodiamond (ND) (aminated and pristine). Cutting-edge AFM-IR technique was used to evaluate the fate of proteins adsorbed onto the individual ND. Our findings highlighted that corona formation on ND occurs within five minutes of exposure to proteins and with the evolution of time, the amount and type of protein bound to ND varies, confirming the dynamics. Furthermore, depending on the physicochemical properties of the ND, proteins compete with each other and preferentially bind to the ND (as seen with the two model proteins BSA and fibronectin). High resolution nanoscale spectra collected using the AFM-IR technique confirmed that irreversible changes to the protein structure, denaturation and aggregation occurred after binding to ND. In addition, depending on the protein bound to the specific class of ND, uptake and cytotoxicity was significantly different. Binding of BSA to ND promoted cell growth whereas fibronectin bound ND showed higher cytotoxic effect on the cells. These finding clearly indicate that investigating the corona formation is crucial to understand the fate of nanoparticles in the biological system and to screen the toxic potential of nanoparticles, as the conformational changes in protein may result in localized inflammation and toxicity.

Figures
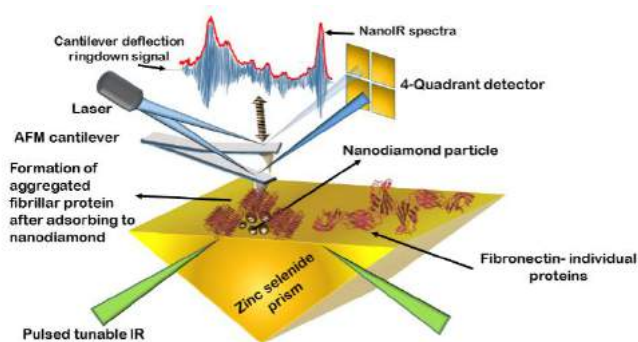
Figure 1. Schematic representation of AFM-IR spectroscopy: conformational changes in the protein structure occurred after exposure to nanodiamond particles resulting in the formation of aggregated fibrillar protein.
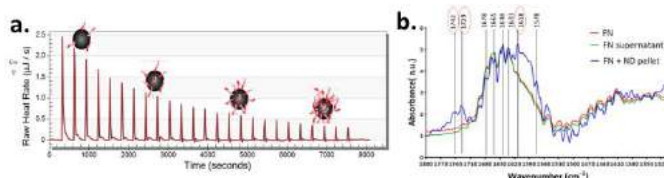
Figure 2. . a) Isothermal calorimetry plot of fibronectin titrated to nanodiamond particles, with increasing number of injections of fibronectin, nanodiamond particle were coated with fibronectin before being saturated by fibronectin adsorption; b) AFM-IR spectra collected from the nanodiamond adsorbed with fibronectin. Formation of aggregated fibrillar fibronectin and denaturation occurred after binding to the nanodiamond: red circles indicate the wavenumbers corresponding to the conformational changes and denaturation of proteins.

Relaxivity of ε-Fe₂₋ₓAlₓO₃ Nanoparticles: A Complex Study

Lenka Kubíčková[1],
Jaroslav Kohout[1], Ondřej Kaman[2], Petr Brázda[2],
Pavel Veverka[2], Tomáš Kmječ[1], Karel Závěta[1],
Petr Dvořák[1], Vít Herynek[3]

[1]Faculty of Mathematics and Physics, Charles University,
V Holešovičkách 2, Prague, Czech Republic
[2]Institute of Physics, Czech Academy of Sciences,
Cukrovarnická 10/112, Prague, Czech Republic
[3]Institute for Clinical and Experimental Medicine,
Vídeňská 1958/9, Prague, Czech Republic

sagittaria.64@gmail.com

Magnetic nanoparticles have received extensive attention in the biomedical research, e.g. as prospective contrast agents for T_2-weighted magnetic resonance imaging (MRI). The ability of a contrast agent to enhance the relaxation rate of hydrogen nuclei in its vicinity is quantified by its relaxivity. In the case of magnetic nanoparticles, the transverse relaxivity $r_2 = (R_2 - R_{H2O})/c$ is more significant, with R_2 and R_{H2O} being relaxation rates of ^{1}H in the examined suspension and in pure water, respectively, and c the molar concentration of the contrast agent in the suspension. In this study, we focused on evaluating r_2 of ε-Fe₂₋ₓAlₓO₃ nanoparticles coated with amorphous silica or citrate — its dependence on external magnetic field, temperature and thickness of silica coating. While most nanoparticles are in superparamagnetic state, nanosized ferrimagnetic ε-Fe₂O₃ is in blocked state due to high magnetocrystalline anisotropy resulting in giant coercive field ∼ 2 T at room temperature [1, 2, 3]. In comparison to ε-Fe₂O₃ nanoparticles, ε-Fe₂₋ₓAlₓO₃ prepared by substituting diamagnetic aluminium atoms for a fraction of iron atoms in ε-Fe₂O₃ was expected to exhibit higher magnetization and thus higher relaxivity.

The nanoparticles were synthesized by impregnation of mesoporous silica template [4] with Fe(NO₃)₃ and Al(NO₃)₃ followed by annealing. After dissolution of the matrix, the particles were coated with amorphous silica [5,6]; one of the samples was stabilized by citrate. The chemical composition of bare ε-Fe₂₋ₓAlₓO₃ particles was determined from XRF spectrum to be 2 − x = 1.77(1) of Fe and x = 0.23(1) of Al. XRPD analysis of the bare sample confirmed the same structure as ε-Fe₂O₃ — orthorhombic crystal system with $Pna2_1$ space group and lattice parameters $a = 5.0757(4)$ Å, $b = 8.7444(7)$ Å and $c = 9.4243(6)$ Å, the volume per formula unit ∼ 52.286(6) Å³. The size of magnetic cores (i.e. bare particles) was $d_c \sim 21$ nm, the thickness of silica coating $L \sim 6$, 10, 17 and 21 nm was used in sample labelling (Figure 1). Magnetization of the ε-Fe₁.₇₇Al₀.₂₃O₃ nanoparticles

(σ_{5T} = 21.1 A.m².kg⁻¹) increased by ∼ 30% when compared to ε-Fe₂O₃, confirming thus our assumption about the influence of Al. ZFC/FC curves indicate that magnetic transitions characteristic to ε-Fe₂O₃ [4] are suppressed by the substitution [7]. The magnetization evinced an approximately linear decrease with temperature in the temperature range examined in the relaxometric study.

The r_2 relaxivity was measured on suspensions of four samples encapsulated in silica and one stabilized by citrate, by means of nuclear magnetic resonance (NMR). The relaxivity was calculated from the linear fit of $R_2(c)$ data obtained for suspensions of various concentrations. Considering the size and magnetic moment of the nanoparticles, the motional averaging regime (MAR) [8] should be used for describing the relaxivity, yielding the relation $r_2 = (4d^2 M^2 v_{mat} \gamma^2 \mu_0^2)/405D$, where d denotes the size of the particles, M volume magnetization of the agent, v_{mat} its molar volume, γ gyromagnetic ratio of ^{1}H and μ_0 permeability of vacuum. Magnetic field dependence (Figure 2) followed approximately the exponential rise to maximum, for which the MAR model is no more applicable. The different slope of relaxivity of the citrated sample in comparison to samples coated with silica suggests different mechanism of interaction of ^{1}H with the coating material. The temperature dependence of relaxivity (Figure 3) of samples coated with silica demonstrated a significant deviation from a simple model based on the pseudo-Arrhenius behaviour of water self-diffusion, which resulted in higher values of relaxivity than predicted by the given model. The experimentally found linear decrease of relaxivity with increasing thickness of the silica coating is also in contrast with the prediction of the MAR model, which suggests the decrease of r_2 proportional to $d_c^2/(1+2L/d_c)^3$. Our results indicate that another mechanism which enhances the transversal relaxivity might be involved. Possible explanation can be suggested based on water molecules bound to the silica coating, i.e. molecules either present inside the pores of silica or physisorbed to the silica surface. The relaxivity of examined samples was also compared to the relaxivity of ε-Fe₂O₃ nanoparticles from previous study; the increase by almost 40 % for particles coated with silica thickness lower than 10 nm was found, while there was no considerable difference in relaxivity for thicker coatings. Consequently, the magnitude of the increase did not meet our expectation and was in contradiction to the prediction of MAR (increase in magnetization by ∼ 30 % was supposed to enhance relaxivity by ∼ 70% irrespective of the thickness of silica coating).

The transverse relaxivity of the examined samples is comparable to or exceeds commercial superparamagnetic iron oxide nanoparticle contrast agents (SPIOs and USPIOs) or those under clinical

investigation [9], whose relaxivity ranges between roughly 20 and 200 $s^{-1}.mmol^{-1}.dm^3$ per Fe at 1.5 T and 37 °C.

We have found that the level of the cytotoxicity of our silica-coated nanoparticles is very low suggesting that the follow-up use of $\varepsilon\text{-Fe}_{2-x}\text{Al}_x\text{O}_3$ cores even with small thickness of silica coating for *in vivo* studies is safe.

References

[1] J. Jin, S. Ohkoshi and K. Hashimoto, *Advanced Materials* 16, 1 (2004) 48–51

[2] J. Tuček, R. Zbořil, A. Namai and S. Ohkoshi, *Chemistry of Materials* 22, 24 (2010) 6483–6505

[3] J. Kohout, P. Brázda, K. Závěta, D. Kubániová, T.Kmječ, L. Kubíčková, M. Klementová, E. Šantavá and A. Lančok, *Journal of Applied Physics* 117, 17 (2015) 17D505

[4] P. Brázda, J. Kohout, P. Bezdička and T. Kmječ, *Crystal Growth & Design* 14, 3 (2014) 1039–1046

[5] Stöber, W., Fink, A. & Bohn, E., *Journal of Colloid and Interface Science* 26, 1 (1968) 62–69

[6] L. Kubíčková, J. Kohout, P. Brázda, M. Veverka, T. Kmječ, D. Kubániová, P. Bezdička, M. Klementová, E. Šantavá and K. Závěta, *Hyperfine Interactions* 237, 1 (2016) 159

[7] A. Namai, S. Sakurai, M. Nakajima, T. Suemoto, K. Matsumoto, M. Goto, S. Sasaki and S.I. Ohkoshi *Journal of the American Chemical Society* 131, 3 (2009) 1170–1173

[8] A. Roch, R. N. Muller and P. Gillis, *The Journal of Chemical Physics*, 110, 11 (1999) 5403–5411

[9] S. Laurent, D. Forge, M. Port, A. Roch, C. Robic, L. Vander Elst, and R. N. Muller, *Chemical Reviews* 108, 6 (2008) 2064–2110

Figures
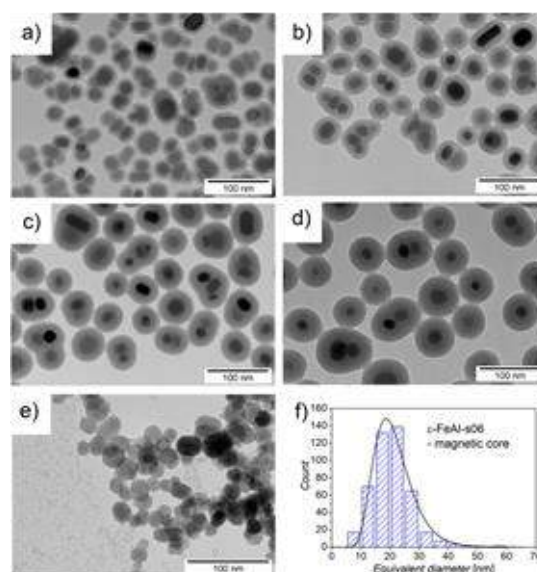
Figure 1. TEM images of samples coated with silica and citrate: a) ε-FeAl-s06, b) ε-FeAl-s10, c) ε-FeAl-s17, d) ε-FeAl-s21, e) ε-FeAl-cit, f) representative histogram of particle sizes from TEM (magnetic core of ε-FeAl-s06; fitted with lognormal distribution).
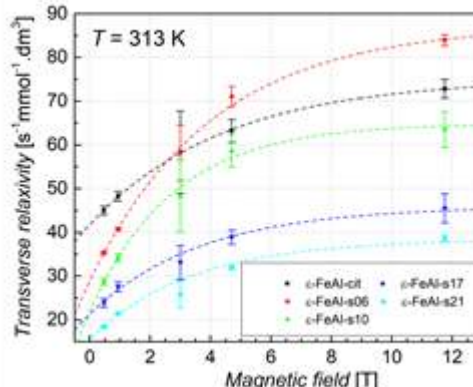
Figure 2. Representative dependence of transverse relaxivity per Fe on external magnetic field at 313 K. Experimental data were fitted by exponential rise to maximum to provide guidelines to the eye.
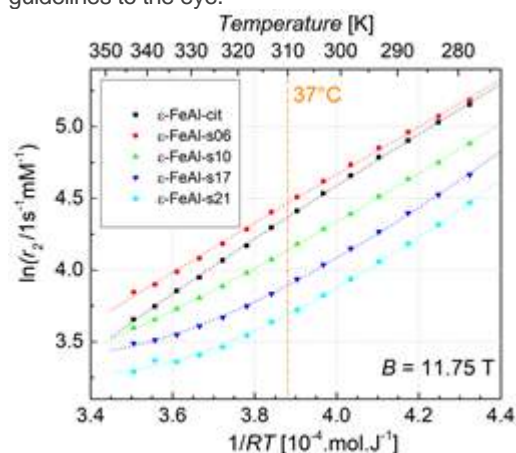
Figure 3. Representative graph showing the dependence of lnr_2 per Fe on 1/RT at 11.75 T, R being the gas constant. The data were fitted with regard to the temperature dependence of magnetization and the Arrhenius-type of behaviour of the self-diffusion coefficient in the MAR. The temperature of the human body 37 °C is highlighted in the graph.

Molecular Dynamics Simulations of Surfactants Adsorption on Carbon Nanotubes Surfaces

Isabel Lado Touriño[1]

Arisbel Cerpa Naranjo[1], Mª Piedad Ros Viñegla[2], Paloma Ballesteros García[3], Sebastián Cerdán García-Esteller[4]

[1]Department of Industrial Engineering and Aeronautics, Universidad Europea de Madrid, 28670-Villaviciosa de Odón, Spain
[2]Department of Pharmacy and Biotechnology, Biomedicine, Faculty, Universidad Europea de Madrid, 28670-Villaviciosa de Odón, Spain
[3]Laboratory of Organic Synthesis and Molecular Imaging by Magnetic Resonance, Faculty of Sciences, UNED, 28040-Madrid, Spain,
[4]LIERM, Institute of Biomedical Research "Alberto Sols", CSIC, 28029-Madrid, Spain.

misabel.lado@universidadeuropea.es

Abstract

During the last years, carbon nanotubes (CNTs) have been increasingly used in the fields of pharmacy and biomedicine [1, 2]. However, since it is an emerging technology, there is very limited information about their toxicity, complications or adverse reactions in the body. The other drawback to these structures is that they are very hydrophobic so that they cannot easily be handled in most solvents of biological interest. Different surfactants have been used to improve their dispersion in aqueous media [3]. In the present work, we investigated the adsorption behavior of two surfactants, sodium dodecyl sulfate (SDS) and sodium dodecyl benzene sulfonate (SDBS), at different concentrations on CNT surfaces by molecular dynamics (MD) simulations [4]. The results are presented in terms of distance between surfactant molecules and CNT surfaces, radial distribution functions and interaction energies. In all the models simulated here, a strong adsorption of both surfactants on CNT surfaces is seen as it is demonstrated by decreasing distances during simulation time and favorable energetic processes.

References

[1]   V. Negri, A. Cerpa, P. López.Larrubia, L. Nieto-Charques, S. Cerdán, P. Ballesteros, Angew. Chem., 122 (2010) 1857

[2]   A. Cerpa, M. Köber, D. Calle, V. Negri, JM Gavira, A. Hernanz, F. Briones, S. Cerdán, P. Ballesteros. Med. Chem. Com., 473 (2013) 270

[3]   I. Lado Touriño, A. Cerpa Naranjo, V. Negri, S. Cerdán, P. Ballesteros, J. Mol. Graphics Modell., 62 (2015) 69

[4]   [3] Materials Studio, (2016). Retrieved from http://accelrys.com/
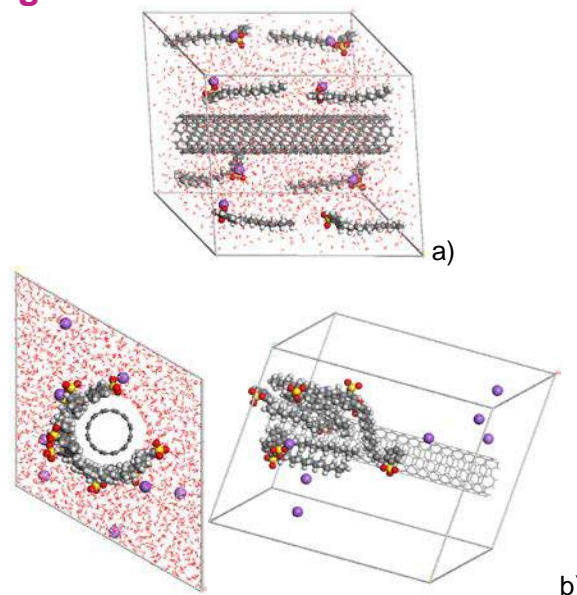
Figures

Figure 1. Initial (a) and final positions (b) of eight SDBS molecules interacting with a CNT obtained from molecular dynamics calculations. In part b) of this figure, two different views of the model are shown.
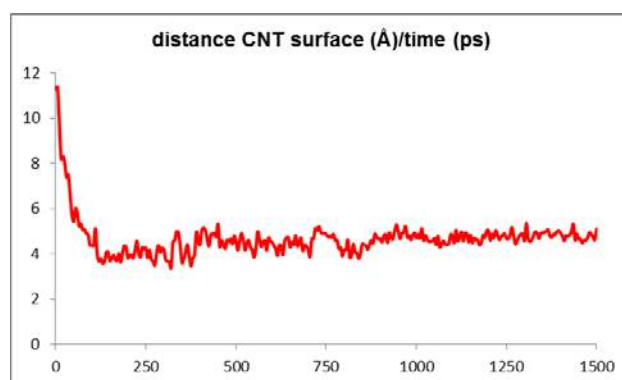
Figure 2. Evolution of the distance between the center of mass of SDBS molecules and the CNT surface with simulation time.

Amoxicillin-loaded lipid nanoparticles: towards a therapeutic approach for *Helicobacter pylori* infections

Daniela Lopes[1],
Rita M. Pinto[1], Catarina Seabra[2], Sofia Lima[1], Bruno Sarmento[2], Cristina Martins[2], Cláudia Nunes[1], Salette Reis[1]

[1]LAQV, REQUIMTE, Departamento de Ciências Químicas, Faculdade de Farmácia, Porto, Portugal
[2]i3s, Instituto de Investigação e Inovação em Saúde and INEB- Instituto de Engenharia Biomédica, Portugal

dplopes@ff.up.pt

Helicobacter pylori (*H. pylori*) is a bacterium that colonizes human gastric mucosa [1] (Figure 1). It is associated with inflammatory processes that lead to chronic gastritis, peptic ulcers, and even gastric cancer [1]. In fact, it is considered a human carcinogenic by the World Health Organization (WHO) [2]. Nevertheless, its eradication is distant from the proposed for infectious diseases by the WHO [1]. This is a consequence of the limitations of the current treatment plan, namely, the degradation of antibiotics under acidic conditions, their low residence time in the stomach, and the incidence of side effects that affects the therapeutic compliance [1]. Even more important, the development of resistant bacterial strains significantly affects the eradication rate of this bacterium [1].

In this work, amoxicillin-loaded solid lipid nanoparticles (Figure 1) were produced by the double emulsion technique. A three-factor, three-level Box-Behnken design was used to optimize the physico-chemical properties of the nanoparticles. Spherical nanoparticles with a mean diameter of 200 nm, a surface charge of -43 mV, and a loading capacity of almost 8% were produced. The nanoparticles were stable for at least 6 months at 4°C. *In vitro* release studies showed a high resistance to harsh conditions (pH 1.6, bile salts, lecithin, and a physiological temperature) and a controlled release at pH 7.4. *In vitro* cytotoxicity studies were performed using reference (L929 fibroblasts) and gastric (MKN28) cell lines. Results showed no cytotoxicity in both cell lines for the tested concentrations. The efficacy of the formulation was evaluated by studying bacterial growth curves in the presence of different concentrations of amoxicillin-loaded nanoparticles. The results revealed a dose-dependent bactericidal effect of the loaded nanoparticles. Furthermore, placebos also had a bactericidal effect. Scanning microscopic images showed a disruption of the *H. pylori* membrane and a consequent release of the cytoplasmic content.
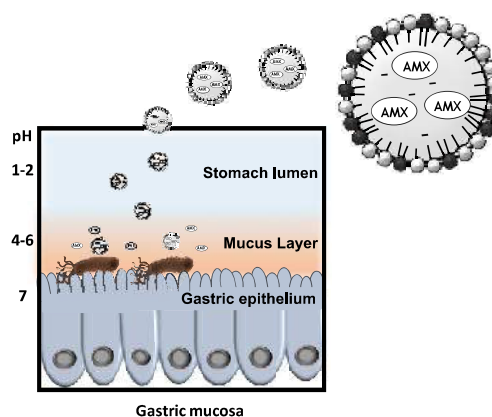
Figure 1. Amoxicillin (AMX)-loaded solid lipid nanoparticles to improve the current treatment against *H. pylori* infections.

In conclusion, the designed formulation presents suitable physico-chemical features for being used in the oral delivery of amoxicillin. The resistance of the nanoparticles under harsh conditions may avoid the degradation of amoxicillin under acidic conditions. Moreover, considering the efficacy of the placebo, multiple mutations would be required to develop resistance against these nanoparticles [3], revealing an interesting therapeutic potential. Combining these results with the *in vitro* efficacy, these nanoparticles are suitable for being ultimately used in the treatment of *H. pylori* infections.

Acknowledgements

References

[1] Lopes, D., et al, Journal of Controlled Release, 189 (2014) page 169-186.
[2] A review of human carcinogens. Part B: biological agents, IARC Working Group on the Evaluation of the carcinogenic risks to humans, Lyon, France (2009).
[3] Pelgrift, R. Y. and Friedman, A. J., Advanced Drug Delivery Reviews, 65 (2013) page 1803-1815.

Microfabrication of Gold colloids, size control, biomedical conjugation applications

Olena Madden *[1]

Mariana Alves[1]

Syed Ansar Md. Tofail[2]

Patrick G. Murray [1,]

[1] CHIMERA Research Group, Shannon ABC, Department of Applied Science, Limerick Institute of Technology, Moylish Park, Limerick, Ireland. Department of Physics, University of Limerick, Limerick, Ireland

*Olena.madden@lit.ie

This work presents a greener, environmentally benign alternative for mycosynthesis gold nanoparticles (NPs) using microbial sources. Gold nanoparticles (AgNPs) are highly valued due to their surface plasmon resonance, a unique quality which causes a charge separation on the surface of the NP. They have found importance in many areas of science and technology including biomedicine and imaging technology. This study achieved a precise tailoring of gold nanospheres down to the nano-seed level using extracellular systems of extremophilic microbes. Control of the size of AgNPs and AuNPs was achieved in a size range between 40nm and 2nm by varying physiochemical conditions of the synthesis. Novel protocol developed to encapsulate biological AuNPs cyclo RGD peptide, c(RGDfC). The peptide selectively binds to the receptors on the surface of cancer cells. Therefore, when conjugated with c(RGDfC), AuNPs can potentially be used in targeted cancer treatments.

Graphical abstract
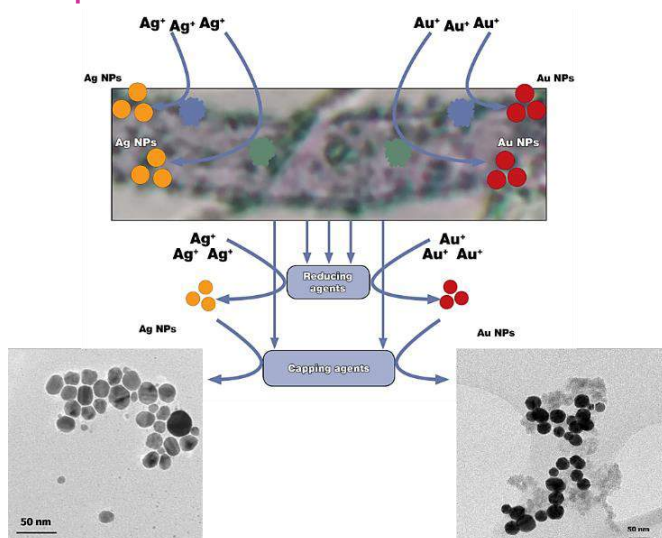
Outcomes

Traditional methods of AuNPs synthesis involve multistep physical and chemical processes that use high temperature and pressure, large amounts of energy, and toxic substances that produce pollution in the environment [1]. Greener, alternative methods of synthesis that utilise a variety of microorganisms including fungi [2] have been explored. However, due to a complexity of biological medium it is difficult to control size and size distribution and to achieve repeatable results. The major parameters that can affect the formation of monodispersed nanoproducts are: the concentrations of the precursor salt, reducing and capping agents, and the temperature of the reaction mixture [3]–[5], i.e. the parameters that determine the rate of the synthetic reaction.

This work demonstrates the precise tailoring of the sizes of gold nanospheres down to the nano-seed level using an active fungal medium.

Size control

Utilising a one-pot, green chemical method AuNPs were synthesised through the reduction of $HAuCl_4$ by a cell-free extract of a thermophilic fungus.

The increase in the ratio of fungal reducing/capping agents to $HAuCl_4$ allowed for the reduction of the AuNP' size to a nano-seed level with the size of 2nm and Standard deviation (StDev) of 0.4nm, Fig 1 (d).
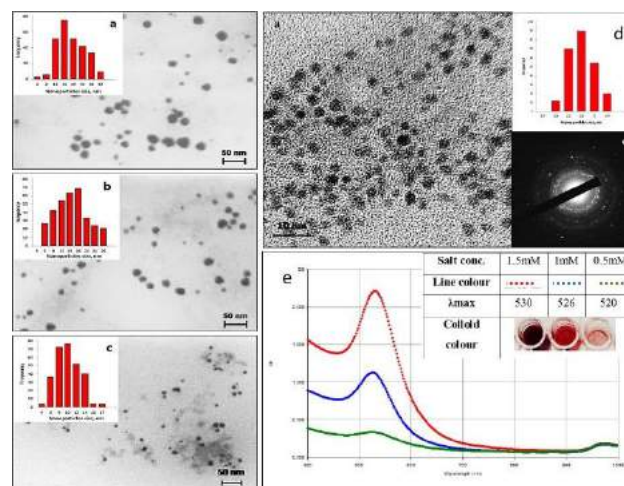
Figure 1 Decrease in size and size distribution of fungal AuNPs with the increase in the ratio of concentrations of reducing/capping molecules to $HAuCl_4$.

A reduction of an average size of the AuNPs from 37.7nm to 14.06nm and a StDev from 20.8nm to of 2.2nm was achieved through the increase in the synthetic reaction temperature, Fig 2.

The increase in temperature significantly promotes the increase of the reduction reaction rate and higher availability of the capping functional groups of fungal proteins, which unfold at high temperatures.

The findings create a potential for the synthesis of gold nanocrystals of different sizes and morphologies through directional growth from nano-seeds using a biological medium.
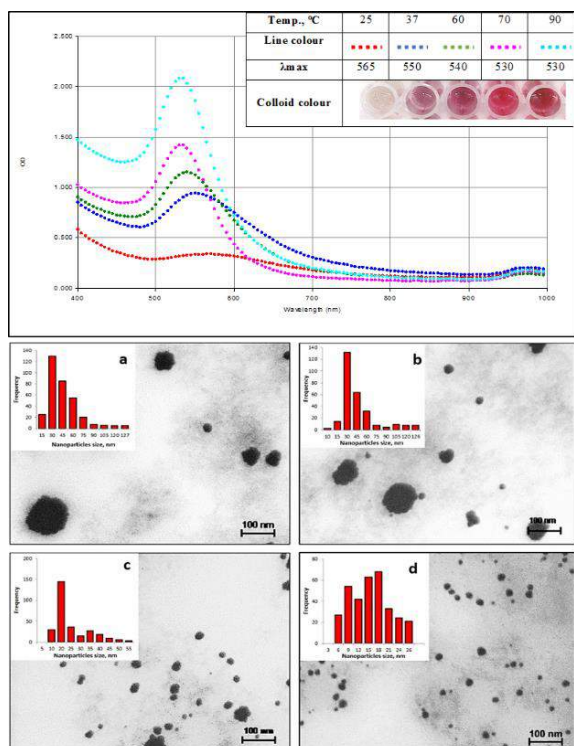
Figure 2 Decrease in AuNPs size distribution with the increase in reaction temperature.

Application

Photothermal therapy (PTT) has great potential for the destruction of cancer cells through selectively induced apoptosis [6]. Both spherical and anisotropic nanoparticles are internalised by cell receptor mediated endocytosis [7] and treated with a laser which produced selective cellular damage of cancer cells [8] For an application in PTT AuNPs are conjugated with targeting moieties to be delivered into the cancer cell and to produce the desired effect. Therefore, as one of the potential applications of AuNPs, the possibility of conjugation of AuNPs generated in this work with a cancer cell-targeting peptide was explored. As such this part of the research was conducted to probe the potential applications of mycogenerated AuNPs and to set a path for the development of novel mycogenerated gold nano-catalysts and potential anti-cancer gold colloids.

AuNPs synthesised using fungal filtrate were capped with a cyclo RGD peptide - *c*(RGDfC). The average size of *c*(RGDfC)-AuNPs produced was 31.2nm with a standard deviation of 4.5nm, Fig 3. This size is very suitable for the application in photothermal therapy as these nanoparticles are large enough not to produce a toxic effect through the generation of reactive oxygen species. At the same time fungal AuNPs-conjugates are of suitable size for endocytosis and have a λmax of 530nm which perfectly correlates with the wavelength commonly used in this application laser.

As such It was demonstrated that the size and size distribution of biologically synthesised AuNPs can be successfully controlled through the variation of physio-chemical conditions of NPs synthesis. And as a novel development these nanoparticles can be conjugated with therapeutic moieties for biomedical applications.
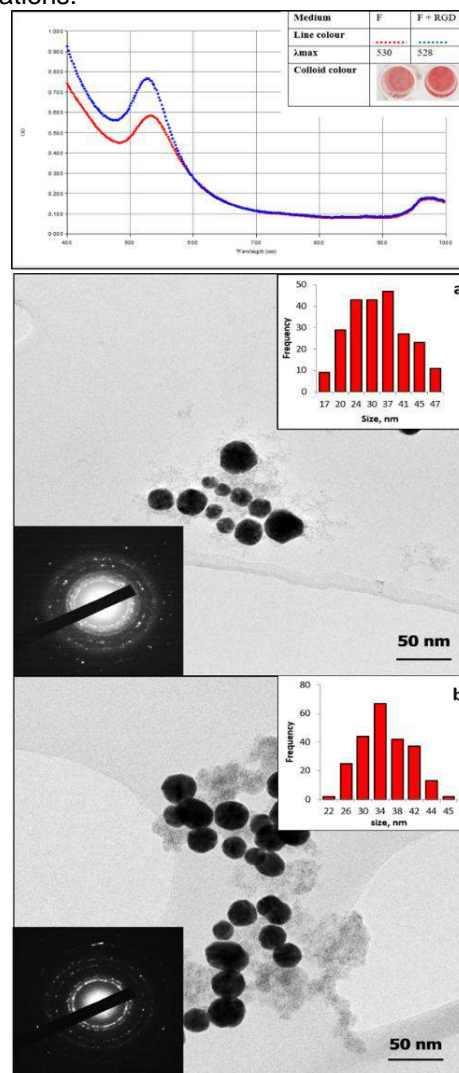
Figure 3 AuNPs(a) and AuNPs-RGD conjugates (b) and their LSPR absorption (top)

References

[1] Nguyen T.K. Thanh and Luke .W. W. Green, *Nano Today*, vol. 5, no. 3, pp. 213–230, Jun. 2010.

[2] E. Castro-Longoria, A. R. Vilchis-Nestor, and M. Avalos-Borja, *Colloids Surfaces B Biointerfaces*, vol. 83, no. 1, pp. 42–48, Mar. 2011.

[3] V. M. Rotello,

[4] C. Burda, X. Chen, R. Narayanan, and M. A. El-Sayed, *Chem. Rev.*, vol. 105, no. 4, pp. 1025–1102, Apr. 2005.

[5] A. Wei, V. Rotello, Ed. on-line: Springer US, 2004, pp. 173–200.

[6] F. K. Storm, W. H. Harrison, R. S. Elliott, and D. L. Morton, pp. 2245–2251, 1979.

[7] J. Shao *et al.*, "Photothermal nanodrugs: potential of TNF-gold nanospheres for cancer theranostics." *Sci. Rep.*, vol. 3, p. 1293, Jan. 2013.

[8] X. Huang *et al.*, *J. Biomed. Opt.*, vol. 15, no. 5, p. 58002, 2010.

Rifampicin-loaded lipid nanoparticles to improve tuberculosis treatment: an active targeting approach

Joana Magalhães[1,2,4],
Alexandre C. Vieira[1], Sónia Rocha[3], Marcos S. Cardoso[3], Susana G. Santos[4], Margarida Borges[3], Marina Pinheiro[1], Salette Reis[1]

[1]LAQV, REQUIMTE, Departamento de Ciências Químicas, Faculdade de Farmácia, Universidade do Porto, Porto, Portugal.
[2]ICBAS, Instituto de Ciências Biomédicas Abel Salazar, Universidade do Porto, Porto, Portugal.
[3]UCIBIO, REQUIMTE, Departamento de Ciências Biológicas, Faculdade de Farmácia, Universidade do Porto, Porto, Portugal.
[4]i3S - Instituto de Investigação e Inovação em Saúde, INEB - Instituto de Engenharia Biomédica, Universidade do Porto, Porto, Portugal.

joanamagalhaesbio@gmail.com

Tuberculosis is a major global health problem of overwhelming proportions [1]. The current treatment is associated with several adverse-effects and noncompliance to therapy [2]. The development of nanodelivery systems represents an interesting alternative for the delivery of anti-tuberculosis drugs to the target site of infection, as an attempt to reduce the required dose, to minimize the side effects, and to enhance patients' compliance [3]. Thus, this work aims to develop a mannosylated nanostructured lipid carrier (NLC) loaded with rifampicin, to improve tuberculosis treatment. An active targeting strategy was used and the nanoparticles were characterized in terms of size, polydispersity, zeta potential, surface morphology, encapsulation efficiency, and *in vitro* drug release. Effects on cell viability were tested using primary mouse bone marrow-derived macrophages (BMDM), and the anti-mycobacteria activity of the nanoformulations was evaluated using *Mycobacterium avium*-infected BMDM. The nanoparticles developed exhibited a size of about 315 nm, and polydispersity below 0.2. The drug encapsulation efficiency was higher than 90%, and its release was sensitive to pH. The mannosylated NLCs showed efficient uptake by BMDM. Further, rifampicin-loaded mannosylated NLCs were more efficient in inducing a decrease of intracellular growth of mycobacteria. The overall results support that mannosylated NLCs constitute a promising strategy for the delivery of rifampicin selectively to macrophages. Moreover, although *in vivo* studies are required to validate the clinical potential of these nanoparticles, the results obtained are a promising proof-of concept, and demonstrate, albeit *in vitro*, the applicability of the nanoformulations developed.

This may ultimately open up new avenues in the fight against the world's deadliest infectious disease.

References

[1] WHO, Global tuberculosis report 2016. WHO Library Cataloguing-in-Publication Data, ISBN 978 92 4 156539 4 (2016).
[2] Zumla A., et al., Tuberculosis treatment and management - an update on treatment regimens, trials, new drugs, and adjunct therapies. The Lancet Respiratory Medicine, 3 (2015) 220-234.
[3] Vieira A.C., et al., Targeted Macrophages delivery of Rifampicin-loaded Lipid Nanoparticles to improve Tuberculosis treatment. Nanomedicine (2017) *in press*.

Figure
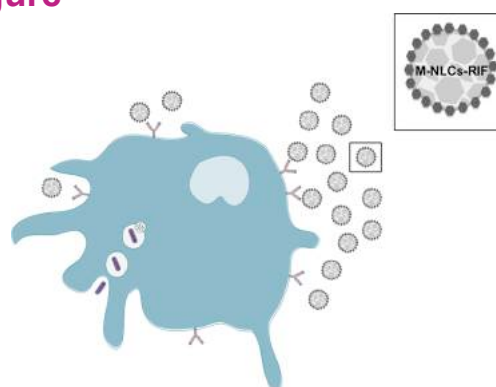
Figure 1. Schematic representation of the active targeting approach used in the present study. Mannosylated nanostructured lipid carriers loaded with rifampicin (M-NLCs-RIF) were developed to target macrophages, the main site of tuberculosis infection.

In vitro toxicity of Polyethylene terephthalate nanoparticles in a Caco-2 model of intestinal barrier

Davdie Magrì[1,2],
Paola Sánchez-Moreno[3], Gianvito Caputo[2],
Athanassia Athanassiou[2], Pierpaolo Pompa[3],
Despina Fragouli[2]

[1] DIBRIS, University of Genova, Via Balbi, 5 - 16145 Genova, Italy
[2] Smart Materials, Istituto Italiano di Tecnologia, Via Morego, 30 - 16163 Genova, Italy
[3] Nanobiointeractions & Nanodiagnostics, Istituto Italiano di Tecnologia, Via Morego, 30 - 16163 Genova, Italy

davide.magri@iit.it

Plastic debris in the environment is increasing in line with the plastic production. The last studies estimate more than 250 MT of plastic floating in the oceans [1,2]. The phenomena related to the breakdown and degradation of the plastic debris in small pieces (micro- and nanoplastics) is principally linked to four main factors: the temperature, the UV radiation, the surrounding media (that enhance the break down into smaller pieces), and the fouling processes [1]. Micro- and nanoplastics may impact the basis of the food chain causing damage to the entire trophic chain, including humans. In fact as already known plastic particles are ingested by a large number of aquatic organisms [3,4]. The potential toxicity of these nanomaterials needs to be characterized. We investigate the impact of polyethylene terephthalate (PET) nanoparticles (NPs) on model of the intestinal barrier obtained using Caco-2 cells. PET is a widespread type of plastic (56 million tons produced in 2013) used for packaging foods and beverages, which accumulate in the ecosystem [5]. Protein Corona complex formation was studied to understand the NPs behaviour in biological media and the stabilizing effect of soft corona proteins was observed. Through confocal microscopy we have evaluated the uptake of PET NPs marked with a fluorescent tag, both in isolated Caco-2 cells and in the intestinal barrier in vitro model (Figure 1). Following NANoREG SOP (Standard Operating Procedure for evaluation of NPs impact on Caco2 cell barrier model) method we analysed the impact of PET NPs on the functionality and on the integrity of the barrier in dependence on the concentration of the NPs and time of exposure. From our cellular studies, it emerged that the PET NPs do not have a decisive effect on the cell viability and membrane integrity, and despite a lack of acute response of Caco-2 barrier, a chronic response is underlined by the variation in TEER (Trans-epithelial Electrical resistance) value and by the increase of the barrier permeability. The results of this work enrich the basic knowledge of this novel class of pollutants and helps to understand their interactions with living organisms.

References

[1] Andrady A.L., Marine pollution bulletin, 62(8) (2011) 1596-1605

[2] Law K.L., Morét-Ferguson S., Maximenko N.A., Proskurowski G., Peacock E.E., Hafner J., Reddy C.M., Science, 329(5996) (2010) 1185-1188

[3] Besseling E., Foekema E.M., Van Franeker J.A., Leopold, M.F., Kuhn S., Rebolledo E.L.B., Heße E., Mielke L., IJzer J., Kamminga P., Koelmans A.A., Marine pollution bulletin, 95 (2015) 248-252

[4] Paul-Pont I., Lacroix C., González Fernández C., Hégaret H., Lambert C., Le Goïc N., Frere L., Cassone A.L., Sussarellu R., Fabioux C., Guyomarch J., Albentosa M, Huvet A, Soudant P., Environmental Pollution, 216 (2016) 724-737

[5] Neufeld L., Stassen F., Sheppard R., Gilman T., World Economic Forum, (2016)

Figures
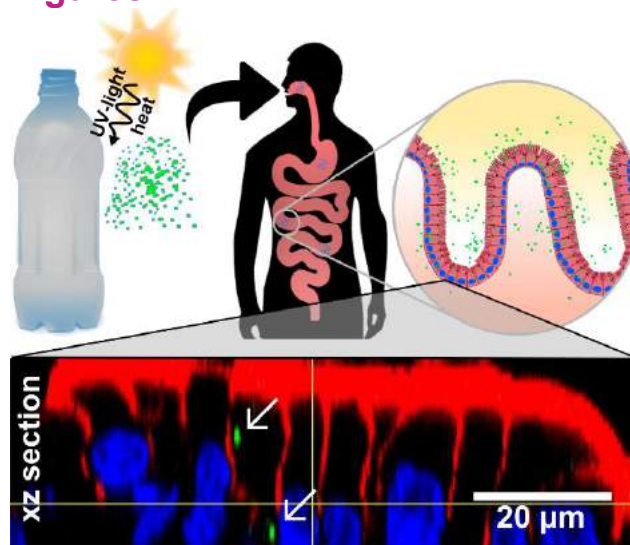
Figure 1. Schematic representation of the PET NPs uptake by human; below xz confocal section of a Caco2 intestinal barrier which internalized PET NPs. Cell nuclei (Hoechst) in blue, actin (Phalloidin) in red and NPs (Fluoresceinamine) are shown green.

Poly(ε-caprolactone) nanoparticles loading doxorubicin: effect in lung cancer

Consolación Melguizo[1,2,3]
Laura Cabeza[1,2,3], Raul Ortiz[1,4], Julia Jiménez-Lopez[1,2,3], Gloria Perazzoli[1,2], Octavio Caba[1,4], Ana R. Rama[1,4], Celia Velez[1,2,3], Maria Carmen Leiva[1,2,3], Jose Carlos Prados[1,2,3], Ángel V. Delgado[5], José L. Arias[1,2,6]

[1]Institute of Biopathology and Regenerative Medicine (IBIMER), Biomedical Research Center (CIBM), Granada University, Av. del Conocimiento, s/n, 18100, Granada, Spain
[2]Biosanitary Institute of Granada (ibs.GRANADA), SAS-Universidad de Granada, Granada, Spain
[3]Department of Anatomy and Embryology, Faculty of Medicine, University of Granada. 18071, Granada, Spain
[4]Department of Health Science, University of Jaén, 23071 Jaén, Spain
[5]Department of Applied Physics, University of Granada, 18071, Granada, Spain
[6]Department of Pharmacy and Pharmaceutical Technology, University of Granada, 18071 Granada, Spain.

melguizo@ugr.es)

Nanotechnology has provided new strategies in biomedicine for the treatment of certain pahologies such as cancer by the development of nanoformulations that transport antitumor drugs improving their solubility, specificity, half-life in blood stream and reducing their toxicity [1]. The tumor pathology more common diagnosed and the main cause of death worldwide for this disease is lung cancer. One of the drug used to treat it is Doxorubicin (DOX) alone or in combination with other drugs. This drug has a good antitumor activity. However, its low specificity for tumor tissues makes it toxic for non-tumor tissues causing severe side effects, especially cardiac toxicity [2]. Our study is based in the development of DOX-loaded poly (ε-caprolactone) (DOX-PCL) nanoparticles (NPs) (Figure 1) that were tested in in vitro and in vivo lung cancer models [3]. For the in vitro model we used human and mouse lung cancer cell lines A549 and LL/2. For the in vivo model immunocompetent C57BL/6 mice were subcutaneously inoculated with LL/2 cell line. Our results showed no toxicity of blank PCL NPs in general in any cell line thus demonstrating its biosafety and biocompatibility. Otherwise, DOX-PCL NPs increased cell death reducing the half-inhibitory concentration (IC50) compared to free drug up to 56.3% and 63.6% in A549 and LL/2 respectively. Nanoformulations showed an intense internalization in tumoral cells in comparison to free drug. (Fig. 1). Furthermore, in vivo assays demonstrated better antitumor activity and survival (Fig. 2) and also a reduction of cardiac toxicity in mice treated with DOX-PCL NPs. These results suggest that PCL NPs are a safe and efficient nanoformulation to improve the treatment of lung cancer.

References

[1] Wang AZ, Langer R, Farokhzad OC. Annu Rev Med. (2012) 185–188.

[2] Angsutararux P, Luanpitpong S, Issaragrisil S. Oxid. Med. Cell. Longev, (2015) 795602.

[3] Cabeza L, Ortiz R, Prados J, Delgado ÁV, Martín-Villena MJ, Clares B, Perazzoli G, Entrena JM, Melguizo C, Arias JL. Eur J Pharm Sci. (2017) 24-34.
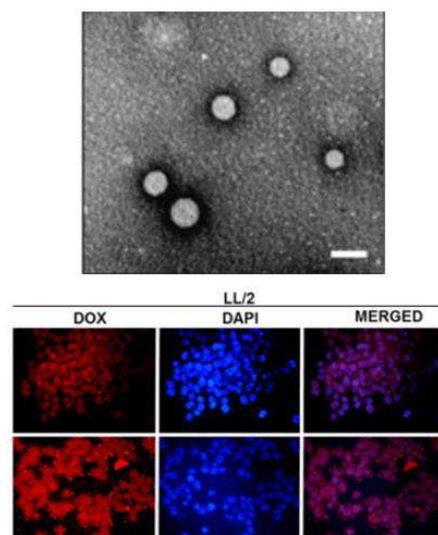
Figures

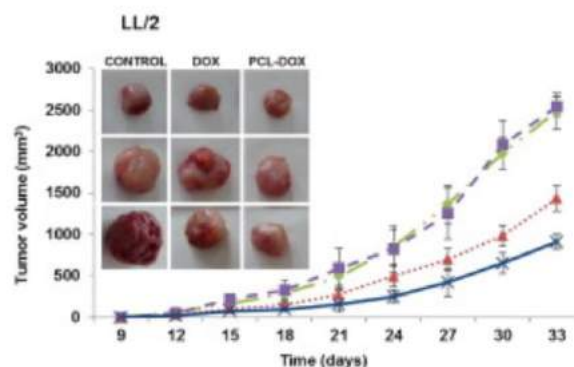**Figure 1.** DOX-loaded poly (ε-caprolactone) (DOX-PCL) NPs. Internalization studies in LL2 cell line.

Figure 2. Evolution along time of tumor volume of mice.

miRNA sensing for disease monitoring.

Salvador Mena Mollá[1],

[1]Department of Physiology. Faculty of Pharmacy. University of Valencia. Valencia.(Spain).

Salvador.mena@uv.es

Cancer progression (proliferation and metastasis) and treatment resistance are a dynamic process due to molecular changes that progress over time. Among these changes are genetic mutations, but also epigenetic changes (chromatin compaction, DNA methylation, histone modifications or change in non-coding RNAs such as miRNAs) that confer characteristics necessary for invasion and aggressiveness.

Therefore, one of the great challenges in clinical practice is the early diagnosis and precision medicine, which allows the application of more individualized treatments leading a higher success rate, better quality of life for the patient and a lower cost for the health system. For this, it is necessary to invest in the identification of biomarkers, but also in the design of new biosensors to detect these biomarkers with a high sensitivity, specificity and low cost-effectiveness.

MicroRNAs (miRNAs) are a family of small (20-22 nucleotides) non-coding RNAs that regulate gene expression by binding to the 3 'region of mRNAs. Each miRNA has distinct target mRNAs and each mRNA has binding sites for distinct miRNAs, so there is a miRNA integration in the regulation of expression. In addition, they are stable, easy to detect and are present in biofluids such as plasma, urine or saliva, so they can be obtained by non-invasive techniques. In this way the miRNAs are ideal candidates to be used as diagnostic biomarkers and prognoses and also as potential therapeutic targets [1].

There are different studies that have found an aberrant profile of miRNAs in pathologies such as cardiovascular or inflammatory disease and in cancer [2].

Regarding the quantification of miRNAs in vitro, it is possible to indicate that currently the most widespread quantification methods are based on sequencing methods, Northern or microarraying, but possibly the most widespread is the PCR, mainly by TaqMan probes or Exiqon technology, which require a retrotranscription pre-stage and a subsequent step of amplification and detection [3], so are time-consuming and laborious.

Molecular Beacon (MB) are specific hairpin-shaped probes containing at the 5 'end a fluorochrome and a 3' molecule that inhibits fluorescence (quencher). The ends of this sequence have 5-7 nucleotides complementary to each other, allowing it to adopt a hairpin structure. Between these extremes there is a sequence specific and complementary to the target to be detected, in this case the 22 nucleotides of the miRNA of interest. Thus, when the miRNA is not present, the MB is in the form of a hairpin, with its proximal ends preventing the emission of the signal. In the presence of the miRNA, it hybridizes to the central sequence of the MB, which acquires an open arrangement, thereby removing the quencher from the fluorochrome allowing the emission of fluorescence [4].

Herein, we have demonstrated that miRNAs can be detected directly using a MB. MiRNA-205 has been detected successfully by molecular beacons in a quantitative and enzyme-free manner. The method developed in this work is simple, fast, and sensitive, so it will offer great opportunities for the high-throughput diagnosis and prognosis of diseases.

References

[1] García-Giménez JL, Sanchis-Gomar F, Lippi G, Mena S, Ivars D, Gomez-Cabrera MC, Viña J, Pallardó FV, Clin Chim Acta. 413 (2012) 1576-82.

[2] Zeng MS, Adv Exp Med Biol. 927 (2016) 391-427.

[3] Egatz-Gomez A, Wang A, Klacsmann F, Pan Z, Marczak S, Wang Y, Sun G, Senapati S, Chang HC, Biomicrofluidics, 10 (2016) 032902.

[4] Lee JH, Kim JA, Jeong S, Rhee WJ, Biosens Bioelectron. 86 (2016) 202-210.

Figures
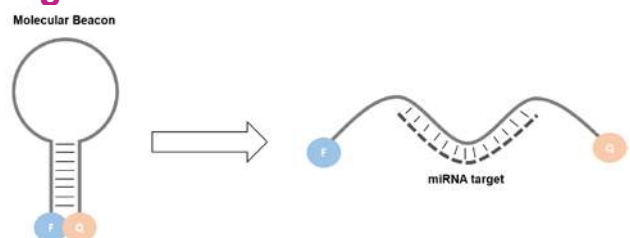
Figure 1. Closed conformation of the MB in the absence of the target miRNA maintains the fluorophore near the quencher, so it does not emit fluorescence. Open conformation in the presence of the target, the fluorophore is kept away from the Quencher and emits fluorescence.

3D Bioprinting of Skeletal Muscle Tissue for the Development of Soft Bio-Robotic Systems

Rafael Mestre[1,2],
Tania Patino[1,2], Ariadna Pérez-Jiménez[1],
Samuel Sánchez[1-3]

[1] Institute for Bioengineering of Catalonia (IBEC), The Barcelona Institute of Science and Technology, Baldiri Reixac 10-12, 08028 Barcelona Spain
[2] Max Planck Institute for Intelligent Systems Institution, Stuttgart, Germany
[3] Institució Catalana de Recerca i Estudis Avancats (ICREA), Barcelona, Spain

rmestre@ibecbarcelona.eu, tpatino@ibecbarcelona.eu
ssanchez@ibecbarcelona.eu

Many recent advances in nanomaterial science have opened up the possibility of combining biological entities with artificial materials to obtain hybrid bio-robotic devices capable of performing different tasks[1]. At the nanoscale, integrating enzymes with nanoparticles is of special interests in nanomedicine and water remediation and, at the microscale, self-motile cells like bacteria can be used to propel microtubes or microparticles. But, how much further can we go?[2]

Several examples in the literature have used cardiac or skeletal muscle cells, in the form of micro-tissues, to develop hybrid bio-actuators that can perform simple movements or actuations[3,4]. These bio-actuators could, in the future, take advantage of naturally-appearing actuators and boost the performance of current soft robotic systems in terms of bio-compatibility, energy efficiency, adaptability, self-healing, damage tolerance or bio-sensing capabilities.

Here, I will present the recent advances in our lab in the development of hybrid bio-actuators[5]. We have used the 3D bioprinting technique to obtain 3D skeletal muscle whose contractions can be completely controlled *via* electrical stimulation. We proved the high controllability of our bio-actuators by both calcium imaging and bright-field tracking during electrical stimulation. These results can be of high relevance not only in the field of bio-robotics, but also in tissue engineering, regenerative medicine and drug testing.

References

[1] Patino, T., Mestre, R. and Sanchez, S. (2016) 'Miniaturized soft bio-hybrid robotics: a step forward into healthcare applications', Lab Chip. Royal Society of Chemistry, 16(19), pp. 3626–3630.

[2] Duffy, R. M. and Feinberg, A. W. (2014) 'Engineered skeletal muscle tissue for soft robotics: Fabrication strategies, current applications, and future challenges', Wiley Interdisciplinary Reviews: Nanomedicine and Nanobiotechnology, 6(2), pp. 178–195.

[3] Park, S. J. et al. (2016) 'Phototactic guidance of a tissue-engineered soft-robotic ray', Science (New York, N.Y.), 353(6295), pp. 158–162.

[4] Raman, R. et al. (2016) 'Optogenetic skeletal muscle-powered adaptive biological machines', Proceedings of the National Academy of Sciences of the United States of America, 113(13), pp. 3497–3502.

[5] Patino, T., Mestre, R., Pérez-Jiménez, A. and Sanchez, S. (2017) '3D Bioprinting of Biological Actuators Based on Skeletal Muscle with Controllable Shape and Contractility'. Submitted.

Figures
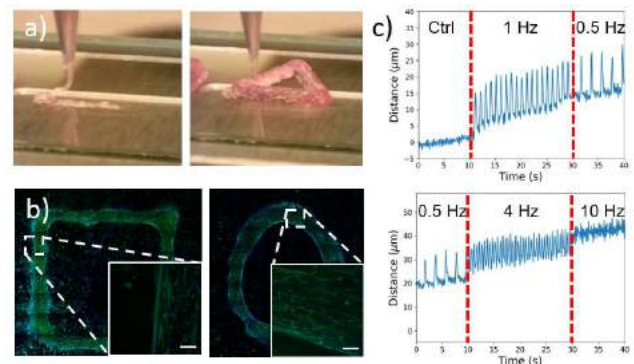
Figure 1. a) Snapshots of a 3D bioprinting process of skeletal muscle tissue. b) Immunostaining of cell nuclei and Myosin Heavy Chain II, where aligned myotubes can be seen. c) Contractions of stimulated skeletal muscle tissue at different frequencies.

Confinement of biomolecules to enhance the efficacy of enzyme-powdered micro/nanomotors

Nerea Murillo-Cremaes[1],
Samuel Sánchez[1,2,3]

[1] Institute for Bioengineering of Catalonia (IBEC), The Barcelona Institute of Science and Technology, Baldiri i Reixac 10-12, Barcelona 08028 (Spain).
[2] Institució Catalana de Estudis Avançats (ICREA), Pg. Lluís Companys 23, Barcelona 0810 (Spain).
[3] Max Planck Institute for Intelligent Systems, Heisenbergstraße 3, Stuttgart 70569 (Spain).

nmurillo@ibecbarcelona.eu

Since the last decade, the engineering of chemically-driven synthetic micro/nanomotors capable of autonomous motion has been attracting much attention. Researchers from different fields have focused on the development of these machines due to their enormous potential applications, such as in nanomedicine.[1] One of the major challenges when designing active systems for biomedicine relies on the use of nontoxic and biocompatible driving forces. Catalytic reactions triggered by enzymes are good candidates to perform the required transformation of chemical energy into mechanical energy upon the presence of the appropriate substrates (fuels).[2] However, the stability and long-term activity of the enzymes is strongly affected by the interactions with the surrounding media. This is specially challenging when enzyme-powdered micro/nanomotors are aimed to address biological tasks at body fluids. It is then crucial to protect these biocatalysts in compartmentalized spaces to maintain their functions in body fluids.[3], [4]

Mesoporous silica particles (MSPs) have emerged as promising materials for the construction of smart devices with biomedical relevance, especially as drug vehicles owing to the advantages that they present over the traditional drug nanocarriers. In regards of biomedical applications, MSPs show unique properties as size and shape control, easy surface chemistry, high loading capacity, biocompatibility and nontoxicity.[5] Moreover, silica provides remarkable chemical and thermal stability when used host material for biomolecules, such as enzymes.

Our strategy is based on the fabrication of microsized hollow MSPs that are functionalized at the inner surface to covalently bind enzymes. In addition to the internal hollow structure, such micromotors present a cavity at the surface that allows both the diffusion of the substrates and the product release for the enzymatic reactions. Since the source of kinetic energy is confined in silica protective capsules, the proposed system might facilitate the particles self-propulsion even in biological fluids. The possibility of using a vast library of enzymes and the easy size tunability of the particles confers remarkable versatility to the motors.

References

[1] X. Ma, A. Jannasch, U.-R. Albrecht, K. Hahn, A. Miguel-López, E. Schäffer, S. Sánchez, Nano Letters, 15 (2015) 7043.

[2] X. Ma, A. C. Hortelão, T. Patiño, S. Sánchez, ACS Nano, 10 (2016) 9111.

[3] M. Nijemeisland, L. K. E. A. Abdelmohsen, W. T. S. Huck, D. A. Wilson, J. C. M. van Hest, ACS Central Science, 2 (2016) 843.

[4] A. Joseph, C. Contini, D. Cecchin, S. Nyberg, L. Ruíz-Perez, J. Gaitzsch, G. Fullstone, X. Tian, J. Azizi, J. Preston, G. Volpe, G. Battaglia, Science Advances, 3 (2017) e1700362..

[5] A. Baeza, D. Ruíz-Molina, M. Vallet-Regí, Expert Opinion on Drug Delivery, 14 (2017) 783.

Leflunomide delivery for Rheumatoid arthritis therapy by folic acid-enhanced PEG-coated magnetic nanoparticles

Ionela Andreea Neacșu[1*],
Patricia Medeșan[2], Florin Iordache[3], Vladimir Ene[1],
Ecaterina Andronescu[1], Anton Ficai[1]

[1] University Politehnica of Bucharest, Faculty of Applied Chemistry and Materials Science, 1-7 Gheorghe Polizu Street, Bucharest, Romania
[2] University Politehnica of Bucharest, Faculty of Medical Engineering, 1-7 Gheorghe Polizu Street, Bucharest, Romania
[3] Institute of Cellular Biology and Pathology of Romanian Academy, "Nicolae Simionescu", Department of Fetal and Adult Stem Cell Therapy, 8, B.P. Hasdeu, 050568 Bucharest, Romania

*neacsu.a.ionela@gmail.com

Nano-sized biomaterials provide a number of benefits that have contributed to the development of the biomedical domain. They have chemical and structural similarity to biological tissues and systems, the comparable size of nanobiomaterials with biomolecules and biomicrostructures provides researchers with the ability to detect, manipulate and mediate these biocomponents and, last but not least, nanostructured materials can be easily adapted to reveal significant variations in surface properties [1].

"Zero-dimensional" nanomaterials [2] are specially formulated to absorb, adsorb or encapsulate an active substance, thus protecting it from potential degradation by either chemical or enzymatic processes. They can be used as adjuvants in vaccines or drug transporters, at which the active compound is dissolved, encapsulated, adsorbed or chemically attached [3]. The main purpose in designing nanoparticles as controlled release systems is to release specifically pharmacologically active agents at optimal rates and doses.

Magnetic iron oxides have been extensively exploited by researchers over centuries, an eloquent example being the use of iron oxide nanoparticles both as contrast agents for in vitro diagnosis and as a support for drug delivery. Eight types of iron oxide are known, among which the most promising and popular candidates are hematite (α-Fe_2O_3), magnetite (Fe_3O_4) and maghemite (γ-Fe_2O_3) as a result of polymorphism involving phase transitions under the influence of temperature. Each of these iron oxides exhibits a number of unique biochemical, magnetic and catalytic characteristics, as well as

properties that provide them with many advantages in technical and biomedical applications [58].

Synthetic magnetic particles, obtained through various synthesis routes, may have large differences in their magnetic properties. These differences are attributed to structural changes, the creation of antiphase boundaries, or the existence of a residual magnetic layer at the surface of particles. The disadvantage of synthesis methods in aqueous solutions is that the pH of the reaction must be adjusted during both the synthesis process and the purification process. The tendency of these nanoparticles to form aggregates and increase in size to minimize total free surface energy represents a critical and difficult to combat [66, 67]. Since particles are attracted magnetically, besides agglomeration due to the Van de Waals forces, alteration of the surface is often indispensable. Various surfactants, such as sodium oleate, dodecylamine, sodium carboxymethyl cellulose or PEG, are commonly used to improve the dispersibility of nanoparticles in aqueous media.

Leflunomide is one of the approved disease-modifying anti-rheumatic drugs and has been widely used for the treatment of rheumatoid arthritis over the past decade. It acts rather as an immunomodulating agent, rather than as an immunosuppressive one. It inhibits dihydroorotate dehydrogenase (an enzyme involved in pyrimidine synthesis) and shows antiproliferative activity. Numerous experimental models in vitro and in vivo have demonstrated an anti-inflammatory, analgesic and antipyretic effect of this active substance, used in rheumatoid arthritis therapy [5].

Folic acid and its derivatives are of great interest in biology and medicine due to the coenzyme functions performed in the body in a series of vital reactions. Rheumatoid arthritis therapy, even if it is used to reduce inflation and joint damage, brings about numerous undesirable systemic effects, which implicitly add to the risk of adverse effects. Improved disease control measures, as well as the use of targeted therapies involving only the affected tissue, are therefore needed [6]. Selective neutralization of synovial macrophage activation is an attractive approach to diminishing local and systemic inflammation as well as preventing irreversible joint damage.

Synthesis is made following a co-precipitation method, where over an NH_3 solution, a mixture of Fe^{2+}, Fe^{3+} and lefluonimide is added drop wise and under continuous stirring. After the precipitate is formed, it is washed with pure water and the nanoparticles (Fe_3O_4@LEF) are dried at 40°C for 48 h. After dispersing the nanoparticles into ultrapure water, a solution of PEG 8000 is added drop wise into the dispersion. The nanosystem (Fe_3O_4@LEF@PEG) is washed and dried. The stabilized nanoparticles are then again dispersed

into ultrapure water where a folic acid solution is added. The complex nanosystem (Fe$_3$O$_4$@LEF@PEG@FA) is washed and dried at 40°C for 48 hours.

The obtained system was structurally and morphologically characterized by several techniques including XRD (Figure 1), SEM, TEM (HRTEM, SAED, EDS) FTIR (Figure 2), release profile of LEF by UV-Vis and also, the evaluation of in vitro biocompatibility was assesed.
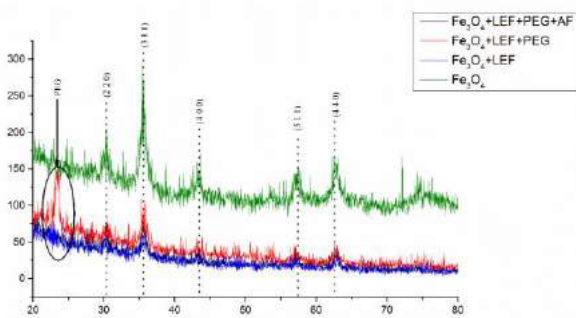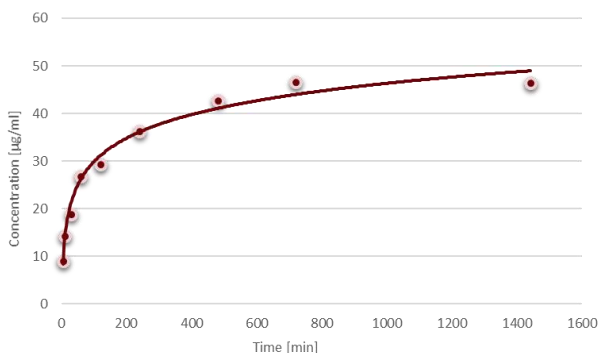
Figures

Figure 1. X-ray diffraction in each stage of the complex system
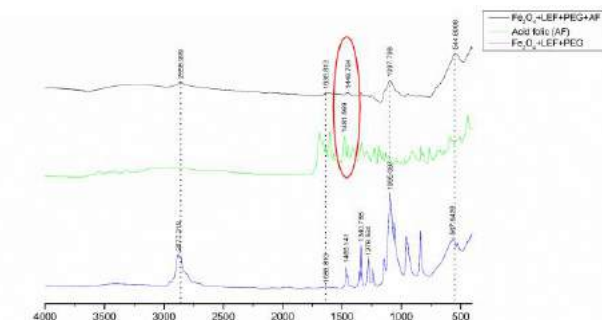
Figure 2. FT-IR spectroscopy in each stage of the complex system

Figure 3. Release profile of LEF by UV-VIS spectroscopy

References

[1] L. Yang, L. Zhang, and T. J. Webster, *Adv. Eng. Mater.*, vol. 13, no. 6 (2011), pages 197–217.

[2] S. Singh, V. K. Pandey, R. P. Tewari, and V. Agarwal, *Indian J. Sci. Technol.*, vol. 4, no. 3 (2011), pages 177–180.

[3] M. E. Davis, Z. (Georgia) Chen, and D. M. Shin, *Nat. Rev. Drug Discov.*, vol. 7, no. 9 (2008), pages 771–782.

[4] M. L. Herrmann, R. Schleyerbach, and B. J. Kirschbaum, *Immunopharmacology*, vol. 47, no. 2–3 (2000), pages 273–289.

[5] C. Marchetti *et al.*, *Onco. Targets. Ther.*, vol. 7 (2014), page 1223.

Extracellular vesicles derived from *Plasmodium*-infected red blood cells: Characterization and drug encapsulation studies

Livia Neves Borgheti-Cardoso[1,2],
Xavier Fernàndez-Busquets[1,2,3]

[1]Nanomalaria Group, Institute for Bioengineering of Catalonia (IBEC), Carrer de Baldiri Reixac, 10-12, Barcelona, Spain
[2]Barcelona Institute for Global Health (ISGlobal), Carrer del Rosselló 149-153, Barcelona, Spain
[3]Nanoscience and Nanotechnology Institute (IN2UB, Universitat de Barcelona), Avd Joan XXIII S/N, Barcelona, Spain

lborgheti@ibecbarcelona.eu

Malaria is one of the main global health concerns: according to the World Health Organization, in 2015 there were 212 million new cases of malaria and 429,000 deaths related to this disease. Malaria is a blood infection by protists of the genus *Plasmodium* transmitted by female *Anopheles* mosquito bites. The parasite has an asexual cycle in the human and a sexual cycle in the mosquito. The rapid multiplication of parasites in red blood cells (RBCs) elicits the clinical manifestations of malaria (fever, chills, prostration and anemia, and, in severe infection, metabolic acidosis, cerebral malaria, multi-organ failure, coma and death) [1]. The treatment of malaria is difficult because of the complex life cycle of *Plasmodium*, the adverse physical environment for drug administration to RBCs and the short half-lives of most antimalarials. To overcome these barriers, several drugs and regimes of administration have been used for more than one-hundred years, but they have consistently failed because of resistance evolution caused mainly by the exposure of the parasite to low amounts [2]. On the other hand, the use of high doses to avoid low local concentrations frequently leads to toxic side effects. The proposition of targeted drug delivery systems is a promising strategy to overcome these problems and advance towards effective treatments. Extracellular vesicles (EVs) have emerged as an interesting targeted drug delivery system because they may provide advantages over other methods such as greater stability in the blood, efficient cargo delivery into the cytosol of the target cell and, possibly, fewer off-target effects. EVs are lipid bilayer-bounded vesicles released by cells into the extracellular space and are involved in cell-to-cell communication [3]. EVs derived from *Plasmodium*-infected RBCs (pRBCs) can contribute to the general inflammatory condition in malaria, are related to the control of balance between virulence and transmission and can spread drug resistance throughout the parasite population. In addition, pRBCs are able to internalize EVs and incorporate their contents into the parasite cytosol [4]. Based on these concepts, we are proposing EVs derived from pRBCs as a targeted drug delivery system for the treatment of malaria. EVs were isolated by differential centrifugation, filtration and density fractionation in a 60% sucrose cushion [5]. Purified EVs were evaluated by dynamic light scattering, cryogenic transmission electron microscopy (cryo-TEM) and flow cytometry. Preliminary studies were performed to evaluate drug encapsulation of the antimalarial compound chloroquine. EVs exhibited a size around 200 nm (Figure 1) and vesicular shape (Figure 2). Flow cytometry data were obtained using an antibody-binding assay to analyze the presence of molecular EV markers. EVs derived from pRBCs have been found to contain glycophorin A and histidine rich protein-2 (HRP2); glycophorin A is an abundant membrane protein present in all RBCs and HRP2 is expressed during most of the *Plasmodium falciparum* life cycle. These characterization results strongly indicate that the purified vesicles were released from malaria-infected RBCs. Drug encapsulation was evaluated by two methods: (1) incubation for 2 h at 37 °C and (2) active encapsulation protocol using a pH gradient [6]. Only the second approach succeeded, resulting in a 15% encapsulation of chloroquine. Further studies evaluating different encapsulation strategies will be performed and the active encapsulation method will be optimized. In addition, other antimalarial drugs will be encapsulated in purified EVs and antimalarial *in vitro* activity will be evaluated.

References

[1] Aditya, N.P. *et al*. Advances in Colloid and Interface Science, 201-202 (2013) 1-17.

[2] Fernandez-Busquets, X. Expert Opinion on Drug Delivery, 5247 (2016) 1-4.

[3] Kooijmans, S.A.A. *et al*. International Journal of Nanomedicine, 7 (2012) 1525-1541.

[4] Mantel, P-Y *et al*. Cellular Microbiology, 3 (2014) 344-354.

[5] Mantel, P-Y *et al*. Cell Host and Microbe, 5 (2013) 521-534.

[6] Mole, E. *et al*. Journal of Controlled Release, 210 (2015) 217-229.

Figures
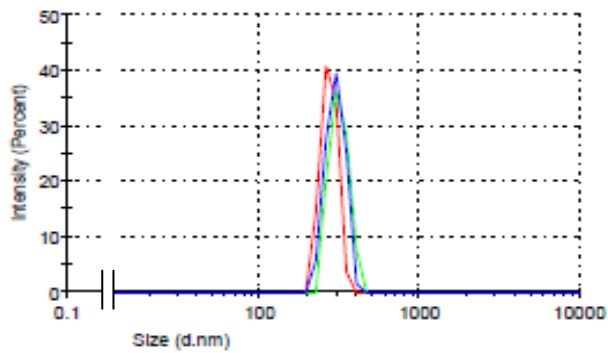
Figure 1. Dynamic light scattering analysis of extracellular vesicles derived from *Plasmodium*-infected RBCs.
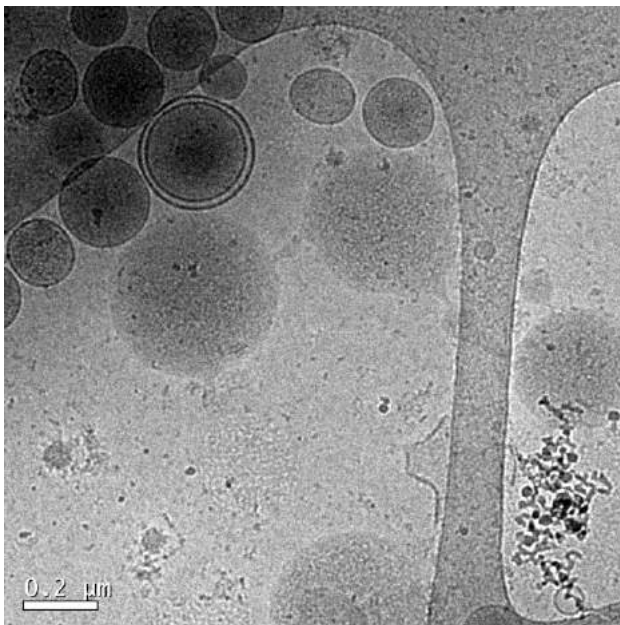
Figure 2. Cryogenic transmission electron microscopy (cryo-TEM) images of extracellular vesicles derived from *Plasmodium*-infected RBCs.

Folic acid-enhanced polyethylene glycol-coated Fe$_3$O$_4$ for Methotrexate delivery

Adrian-Ionuț Nicoară[1],
Patricia Medeșan[2], Ionela Andreea Neacșu[1*],
Bogdan Vasile[1], Florin Iordache[3], Ecaterina Andronescu[1], Anton Ficai[1]

[1]University Politehnica of Bucharest, Faculty of Applied Chemistry and Materials Science, 1-7 Gheorghe Polizu Street, Bucharest, Romania
[2]University Politehnica of Bucharest, Faculty of Medical Engineering, 1-7 Gheorghe Polizu Street, Bucharest, Romania
[3] Institute of Cellular Biology and Pathology of Romanian Academy, "Nicolae Simionescu", Department of Fetal and Adult Stem Cell Therapy, 8, B.P. Hasdeu, 050568 Bucharest, Romania

*neacsu.a.ionela@gmail.com

Nanotransporters are systems that offer unique possibilities to overcome cellular barriers in order to improve the delivery of numerous active substances such as drugs and therapeutic biomedical molecules [1].

Magnetic nanoparticles have a wide range of features that recommend them as promising candidates for controlled release systems. Some of these features are: easy manipulation of nanoparticles by applying an external magnetic field, the possibility of using passive and active substance release strategies, the ability to be visualized by imaging techniques such as nuclear magnetic resonance, and efficient internalization by target tissues, ensuring optimal treatment for optimal therapeutic doses [2].

In the absence of a coating, the iron oxide magnetic particles have hydrophobic surfaces with a high surface / volume ratio. Due to the hydrophobic interactions between the particles, the latter agglomerate, forming clusters (aggregates), leading to particle size increase. For effective stabilization of iron oxide nanoparticles, it is recommended to cover them with stabilizers such as surfactants or macromolecules (polymers), which will ultimately prevent the aggregation of magnetic nanoparticles.

Methotrexate, also known as Amethopterin, is a chemotherapeutic agent and a suppressor of the immune system. It is used in the treatment of cancer (breast cancer, leukemia, lung cancer, lymphoma and osteosarcoma), autoimmune diseases (such as psoriasis, rheumatoid arthritis and Crohn's disease) and ectopic pregnancies. It is a folate analogue and therefore has structural and physico-chemical properties similar to [3].

PEG is used as a stabilizer because of its ability to not adsorb blood proteins, to improve the bioavailability of active substances, and to slow down the degradation processes of materials used to obtain controlled release systems (micelles, liposomes, dendrimers or nanoparticles).

Folic acid is a ligand that has an increased affinity for FR (folic acid receptors). Folic acid receptors mediate the cellular internalization of follicular conjugates via receptor mediated endocytosis. In fact, the small size of the ligand allows effective tissue penetration and faster acceptance by affected tissue receptors. Conjugation of folic acid is therefore a valid method in the targeted delivery of therapeutic agents [4]. The schematic representation of folic acid-mediated endocytosis can be seen in Figure 1.

Synthesis consists of a co-precipitation rute, where a stoichiometric mixture of Fe^{2+} and Fe^{3+} that also contains the methotrexate is added dropwise into an NH$_3$ solution subjected to continous stirring. After complete addition of the iron precursor mixture, the precipitate is washed several times until complete removal of Cl$^-$ ions (from precursors) and the nanoparticles (Fe$_3$O$_4$@MTX) are dried inside an oven at 40°C for 2 days. After dispersing the nanoparticles into ultrapure water with an ultrasonic probe, a solution of PEG 8000 is added dropwise into the dispersion. The nanosystem (Fe$_3$O$_4$@MTX@PEG) is washed and dried in the same conditions as the above precipitate. The stabilized nanoparticles are then again dispersed into ultrapure water and a folic acid solution is dripped over it. The complex nanosystem (Fe$_3$O$_4$@MTX@PEG@FA) is washed and dried at 40°C for 2 days.
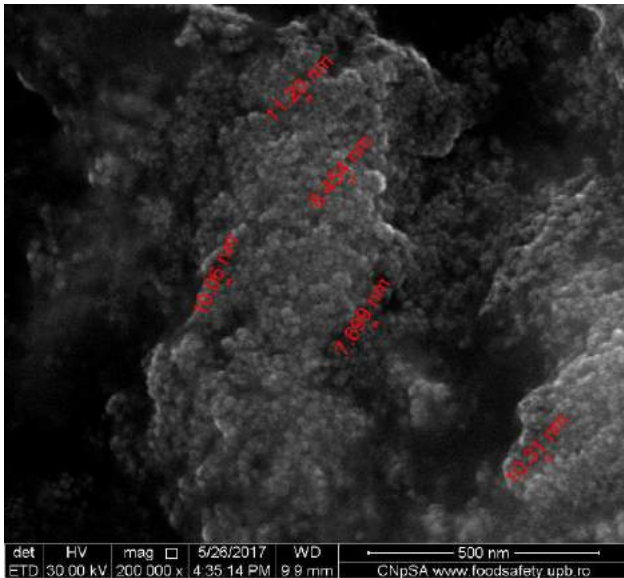
The obtained system was structurally and morphologically characterized by several techniques including XRD, SEM (Figure 2), TEM (Figure 3) (HRTEM, SAED, EDS) FTIR, Release profile of MTX by UV-Vis and also, the evaluation of in vitro biocompatibility was assesed.

Fourier transform infrared spectroscopy analysis confirms that the nanosystems comprise all the target compounds identified by the presence of characteristic absorption bands. The release profile for Fe$_3$O$_4$@MTX exhibits classic two-step release behavior, typically for active substance-bearing nanoparticles. Following in vitro biocompatibility tests, it was concluded that the only system that could induce a cytotoxic effect on mesenchymal stem cells isolated from amniotic fluid (AFSC) is the Fe3O4 + MTX complex. Also, the addition of the macromolecular compound and folic acid, respectively, significantly reduces the negative effects of nanosystems on AFSC.
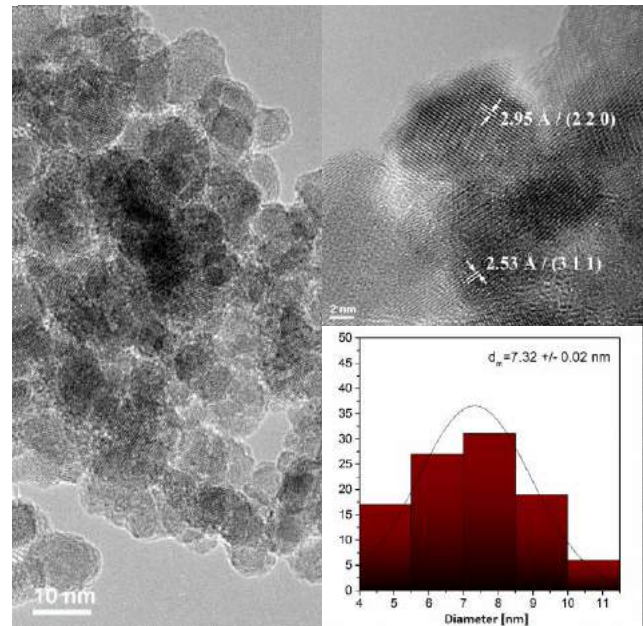
Figures

Figure 1. Schematic representation of folic acid mediated endocitosys
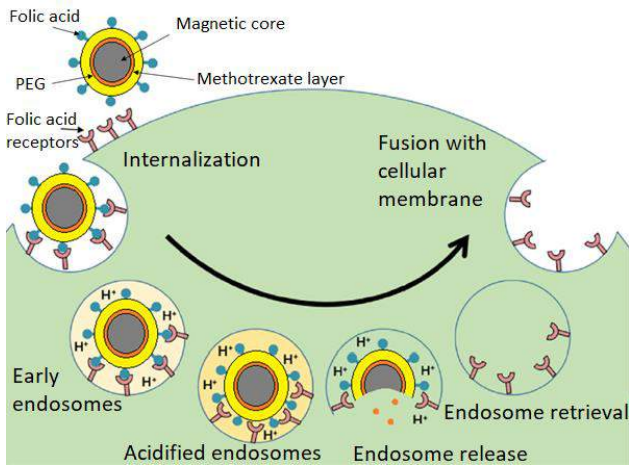
Figure 3. Transmission electron microscopy (TEM) and HR-TEM for Fe_3O_4@MTX@PEG@FA

Figure 2. Scanning electron microscopy for Fe_3O_4@MTX@PEG@FA

References

[1] H. Hillaireau and P. Couvreur, *Cell. Mol. Life Sci*, vol. 66, no. 17 (2009), page 2873-2896;

[2] M. Arruebo, et al., *Nano Today*, vol 2, no. 3 (2007), page 22-32;

[3] E. G. Favalli, M. Biggioggero, and P. L. Meroni, Autoimmun. Rev., vol. 13, no. 11 (2014), pages 1102–1108;

[4] C. M. Paulos, B. Varghese, W. R. Widmer, G. J. Breur, E. Vlashi, and P. S. Low, Arthritis Res. Ther., vol. 8, no. 3 (2006), page 77.

Antimicrobial PVA/Alginate macroporous foam scaffold for wound dressing

Jorge Pamplona Pagnossa[1],
Pedro H. S. Cesar[1], Tamara L. dos Santos[1],
Juliano E. de Oliveira[1], Eduardo Alves[1],
Roberta H. Piccoli[1], Silvana Marcussi[1]

[1]Universidade Federal de Lavras - UFLA,
Lavras, Minas Gerais, Brasil

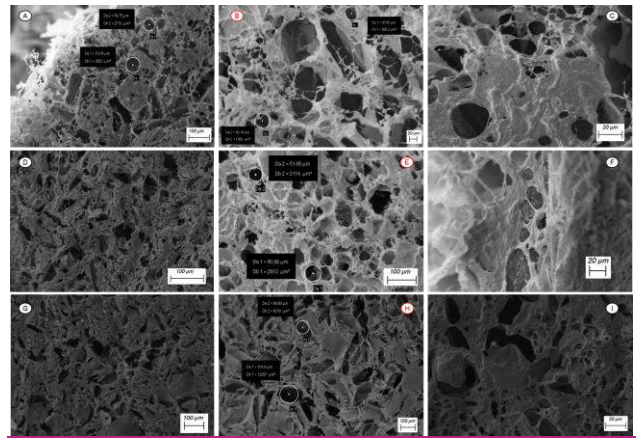jorgepamplona@posgrad.ufla.br

Figures

Figure 1. SEM images of PVA/Alginate formulations (A, B, C: 50/50%; D, E, F: 75/25%; and G, H, I: 25/75%). Red-labeled images (B, E, and H) shows cross-link treated polymers.
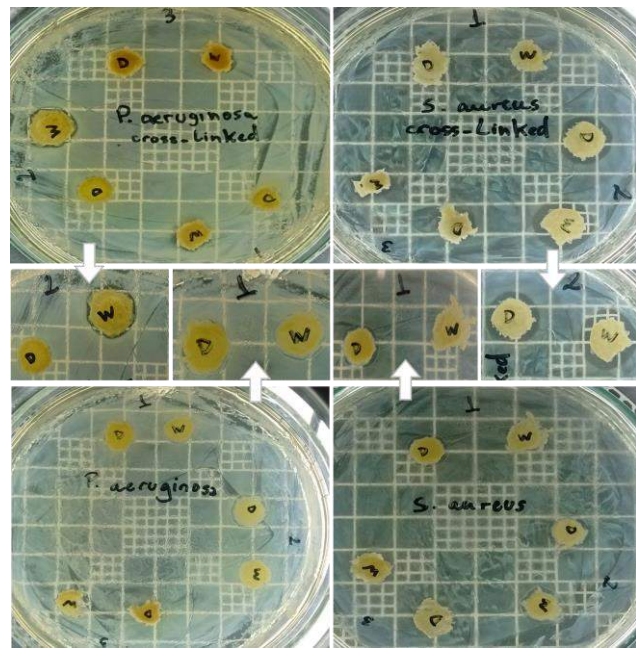

Figure 2. Disk-diffusion tests showing inhibition halos of *P. aeruginosa* and *S. aureus*. In some cases, cross-link treatment (above) and PBS buffer application (W) induced the release of bactericidal compounds rather than non cross-linked (under) or without PBS application (D).

Modern wound dressings are currently being produced from several biocompatible polymers, tailored to meet the optimum conditions for wound healing such as alginate and poly (vinyl alcohol). In some cases, these scaffolds are loaded with growth factors and antimicrobial agents to enhance wound healing and prevent infection. The use of such agents affects the efficacy, cytotoxicity, allergenicity and the cost of production [1]. It is well known that inexpensive natural compounds such as propolis, has many important pharmaceutical properties, while some retinols act as a regenerative compound in damaged human tissues. Thus, in this preliminary work we developed three PVA/Alginate dressings loaded with 10% propolis and 0,001% vitamin A (retinoic acid, retinol palmitate and retinol acetate) to investigate their pore sizes and bactericidal potential relations. Samples were prepared as (1) 50/50 (PVA:Alginate, w:w); (2) 75/25; and (3) 25/75%, with or without cross-linking with glutaraldehyde (0,5%). Samples were analyzed by SEM to measure the pore sizes, and disk-diffusion tests to evaluate the bactericidal activity against *Pseudomonas aeruginosa* INCQS0025 and *Staphylococcus aureus* ATCC 25923 strains. By increasing the concentration of PVA it is observable the formation of smaller and more uniform pores (Figure 1), this fact is related to the formation of smaller ice crystals between the PVA chains, what impacts in the release of propolis and vitamin A, and the mechanical properties. Disk-diffusion tests showed visible inhibition halos for *P. aeruginosa* and *S. aureus* strains. Higher PVA formulation (75%) and cross-link treated samples exhibited wider halos, which can be related to faster release of active compounds, while higher alginate content had more controlled release noticing bactericidal effect only in the zone of contact (Figure 2). Further studies will be performed to better understand PVA/Alginate compositions in drug release kinetics and scaffold mechanical properties.

References

[1] Vowden, K., Vowden, P., Surgery 32:9 (2014), 462-467.
[2] Dhivyaa, S., Padma, V. V., Santhini, E., Biomedicine, 5:4 (2015), 24-28.

Colloidal quantum dots@SiO2 as platform for enzymes detection.

Sofia Paulo[1,2],
Santi Gené[1], Roger Mallol[1] and Emilio Palomares[1,3]

[1]Institute of Chemical Research of Catalonia (ICIQ), The Barcelona Institute of Science and Technology (BIST), Avinguda del Països Catalans 16, 43007 Tarragona, Spain.
[2]CentreFundació Eurecat. Av. d'Ernest Lluch 36, Parc Científic i de la Innovació TecnoCampus, E-08302, Mataró, Barcelona.
[3]Catalan Institution for Research and Advanced Studies (ICREA), Passeig de Lluis Companys 23, 08010 Barcelona, Spain. Fax: +34 977920224; Tel: +34 977920200

spaulo@iciq.es, epalomares@iciq.es

Colloidal quantum dots (QDs) have been extensively studied due to 1) their optoelectronic properties, such as narrow emission and color tuneability, and 2) their potential for applications in electronic and biological systems[1,2]. In this study, we used QDs as a detector to determine elastase and trypsin concentration in human stool samples for cystic fibrosis diagnosis.

Two different quantum dots (λ_{em}(CdSeS)= 500nm and λ_{em}(CdTe)= 650nm) were encapsulated in silica nanospheres using a reverse microemulsion method described elsewhere.[3] Then, a short peptide marked with a 5-TAMRA dye (5-Carboxytetramethyl-Rhodamine, with a fluorescence band at 550nm) was attached to the surface of the nanosphere (nanoSi) (Figure 1). The 2nanoSi system composed of 80nm silica nanospheres on average (Figure 2) showed three emission bands at 500nm, 550nm and 660nm when analyzed using a fluorimeter (Figure 3).

Our system is based on a simple mechanism. Briefly, when blue QDs are relaxed after being excited with a lamp, radiative and nonradiative recombinations take place. Some of this energy is transferred to the photosensitizer dye by FRET (Fösrster Resonance Energy Transfer). This phenomenon is noticed because the emission band of QDs decreases. To allow this process to happen, two requisites are necessary: 1) the donor emission band has to overlap to the acceptor absorption band and 2) the acceptor and the donor must be spatially close. On the other hand, red QDs work as a control signal, meaning that their emission band must remain constant during all the procedure.

We can plot a linear curve fitting the ratio between blue and red emission bands with different concentrations of porcine elastase (Figures 4 and 5). The calibration curve showed an excellent linear respond (χ^2 = 0.96) and using this system, we were able to quantify the concentration of elastase and trypsin[4], in human stool samples.

Overall, this system will allow the development of a non-invasive, low-cost, fast and easy-to-use device for the detection of diseases such as cystic fibrosis.

References

(1)   Bonacchi, S.; Genovese, D.; Juris, R.; Montalti, M.; Prodi, L.; Rampazzo, E.; Sgarzi, M.; Zaccheroni, N.: Luminescent Chemosensors Based on Silica Nanoparticles. In Luminescence Applied in Sensor Science; Prodi, L., Montalti, M., Zaccheroni, N., Eds.; Springer Berlin Heidelberg: Berlin, Heidelberg, 2011; pp 93-138.
(2)   Michalet, X.; Pinaud, F. F.; Bentolila, L. A.; Tsay, J. M.; Doose, S.; Li, J. J.; Sundaresan, G.; Wu, A. M.; Gambhir, S. S.; Weiss, S.: Quantum Dots for Live Cells, in Vivo Imaging, and Diagnostics. Science 2005, 307, 538-544.
(3)   Ma, Q.; Li, Y.; Lin, Z.-H.; Tang, G.; Su, X.-G.: A novel ascorbic acid sensor based on the Fe3+/Fe2+ modulated photoluminescence of CdTe quantum dots@SiO2 nanobeads. Nanoscale 2013, 5, 9726-9731.
(4)   Castello Serrano, I.; Stoica, G.; Matas Adams, A.; Palomares, E.: Dual core quantum dots for highly quantitative ratiometric detection of trypsin activity in cystic fibrosis patients. Nanoscale 2014, 6, 13623-13629.
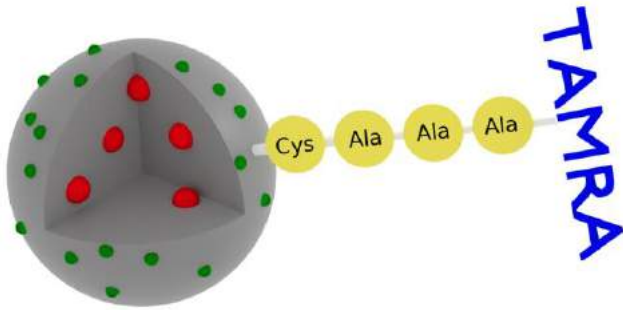
Figures

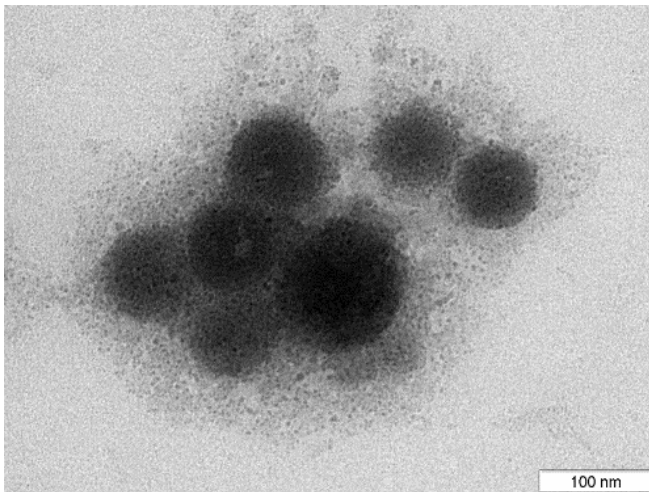**Figure 1.** Pictoral description of the nanoSi system.

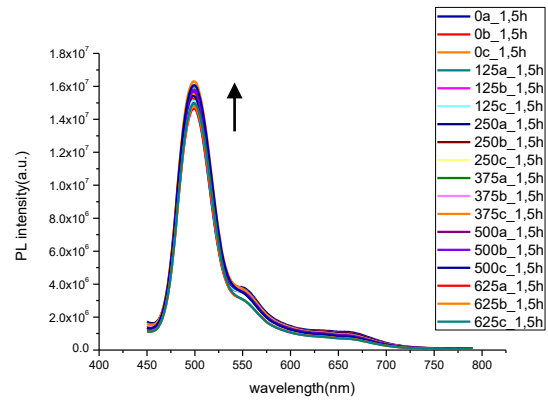**Figure 2.** TEM images of nanoSi. Dint= 71,23nm Dext= 96,26; DCdTe QDs= 4nm; DZnCdSe=2nm

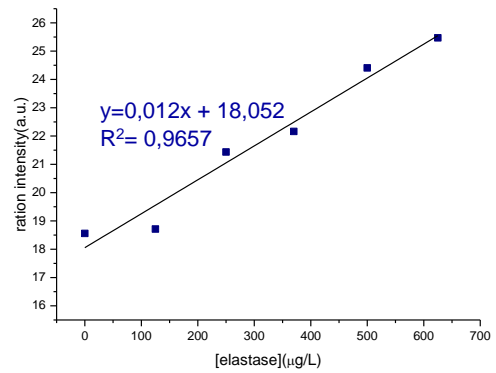**Figure 3.** PL spectra of calibration curve Stirring time 1,5h.

$y=0,012x + 18,052$
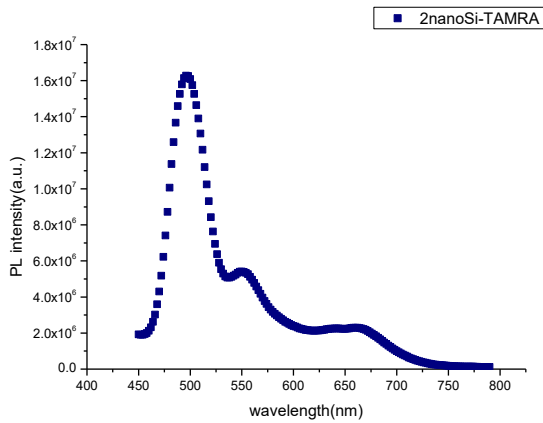$R^2= 0,9657$

Figure 4. Calibration curve.

Figure 3. PL spectrum of Nanospheres.

Potential Medical Applications of Ultra Small Copper Oxide Nanoparticles

Or Perlman[1],
Iris S. Weitz[2] and Haim Azhari[1]

[1]Technion – Israel Institute of Technology, Haifa, Israel
[2]ORT Braude College, Karmiel, Israel

irisweitz@braude.ac.il
haim@bm.technion.ac.il

Due to the deficient structure of the cancerous vasculature system, nanoparticles hold a great promise for increased tumor permeability [1]. In the medical imaging arena, several nano-based contrast agents were previously approved for clinical use [2], yielding enhanced detection of the pathological tissue. Extensive efforts are continuously taken to further incorporate nano-based materials for various medical imaging modalities. In the therapeutic arena, a growing field of interest is the utilization of nano-scaled complexes as thermal treatment enhancers [3]. In such procedures, a semi-invasive or an utterly noninvasive energy applicator is used to heat the cancerous tissue. This may improve the efficiency of chemotherapy or radiotherapy, or completely ablate the tumor tissue.

Copper oxide nanoparticles (CuO-NPs) were recently demonstrated as capable of inducing tumor cell death using *in vitro* and *in vivo* models [4]-[6]. Herein, we shall describe our recent efforts to incorporate copper oxide based nanomaterials for additional and multiple medical applications. The main goal of the research was to investigate whether these nanoparticles may also serve as an imaging contrast agent and therefore, be monitored during their therapeutic application. Seven nanometer in diameter CuO-NPs were synthesized and their properties characterized. The particles improved magnetic resonance imaging (MRI) contrast (e.g., in figure 1), based on the longitudinal magnetic relaxation time property. The CuO-NPs were also well visualized using ultrasound, thus, providing a multimodal imaging capability [7]. Using a unique approach, termed through-transmission ultrasonography, the particles were also useful for cancer thermal treatments image monitoring, when performed using a minimal-invasive microwave applicator [8]. In conclusion, CuO-NPs hold a unique potential to serve as an imaging-therapeutic combined nano-material.

Acknowledgments

References

[1] V. Torchilin, Adv. Drug Delivery Rev., 63 (2011), 131-135.

[2] Y.-X. J. Wang, Quantitative imaging in medicine and surgery, 1 (2011), 35.

[3] X. Wang, H. Chen, Y. Zheng, M. Ma, Y. Chen, K. Zhang, D. Zeng and J. Shi, Biomaterials, 34 (2013), 2057-2068.

[4] T. Sun, Y. Yan, Y. Zhao, F. Guo and C. Jiang, PLoS One, 7 (2012), e43442.

[5] M. A. Siddiqui, H. A. Alhadlaq, J. Ahmad, A. A. Al-Khedhairy, J. Musarrat and M. Ahamed, PLoS One, 8 (2013), e69534.

[6] D. Laha, A. Pramanik, S. Chattopadhyay, S. kumar Dash, S. Roy, P. Pramanik and P. Karmakar, RSC Advances, 5 (2015), 68169-68178.

[7] O. Perlman, I. S. Weitz and H. Azhari, Physics in medicine and biology, 60 (2015), 5767

[8] O. Perlman, I. S. Weitz and H. Azhari, submitted for publication.

Figures
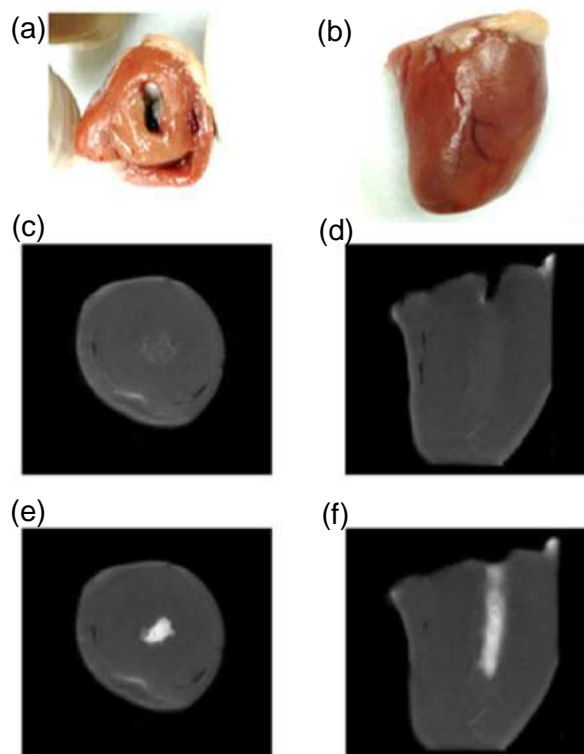
Figure 1. Magnetic resonance imaging (MRI) of an *ex vivo* poultry heart injected with copper oxide nanoparticles. (a)-(b). Top and frontal views respectively of the imaged specimen. (c)-(d). Axial and coronal MRI images respectively of the left ventricle, as the chamber was filled with water. (e)-(f). Axial and Coronal MRI images respectively of the left ventricle, after injecting copper oxide nanoparticles into the chamber.

Nanodispersions as carriers of novel bioactive compounds - Biological Applications

Vasiliki Pletsa,
Ioanna Theochari, Vassiliki Papadimitriou,
Dimitrios Papahatjis, Aristotelis Xenakis

Institute of Biology, Medicinal Chemistry & Biotechnology, National Hellenic Research Foundation, 48 Vassileos Constantinou Avenue, 11635, Athens, Greece

vpletsa@eie.gr

Targeted delivery of chemotherapeutics in order to overcome side effects and enhance chemosensitivity remains a major issue in cancer research worldwide. In this context, biocompatible O/W micro-emulsions were developed as matrices for the encapsulation of bioactive molecules, which are slightly soluble or insoluble in water [1]. DPS-2 is a novel bioactive compound, exhibiting high cytotoxicity in various cancer cell lines, among them the MW 164 skin melanoma cell line and the CaCO-2 human epithelial colorectal adenocarcinoma cell line. The delivery system, composed of 81.5% w/w PBS buffer, 10.6% w/w Tween 80 and 7.9% w/w triacetin [2], was structurally characterized by Dynamic Light Scattering (DLS), Cryogenic-transmission electron microscopy (Cryo-TEM) and Electron Paramagnetic Resonance (EPR) in order to characterize its internal structure and investigate the degree of encapsulation of the bioactive compound [3,4]. The effective release of a lipophilic compound was evaluated via Confocal Microscopy. The cytotoxic effect of O/W micro-emulsions, in the presence and absence of DPS-2, in MW 164 and CaCO-2 cells, was examined through the MTT cell proliferation and Trypan Blue exclusion assays. The O/W micro-emulsion, as nanocarrier, had no effect on cell lines' viability while DPS-2 exhibited significant cytotoxicity in both cell lines when loaded in micro-emulsion. A deep understanding of how a given chemotherapy affects cell signalling pathways involved in cell death is highly relevant in order to develop more effective therapeutics [5]. The molecular mechanism of the induced cell death is being investigated through experimental approaches such as Fluorescence -activated cell sorting (FACS) analysis and Western Blotting. Preliminary results indicate lack of apoptosis and S-phase arrest in both cell lines. Currently, further characterization of the type of the cell death induced as well as identification of the molecular pathways involved, in each cell type, is ongoing.

References

[1] M. J. Lawrence, G. D. Rees, Advanced Drug Delivery Reviews, 64, (2012) 175–193.
[2] I. Theochari, M. Goulielmaki, D. Danino, V. Papadimitriou, A. Pintzas, A. Xenakis, Colloids and Surfaces B: Biointerfaces, 154 (2017) 350-356.
[3] D. Danino, Cryo-TEM of soft molecular assemblies, Curr. Opin. Colloid Interface Sci., 17 (2012) 316-329.
[4] A. Kalaitzaki, N. E. Papanikolaou, F. Karamaouna, V. Dourtoglou, A. Xenakis, V. Papadimitriou, Langmuir, 31 (2015) 5722-5730.
[5] Papadodima O, Moulos P, Koryllou A, Piroti G, Kolisis F, Chatziioannou A, Pletsa V, PLoS One. 11(2016) e0160248.

Figures
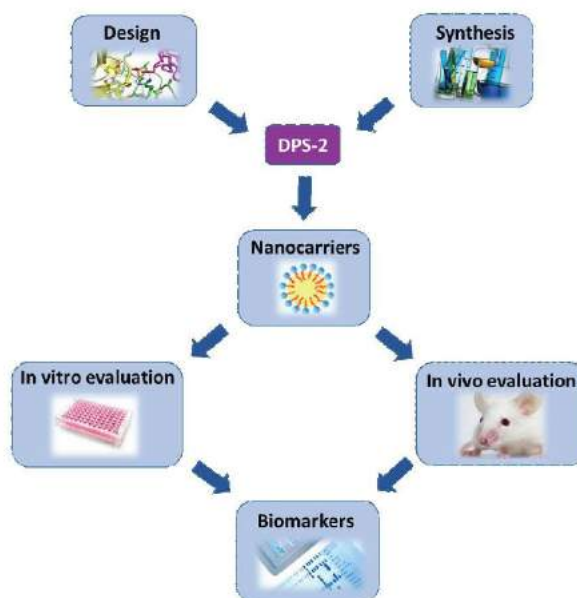
Figure 1. Schematic representation of the several phases of the study and their interactions

Interferometric real time monitoring Streptavidin bioconjugation in Nanoporous Anodic Alumina

L. Pol

L.K. Acosta, A J. Ferré-Borrull, L.F. Marsal

Departament d'Enginyeria Electrònica, Elèctrica i Automàtica,ETSE, Universitat Rovira i Virgili

Lluis.marsal@urv.cat

Nanoporous Anodic Alumina (NAA) is a material with growing interest in nanotechnology as it consists of an array of regularly ordered straight pores perpendicular to the material surface [1] obtained by the electrochemical anodization of aluminum in the appropriate conditions [2,3,].

Because of its high surface-to-volume ratio, tailorable geometry and chemical stability one of the main applications of NAA is as a biosensing platform [4], for this propose the surface modification of NAA by grafting functional molecules is a key step.
The Streptavidin-Biotin interaction system is widely used in biosensors. Thanks to their strong affinity and specificity, it is easy immobilize any biotinylated molecule on a biosensor surface previously functionalized with Streptavidin [5][6].
Optical biosensing with NAA has been demonstrated with the Reflection Interference Spectroscopy (RIfS) method [7]: the attachment of a specific molecule to the inner pore surface (conveniently modified) of a NAA thin film is detected by a change in the reflectance spectrum, quantified as a shift in the film effective optical thickness (EOT).
In this work we study two pathways to accomplish the attachment of Streptavidin to the NAA surface by means of RIFS in real time. The first step is common in both pathways and consists of grafting aminopropyl triethoxysilane (APTES) to the NAA surface, while the difference between the two pathways consists in considering two different cross-linking methods able to attach Streptavidin: glutaraldehyde (GTA) or EDC/NHS. Both functionalization pathways have previously been studied for the attachment of proteins to the NAA surface [8].

Here we study in real time the streptavidin attachment process and study the effect of depositing a thin film (10 nm of thickness) of gold on top of the NAA porous structure as it can contribute to improve the interferometric signal in the reflectance spectrum of the NAA.
NAA samples were prepared following the well-established two-step anodization procedure [1] using 0.3 M oxalic acid and a thin film of gold was deposited by sputtering on half of the samples while the other half was used as produced.

Grafting APTES to the NAA samples was accomplished by incubation of 2µl of APTES in 20ml of dry Toluene under Nitrogen flux, half of the samples were then functionalized with GTA (both as-produced NAA and gold-coated NAA samples) raised in GTA solution and the other half was functionalized only with APTES using EDC/NHS to activate the carboxyl group that will be binding with the Streptavidin.
The attachment of streptavidin to the NAA samples was monitored in real time by means of RIFS in sequential injections of Streptavidin and buffer solution, Phosphate buffer saline (PBS) in the case of the GTA and, 2-(N-morpholino)ethanesulfonic (MES) in the case of ECD-NHS.
In all the experiments, pure buffer is first flown until the measured EOT is stable. At this point, the corresponding Streptavidin solution with a concentration of 100µg/ml is injected and the change of EOT is registered as a function of time, until it reaches a stable value. Finally, buffer is injected again in the flow cell to rinse the non-attached molecules.

Figure 1 shows two reflectance spectra corresponding to one sample measured after functionalization with APTES and Streptavidin (red line) and to another equivalent sample measured after the sputtering of 10 nm of gold on top of the NAA structure (blue line), both spectra show successive maxima and minima resulting from the Fabry-Pérot interferences in the NAA porous thin film, it can be observed that the gold layer increases the contrast between the maxima and minima in the spectrum.

Figure 2 shows the results of four real-time RIfS experiments of streptavidin injection in flow cell. The graphs show the variation of the estimated EOT as a function of time. Graphs a) and b) correspond to as-produced samples, while graphs c) and d) to samples with sputtered gold. On the other hand, graphs a) and c) correspond to samples functionalized with the GTA cross-linker while b) and d) correspond to the EDC-NHS activating method.

The results for the EDC cross-linker show a fast increase of EOT after the streptavidin injection, with an EOT increment of approximately 40 nm in 100 s. However, after the injection of the PBS buffer, the EOT recovers its original level in the same time.
For the EDC cross-linker the increment in EOT after the streptavidin injection reaches a smaller value (between 20 nm and 25 nm) and at a much smaller rate (approximately 700 s). Furthermore, after the injection of the MES buffer, the EOT decreases 15 nm in the case of the as-produced sample and maintains its level for the sample sputtered with gold.

These results indicate that using GTA as cross-linker does not result in an effective attachment of the streptavidin to the NAA pore walls.

This can be caused by the fact that the APTES-GTA binding reaction is reversible in water-based solvents. Instead using EDC-NHS results in a noticeable change in EOT, this is maintained after MES injection indicating a good attachment of Streptavidin.

These results demonstrate that the RIfS method is able to detect the streptavidin attachment to the NAA pore wall, and that is a good tool to investigate the attachment dynamics. On the other hand, the results also show that depositing a thin film of gold contributes to enhance the spectral signal and to reduce noise in the measurement of the EOT.

References

[1]   W. Lee et al., Chem. Rev., vol. 114, no. 15, (2014) 7487–7556.
[2]   Santos, Abel *et al.*, Journal of Electroanalytical Chemistry, vol. 655 no. 1, (2011) 73-78.
[3]   J. Ferré-Borrull et al., Materials, vol. 7, no. 7, (2014) 5225–5253.
[4]   J. Ferré-Borrull, et al., D. Losic and A. Santos, Eds. Cham: Springer International Publishing, (2015) 185–217.
[5]   T. Kumeria, et al. Biosens. Bioelectron., vol. 35, (2012). 167–173.
[6]   S. D. Alvarez et al., ACS Nano, vol. 3, no. 10, (2009) 3301–3307.
[7]   Z. Lin et al., vol. 75, (2008) 965–972.
[8]   M. Baranowska et al., Colloids Surfaces B Biointerfaces, vol. 122, (2014) 375-383.

Figures
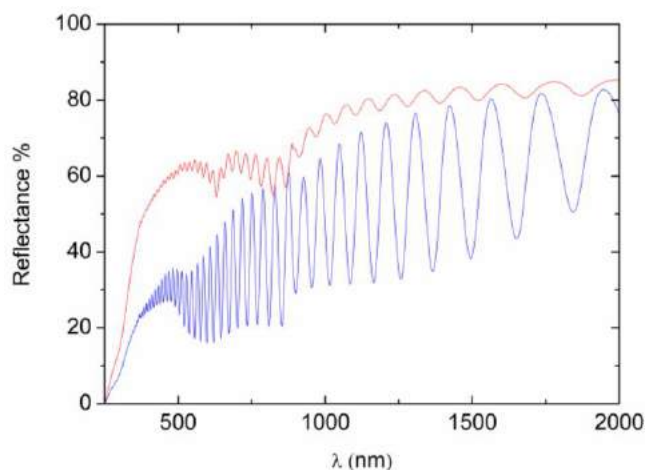
Figure 1. Reflectance spectra of NAA measured after functionalization with APTES and Streptavidin in a as produce NAA (red line) and after the sputtering of 10 nm of gold on top of the NAA (blue line).
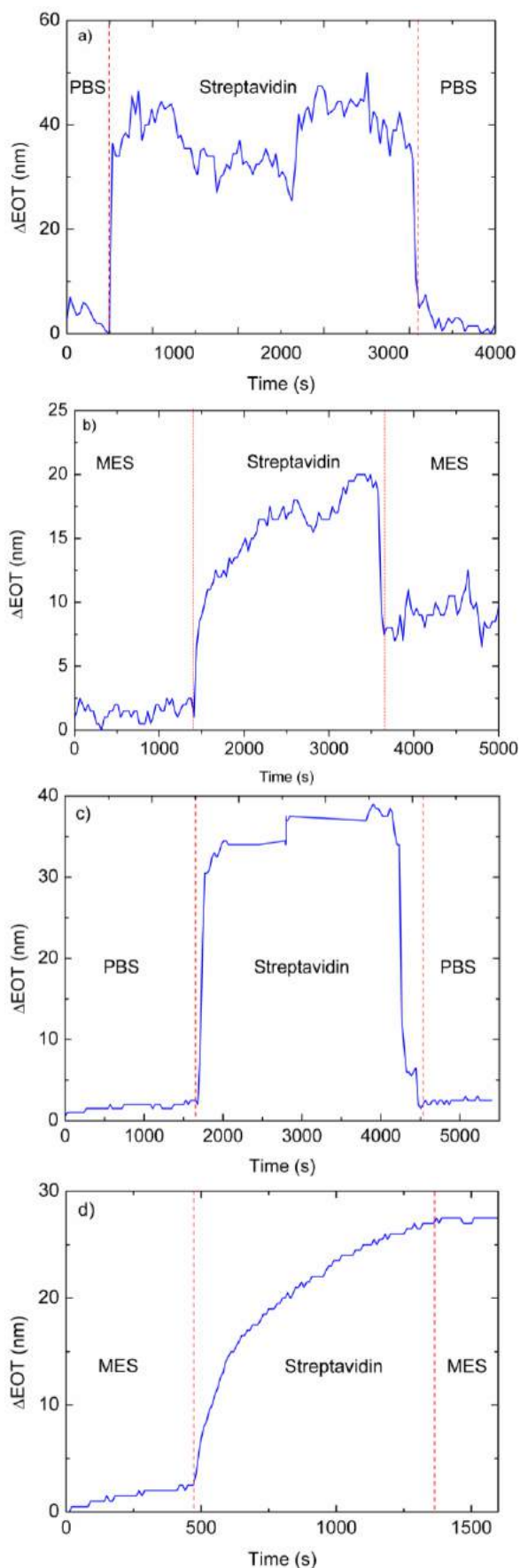
Figure 2. Real-time EOT of streptavidin injections at 100µg/ml in flow cell in NAA as-produced a) and b), and NAA covered with gold c) and **d).**

Nanoporous Anodic Alumina Three-Dimentional Structures for Drug Delivery

Maria Porta-i-Batalla,
Elisabet Xifré-Pérez, Chris Eckstein,
Josep Ferré-Borrull and Lluis F. Marsal

Departament d'Enginyeria Electrònica, Elèctrica i Automàtica, ETSE, Universitat Rovira i Virgili, Avda. Països Catalans 26, 43007 Tarragona, Spain

maria.porta@urv.cat / lluis.marsal@urv.cat

Abstract

The release of drugs loaded inside Nanoporous Anodic Alumina (NAA) pores is complex and depends on the morphology of those pores. In this study, NAA with different three-dimensional (3D) pore structures were fabricated, and their respective drug release rates were studied and modeled. The obtained results reveal optimal modeling of all 3D pore structures, discriminating two drug release stages: short term and long term stages. Higuchi and Korsmeyer–Peppas equations, successfully modeled a short-term and a long-term release respectively. This study proves the effect of pore geometries on drug release rates.

Experimental Section

Ordered nanoporous anodic alumina (NAA) was prepared by the two-step anodization method. To suppress breakdown effects and to enable uniform oxide film growth at high voltage (195 V in phosphoric acid) a protective layer at lower voltage (174 V also in phosphoric acid) was performed for 180 min. After the first anodization (first step), the disordered porous alumina grown on the aluminium surface was removed by a wet chemical etching in a mixture of phosphoric acid (0,4M) and chromic acid (0,2M) (1:1 volume ratio) at 70ºC. The second anodization step was performed under the same experimental conditions (195V) as they were used in the first step in order to obtain ordered nanoporous alumina. The layer length or pore depth was controlled by the total charge that is going through the electrodes because it has a direct relation with the amount of Nanoporous Anodic Alumina created [1,2].
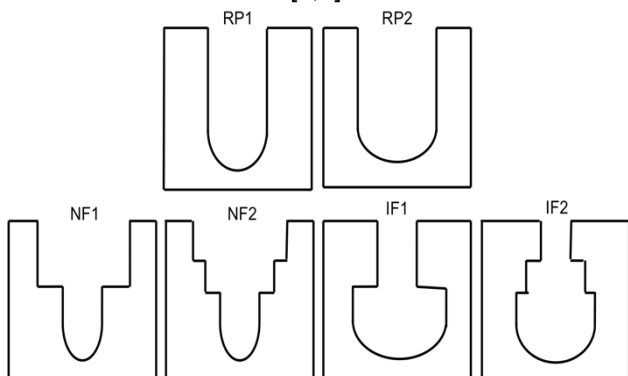
Figure 1. Schematic illustration of the different pore shapes. The name of every pore shape is written in the upper part.

Regular pore shapes (RP) or straight pores were achieved by electrochemical anodization. Then pores with different pore diameters were realised using wet chemical dissolution (pore widening) of the pore walls in order to obtain pores with similar top pore diameter and be able to compare them.

Normal Funnels (NF) samples were performed alternating anodization process and pore widening process. Depending on the number of layers the samples were named NF2 (Normal Funnels of 2 layers) or NF3 (Normal Funnels of 3 layers) (Figure 1 and 2).
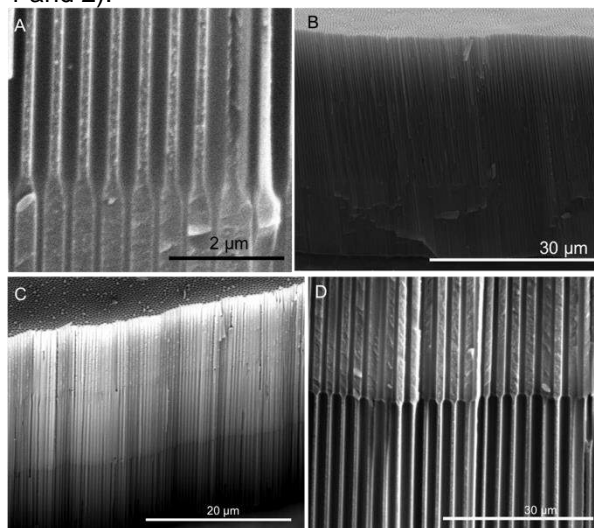
Figure 2. Cross section ESEM images of Normal and Inverted Funnel sample A) Two layered Normal Funnel B) Three layered Normal funnel sample. C) Three layered Inverted Funnel sample D) Cross-section of a two layered inverted funnel sample.

In order to achieve the Inverted Funnels (IF) structures, a thermal treatment to change the amorphous crystallographic phase of the alumina to gamma crystallographic phase was used [3]. Temperatures treatments about 250ºC and 500ºC were applied, and finally a pore widening procedure was applied. Inverted funnels were named IF2 (Inverted Funnels 2 layers) or IF3 (Inverted Funnels 3 layers) depending on the number of layers (Figure 1 and 2).

Drug Loading and Release Studies

Doxorubicin (DOX), which is a self-fluorescent drug, was selected as a model drug. DOX solution at 1mg/ml concentration was loaded into the templates for the release studies. The release studies were performed in vitro using phosphate-buffered saline (PBS. DOX was measured directly in the release medium. The photoluminescence measurements were taken on a fluorescence spectrophotometer using an excitation wavelength (λ_{ex}) of 480 nm and emission wavelength of 590 nm.

Results and Discussion

Regular pores (RP), Normal Funnels (NF) and Inverted Funnels (IF) were successfully achieved. Figure 2 shows ESEM cross-section pictures of the normal and inverted funnels samples.
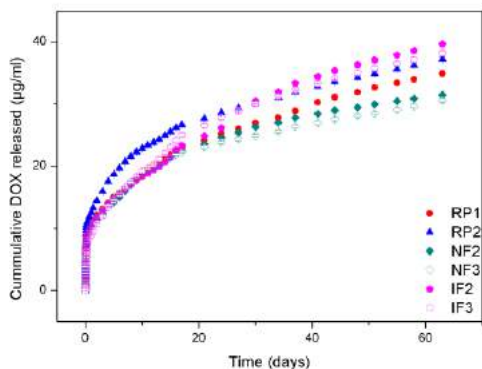
Figure 3. Graphs showing the cumulative drug release of different sample shapes in days.

In figure 3 a general release profile is shown for straight pores and for every type of funnels. We can observe a burst release within the first minutes, and then the release rate is decreasing slowly, for this reason we distinguished between two release ranges: the short-term and the long-term release. In order to identify the release constant for the burst release we used Origin software to find the equation witch best describes the drug liberation. A variation of the Higuchi equation was used:

$$M_t = M_0 + K\sqrt{t} \tag{1}$$

Where M_t is the cumulative release at time t, M_0 is the intercept value when time is zero and k is the release constant [4,5].

A correlation between the top pore diameter and the release rate (K) was found in this study within the first minutes in the case of regular pores. For this reason we plotted the release rate (k) against the top pore diameter for the different pore structures (figure 4).
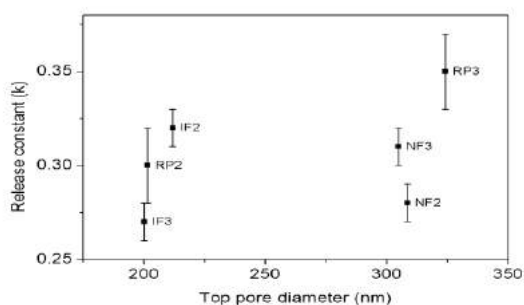
Figure 4. Graph showing the relation between the slope (K) and the top pore diameter.

To continue with the identification of the release mechanism model we used the Korsmeyer-Peppas (equation 2) for the long time release (from day 2 to day 63).

$$M_t = M_{t0} \left(\frac{t}{t_0}\right)^n \tag{2}$$

Where M_t is the proportion of drug released at given time t, M_{t0} is the amount of drug released at the reference time t_0 (1day), t is time in days and n is the release parameter related to the release rate.

This time the release rate was obtained as the first derivative of the equation 2 and we could also found a relation of the release rates and the top pore diameter on the regular pores. For this reason a graph relating the release rate and the top pore diameter (figure 5) was prepared [6].
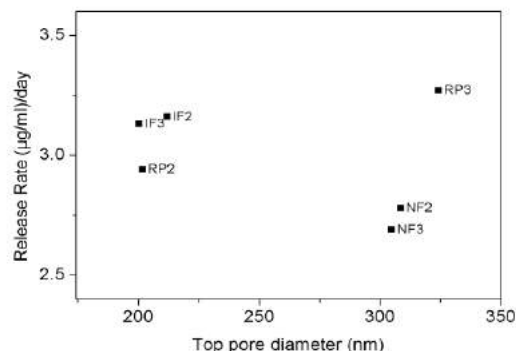
Figure 5. Graph relating the release rate and the top pore diameter for the long time release.

Conclusions
The quantitative dynamics of the release has been studied in two different regimes: A short-term release and a long-term release. During the short-term release the results were fitted by the Higuchi model. Normal Funnels samples show a lower release constant (K) during the bust release than the regular pores

For the long-term release, the data has been fitted by the Korsmeyer-Peppas model. This time release rates in Inverted Funnels were higher than the regular pores with the same top pore diameter, and the Normal Funnels values were lower than the regular pores with the same top pore diameter. Those results reveal that the Inverted Funnels structures retain inside the pores a higher quantity of drug than the Normal Funnels or the regular pores with the same volume, area or top pore diameter. This retention allows this pore structure to release the active molecule in a sustained way.

References
[1] Losic D. et al. Expert Opin Drug Deliv 6 (2009) 1363.
[2] Santos A. et al. Phys Status Solidi Appl Mater Sci 208 (2011) 668.
[3] Santos, A. et al. Nanoscale 6 (2014) 9991
[4] Porta-i-Batalla M. et al. Nanoscale Res Lett 11 (2016) 372.
[5] Kang H-J. et al. Thin Solid Films 515 (2007) 5184–5187.
[6] Porta-i-Batalla M. et al. Nanomaterials 7 (2017) 227

Paclitaxel loading Poly(4-vinylpyridine) and Tripalmitin Nanoparticles for Breast Cancer Therapy

Jose Carlos Prados [1,2,3*]
Maria Carmen Leiva[1,2,3], Rafael Contreras-Cáceres[4], Amelia Díaz[4], Miguel A. Casado-Rodríguez[4], Jose M. Baeyens[5], Gloria Perazzoli[1,2], Laura Cabeza[1,2], Julia Jiménez-Lopez[1,2,3], Raul Ortiz[1,6], Consolación Melguizo[1,2,3], Juan M. López-Romero[4]
*Equal contribution

[1]Institute of Biopathology and Regenerative Medicine (IBIMER), Biomedical Research Center (CIBM), Granada University, Av. del Conocimiento, s/n, 18100, Granada, Spain
[2]Biosanitary Institute of Granada (ibs.GRANADA), SAS-Universidad de Granada, Granada, Spain
[3]Department of Anatomy and Embryology, Faculty of Medicine, University of Granada. 18071, Granada, Spain
[4]Department of Organic Chemistry, Faculty of Science. University of Málaga, 29071, Málaga, Spain
[5] Department of Pharmacology, Institute of Neuroscience, Biomedical Research Center (CIBM), University of Granada, 18100, Granada, Spain.
[6]Department of Health Science, University of Jaén, 23071 Jaén, Spain

jprados@ugr.es

Paclitaxel (PTX) is one of the chemotherapics of election for the treatment of breast cancer. However, this drug presents some limitations as low solubility, poor tumor specificity and the appearance of side effects (1). The use of nanoparticles (NPs) is an asset to improve PTX antitumor efficacy, avoid toxicity and target the drug action specifically on the tumor tissue (2). For these reasons, we have developed a delivery sistem, consisting on Tripalmitin solid lipid NPs (Tripalm-NPs) for PTX encapsulation (Tripalm-NPs-PTX) (3). These NPs (Figure 1) have been assayed in a wide range of breast tumor models, consisting on a human breast cancer cells (MCF7); multicellular tumor spheroids (MTS) derived from MCF7, that mimic a tumor mass (Figure 2); a resistant cells line through P-glycoprotein (P-gp) overexpression (HCT-15) and breast cancer stem cells (CSCs) obtained from MCF7, which are very often responsible for recurrences and recidives. In order to asses the antitumor efficacy of these PTX-loaded NPs, treatments were added at increasing concentractions and a cytotoxicity assay was performed by the sulphorrodamine B method after 96 hours. MTS were obtained from MCF7, and their volume after being treated were monitored by microscopy at different times of the experience. Finally, for CSCs obtention, MCF7 were incubated with an induction medium for two weeks, treatments were administered for 48 hours, and the cytotoxicity assay was carried out using a Cell Counting Kit

(CCK-8, Dojindo, Japan). The results obtained prove an improvement in the antitumor efficacy of PTX after its incorporation in Tripalm-NPs-PTX over MCF7 cells and MTS (Figure 2). Further, they were also able to increase PTX effect against a resistant cell line, and CSCs, with a significant (p<0.001) decrease in cell viability in all the cases. According to these results, Tripalm-NPs-PTX are very promising delivery systems to improve breast cancer treatment efficacy and avoid treatment failure.

References

[1] Guchelaar, H. J.; ten Napel, C. H.; de Vries, E. G.; Mulder, N. H., Clin. Oncol., 6 (1994) 40-48.
[2] Surapaneni, M. S.; Das, S. K.; Das, N. G., ISRN Pharmacol., 10 (2012) 12.
[3] Leiva MC, Ortiz R, Contreras-Cáceres R, Perazzoli G, Mayevych I, López-Romero JM, Sarabia F, Baeyens JM, Melguizo C, Prados J. Sci Rep. 7 (2017) 13506.
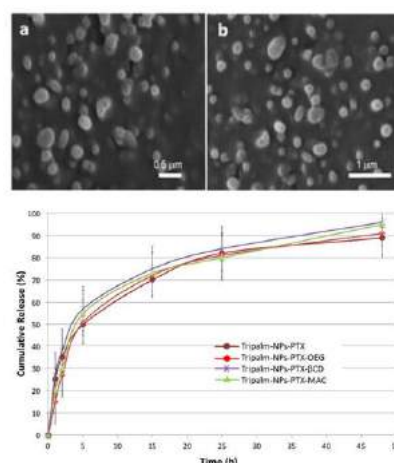
Figures

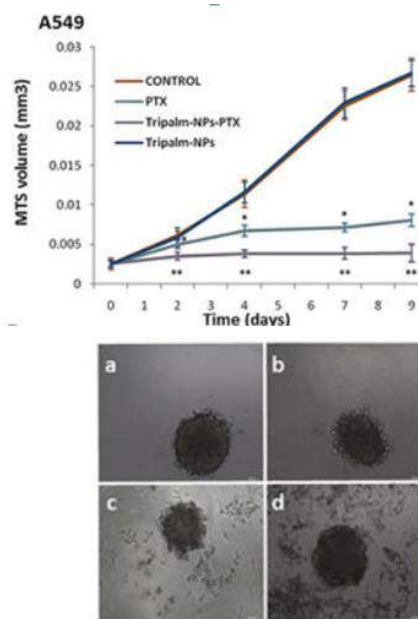**Figure 1.** Tripalmitin solid lipid NPs (Tripalm-NPs) NP-loading PTX. Entrapment efficiency.

Figure 2. Analysis of the tripalmitin solid lipid NPs (Tripalm-NPs) NP-loading PTX effect in MTS volume.

Nanocarriers for Alzheimer's disease treatment: from bench to bedside

Amira Sayed Hanafy

Department of Pharmaceutics and Drug manufacturing, Faculty of Pharmacy & Drug Manufacturing, Pharos University in Alexandria, Egypt

amira.sayed@pua.edu.eg

Alzheimer's disease (AD) is a slowly developing neurodegenerative disease that is prevalent among the elderly. AD progression might start 20 years before symptoms are apparent. Several hypotheses were proposed to explain AD pathogenesis. Understanding the key players in AD neuropathogenesis helps identifying the possible therapeutic targets. AD could be managed via symptomatic or disease-modifying treatments. Symptomatic treatments improve memory and cognition; while disease-modifying treatments stop or slow down the disease progression. Recent advances in nanotechnology have provided superior opportunities in the management of AD. Loading a drug in a suitably formulated nanocarrier can increase drug accumulation in the brain via surface functionalization; increasing its blood-brain barrier crossing ability. In spite of the research ongoing for decades, the clinical trials on nanocarriers for AD drug delivery are very limited; hindering their transfer from bench to bedside. It appears that the nanotoxicity and large scale processibility challenge their success. In this presentation, different types of nanocarriers for AD management will be overviewed. Toxicity and scaling up aspects of these nanocarriers will be highlighted.

Magnetically controlled cells movement after internalization of synthesised metal nanostructures

Albert Serrà[1,2]
Jose García-Torres[1,2,3], Elisa Vallés[1,2]

[1]Materials Science and Physical Chemistry Department, University of Barcelona, Martí I Franqués, 1 (08028), Barcelona, Spain
[2]Institue of Nanoscience and Nanotechnology (IN2UB), University of Barcelona, Martí I Franqués, 1 (08028), Barcelona, Spain
[1]Condensed Matter Physics Department, University of Barcelona, Martí I Franqués, 1 (08028), Barcelona, Spain

aserra@ub.edu

Various methods have been used to control and manipulate living cells, for example those involving nano- and micromotors propelled by remote triggers such as acoustic and ultrasonic waves [1,2], temperature [3] or electrophoretic and dielectrophoretic forces [4,5]. Among these external stimuli, actuation by magnetic fields has garnered great attention as it offers advantages like easy manipulation, control of the swimming dynamics by the applied magnetic field, wireless control or no harmful effect to the body [6,7].

Magnetic nanostructures have received increased attention as micromotors during the last years for biomedical applications like marking and cells separation, drug-delivery or theranostics. The incorporation of magnetic nanostructures into living cells and their manipulation using steering magnetic fields is a challenge to widen the applicability of nanobiomedicine. Locomotion of these nanostructures represents the first challenge. At low Reynolds number environment the viscous forces dominates over the inertial ones. Consequently, hydrodynamics becomes time reversible and no net motion is observed. The second challenge is the possible cytotoxicity of the metallic nanostructures.

Thus, we present here the synthesis of Ni/Au nanorods (NRs) in two different configurations - core@shell and bi-segmented NRs- and their further internalization into test yeast cells. The two configurations will allow the systems to be biocompatible and their actuation via magnetic fields. The internalization of the NR will allow obtaining a cell-NR biohybrid asymmetric microstructure able to be moved, at the micrometric level, by controlled magnetic fields.

The fabrication of the NWs is performed by using electrochemical method. The electrosynthesis requires the use of a porous membrane as a template where growing the metallic NRs. The diameter and length of the NRs is controlled by the diameter of the template channels and the electrodeposition charge respectively. Different electrochemical strategies have been used for the synthesis. Electrodeposition of Ni NRs of a few microns of length and 100 nm of diameter, followed by the galvanic displacement of the superficial nickel by a gold layer allows to fabricate Ni@Au NRs (Figure 1) in which the gold layer avoids the dissolution of nickel in cellular medium. Electrodeposition of bi-segmented Ni-Au NRs, and posterior oxidation of the nickel surface in alkaline solution allows obtaining Ni@NiO-Au asymmetric NRs of a few microns in length and 100 nm of diameter (Figure 2); in this case the biocompatibility and stability of the nanostructures is assured by the presence of gold and NiO surfaces. Both kinds of NRs are easily manipulated by means of magnetic fields.

After that, NRs were incubated during 24h with yeast cells dispersed in water. After this time, the correct internalization of the NRs inside the cells was corroborated by FE-SEM microscopy (Figure 3). Finally, the biohybrid micromotor was propelled using different rotating magnetic fields. The magnetic fields were generated by custom-made coils oriented along three perpendicular directions and connected to a waveform generator and a current amplifier.

The velocity and direction of the movement can be controlled by the field strength, the frequency and the sense of rotation of the magnetic field. Figure 4 shows how the yeast cell can be transported to the target area by changing the magnetic fields. No significant differences are observed for the two types of NRs, and the conditions for the maximum velocity are determined. The work opens the possibility of using the proposed strategy for cells separation of precise motion of cells at the micrometric level.

References

[1] H. Mulvana, S. Cochran, M. Hill, Advanced Drug Delivery Reviews 65 (2013) 1600

[2] X. L. Dong, J. Cai, Z. Wang, 5th International Conference on Manipulation, Manufacturing and Measurement on the Nanoscale, 3M-NANO 2015 - Conference Proceedings 7425517, p. 259

[3] A. Sutton, T. Shirman, J.V.I. Timonen, G.T. England, P. Kim, M. kolle, T. Ferrante, L.D. Zarzar, E. Strong, J. Aizenberg, Nature Communications, 8 (2017) 14700

[4] F. Gerzt, A. Kitun, AIP Advances 6 (2016) 025308

[5] K. Park, S. Kabiri, S. Sonkusale, Biomedical Microdevices 18 (2016 1

[6] F. Gertz, A. Khitun, AIP Advances 6 (2016) 025308

[7] G. Lucarini, V. Iacovacci, L. Ricotti, L., N. Comisso, P. Dario, A., Proceedings of the Annual International Conference of the IEEE Engineering in Medicine and Biology Society, EMBS, 2015

Figures

Figure 1. Ni@Au NWs: Ni NWs fabricated by templated assisted electrodeposition and covered with a gold layer by galvanic displacement in a Au(III) solution. Scale bar: 200 nm
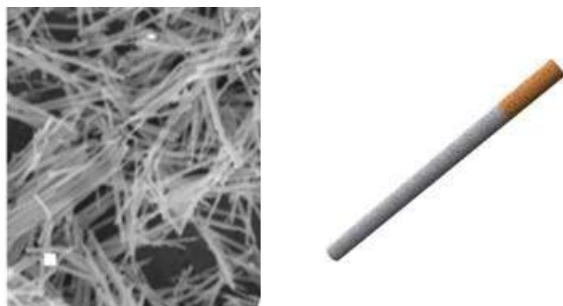
Figure 2. Asymmetric Ni@NiO-Au NWs: Ni-Au NWs fabricated by templated assisted electrodeposition in a single solution and pulsed technology, and posterior oxidation of the Ni surface in alkaline solution. Scale bar: 200 nm
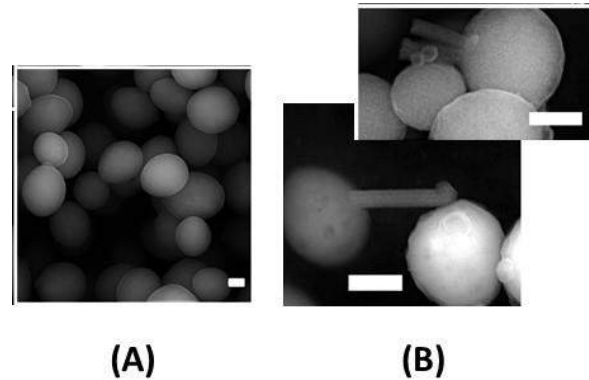
Figure 3. FE-SEM pictures of the yeast cells before (A) and after (B) internalization of magnetic NWs..Scale bar: 400 nm
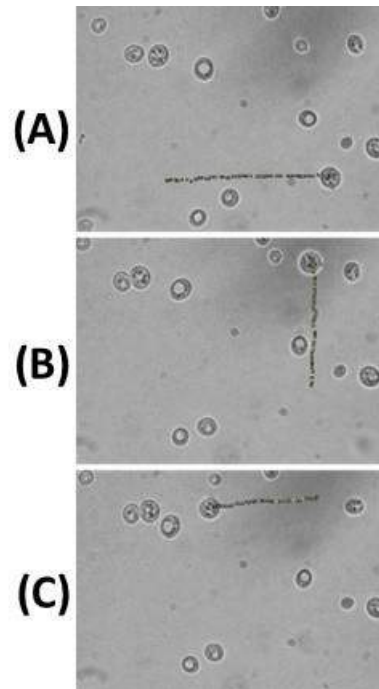
Figure 4. Motion of the yeast cell-NR biohybrid micromotor in different directions depending on the applied rotating magnetic field: (A) rotating magnetic field in the xz plane, 4.5 mT, 5Hz, (B) rotating magnetic field in the yz plane, 4.5 mT, 5Hz, (C) rotating magnetic field in the xz plane, 4.5 mT, 5Hz. The sense of rotation of the magnetic field is opposite to the field in (A).

Preparation and evaluation of multifunctional (Mg, Fe)$_3$O$_4$ nanoparticles designed for cancer therapy

V. Spasojevic[1]

I. Spasojevic[1], M. Ognjanovic[1], M. Mirkovic[1], M. Radovic[1], S. Vranjes Djuric[1], T. Stanojkovic[2], Z. Prijovic[1] and B. Antic[1]

[1]"Vinca" Institute of Nuclear Sciences, University of Belgrade PO Box 522, 11000 Belgrade, Serbia
[2] Institute of Oncology and Radiology of Serbia , Pasterova 14, RS-11000 Belgrade

vojas@vinca.rs

Several sets of ferrofluids, consisting of Mg$_x$Fe$_{3-x}$O$_4$ nanoparticles ($0 \leq x \leq 0.6$), which are coated with citric acid (CA), oleic acid (OA) and polyethylene glycol (PEG), were synthesized by using hydrothermal method. Some of these magnetic nanoparticles (MNPs) were additionally radiolabeled by β-emitter yttrium-90 (^{90}Y). The main objective was to test the MNPS and optimize their characteristics for magnetic hyperthermia and regional radiotherapy, which can be used either individually or simultaneously in cancer treatment. A complete characterization was made for all samples from which information about external morphology of MNPs, their size distribution and magnetic characteristics was obtained. For coated MNPs measurements of ζ-potential and hydrodynamic radii were done, from where the dependence on Mg concentration x was found.

The cytotoxicity of the coated MNPs was tested in vitro on four cell lines: HeLa (human cervical adenocarcinoma cells), LC174 (human colon cancer cells), A549 (lung cancer cells) and MRC5 (healthy fetal lung fibroblast cells).

The obtained results show that the examined cancer lines demonstrate different sensitivity to MNPs and that cytotoxicity depends on the type of nanoparticle coating. For example, the Mg$_{0.6}$Fe$_{2.4}$O$_4$/OA sample shows very good cytotoxicity to all of the used cell lines, whereas the same PEG-coated magnetic nanoparticles have a negligible cytotoxicity. Also, it was found that HeLa cells exhibit the highest sensitivity, regardless of the type of coating while at the same time healthy cells are almoust insensitiv to MNPs.

The labeling yield for all MNPs is very high and for citric acid coated MNPs is 75%, while for PEG coated nanoparticles is almost 100%. Stability of ^{90}Y-labeled MNPs was investigated in both saline and human serum at 37°C up to 72h. It was found that MNPs/PEG/^{90}Y stability is almost 100% while citric acid nanoparticles (MNPs/CA/^{90}Y) demonstrate lower stability of 65%.

Magnetic hyperthermia measurements show that all samples have good heating ability. SPA values of MNPs doped with Mg are increasing with concentration x and applied frequency, showing improvement of heating efficiency comparing to pure magnetite. Measured SPA values are comparable or higher with so far known commercial ferrofluids [1].

References

[1]   M. Kallumadil, M. Tada, T. Nakagawa, M. Abe, P. Southern, Q.A. Pankhurst, Suitability of commercial colloids for magnetic hyperthermia, J. Mag. Mag. Mat, 321(21) (2009) 3650-3651.

Determination of nanoparticle batch reproducibility via stimuli-induced heating

Lukas Steinmetz[1],
Christoph Geers[1], Laura Rodriguez-Lorenzo[1],
Mathias Bonmarin[2], Barbara Rothen-Rutishauser[1],
Alke Petri-Fink[1,3]

[1]Adolphe Merkle Institute, Chemin des Verdiers 4, Fribourg, Switzerland
[2]Institute of Computational Physics, Zurich University of Applied Sciences, Technikumstrasse 9, 8400 Winterthur, Switzerland
[3]University of Fribourg – Chemistry Department, Chemin du Musée 9, Fribourg, Switzerland

lukas.steinmetz@unifr.ch

Ensuring the reproducibility of nanoparticle (NP) synthesis in terms of particle size, size distribution, particle uniformity or colloidal stability is crucial for (i) applications, (ii) basic and applied research or (iii) exploit nano related physical properties. Standard analytical methods, such as electron microscopy, static or dynamic light scattering (DLS), or x-ray diffraction can deliver precise results, but often sample preparation and measurements are time consuming, prone to artifacts, or require expert knowledge for data treatment [1].

Hence we were looking for a quantitative, non-destructive measurement method with high precision and accuracy, which overcomes the above-mentioned disadvantages.

We stimulated thermally responsive nanoparticles with a homogeneous light source and measured the heat generated by the NPs. The thermal signal was detected with lock-in thermography (LIT) [2], an ultra-sensitive infrared imaging technique, commonly used to test composites and electronic components (e.g. solar panels) [3].

The result is a 2D heat map, which allows quantifying of the heat produced with respect to the applied light intensity. The method has been successfully applied to rapidly and efficiently test and compare different NP batches. In addition, the method can be used to investigate the particles' shelf-life over several weeks or analyze particle aggregation. Sample preparation is extremely straight-forward, as the NPs can be measured in their dispersed state. To stimulate different types of NPs, such as gold (Au) or silver (Ag), the excitation wavelength can be changed, ranging from the UV- to the IR-spectrum [4].

We investigated Au and Ag NPs with different size distributions and polydispersities to test the versatility of this method.

In addition to those model plasmonic NPs, we also analyzed the applicability of our method to much more real and complex particles, such as carbon nanotubes. Their composition, shape anisotropy and polydispersity make them challenging candidates for qualitative and quantitative analysis. Complementary methods, such as transmission electron microscopy (TEM), DLS and Taylor Dispersion Analysis (TDA) have been used to analyze the particles and to understand the origin of the difference in heating behavior.

References

[1] B. Michen, C. Geers, D. Vanhecke, C. Endes, B. Rothen-Rutishauser, S. Balog, A. Petri-Fink, *Scientific Reports*, 5 (2015) 9793-9799

[2] S. Huth, O. Breitenstein, A. Huber, D. Dantz, U. Lambert, F. Altmann, *Solid State Phenomena*, Vol. 82-84 (2002) 741-746

[3] C. A. Monnier, M. Lattuada, D. Burnand, J. C. Martinez-Garcia, A. M. Hirt, B. Rothen-Rutishauser, M. Bonmarin, A. Petri-Fink, *Nanoscale*, 8 (2015) 13321-13332

[4] A. O. Govorov, H. H. Richardson, *Nano Today*, Vol. 2 (2007) 30-38

Figures
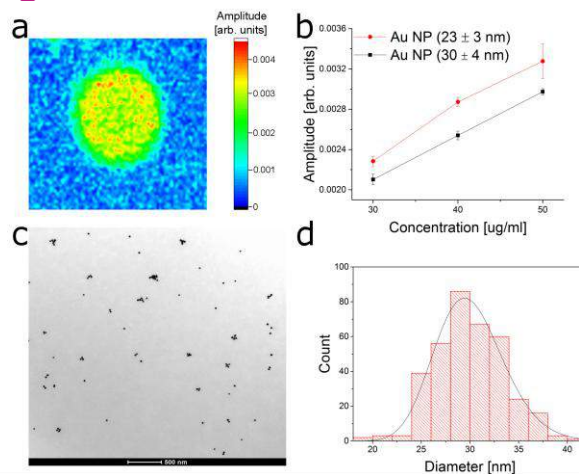
Figure 1. a. 2D LIT heat signal of 30nm Au NPs. **b**. Comparison of two Au NP batches at different concentrations. **c**. TEM micrograph of 30nm Au NPs (scale is 500nm). **d**. Histogram of 30nm Au NPs.

Towards targeted drug delivery: A highly efficient system for production and functionalization of Hepatitis C virus like particles employing transient expression in plants

Edgar Fernando Suarez Zamora[1],
Miguel Angel Gomez Lim[1], Bogdan Dragnea[2]

[1]Department of genetic engineer,
Center for Research and Advanced Studies of the
National Polytechnic Institute (CINVESTAV),
Irapuato, Guanajuato 3682, Mexico
[2]Department of Chemistry, Indiana University,
Bloomington, Indiana 47405, United States

fsuarezam@gmail.com

Hepatitis C is an enveloped, positive-stranded RNA virus belonging to the *hepacivirus* genus in the *Flaviviridae* family. It is comprised of a nucleocapsid (Core) surrounded by a host-derived membrane containing the E1 and E2 HCV glycoproteins and has a specific tropism to liver hepatocytes [1]. Cell-culture (cc) systems for the production of infectious and non-infectious Hepatitis C Virus (HCV) particles (HCVcc) had been developed in mammals [2], insect [3] and free cell systems [4]. Transient expression in plants of viral proteins and particles has been exploited for production of enveloped and non-enveloped plant-related and heterologous viruses and virus like-particles (VLPs), due their relatively low cost of production, high yields of biomass production and efficient eukaryotic post-traductional modifications required for mammalian hosts viruses [5].

We report for the first time the successful production of HCV VLPs in a plant system (*N. Benthamiana*). Transient overexpression of plant-codon optimized, cDNA of the structural proteins (E1, E2 and Core) from the strain 1a of Hepatitis C results in formation of fully assembled VLPs.

Negative staining transmission electron microscopy (TEM) and size distribution analysis after Heparin affinity chromatography purification and isopicnyc centrifugation in sucrose and Iodixanol gradients, showed pleomorphic particles populations ranging in size from 29nm to 110nm, with 2 mayor populations of 50nm and 99nm in diameter resembling particles produced in other HCVcc systems [6,7] (Figure 1).

SDS-Page and Western-Blot analysis showed the presence of the 3 structural proteins at the previously reported buoyant density for HCVcc particles of 1.1g/ml [8].

VLPs were fluorescently labeled and fused (pH=6, sonication 30s) with previously functionalized fluorescent liposomes. Co-localization was showed using single-particle multi-fluorophore confocal microscopy (Figure 2).

References

[1] Zhu, Y. Z., Qian, X. J., Zhao, P., & Qi, Z. T., World Journal of Gastroenterology, Vol. 20 (2013), 3457–3467.

[2] Catanese, M. T., Uryu, K., Kopp, M., Edwards, T. J., Andrus, L., Rice, W. J., Rice, C. M, Proceedings of the National Academy of Sciences of the United States of America, Vol. 110 (2013), 9505–9510.

[3] Baumert, T. F., Ito, S., Wong, D. T., & Liang, T. J., Journal of Virology, vol. 72 (1998), 3827–3836.

[4] Klein, K. C., Dellos, S. R., & Lingappa, J. R., Journal of Virology, Vol. 79 (2005), 6814-6826.

[5] Santi, L., Huang, Z., & Mason, H., Methods Vol. 40 (2006), 66–76.

[6] Piver, E., Boyer, A., Gaillard, J., Bull, A., Beaumont, E., Roingeard, P., & Meunier, J.-C. Gut, gutjnl-2016-311726.

[7] Catanese, M. T., Uryu, K., Kopp, M., Edwards, T. J., Andrus, L., Rice, W. J., … Rice, C. M., Proceedings of the National Academy of Sciences of the United States of America, Vol. 110 (2013), 9505–10.

[8] Gastaminza, P., Dryden, K. a, Boyd, B., Wood, M. R., Law, M., Yeager, M., & Chisari, F. V. Journal of Virology, 84 (2010),10999–11009.
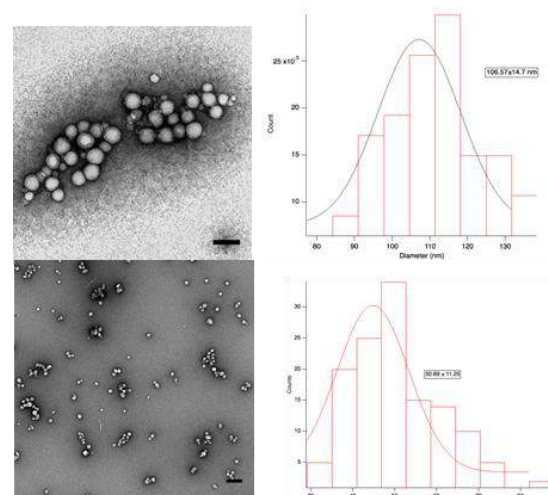
Figures

Figure 1. TEM of VLPs from HepC and Size Distribution. Scale=200nm.
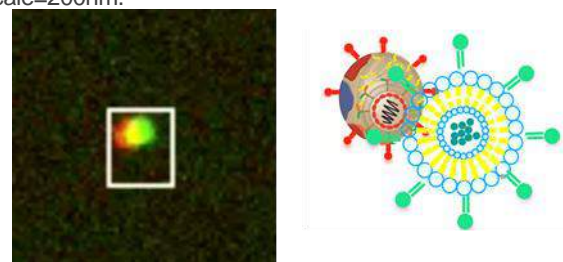

Figure 2. Confocal microscopy of multi-fluorophore co-localization of VLPs of HepC and Liposomes.

Mesoporous silica microtubes as promising chassis for micromotor medical applications

D. Vilela[1,2], M.M. Stanton[2], Ana C. Hortelao[1,2], S.Sanchez[1,2,3]

[1] *Institute for Bioengineering of Catalonia (IBEC), The Barcelona Institute of Science and Technology, Baldiri Reixac 10-12, 08028 Barcelona Spain.*
[2] *Max Planck Institute for Intelligent Systems Institution, Heisenbergstraße 3, 70569 Stuttgart, Germany.*
[3] *Institució Catalana de Recerca i Estudis Avancats (ICREA), Pg. Lluís Companys 23, 08010, Barcelona, Spain*

dvilela@ibecbarcelona.eu

In last decade, micro and nanomotors have demonstrated to be useful tools for biomedical application and have a great potential for the development of future disease treatments and microsurgeries since they can eventually move through the body to perform complex medical tasks. In particular, tubular micro-jets have one of the most promising structures and several methods have been designed for its preparation, such as rolling-up of thin films[1,2], electrochemical deposition[3,4] and template-based self-assembly techniques[5,6].

However, despite the promising future of micro/nanomotors in medicine, most of the current tubular micro-jets cannot be used due to the presence of toxic fuels (H_2O_2) necessary for their propulsion. Biohybrids, which consist on a micro or nanoscale structure propelled by a cell, have showed a recent progress and are also promising systems since they can swim without requiring any fuel.[7]

Here, we demonstrated that a non-pathogenic magnetotactic bacteria, Magnetosopirrillum gryphiswalense (MSR-1), can be integrated with drug-loaded mesoporous silica tubes (MSTs) to build controllable microswimmers (biohybrids).

Mesoporous silica is advantageous for the construction of micro-motors due to its extremely high surface area, large pore volume, transparency and ease of surface chemical modifications which can endow the tubular micro-tubes strong capability of cargo loading *via* physical adsorption on the large surface or encapsulation into the nanopores' cavities. First, MSTs were synthesized without requiring the use of any equipment, using as template a cyclopore polycarbonate membrane, containing conical-shaped micropores with 2 μm maximum diameter. After growing the MSTs, the polycarbonate membrane was rinsed with water and polished using a cotton swab to be consecutively dissolved using organic solvents and then washed in ethanol and water[8].

An optical image of a MST reveals their biconical shape, their length which was found to be 17±1μm (n=20) and their transparent properties (**Figure 1a**). **Figure 1b-d** illustrate the heterogeneous surface of the

MST using TEM. Furthermore, the mesoporous structure of MSTs was evaluated using BET finding the estimated average pore size approximately 3.8 nm of diameter[8].
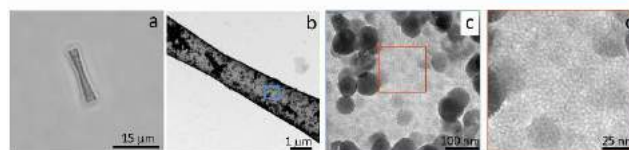
Figure 1. Characterization of MSTs. (A) Mesoporous silica microtube (MST): (a) optical image of a MST, (b) TEM image of a MST and TEM images of MST surface at low (c) and (d) high magnification.

Then, MSR-1 (**Figure 2A**) were integrated with drug-loaded MSTs to build controllable biohybrids (**Figure 2B**) for the antibiotic delivery to target infectious biofilm. Applying external magnetic guidance capability and swimming power of the MSR-1 cells (**Figure 2C**), the biohybrids are directed to and forcefully pushed into matured Escherichia coli (E. coli) biofilms. Release of the antibiotic, ciprofloxacin (CFX), is triggered by the acidic microenvironment of the biofilm ensuring an efficient drug delivery system (**Figure 2D-E**). Our results reveal the capabilities of a non-pathogenic bacteria species to target and dismantle harmful biofilms, indicating biohybrid systems have great potential for anti-biofilm applications[9].

In conclusion, the easy fabricated novel MSTs presented in this work were proved as efficient and active drug delivery vehicles for potential medical applications. In addition, we have demonstrated the anti-biofilm capacity of biohybrids as drug delivery systems by using a living benign bacteria power source with a natural magnetic sensor. This report also demonstrates the advantages of microswimmer technology for the clinically relevant and considerable problem of biofilm formation and how biohybrids have great targeting and therapeutic capabilities for medical applications.
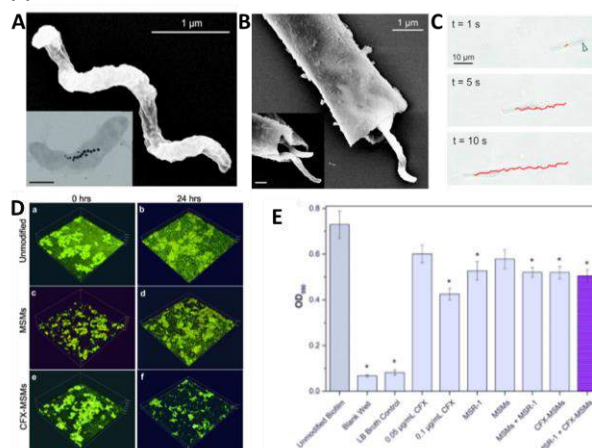
Figure 2. Characterizing bacteria driven biohybrid microswimmers. (A) SEM image of MSR-1 bacterium. Inset displays TEM of MSR-1 and internal magnetosome chain. Inset Scale bar = 500 nm. (B) SEM of MSR-1 cells captured within microtube. Inset displays increased magnification of bacteria in tube. Inset scale bar = 500 nm. (C) Bright field microscopy images of MSR-1 powered biohybrid swimming. Blue arrow indicates location of MSR-1 inside the microtube. Red track indicates the trajectory of the biohybrid. (D) E. coli biofilm disruption. Overnight cultured biofilms had live (green) and dead cells (red) compared in 350 x 350 µm2 3D confocal

images. (a-b) Unmodified control biofilms, (c-d) biofilms with MSMs, and (e-f) biofilms with CFX-MSMs were compared at the time of incubation with the microtubes (0 hours) and 24 hours later. CFX fluorescence is shown in e and f in cyan. (E) CV absorbance analysis of biofilms after 24 hours incubation with biohybrids and control groups. Error bars indicate the s.d. of the mean (n = 15) and the statistical significance (with p < 0.01) is indicated with * for those values which are significantly different from the 'Unmodified Biofilm' control group.

References

[1] S. M. Harazim, W. Xi, C. K. Schmidt, S. Sanchez and O. G. Schmidt, Journal of Materials Chemistry, 22 (2012) 2878-2884.

[2] A.A. Solovev, Y. Mei, E. Bermudez Ureña, G. Huang and O. G. Schmidt, Small 5 (2009) 1688-1692.

[3] W. Gao, S. Sattayasamitsathit, J. Orozco and J. Wang, Journal of the American Chemical Society, 133 (2011) 11862-11864.

[4] D. Vilela, J. Parmar, Y. Zeng, Y. Zhao and S. Sánchez, Nano Letters, 16 (2016) 2860-2866.

[5] Z. Wu, X. Lin, Y. Wu, T. Si, J. Sun and Q. He, ACS Nano, 2014, 8, 6097-6105.

[6] Z. Wu, Y. Wu, W. He, X. Lin, J. Sun and Q. He, Angewandte Chemie International Edition, 2013, 52, 7000-7003.

[7] M. M. Stanton; B.-W. Park; A. Miguel-López; X. Ma; M. Sitti; S. Sánchez, Small 13 (2017) 1603679.

[8] D. Vilela, A. C. Hortelao, R. Balderas-Xicohténcatl, M. Hirscher, K. Hahn X. Ma and S. Sanchez, Nanoscale, 9 (2017) 13990-13997.

[9] M. M. Stanton, B.-W. Park, D. Vilela, K. Bente, D. Faivre, M. Sitti, and S. Sánchez. ACS Nano (2017)10.1021/acsnano.7b04128.

Structural characterisation of antimicrobial Copper oxides and its leaching study using inductively coupled plasma optical emission spectrometry (ICP-OES)

Xiuyi Yang[1],
Yuen-Ki Cheong[1], Jacqueline Stair[2]
and Guogang Ren[1]

[1]School of Engineering and technology,
University of Hertfordshire, College Lane
Hatfield AL10 9AB, United Kingdom

[2]School of Life and Medical Sciences
University of Hertfordshire, College Lane
Hatfield AL10 9AB, United Kingdom

x.yang5@herts.ac.uk

Nanoparticles such silver, mercury and copper are known to have more efficient antibacterial properties as compared with traditional bulk materials [1]. According to previous studies [2], QNA copper oxide (CuO) nanoparticles generated by thermal plasma technology, as displayed in Figure 1, showed to have effectively in killing a range of Gram-positive and Gram-negative bacteria. The minimum bactericidal concentration (MBC) required to counteract pathogens including *Pseudomonas aeruginosa* and *Escherichia coli* were found in ranging from 100 μg/mL to 5000 μg/mL. Another reaserch demonstratd that such nanoparticles have minimum inhibitory (bacteriostatic) concentration (MIC) value in the range of 250 μg/mL to 500 μg/mL against *Prevotella intermedia*, *Porphyromonas gingivalis*, *Fusobacterium nucleatum* and *Aggregatibacter actinomycetemcomitans* [3].
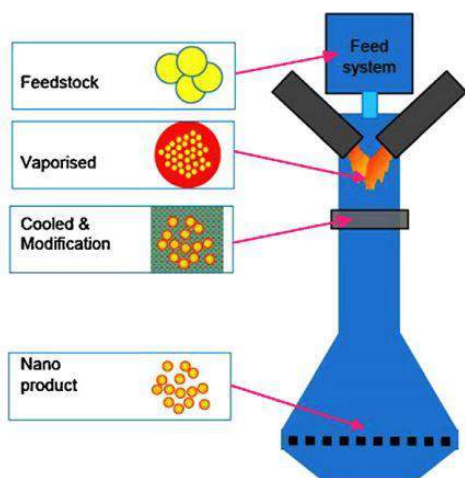

Figure 1. Tesima^TM thermal plasma process to generate nanoparticles

In our study, two different grades of CuO nanopowder (NF CuO and QNA CuO) were investigated. QNA CuO, as mentioned above, was prepared by Intrinsiq Materials Ltd. (Farnborough, UK) using thermal plasma process, while NF CuO nanoparticle was purchased by Suzhou Canfuo Nanotechnology Co.,Ltd (Suzhou, China). Both are deep brown or black powder. Scanning electron microscope (SEM) was used to study the shapes and to estimate sizes of these particles. As shown in Figure 2, SEM images indicated NF CuO nanoparticle has long-rods crystalline with 40 nm diameter, while QNA CuO is fluff-like with very fine nanoparticles.
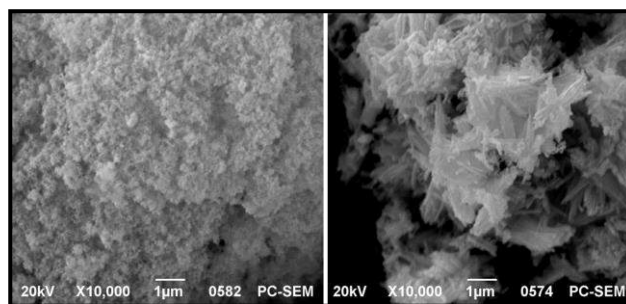

Figure 2. SEM images of QNA CuO (left) and NF CuO (right)

Raman spectroscopy was used to analyse intra- and inter- molecular vibrational modes absorbed through metal oxides bonds, as well as to identify present of any organic impurities. The presence of CuO in both samples were identified by KnowItAll® database software. Figure 3 shows Raman spectra of NF CuO and QNA CuO nanoparticles, both matched well with spectral profile signals resonated at 1100 cm^-1 and 260 cm^-1. A strong and braod vibrational stretch observed at 2240-2650 cm^-1 in QNA CuO (Fig. 3 Top) indicates presence of intermolecular hydrogen bonding, which suggested sample was relatively damp.
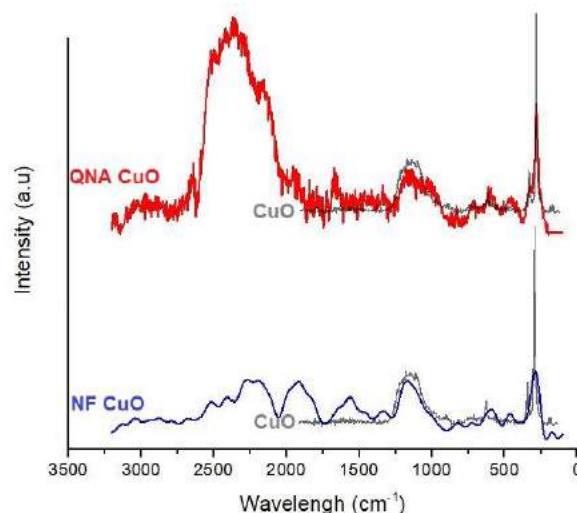

Figure 3. Raman spectra of QNA CuO and NF CuO

Although it is not shown here, further analysis of QNA CuO performed by powder X-ray diffraction has determined the corresponding crystal system as monoclinic and that CuO (Tenorite) was the only visble compound found in the diffractogram.

The aim of this study is to measure Cu ion released from different grades of CuO suspended in various aqueous media (water vs saline). As if such antimicrobial nanopowder is to be used in healthcare or medical applications, it is important to investigate leaching effects produced by these potentially toxic materials. Therefore, the following analytical experiment was designed not to digest the nanoparticles in full but to only measure the ion release in the supernatant isolated from the corresponding suspension samples.

Inductively coupled plasma optical emission spectrometry (ICP-OES) is a highly sensitive elemental tracing technique, metals with concentrations as low as part per million scales can be detected using this method. An ICP-OES is composed of an ICP source, which allow ions to be converted into their excited states, different electronic states and their emitted frequencies are then detected and quantified by the equipped optical emission spectrometry. Prior the measurement of Cu ion in our samples, serial dilutions Cu standard were first analysed to allow selection of optimum Cu emissions as well as to obtain the best fit calibration curve ($R^2 = 1$). Figure 4 shows a total of nine different Cu ion emissions with different wavelengths detected by the OES at standardised Cu concentrations of 0.05 ppm, 0.1 ppm, 0.5 ppm, 1 ppm, 5 ppm and 10 ppm.
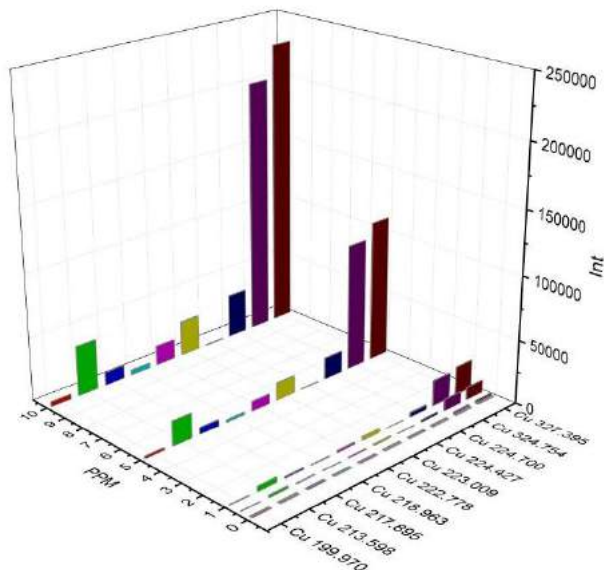

Figure 4. Cu ion emissions detected from standard calibration in ICP experiment

Figure 5 shows Cu ion release detected in both QNA and NF CuO nanoparticle suspensions which were dispersed using 0.1 wt/v % (1000 ppm) of nanopowder in either pure water or Saline. The relative Cu ion concentrations (in ppm) were calculated using formula y=mx+C obtained from the calibration curves according to the emission intensity recorded from the standardised Cu references. In general, low Cu ion concentrations (< 3.4 ppm) were found in all four suspensions, hence, none of the CuO NPs leaching in dangerous level after being

suspended in aqueous media. In particular, NF CuO appeared to leach the minimal in both water and salted saline (0.9% NaCl) when comparing with the QNA engineered CuO samples. In contrast, Cu release found in saline suspensions were approximately three times lower than in the water samples. This may have caused by the difference of pH levels in the water and saline suspensions. More investigations are being carried out to understand the leaching properties of these antimicrobial nanoparticles. It is also worth noting that, this Cu ion release study may also be used to explain antimicrobial activities of different CuO nanoparticles, especially when the biological mechanism of microbial inhibition involves manipulation of protein ion channels.
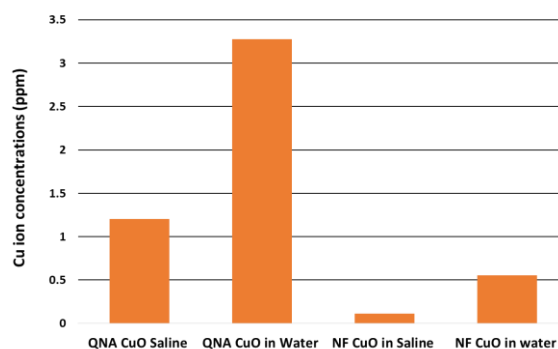

Figure 5. Relative ionic concentration release of NF CuO and QNA CuO in water and saline

References

[1] Tolochko N. History of nanotechnology. Nanoscience and nanotechnology. Encyclopaedia of life Support Systems (EOLSS), Developed under the auspices of the UNESCO, SEolss Published, oxford, 2009.

[2] Ren G, Hu D, Cheng E W C, et al. Characterisation of copper oxide nanoparticles for antimicrobial applications. *International journal of antimicrobial agents*, 2009, 33(6): 587-590.

[3] Vargas-Reus M A, Memarzadeh K, Huang J, et al. Antimicrobial activity of nanoparticulate metal oxides against peri-implantitis pathogens. *International journal of antimicrobial agents*, 2012, 40(2): 135-139.

Acknowledgement

Hepatitis E virus-like particles (VLPs) produced in plants as nanoparticle-based bivalent vaccine

Gergana Zahmanova [1,2],
Valentina Toneva [1,2] and Ivan Minkov [2,3]

[1]Plovdiv University, Department of Plant Physiology and Molecular Biology, 24 Tsar Assen Str., Plovdiv 4000, Bulgaria
[2]Institute of Molecular Biology and Biotechnologies, 105 Ruski Boulevard, Plovdiv 4000, Bulgaria
[3]Center of Plant Systems Biology and Biotechnology, 139 Ruski Boulevard, Plovdiv 4000, Bulgaria

gerganaz@uni-povdiv.bg

Viruses are a great example of natural nanomaterials because of their excellent architectural templates and well characterized genomes and nucleocapsid proteins. Viral nanotechnology and the use of viral nanoparticles (VNPs) as carriers, containers and scaffolds for therapeutics and vaccines has received increasing interest over the last two decades. The immunogenicity of small proteins can be significantly increased by their presentation on particulate carriers such as the capsid protein of hepatitis E virus (HEV). The HEV open reading frame-2 (ORF-2) capsid protein is highly immunogenic and spontaneously assemble into spherical nanoparticles. These VLPs offer the possibility of displaying foreign peptides at different positions on the protruding domain of the capsid protein. Here, we investigated whether HEV-like particles can be used as a vaccine carrier of M2e avian influenza peptide. M2 protein is remarkably conserved in all influenza strains and is therefore a promising vaccine candidate. However, the extracellular domain of M2 protein, M2e protein, is weakly immunogenic and needs to be attached to a carrier to achieve efficacy. The sequences encoding the truncated HEV ORF2 capsid protein and the chimeric HEV ORF2 M2e protein have been inserted into a CPMV-HT vector [1] and expressed in *Nicotiana benthamiana* plants. Expressions of the HEV ORF2 construct and the chimeric construct have been examined by imunoblot analysis and SDS PAGE. Molecular analyses confirmed that inoculated plants produced HEV ORF2 capsid protein and chimeric HEV ORF2 M2e protein. Gradient purified nucleocapsid proteins and M2e chimeric proteins have been examined by electron microscopy, which showed that the plants made truncated HEV ORF2 capsid proteins [Fig. 1] and chimeric HEV ORF2 capsid proteins [Fig. 2]. bearing the M2e spontaneously assembled in VLPs. This study further affirms the suitability of HEV viral nanoparticles as scaffolds of foreign epitopes and their possible application for the generation of monovalent or bivalent vaccines in plants. Hence, plants may be a novel source for the cost-effective production of viral nanoparticle-based bivalent vaccine.

Conclusions: We describe a high-yield, low-cost, and simple method for the production of HEV VLPs and chimeric HEV M2e VLPs in *N. benthamiana* and the potential usefulness of these VLPs for vaccine production.
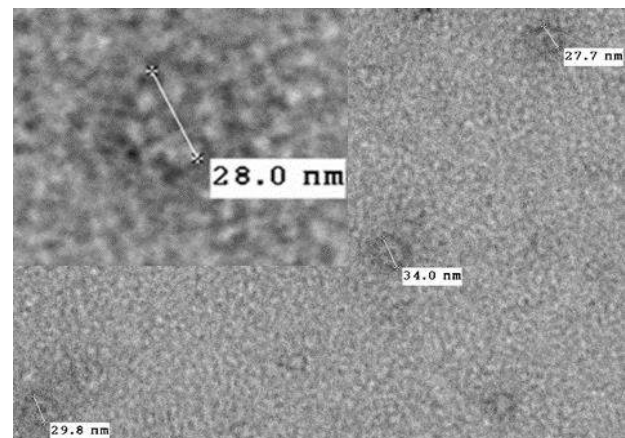
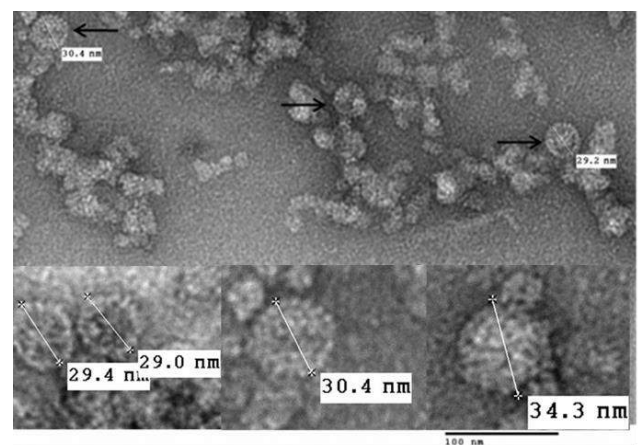**Key Words:** Hepatitis E virus, Transient expression, Nicotiana benthamiana

References

[1] Sainsbury F, Lomonossoff GP. Plant Physiol 2008; 148 (3) 212-18

Figures

Figure 1. Electron microscopy of the HEV ORF2 capsid protein and VLPs.

Figure 2. Electron microscopy of the HEV ORF2 M2e chimeric protein and VLPs.

Enhanced dark-field optical microscopy with high resolution hyperspectral imaging for nanoscale bioimaging and analysis

Paula Zamora Perez[12],
Dionysia Tsoutsi[12], Ruixue Xu[12], Pilar Rivera Gil[12]

[1] Department of Experimental and Health Sciences, Universitat Pompeu Fabra, Doctor Aiguader 88, Barcelona, Spain
[2] Parc de Recerca Biomèdica de Barcelona (PRBB), Aiguader 88, Barcelona, Spain

paula.zamora@upf.edu

Nanoscale imaging techniques are essential for enquiring the behavior of nanoscale materials in different environments and their interactions with biological systems. Parameters such as viscosity, polarity, pH and ionic strength features of the media and other more complex environments as the intracellular milieu, change the physicochemical properties of nanomaterials. Thus, it critically determines the functionality of the material for diagnosis and treatment. For this purpose, enhanced dark-field optical microscopy with high resolution hyperspectral imaging is a very powerful tool that allows real-time optical and light scattering spectral monitoring of unlabeled nanomaterials, in diverse conditions, at single particle level. This imaging system empowers the study of cell and tissue responses to nanosystems with different physicochemical properties, which are relevant for nanodrug delivery and nanotoxicology evaluation.

For example, many nanoscale materials are poor soluble in water and they must be solubilized in solvents with different polarity as ethanol or chloroform. Upon interaction with cell media conditions (rich in salts and proteins) the polarity of the solvent changes and the colloidal stability can be compromised. At the same time, proteins are prone to interact electrostatically with the charge of the nanomaterial, creating a shell on its surface and stabilizing them in solution.

Another example of environmental change, is the exposition of the nanoparticles to an acidic pH. With this procedure the lysosomal pH conditions after cell uptake can be mimicked, to see the changes in the scattering properties that it generates. It makes feasible to track the particles with these spectral features inside the cells.

All this changes on the surface chemistry of the nanomaterials drive different spectral responses, which are traceable with this imaging platform. We are able to study these biological interactions to elucidate different particle behaviors and their potential biological effects.

Multifunctional Platform of Nanocapsules as Drug Carrier for Angiogenic Therapies

Yajie Zhang[1], Irene Anton Sales[1], Alba Grayston[2], Ignasi Barba[2], Anna Rosell[2], Anna Roig[1]

[1]Institute of Materials Science of Barcelona (ICMAB-CSIC), Bellaterra, Spain
[2]Vall d'Hebrón Research Institute (VHIR), Barcelona, Spain

yzhang@icmab.es

Cerebral stroke is a leading cause of mortality and disability that affects 15 million people each year worldwide. Our project focuses on developing a novel nanomedicine-based therapy to promote angiogenesis to address neurorepair after stroke. Previous results demonstrated that the factors secreted by endothelial progenitor cells (EPCs-secretome) have therapeutic potential to promote vascular remodeling in the ischemic brain[1]. Compared to the use of EPCs as a cell therapy[2] or the encapsulation of a single growth factor, i.e., VEGF[3], the encapsulation and controlled delivery of EPCs-secretome as therapeutic agent is clinically interesting in terms of efficiency and safety. In this context, our aim is to take advantage of a nanotechnology approach to achieve the delivery and accumulation of EPCs-secretome in the peri-infracted brain area to promote neurorepair. Specifically, we have engineered a multifunctional polymer nanocapsule platform to encapsulate the EPCs-secretome. This drug delivery system combines the treatment strategy with several diagnostic capabilities. Biodegradable and biocompatible poly(lactic-co-glycolic acid) (PLGA) nanocapsules are synthesized by a double emulsion-solvent evaporation method[3]. PLGA could be further co-polymerized with PEG (to increase the stealth nature of the capsules) and with an intrinsic fluorescent polymer (to *in vivo* track the particles by fluorescence). Further functionalization is achieved by adding magnetic nanoparticles to the organic phase during the synthesis (to magnetically accumulate the capsules in the area of interest with a magnetic field and track them by MRI). Finally, the synthesis method can be modified to attach PET sensitive radiolabels. The presentation will highlight our recent advances in the development of these multifunctional polymeric nanocapsules and their use for neurorepair after stroke.

References

[1]   Rosell A, Morancho A, Navarro-Sobrino M, Martínez-Saez E, Hernández-Guillamon M, Lope-Piedrafita S, Barceló V, Borrás F, Penalba A, García-Bonilla L, Montaner J. PloS one. 2013;8(9):e73244.

[2]   Carenza E, Barceló V, Morancho A, Montaner J, Rosell A, Roig A. Acta -Biomaterialia. 2014;10(8):3775-85.

[3]   Carenza E, Jordan O, Martinez-San Segundo P, Jiřík R, Starčuk jr Z, Borchard G, Rosell A, Roig A. Journal of Materials Chemistry B. 2015;3(12):2538-44.
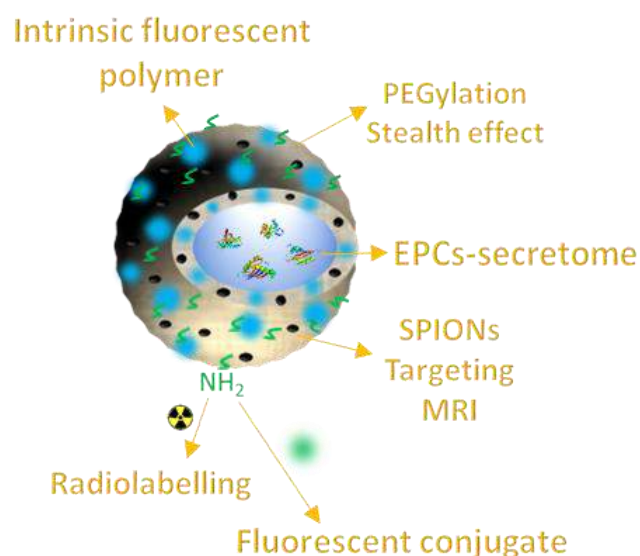
Figures

Figure 1. Schematic illustration of the multifunctional PLGA nanocapsules as EPCs-secretome carrier.